

## MIMER MEDICAL COLLEGE, TALEGAON (D)

### Index

#### 3.3.3 Average number of research papers published per teacher in the Journals notified on UGC -CARE list in the UGC website/Scopus/ Web of Science/ PubMed during the last five years






Sr. No.	Publication Title	Journal-name	Year	Page No.
1	Nanocarrier anticancer drug-conjugates cause higher cellular deformations: culpable for mischief	Biomaterials Science	2020	3-4
2	Prospective study of gross motor milestones in children with severe Idiopathic club foot treated by pontesi method	Indian Journal of Orthopedics	2020	5-9
3	Cellular regeneration and proliferation on polymeric 3D inverse-space substrates and the effect of doxorubicin	Nanoscale Advances	2020	10-21
4	Self-Propelling Targeted Magneto-Nanobots for Deep Tumor Penetration and pH-Responsive Intracellular Drug Delivery	Scientific Reports	2020	22-37
5	Cell deformation and acquired drug resistance: elucidating the major influence of drug-nanocarrier delivery systems	Journal of Materials Chemistry B	2020	38
6	Does the Angle of Rigid Endoscope Makes a Difference in video laryngoscopy?	Indian J Otolaryngology Head Neck Surgery	2019	39-43
7	Variability of small bowel length: Correlation with height, waist circumference and gender	Italian Journal of Anatomy and Embryology	2018	44-51
8	Effect of physical training on pulmonary function test in young adults of a physical training academy	Global journal for research analysis	2018	52-53
9	Morphologic and Cytometric Evaluation of Anemia in geriatric patients	International Journal of Scientific Research	2018	54-56
10	Comparison between tamsulosin vs tamsulosin deflazacort in expulsion of lower ureteric calculi	Indian Journal of Applied Research	2018	57-58
11	Clinical experience of the Tubeless PCNL using standard equipment's	Indian Journal of Applied Research	2018	59-60
12	Clinico- Pathological Study of Ovarian Tumors at A tertiary Care Institute	International Journal of Scientific Research	2018	61-64
13	Do Aesthetic Average Nasal Parameters Matter for Rhinoplasty in India?	Indian J Otolaryngology Head Neck Surgery	2018	65-72
14	Minimal Invasive Endoscopic Ear Surgery: A two handed Technique	Indian J Otolaryngology Head Neck Surgery	2018	73-81
15	Novel horizontal and vertical integrated bioethics curriculum for medical courses	Medical Teacher	2018	82-87
16	Neonatal Screening for Prevalence of Hearing Impairment in Rural Areas	Indian J Otolaryngology Head Neck Surgery	2018	88-94
17	Selective Cell Isolation by Transferrin Functionalized Silane-Carbon Soot Mediated Superhydrophobic Micropatterns	Advanced Materials Interfaces	2018	95-100
18	An insight into hardiness status of medical undergraduates	Indian Journal of Community Health	2017	101-103
19	Biofunctionalized Capillary Flow Channel Platform Integrated 3D Nanostructured Matrix to Capture Circulating Tumor Cells	Advanced Materials Interfaces	2017	104-112
20	Epidemiological Study Of Hardiness Profile Of Blind People	Annals Of Tropical Medicine And Public health	2017	113-121
21	Pattern of Gastric Cancer at Tertiary Rural Hospital in Central India - 10 Year Retrospective study	Paripex- Indian journal of research	2016	122-123
22	Budding trends in integrated pest management using advanced micro- and nano-materials: Challenges and perspectives	Journal of Environmental Management	2016	124-137
23	Novel Concept of Attaching Endoscope Holder to Microscope for Two Handed Endoscopic Tympanoplasty.	Indian Journal of Laryngology and Head and Neck Surgery	2016	138-148

24	Endoscopic cartilage tympanoplasty: A two-handed technique using an endoscope holder.	The Laryngoscope	2016	149-150
25	Hepatoprotective effect of Eclipta Alba and Phyllanthus Fraternus extract in animal model (Rats)	Paripex- Indian journal of research.	2016	151-152
26	Evaluation of possum score – A clinical predictor of morbidity and mortality in gastrointestinal surgeries.	Paripex- Indian journal of research.	2016	153-156
27	Endoscopic management of cholesteatoma with Khan's Endo holder	The Journal of Laryngology & Otology	2016	157-158
28	Awareness of Infectious Occupational Health Risks and the Compliance of Recommended Vaccines Amongst the Medical Interns at Rural Hospital – A Pilot Study	International Journal of Scientific Research	2016	159-161
29	Epidemiological determinants of obesity in adolescent population	Indian Journal of Community Health	2016	162-167
30	Pirfenidone induced phototoxic reaction in an elderly man	Indian Journal of Dermatology, Venereology and Leprology (IJDVL)	2016	168-170
31	Cellular cannibalism in giant Cells of central giant cell Granuloma of jaw bones and Giant cell tumors of long bones	Journal of Investigative and clinical dentistry	2016	171-172



*[Signature]*  
**PRINCIPAL**  
MIMER MEDICAL COLLEGE  
TALEGAON DABHADE  
PUNE -410507

# Nanocarrier anticancer drug-conjugates cause higher cellular deformations: culpable for mischief†

[Narendra Kale](#),  <sup>†a</sup> [Semonti Nandi](#),  <sup>†a</sup> [Ashwini Patil](#),<sup>a</sup> [Yuvraj Patil](#),  <sup>b</sup> [Shashwat Banerjee](#)  <sup>\*b</sup> and [Jayant Khandare](#)  <sup>\*cd</sup>  
[Author affiliations](#)

\*Corresponding authors

<sup>a</sup>MAEER's Maharashtra Institute of Pharmacy, Kothrud, Pune 411038, India

<sup>b</sup>Maharashtra Institute of Medical Education and Research, Talegaon Dabhade, Pune 410507, India

E-mail: [shashwatbanerjee@mitmimer.com](mailto:shashwatbanerjee@mitmimer.com)

<sup>c</sup>School of Pharmacy, Dr. Vishwanath Karad Maharashtra Institute of Technology-World Peace University, Kothrud, Pune 411038, India

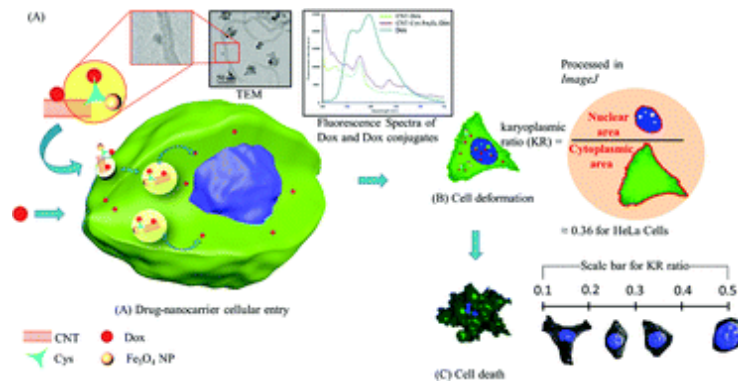
E-mail: [jayant.khandare@mippune.edu.in](mailto:jayant.khandare@mippune.edu.in)

<sup>d</sup>School of Consciousness, Dr. Vishwanath Karad Maharashtra Institute of Technology-World Peace University, Kothrud, Pune 411038, India

## Abstract

Here we report nanocarrier-anticancer drug conjugates culpable for cellular deformations, critically evidenced through image-based analysis as a measure of karyoplasmic ratio (KR) and nuclear surface area (NSA). Multiwalled carbon nanotubes (MWCNTs) were coordinated additionally with Fe<sub>3</sub>O<sub>4</sub> nanoparticles (NPs) to evaluate the symbiotic influence, and further conjugated to Dox for evaluating the cellular kinetics and for measuring cell deformations. Cellular entry kinetics of the CNT (CNT-Dox and CNT-Cys-Fe<sub>3</sub>O<sub>4</sub>-Dox) nanocarriers and their efficiency in nuclear localization were evaluated using cervical cancer (HeLa) cells. Of note, the Dox-bound nanocarriers showed significantly enhanced cell toxicity over the free form of the drug. CNT-Dox and CNT-Cys-Fe<sub>3</sub>O<sub>4</sub>-Dox influx occurred within 4 hours, while maximum cellular retention of Dox was observed for CNT-Dox at 24 h. However, the highest KR (~0.51) was observed for CNT-Dox within 8 hours indicating similar cellular deformations using nanocarrier anticancer drug-conjugates to that of free Dox (KR ~0.50) at 4 hours. In addition, we observed increased NSA at 4 h in Dox treatment whereas in the case of the Dox conjugated nanocarrier, increased NSA was noted at 8 h treatment. At 8 h exposure of HeLa cells with Dox conjugates, we observed that the cells fall into distinct regions of

the morphospace with respect to KR and NSA. Conclusively, nano delivery systems considered for clinical and biomedical translations must take into account the possible negative influences imparting higher cellular deformations and secondary adverse effects over the free form of the drug.





# Prospective Study of Gross Motor Milestones in Children with Severe Idiopathic Clubfoot Treated by Ponseti Method

Chaitrali Shrikant Gundawar<sup>1</sup> · Sameer Shrikrishna Desai<sup>2,5</sup>  · Santosh Shridhar Borkar<sup>3</sup> · Ashish Ranade<sup>4</sup> · Shyamal Patel<sup>2</sup> · Amrut V. Oswal<sup>2</sup>

Received: 12 May 2020 / Accepted: 23 July 2020  
© Indian Orthopaedics Association 2020

## Abstract

**Background** A prospective study of motor milestones achieved in severe clubfeet treated by Ponseti method and comparison between unilateral and bilateral clubfoot will help us gain further insight of motor milestones in these children.

**Methods** Prospective study of 150 consecutive children with idiopathic clubfoot who were treated by Ponseti method and in whom percutaneous tendoachilles tenotomy was performed. The gross motor milestones recorded were: rolls from back to stomach, sitting without support, standing with assistance, walks with assistance, standing alone, walking alone. This was compared with published regional and World Health Organization (WHO) normal data.

**Result** 15 patients were excluded due to non-compliance and recurrence. Children with unilateral clubfoot (80 children) and bilateral clubfoot (55 children) showed a delay of 0.2–2.1 months in various milestones, and this was statistically significant when compared with both normal data. 95% children with unilateral clubfoot had independent ambulation by 17 months and in bilateral ambulation by 17.8 months. There was also a statistically significant difference in unilateral and bilateral clubfeet in all variables except sitting without support and walking with support.

**Conclusion** There is a delay in achievement in all children with clubfoot, with more delay in bilateral clubfoot as compared to unilateral clubfoot. The probable reasons could be plaster treatment, possible weakness due to tendoachilles tenotomy, use of orthosis or the inherent pathology associated with clubfeet. Parents hence need to be explained about this delay.

**Keywords** Motor milestones · Idiopathic clubfoot · Ponseti method · Tendoachilles tenotomy

## Introduction

Ponseti method of correction is currently the most widely used method for the treatment of clubfoot [1–3]. Treatment includes serial plasters followed by percutaneous tendoachilles tenotomy and use of foot abduction orthosis for a minimum of 3–4 years. Bracing is an integral and important part of the treatment and it has been shown to decrease the relapse rate [4]. As parents are usually concerned about the motor milestones of these children, proper information about motor milestones given to these parents based on the published data will help decrease their apprehensions. There are very few prospective studies performed on motor milestones in children with clubfoot and its comparison with published normal regional growth along with World Health Organization (WHO) multi-centric growth reference standards [5–7]. Hence we decided to undertake a prospective study using a selected subset of children with severe idiopathic clubfoot in whom tendoachilles tenotomy was performed.

✉ Sameer Shrikrishna Desai  
doctorsamdesai@yahoo.co.in

Chaitrali Shrikant Gundawar  
gundawarchaitrali@gmail.com

Santosh Shridhar Borkar  
santoshborkar197616@gmail.com

Ashish Ranade  
ashishranade@yahoo.com

Shyamal Patel  
patelshyamalk@yahoo.com

Amrut V. Oswal  
dr.amrut.oswal@gmail.com

<sup>1</sup> Ruby Hall Clinic, Pune, India

<sup>2</sup> KEM Hospital, Rasta Peth, Pune, India

<sup>3</sup> Borkar Hospital, Wada Road, Pune, India

<sup>4</sup> Deenanath Mangeshkar Hospital, Pune, India

<sup>5</sup> Pune, Maharashtra 411009, India

## Materials and Methods

178 consecutive children diagnosed with idiopathic clubfoot attended our clinic from 2013 to 2017. Approval of our ethics committee and institutional review board was taken. Informed consent was taken from parents. To avoid selection bias, it was decided to include only those children in whom tendoachilles tenotomy was performed. Out of these, 158 children underwent a percutaneous tendoachilles tenotomy. Inclusion criteria were: children less than 3 months old with no previous treatment for clubfoot, no other orthopaedic condition like dislocation of hip or torticollis, full-term babies weighing more than 2 kg with no history of any birth injuries or neonatal complications. 8 children did not meet the above criteria. Hence we had 150 children who underwent a percutaneous tendoachilles tenotomy and did not have any other complicating factors and were included in the study group. The children were divided in two groups. Group 1: unilateral clubfoot, Group 2: bilateral clubfoot. All children were treated by serial plasters using the Ponseti method. All plasters were applied by the principal investigator who is a fellowship-trained Paediatric Orthopaedic Surgeon. 150 children underwent a percutaneous tendoachilles tenotomy when foot abduction of 40°–50° was achieved and the Pirani midfoot score was zero. This plaster was applied for 3 weeks. A foot abduction orthosis was used for 23 h for 3 months followed by 12 h every night for 3 years.

After removal of the final plaster, parents were taught about the motor milestones and printed graphical information about the milestones was given to them. They were followed up every 15 days where the principal investigator or co-authors would confirm the milestones achieved by the child and would answer all their doubts. The motor milestones were recorded till the child started walking independently, which was the endpoint of our study. The children were from surrounding location and parents were motivated to come for followup for the study. They were charged as per their income status for followup visits. If there was a discrepancy in the reading of milestones by the parents and the author then the date recorded and personally observed by one of the authors was considered. The motor milestones that were recorded were (1) rolls from back to stomach, (2) sitting without support, (3) standing with assistance, (4) walks with assistance, (5) standing alone (6) walking alone. These were then compared with the historical and published normative data from developmental assessment scales for Indian infants (DASII) and WHO published data. Rolling from back to stomach was not studied in the WHO group and hence it could not be compared. Hand and knee crawling was studied in the WHO group, but was not done in our group. Hence it could not be compared. All other milestones were compared.

## Statistical Analysis

Statistical analysis was performed using SPSS version 20.0. Independent sample *t* test was used to compare the clinical variable in these two groups (unilateral clubfoot patients and bilateral clubfoot patients). Comparison of each group with published normal data of Development Assessment of Indian Infants (DASII) and with WHO published normal data was done. Since all the clinical variables are nominal variables with parametric data, independent sample *t* test was the appropriate test to compare their mean. For the two comparisons,  $p < 0.05$  was considered to be the significance threshold.

## Results

Ten patients were excluded from the study as they were not compliant with brace wear and were not regular with their follow-up. Five patients were excluded as there was a recurrence and they had to undergo repeated plasters or surgery. Hence a total of 135 children were included in the study. There were 80 children with unilateral clubfoot (Group 1). There were 55 children with bilateral clubfoot (Group 2). Both groups were comparable in terms of demographic data. The mean age at which the plaster was first applied in both groups was 13.5 days (range 7–90 days). In group 1, 48 (60%) were males and 32 (40%) were females. In group 2, 30 (55%) were males and 25 (45%) were females. The mean pre-operative Pirani score in Group 1 was 5.4 (range 4–6) and in Group 2 was 5.3 (range 4–6). The average duration of plaster treatment in both groups was for 2 months, with children in both groups requiring a mean of 5.7 plasters (range 5–8).

Comparison of typically developing children (regional data reference) and children with unilateral clubfoot (Table 1): Rolling from back to stomach was the same as in normal children. Sitting without support showed a delay of 1.3 months. Standing holding to a chair showed a delay of 0.3 months and walks with support showed a delay of 1.1 months. Standing alone showed a delay of 1.6 months and walking alone showed a delay of 0.7 months. All these differences were statistically significant.

Comparison of typically developing children (regional data reference) and children with bilateral clubfoot: Rolling from back to stomach showed a delay of 0.2 months, sitting without support showed a delay of 1.2 months. Standing next to the chair showed a delay of 0.5 months and walks with support showed a delay of 1.1 months. Standing alone showed a delay of 2.1 months and walking alone showed a delay of 1.7 months. All these differences were statistically significant.

**Table 1** Comparison of children with unilateral clubfoot, bilateral clubfoot and typically developing children using the Developmental assessment scales for Indian infants

Motor milestone	typically developing child (months)	Unilateral clubfoot (months)	Comparison of typically developing child and unilateral clubfoot ( <i>p</i> value)	Bilateral clubfoot (months)	Comparison of typically developing child and bilateral clubfoot ( <i>p</i> value)	Comparison of unilateral and bilateral clubfoot ( <i>p</i> value)
Roll	4.684	4.684	0.03	4.85	0.001	0.03
Sitting without support	5.7	7.067	0.0001	6.96	0.001	0.183
Stand with support	7.9	8.249	0.0001	8.5	0.001	0.041
Walks with support	8.5	9.663	0.0001	9.67	0.001	0.4
Stand alone	10.1	11.722	0.0001	12.20	0.001	0.029
Walk alone	12	12.787	0.0001	13.77	0.001	0.004

The results are ages of children in months

There was also a statistically significant difference in unilateral and bilateral clubfeet in all variables except sitting without support and walking with support.

Our study group was then compared with the WHO group (Table 2). Sitting without support (delay of 1.01–1.1 month), standing next to chair (delay of 0.8–1.1 months), walking with support (delay of 0.6 months), standing alone (delay of 0.9–1.4 months) and walking alone (delay of 0.7–1.7 months) showed a statistically significant difference and a delay.

## Discussion

Untreated children with unilateral or bilateral clubfoot are independent ambulators, though there are a very few published studies about the achievement of motor milestones in them. The hypothesis before the start of this study was that casts and braces wear should not affect the gross motor milestones of children with clubfoot. To mitigate the influence of other confounding variables, the children who were full-term and without any other orthopaedic problem were included in the study. We decided to include only those children with idiopathic clubfoot in whom percutaneous tendoachilles

tenotomy was performed. The other strength of this study is the prospective nature of this study. There are various studies which show the pitfalls of actual and recalled ages of milestone achievement [8, 9]. To maximise the accuracy of the actual age in this study, the parents were initially taught about the milestones and a printed form with photos was given to the parents. The parents were called every 15 days for follow-up and the accuracy of the date of achievement of a particular milestone was confirmed by the author.

Ethnicity, social habits and culture also play an important role in the development of motor milestones. Hence we decided to compare our results with published normal regional standards along with WHO standards. The DASII scoring system is a simple and quick test for an outpatient clinic [10]. Six milestones as already described were studied in children with clubfoot. All these milestones are very easy to identify and parents were taught about the same at the beginning of the study. We did not compare our study with other studies of typically developing children from other countries as the cultures and habits are different. However, we have compared our results with WHO published data in typically developing children. In WHO group we studied five motor milestones. All milestones were assessed using standardized procedures.

**Table 2** Comparison of children with unilateral clubfoot and bilateral clubfoot with typically developing children as in World Health Organization Multicentre Growth Reference Study Group

Motor milestones	typically developing child (months)	Unilateral clubfoot (months)	Comparison of typically developing child and unilateral clubfoot ( <i>p</i> value)	Bilateral clubfoot (months)	Comparison of typically developing child and bilateral clubfoot ( <i>p</i> value)
Sitting without support	5.9	7.067	0.0001	6.96	0.0001
Stand with support	7.4	8.249	0.0001	8.5	0.0001
Walks with support	9.0	9.663	0.0001	9.67	0.0001
Stand alone	10.8	11.722	0.0001	12.20	0.0001
Walk alone	12.0	12.787	0.0001	13.77	0.0001

Results are the age of children in months



From the current study, we can conclude that there is a delay in motor milestones in children with unilateral and bilateral clubfoot. When compared with each other, children with bilateral clubfoot showed a slight delay as compared to unilateral clubfoot. However, the reason for the delay in pre-ambulatory milestones like rolling and sitting without support cannot be explained. The probable reasons for delay in milestones in children with clubfoot could be prolonged immobilization in above knee casts during the treatment, partial restriction of movement due to use of a brace and the primary pathology of clubfoot itself.

Sala et al. have published a study on motor milestones in 51 children with idiopathic clubfoot [11]. They found a delay of 1.5–2 months in perambulatory and ambulatory milestones in their group. However, their sample size was small and they have not studied unilateral and bilateral clubfoot separately. Tendoachilles tenotomy was performed in only 59% of children studied by them. We have included only those children in whom a tenotomy was performed.

Zionts et al. also studied walking age in clubfoot children treated by Ponseti method and they observed that independent walking was seen approximately 2 months later when compared to infants without clubfoot [12]. A greater delay may be expected for those patients who have a very severe deformity or those who experience a deformity relapse. However, they did not study other milestones and did not differentiate between unilateral and bilateral clubfeet.

In a study by Garcia et al., 26 babies with clubfeet treated with various methods (Ponseti method, French method and combination) were compared with 26 babies who were typically developing children. The gross motor performance was evaluated with the Albert Infant Motor Scale for six motor milestones. The researchers found that the babies with clubfeet had a mild delay in the gross motor skills and this delay became apparent around the age of 9 months. Babies without clubfeet were significantly more likely to walk at 12 months than babies with clubfoot [13].

Loof has shown that gross motor deficits and asymmetries are known to be present in children of 5 years of age with clubfoot. In unilateral clubfoot, the normal foot modifies in gait and foot motion just as the side with clubfoot. According to them, future studies are needed to prospectively study gross motor skills in children from the period of infancy [14].

A possible delay in milestones needs to be explained to parents before the start of treatment. Though all milestones are important, usually parents are more concerned about independent ambulation. There was a delay of 0.7 months for independent walking in children with unilateral clubfoot. 95% of children were walking independently by 17 months. There was a delay of 1.7 months for independent walking in children with bilateral clubfoot. 95% of children were walking independently by 17.8 months. We have shown that there

is a difference in motor milestones in children with unilateral clubfoot and bilateral clubfoot. We have also compared our results with both regional and WHO reference standards and the results show a significant delay in milestones. Parents need to be explained that these delays are mild with no long-lasting implications and they should adhere to the brace protocol to avoid recurrences.

**Funding** None of the authors received financial support for this study.

## Compliance with Ethical Standards

**Conflict of interest** The authors declare no conflicts of interest.

**Ethical standard statement** This article does not contain any studies with human or animal subjects performed by the any of the authors.

**Informed consent** Informed consent was obtained of all parents about the study.

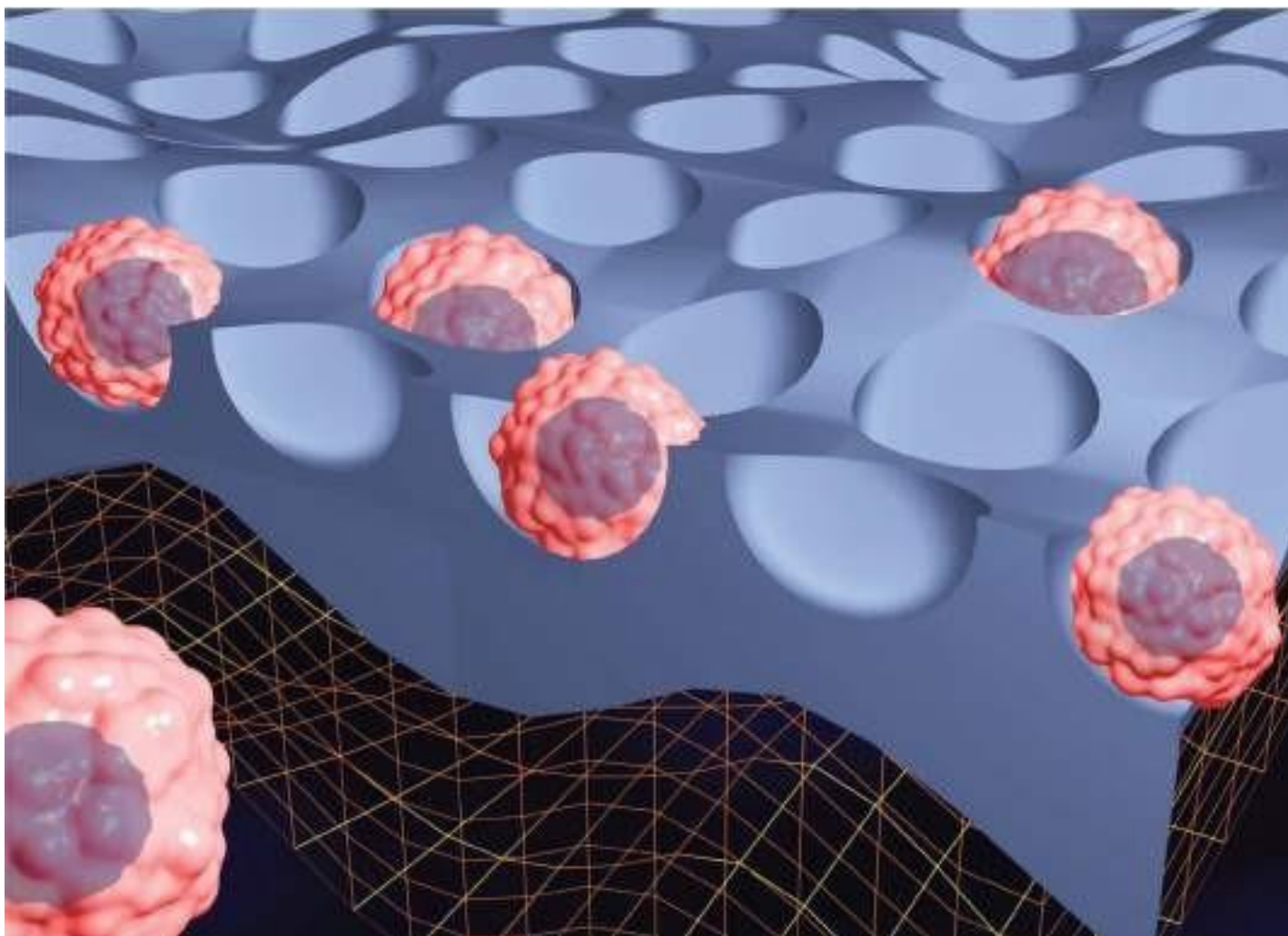
## References

1. Ponseti, I. V. (1996). *Congenital clubfoot. Fundamentals of treatment*. New York: Oxford University Press.
2. Laaveg, S. J., & Ponseti, I. V. (1980). Long-term results of treatment of congenital club foot. *The Journal of Bone and Joint Surgery American Volume*, 62, 23–31.
3. Herzenberg, J. E., Radler, C., & Bor, N. (2002). Ponseti versus traditional methods of casting for idiopathic clubfoot. *Journal of Pediatric Orthopaedics*, 22, 517–521.
4. Thacker, M. M., Scher, D. M., Sala, D. A., et al. (2005). Use of foot abduction orthosis following Ponseti casts: Is it essential? *Journal of Pediatric Orthopaedics*, 25, 225–228.
5. Phatak, P. (1998). *Developmental assessment scales for Indian infants*. Pune: Anand Agencies.
6. Phatak, A. T., & Khurana, B. (1991). Baroda development screening test for infants. *Indian Pediatrics*, 28(1), 31–37.
7. WHO Multicentre Growth Reference Study Group. (2006). WHO Motor Development Study: Windows of achievement for six gross motor development milestones. *Acta Paediatrica Supplement*, 450, 86–95.
8. Donoghue, E. C., & Shakespeare, R. A. (1967). The reliability of paediatric case-history milestones. *Developmental Medicine & Child Neurology*, 9, 64–69.
9. Majnemer, A., & Rosenblatt, B. (1994). Reliability of parental recall of developmental milestones. *Pediatric Neurology*, 10, 304–308.
10. Phatak, P., Dhapre, M., Pandit, A. N., et al. (1991). A study of Baroda Development Screening Test for infants. *Indian Pediatrics*, 28(8), 843–849.
11. Sala, D. A., Chu, A., Lehman, W. B., et al. (2013). Achievement of gross motor milestones in children with idiopathic clubfoot treated with the Ponseti method. *Journal of Pediatric Orthopaedics*, 33(1), 55–58.
12. Zionts, L. E., Packer, D. F., Cooper, S., et al. (2014). Walking age of infants with idiopathic clubfoot treated using the ponseti method. *The Journal of Bone and Joint Surgery American Volume*, 96(19), e164.



13. Garcia, N. L., McMulkin, M. L., Tompkins, B. J., et al. (2011). Gross motor development in babies with treated idiopathic clubfoot. *Pediatric Physical Therapy*, 23(4), 347–352.
14. Lööf, E., Andriessse, H., André, M., Böhm, S., et al. (2019). Gross motor skills in children with idiopathic clubfoot and the association between gross motor skills, foot involvement, gait, and foot motion. *Journal of Pediatric Orthopaedics*, 39(7), 359–365.

**Publisher's Note** Springer Nature remains neutral with regard to jurisdictional claims in published maps and institutional affiliations.

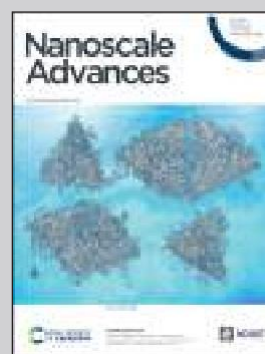


Showcasing the research from Prof. Jayant Khandare's group at School of Pharmacy, Dr Vishwanath Karad MIT World Peace University, Pune and Dr. Yuvraj Patil at MIMER Medical College, Pune, India.

Cellular regeneration and proliferation on polymeric 3D inverse-space substrates and the effect of doxorubicin

3D inverse spaces (3DIS) in polymeric matrices show a robust platform for 3D cell growth and cell regeneration in sharp contrast to flattened cells cultured on conventional 2D cell culture substrates. 3DIS milieu system leverage the growth of the cells potentially restoring intrinsic morphology versus in 2D culture, and also altered exemplified in drug dose-responses.





As featured in:



See Yuvraj N. Patil,  
Jayant J. Khandare *et al.*,  
*Nanoscale Adv.*, 2020, 2, 2315.

Cite this: *Nanoscale Adv.*, 2020, 2, 2315

# Cellular regeneration and proliferation on polymeric 3D inverse-space substrates and the effect of doxorubicin†

Chandrashekar D. Bobade,<sup>‡a</sup> Semonti Nandi, <sup>‡a</sup> Narendra R. Kale,<sup>a</sup>  
Shashwat S. Banerjee, <sup>b</sup> Yuvraj N. Patil <sup>\*b</sup> and Jayant J. Khandare <sup>\*c</sup>

Spatial arrangement for cells and the opportunity thereof have implications in cell regeneration and cell proliferation. 3D inverse space (3DIS) substrates with micron-sized pores are fabricated under controlled environmental conditions from polymers such as poly(lactic-co-glycolic) acid (PLGA), poly(lactic acid) (PLA) and poly(styrene) (PS). The characterization of 3DIS substrates by optical microscopy, scanning probe microscopy (SPM), *etc.* shows pores within 1–18 μm diameter and prominent surface roughness extending up to 3.9 μm in height over its base. Conversely, to compare two-dimensional (2D) *versus* 3DIS substrates, the crucial variables of cell height, cell spreading area and cell volume are compared using lung adenocarcinoma (A549) cells. The results indicate an average cell thickness of ~6 μm on a glass substrate whereas cells on PLGA 3DIS were ~12 μm in height, occasionally reaching 20 μm, with a 40% decreased cell spreading area. A549 cells cultured on polymer 3DIS substrates show a cell regeneration growth pattern, dependent on the available spatial volume. Furthermore, PLGA 3DIS cell culture systems with and without graded doxorubicin (DOX) pre-treatment result in potent cell inhibition and cell proliferation, respectively. Additionally, standard DOX administration to A549 cells in the PLGA 3DIS system revealed altered drug sensitivity. 3DIS demonstrates utility in facilitating cellular regeneration and mimicking cell proliferation in defined spatial arrangements.

Received 27th January 2020  
Accepted 1st April 2020

DOI: 10.1039/d0na00075b

rsc.li/nanoscale-advances

## Introduction

Synthetic biodegradable polymers such as poly(L-lactic acid) (PLLA), poly(glycolic acid) (PGA), PLGA, poly(ε-caprolactone) (PCL) *etc.* have been previously reported as scaffolding materials to exhibit cellular behavior and characteristics.<sup>1–3</sup> Tissue regeneration and wound healing has been extensively studied in cell culture models.<sup>4–6</sup> Comparably, the use of 3D cell culture tools in cell proliferation and drug-mediated cytotoxicity studies is limited, and is primarily studied using 2D cell cultures.<sup>7</sup> An observable issue with such planar tools as a cell attachment/proliferation model is the morphological change induced in 2D cultured cells; the cells appear thinly spread with a predominantly flattened profile.<sup>8</sup> While enhanced cell adhesion as a feature is desirable for cell studies, structurally altered

biological features may be responsible for a varied cell response and function in such cells.<sup>8–10</sup> Cell adhesion and interfacial interactions exert morphological changes based on attachment-substrate geometry, surface texture and stiffness among others.<sup>11,12</sup>

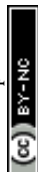
Tissue regeneration/wound healing involves healthy cells utilizing interactive feedback such as contact inhibition, preventing healthy cells from multiplying and stacking beyond their physiological role.<sup>13,14</sup> On the other hand, cancerous cells continue to proliferate beyond spatial contact inhibition and often grow as uncontrolled tumor masses as well as enable dissemination of cancerous cells leading to metastasis.<sup>13</sup> Planar cell culture models with enhanced cell adhesion features significantly lack a vertical profile and may not reflect the ability of cells to simulate wound closure based on cell–cell interaction alone.<sup>2,15</sup> Furthermore, structural components of *in vivo* tissues support a more spatially relaxed cell profile, compared to glass or compatible planar surfaces, where tissue sections reveal more geometrically shaped cells which can stack against each other.<sup>16,17</sup>

3DIS is a 3D-embedded negative or ‘inverted’ space, embodied by porous cavities. While true 3D structures have mass and distinct spatial coordinates, 3DIS presents a niche which can be exploited for cell attachment, growth and culture. The 3D matrix surrounding the 3DIS pore constitutes the cell

<sup>a</sup>MAAER's Maharashtra Institute of Pharmacy, Kothrud, Pune 411038, India<sup>b</sup>Maharashtra Institute of Medical Education and Research Medical College, Talegaon-Dabhade, Pune 410507, India. E-mail: yuvrajpatil@mitmimer.com<sup>c</sup>School of Pharmacy, Dr Vishwanath Karad MIT World Peace University, MIT Campus, S. No. 124, Paud Road, Kothrud, Pune 411038, India. E-mail: jayant.khandare@mippune.edu.in

† Electronic supplementary information (ESI) available: Fig. S1, Fig. S2, Fig. S3, video 1, video 2, video 3 and video 4. See DOI: 10.1039/d0na00075b

‡ C. D. B. and S. N. contributed equally to this work.



scaffolding. We hypothesize that the 3DIS substrates and the corresponding cell culturing strategies may offer greater spatial opportunity compared to 2D substrates. 3DIS substrates with their predicted optimal cell attachment properties are further hypothesized to retain cell topography to mimic *ex vivo* cells in their natural environment. In the present study, the correlation of chemotherapy failure due to sub-lethal anticancer therapy leading to tumor cell regression and cell proliferation, thereafter using 3DIS *ex vivo* polymeric systems, is envisioned. Thus, the objectives of the study were (a) to design 3DIS substrates composed of PS, PLA and PLGA and characterize the same; (b) to demonstrate the utility of spatial scaffolding to allow cells to grow freely in a 3D microenvironment, thereby enabling a near-physiological outcome of DOX exposure to cancerous cells and (c) to compare the differences in 2D and 3DIS cell cultures, with regard to their effect on cell morphology and the effect of the substrate juxtaposed with DOX exposure and the fate of the cells thereof.

## Experimental section

### Materials

PLGA with lactide : glycolide (ratio 75 : 25) and a  $M_w \sim 66$ –107 kDa and PLA with an average  $M_n \sim 40$  kDa were obtained from Sigma Aldrich, PS with a  $M_w \sim 40$ –60 kDa was obtained from Analab Fine Chemicals, India. Doxorubicin hydrochloride (DOX) was obtained from Sigma Aldrich. Toluidine blue O (TBO) was obtained from SRL Pvt. Ltd, India. Methanol, chloroform, and dimethylsulfoxide (DMSO) were of analytical grade.

### Preparation of glass, PLGA, PS and PLA substrates

Plane, unmodified microscopic cover glasses were obtained and used as substrates for cell culture post sterilization. PLGA, PS and PLA 3DIS substrates were prepared through a typical breath figure approach. First, 18 mm × 18 mm glass cover slips were washed with methanol to remove impurities. 5 mg. ml<sup>-1</sup> polymer solution of PLGA, PS and PLA was prepared in chloroform; 50 ml of the resultant polymer solution was placed with the aid of a pipette slowly onto the glass slide under humid atmospheric conditions (~80–90% Relative Humidity (RH) and temperature 22.5 to 23.5 °C) in a sealed acrylic chamber. The prepared 3DIS polymeric substrates were observed under bright field microscopy. The smooth polymeric substrates (lacking inverted 3D structures) were prepared using the same method under dry conditions (40% RH and temperature 26 °C).

### Characterization of the polymeric scaffold

Morphological characters such as pore diameter, rim width and substrate thickness of PLGA, PS and PLA substrates were determined by calculating the average of three-point measurements. The surface area for smooth and 3DIS substrates was determined by image analysis. SPM (JSPM-5200, JEOL) analysis provided the topography data of the designed polymer substrates. Other parameters noted were polymer substrate stability in various exposure conditions such as chemical reagents, pH sensitivity, ultraviolet radiation *etc.*

### Determination of surface carboxyl (–COOH) groups using the TBO assay

The substrates were immersed in 1.5 ml of 2 mM TBO solution for 24 h at room temperature (25 °C), during which the dye bound *via* electrostatic interaction to the ionized acidic charges. Substrates were thoroughly rinsed with 0.015 M NaCl at pH 11.0 to wash away the unbound dye molecules. Once air dried, the substrates were placed in 1 ml of 0.2 M NaCl solution at pH 2.0 for 60 min while stirring. During this step, the TBO molecules bound to the acidic groups of the substrate were eluted from the analyzed surface and diffused into the solution, coloring it blue. The light absorbance of the solutions at 630.8 nm wavelength was measured. The blank consisted of a 0.2 M NaCl solution at pH 2.0.

### Measurement of wettability

The contact angle ( $\theta$ ) of the prepared substrates was studied and correlated with the structural geometry and wettability characteristics of the prepared substrates. A deionized water drop of 5  $\mu$ l, ( $n = 1.33$ ) was placed on dry substrates (PLGA, PS and PLA smooth and 3DIS architecture) at room temperature and images of the wetting process of the placed water drop were captured with a high speed digital camera. The captured images were processed using LBDSA Drop Shape plug-in the image analysis software ImageJ (NIH, Bethesda, MD) for  $\theta$  determination.

### Preparation of Dox pre-treated PLGA substrates

DOX solution volumes which are mole-identical to IC<sub>50</sub> and IC<sub>25</sub> of free DOX were pipetted onto PLGA (smooth and 3DIS) substrates and air dried to leave a DOX coat onto the film. These prepared substrates were further used for A549 cell culturing and analyzed for morphological parameters.

### Cell culture

The prepared substrates were rinsed in 70% ethanol solution and kept for 30 min under UV light to sterilize before cell seeding. The substrates were immersed in Dulbecco's Modified Eagle's Media (DMEM) supplemented with 10% fetal bovine serum (FBS) and 1% penicillin–streptomycin. A549 cells (National Center for Cell Science, Pune) were used for the cell study. After rinsing cells in the flask with phosphate buffered saline (PBS) (pH 7.4), cells were harvested with trypsin (0.5%) ethylenediaminetetraacetic acid (EDTA). A549 cells were seeded at a high density (400 000 cells per ml) on the substrates in 12 well plates and cultured for 3, 6, 24 and 48 h in 5% CO<sub>2</sub> in a humidified incubator.

### Cell imaging and quantification

Cell morphology was characterized using an inverted fluorescence microscope Axio Observer A1 (Carl Zeiss, Germany). The cells were fixed with 4% paraformaldehyde for 20 min. The substrates were mounted on glass slides and observed under 20× magnification. The microscopic images of cell morphology were visualized with fluorescent dyes FITC (cytoplasm) and 4',6-diamidino-2-phenylindole (DAPI) (nuclei) and were





quantitatively analyzed using ImageJ® software (NIH, Bethesda, MD). High resolution images were obtained using a Confocal Laser Scanning Microscope (Leica Microsystems); Z-stack images for spatial data were obtained for all samples. Quantification and visual data were extracted with Fiji® software (NIH, Bethesda, MD). The volume of cells was obtained by defining specific regions of interest, followed by signal thresholding. The resulting spatial signal was compiled with the Voxel Counter plug-in in Fiji® and calculated as the volume in cubic microns. Imaging was carried out four separate times with multiple samples. The calculated data is expressed as the mean data with a standard error of mean.

### Biocompatibility/cell viability test

The cell viability of A549 cells on glass and PLGA polymer substrate samples, both smooth and 3DIS, was quantitatively determined by the 3-(4,5-dimethylthiazol-2-yl)-2,5-diphenyl tetrazolium bromide (MTT) assay. Briefly, 10 000 cells per well were seeded on each substrate in a 48-well plate and maintained for 24 h at 37 °C in 180 ml DMEM supplemented with 10% FBS, following which a stock MTT reagent, (20 ml) was added and cells were incubated for 4 h. After 4 h, the entire media was aspirated and DMSO (100 ml) was added to each well. DMSO dissolved the precipitate following which the absorbance was measured at 570 nm. Background readings (blank) were obtained from cell-free wells containing only DMSO. A549 cells grown on glass substrates were considered as the control. Percentage cell viability was calculated as

$$(A \times 100)/C \quad (1)$$

where,  $A$  ¼ polymer substrate MTT absorbance and  $C$  ¼ glass control MTT absorbance.

### PLGA-3DIS DOX release study

PLGA substrates (smooth and 3DIS) were surface coated with 200 mg DOX and dried. PBS (pH 7.4) was used as the dissolution media of which 1 ml was added to the substrates and aliquots were collected at fixed time intervals (1, 3, 6, 24 and 48 h). Fresh PBS was replaced at every time point to maintain constant media volume. Fluorescence emission intensity was measured at 590 nm upon excitation at 480 nm. The DOX released was calculated as the % cumulative release against all time points. All experiments were performed in triplicate.

### Statistical analysis

A student *t*-test was performed on the data sets to determine the *p*-value for testing the significance of quantified data (volume, area, height, drug concentration *etc.*). A *p*-value of 0.05 was assumed as the limit of significance. Statistical processing was carried out with GraphPadPrism, GraphPad Software, San Diego, California, USA.

## Results

The complex model for tissue repair or regeneration utilizing multiple cell types and signaling components, as depicted in Fig. 1A, may not be easily replicated *in vitro*; however, the ability of epithelial cells to mimic the gap-bridging may be studied *in vitro* using appropriate 3D substrate architecture. Conversely,

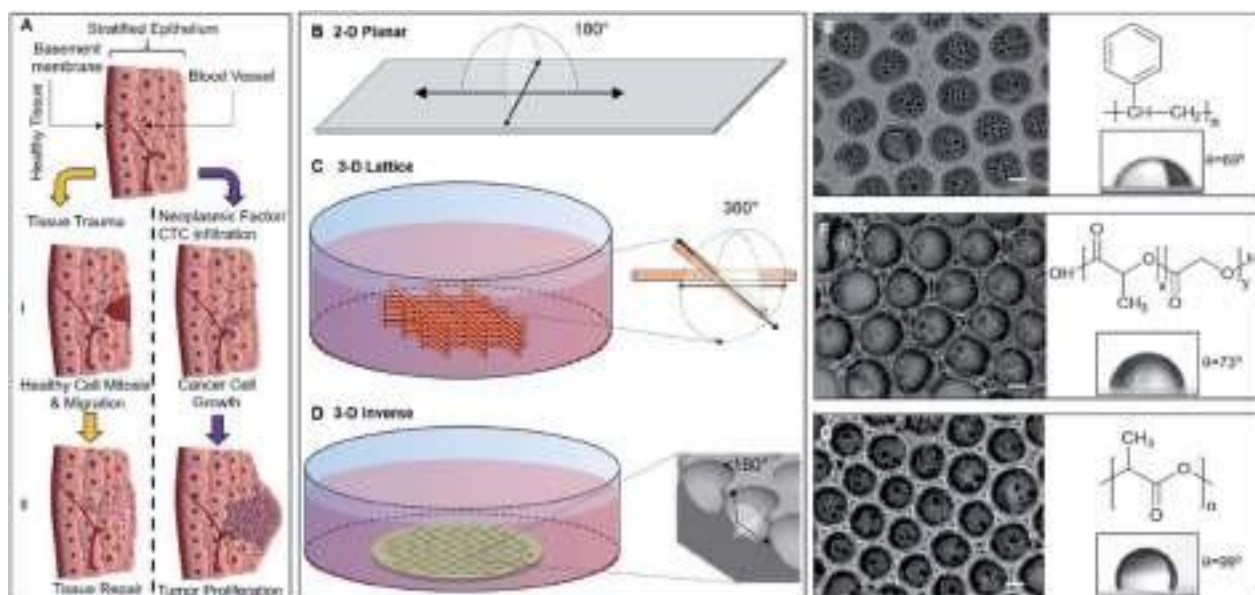


Fig. 1 Apparent degrees of freedom in cell culturing substrates. (A) Schematic comparing the tissue cell growth and repair mechanism in normal healthy cells after an injury or trauma and tumour cells presenting uncontrolled and unregulated cell multiplication leading to rapid tissue proliferation. (B) 2D plane surfaces provide 180° of freedom for cells to spread along a hypothetical hemispherical zone. (C) The 3D lattice may allow unrestricted growth with 360° of spatial freedom and cells may spread entirely along the scaffold surface. (D) 3DIS involves a limited volume within a material matrix which markedly reduces the available spatial freedom (<180°) for cell spreading. Brightfield images, chemical structures and contact angles of (E) PS 3DIS, (F) PLGA 3DIS, and (G) PLA 3DIS are depicted. Scale bar is 10 μm.



while cancer cell proliferation also presents a complex model of unregulated cell division, the changes in cell morphology are readily observed. Fig. 1A depicts the cellular fates a healthy tissue may experience upon being subjected to physical injury or cellular insult with onco-genetic potential, including in infiltration of circulating or metastatic tumor cells. The 3DIS platform proposed here mimics tissue substratum offering cultured cancer cells the spatial opportunity for proliferation as well as presenting a broken surface simulating tissue trauma which in turn presents a spatial opportunity for studying tissue monolayer repair and rebuilding.

#### Apparent degrees of freedom of cell culturing substrates

2D surfaces such as tissue culture flasks or glass offer 180° of spatial freedom for cell growth (Fig. 1B). Some 3D culture methods utilizing cell substrates as scaffolding may even approach 360° of freedom allowing cells to spread along any accessible direction (Fig. 1C). Conversely, 3DIS reduces available spatial freedom (<180°) and cells are confined to a restricted volume while allowing spatial cell adhesion opportunity (Fig. 1D), virtually absent in the above two models.

#### Mechanism of formation of 3DIS polymer architecture

The polymer 3DIS films were generated by a method known as the 'breath-figure' method which exploits higher atmospheric/environmental moisture content or humidity to accelerate pore formation on the film surface during the course of film

drying. When a drop of polymer solution is cast on a substrate, the volatile solvent begins to evaporate in the humid atmosphere. During evaporation, the latent heat of vaporization is absorbed due to which the temperature at the solution surface decreases to a point at which condensation begins. These condensed water droplets interact and rearrange on the solution surface to remain isolated from each other. When the temperature of the solution surface increases high enough, further condensation cannot occur. Thus, the water droplets begin to evaporate from the solution surface and the polymer precipitates around each water droplet which leaves behind cavities (pores) in the solid polymer film, after complete evaporation.<sup>18,19</sup> The greater the humidity, the greater is the water vapor sequestration in the chloroform-polymer slurry leading to condensation of water droplets onto the drying film. Thus with a greater water content, smaller pores coalesce and form larger pores (>10 nm).

#### Physicochemical traits of 3DIS substrates

Polymer substrates on glass cover slips were fabricated from PS, PLGA and PLA (chemical structures depicted in Fig. 1E, F, G respectively) and analyzed to verify either the smooth or 3DIS geometry of the substrates (Fig. 1E, F, G). The 3DIS substrates were distinguished as 3DIS(+) or 3DIS(−) based on their large (>12 nm) or small (<10 nm) pore sizes, respectively. Each of the substrates showed an even distribution of the 3DIS aspect with even rim-width and pore sizes (12–18 nm). The pore size of 3DIS

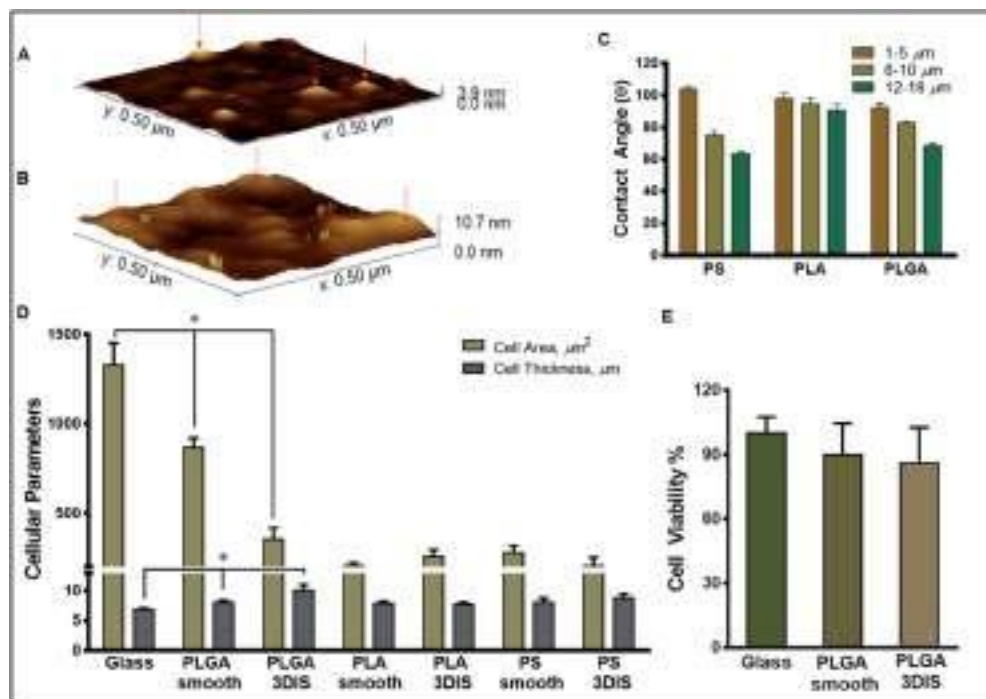


Fig. 2 Physical characterization of 2D glass and 3DIS polymer architectures and polymer biocompatibility evaluation. SPM images of (A) the PLGA film and (B) glass showing surface topography. The red arrows indicate surface features. (C) The  $\theta$  value varied with the polymer nature (PS, PLA or PLGA) and polymer 3DIS pore sizes (1–5 nm, 6–10 nm, and 12–18 nm). (D) Cell area and cell thickness were evaluated on different 2D surfaces and 3DIS composed of PS, PLA and PLGA. (E) Cell viability of A549 cells on PLGA smooth (90%) and 3DIS (86.2%) films in comparison to glass as the control. \* represents statistical significance,  $p < 0.01$ .



increased (1 mm to 18 mm) with increasing polymer strength (0.3–0.7% w/v) and also with greater environmental moisture content and temperature ( $\sim 80$ – $90\%$  RH and  $22.5$  to  $23.5$  °C, (Fig. S1A and B<sup>†</sup>)). The polymer substrates cast on the glass surface had an average thickness of  $25.4 \pm 9$  mm. The total surface area of 3DIS substrates was computed using the following rationale:

$$[pR^2 + (2pr^2 \times n)] - pr^2 \times n \quad (2)$$

where  $R$  is radius of the circular cast substrate,  $r$  is radius of one pore, and  $n$  is the total number of pores. Thus, for a 3DIS substrate with an average pore size of  $15$  mm, the total surface area was computed to be  $89.5$  mm<sup>2</sup> for a substrate of  $1$  cm diameter; with the average distance between pores as  $5$  mm. The porous architecture of the polymer substrates increased the exposed surface area by about  $14\%$ .

The roughness of the glass surface and PLGA substrates was evaluated with SPM. The analyzed area ( $0.5$  mm  $\times$   $0.5$  mm) for

PLGA revealed an intermittently textured area with prominent outgrowths not greater than  $3.9$  nm in height over the substrate base (Fig. 2A). Further, the calculated roughness depicted smaller features distributed about  $10$  nm apart. In comparison, the SPM image of glass showed significantly greater surface roughness with frequent protrusions extending up to  $10$  nm in height (Fig. 2B).

Further, we analyzed free active carboxyl groups using titrimetric analysis of the polymer surfaces which revealed higher surface carboxylic acid content on 3DIS substrates compared to smooth substrates ( $\sim 30\%$  for PLA and  $\sim 33\%$  for PLGA). PS substrates do not carry free carboxyl groups. It was determined that the test materials, PS, PLA and PLGA were chemically and physically stable against surface sterilization techniques such as exposure to  $70\%$  ethanol/isopropyl alcohol solution and UV radiation ( $1 \frac{1}{4}$   $253.7$  nm) for  $30$  min. Similarly, 3DIS and smooth polymer substrates immersed in cell culture media at pH  $7.4$  for a period of  $30$  days failed to demonstrate substrate fractures or

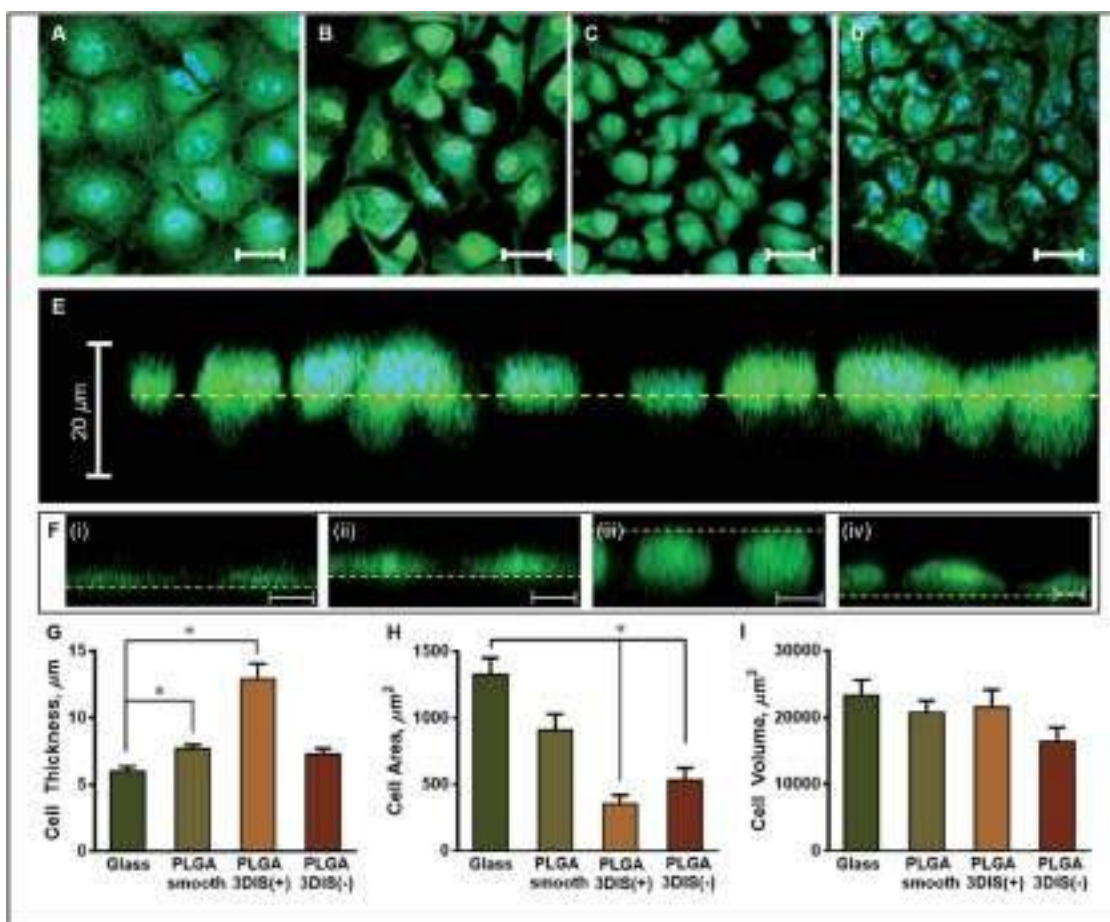


Fig. 3 Influence of substrate geometry on A549 cell morphology. Fluorescent confocal microscopy images of fluorescein isothiocyanate (FITC) labeled cytoplasm (green) and nuclear DAPI (blue) in A549 cells on (A) glass, (B) the PLGA smooth film, (C) PLGA 3DIS(+), and (D) PLGA 3DIS(−) substrates after 48 h; scale bar indicates 5 mm length. (E) Enlarged orthogonal confocal view of A549 cells on PLGA 3DIS; scale bar indicates 20 mm. (F) Orthogonal sections of confocal microscopy images depicting cell morphology behavior on (i) glass, (ii) PLGA smooth, (iii) PLGA 3DIS(+) and (iv) PLGA 3DIS(−) surfaces. The green mass is a representative orthogonal view of the cytoplasm of the attached cell. Scale bar indicates 10 mm. Morphological features such as (G) thickness, (H) area, and (I) volume of A549 cells grown on glass and various PLGA microarchitecture substrates. The yellow dotted lines across the images demarcates the top surface of the pore. \* represents statistical significance,  $p < 0.0001$ .





physical deformation, indicating polymer resistance against mechanical degradation.

### Wettability

As Fig. 2C depicts, with an increasing range of pore sizes (1 mm to 18 mm), PLGA demonstrated a decreased contact angle ( $\theta$ ) from  $92.67 \pm 2.52^\circ$  to  $68.67 \pm 1.53^\circ$ . Similarly,  $\theta$  for PS at the 1–5 mm pore size was  $104.33 \pm 1.53^\circ$  which lowered to  $75.33 \pm 2.52^\circ$  for the 6–10 mm pore size and further decreased to  $64.0 \pm 1.53^\circ$  for the 12–18 mm pore size range. Interestingly, the PLA substrate did not display a strong correlation between pore size and wettability and  $\theta$  ranged between  $100.13 \pm 2.87^\circ$  to  $90.84 \pm 3.90^\circ$  for the entire pore size range (1 mm to 18 mm).

### PLGA DOX release study

Pretreatment of DOX on PLGA 3DIS followed by cell media immersion revealed a cumulative DOX release profile depicting a biphasic trend suggesting a more rapid drug release in the first six hours ( $\sim 36\%$ ) followed by a steady slower release up to  $\sim 66\%$  in 48 h (Fig. S2A<sup>†</sup>).

### 3DIS architecture mimics *in vivo* cancer cell microenvironment

Morphological analysis and polymer biocompatibility evaluation. A549 cell spreading was maximum on the glass surface ( $1329 \pm 122.11 \text{ mm}^2$ ) compared to all test surfaces, evaluated after 48 h of incubation (Fig. 2D). Cell thickness was the greatest in PLGA 3DIS ( $10.12 \pm 0.92 \text{ mm}$ ) followed by PLGA smooth substrates ( $7.7 \pm 0.282 \text{ mm}$ ), whereas cells on glass were the least thick ( $6.4 \pm 0.35 \text{ mm}$ ). Among the three polymers studied, the PLGA-smooth surface demonstrated a notably large cellular area ( $867.69 \pm 52.31 \text{ mm}^2$ ), compared to PLA ( $207.59 \pm 16.77 \text{ mm}^2$ ) and PS ( $280.85 \pm 38.73 \text{ mm}^2$ ). The biocompatibility of PLGA for A549 cell proliferation was determined by the statistically similar cell viability on PLGA 3DIS (86.26%) and PLGA smooth (90.01%) compared to that of A549 control cells cultured on glass (Fig. 2E).

Influence of substrate geometry on morphology. A549 cells were cultured on glass, PLGA smooth substrates, PLGA 3DIS(+) and 3DIS(–) (Fig. 3A–D). Fig. 3E demonstrates the enlarged orthogonal confocal view of A549 cells on PLGA 3DIS(+). Culturing on PLGA 3DIS(+) surfaces virtually doubled the thickness of the cells, compared to cells grown on glass, PLGA smooth and 3DIS(–) surfaces as depicted in the orthogonal projections in Fig. 3F(i–iv).

The orthogonal confocal sectioning of cells on the glass surface (ESI video 1<sup>†</sup>) highlighted a thinner spreading of the attached cells (cell height  $\sim 6.4 \pm 0.35 \text{ mm}$ ), whereas the orthogonal section of PLGA smooth substrates revealed a raised cell profile with an increased cell thickness ( $7.7 \pm 0.28 \text{ mm}$ ) (Fig. 3G). The sub-surface cytoplasmic regions appeared nestled inside the pores. The cells on PLGA 3DIS(+) displayed up to 18 mm thickness with an average cell thickness of  $12.9 \pm 1.15 \text{ mm}$  (ESI video 2<sup>†</sup>). The quantification of the cellular area on the glass surface after 48 h revealed a significant cytoplasmic area ( $1329.68 \pm 122.11 \text{ mm}^2$ ) while the dorso-ventrally flattened

nucleus was  $241 \pm 12 \text{ mm}^2$ . Phalloidin stained actin filaments spanned the volume of the cell attached on the glass cover slip, and the dense terminal protrusions of the actin filaments indicate the cell adhesion points (Fig. S2B<sup>†</sup>). However, A549 cells on PLGA smooth substrates demonstrated comparatively reduced cellular spreading area with cellular projections indicating substantial cell adhesion (Fig. 3H).

On 3DIS(–) substrates, the cells appeared to have little to no access to the depth of the pores, resulting in cells spreading over the porous structures with cytoplasmic area  $\sim 533.6 \pm 91.08 \text{ mm}^2$  and a corresponding cell thickness of  $\sim 7.3 \pm 0.41 \text{ mm}$  (ESI video 3<sup>†</sup>). The surface area of the cells on PLGA 3DIS(+) was sharply reduced, and compared to glass and PLGA smooth, the decrease in area was  $\sim 74\%$  and  $\sim 60\%$  respectively. The cells cultured on glass and PLGA-smooth substrates showed statistically similar cellular volume ( $23 \pm 424 \pm 2243.40 \text{ mm}^3$  and  $20 \pm 798 \pm 1729.90 \text{ mm}^3$  respectively) (Fig. 3I). PLGA 3DIS(+) cells showed the maximum thickness which compensated for the gross decrease in cell area and consequently the cells grown on glass, PLGA smooth and PLGA 3DIS(+) surfaces were statistically comparable with cell volumes varying between  $23 \pm 424 \pm 2243.40 \text{ mm}^3$  to  $21 \pm 618 \pm 2601.03 \text{ mm}^3$ .

3DIS as a cell repair/regeneration platform. A549 cells cultured on PLGA 3DIS substrates over 48 h showed a confluence similar to that seen in culture flasks or on glass.

The cells showed a tendency to occupy 3DIS evenly and to form monolayers, bridging the pore gaps (ESI video 4<sup>†</sup>). As depicted in Fig. 4A–D, the ability of the 3D (spatially restored) cells in bridging small ( $\sim 15 \text{ mm}$ ) gaps was demonstrated. In Fig. 4F, as few as two cells were shown capable of bridging a micro-gap and forming cell–cell and cell–substrate adhesions.

Multiple cells are shown to fill the large ( $\sim 65 \text{ mm}$ ) pores in Fig. 4G and H effectively demonstrating the ability of PLGA 3DIS in allowing cells to grow spatially and create cell–cell adhesions as well. The 3DIS pore-rims serve as foot and hand holds for cells (Fig. 4G and H).

Influence on the drug-cellular response by cancer cell morphology. The DOX treatments conducted in this study

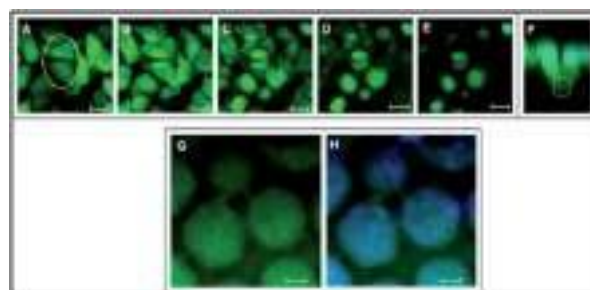


Fig. 4 PLGA 3DIS as a tissue cell repair/regeneration platform. (A–E) Confocal microscope images of the z-planes of PLGA 3DIS(+) showing the convergence of two A549 cells to fill a 3DIS pore at the 48 h time point; (F) orthogonal view depicting cell–cell adhesion in 3DIS bridging the pore gap; scale bar indicates 15 mm. (G) Fluorescence microscope image of A549 cells in 3DIS with  $\sim 50 \text{ mm}$  diameter, demonstrating confluence of cells after 7 days. (H) Composite image with DAPI indicates the presence of multiple cells; scale bar indicates 20 mm.



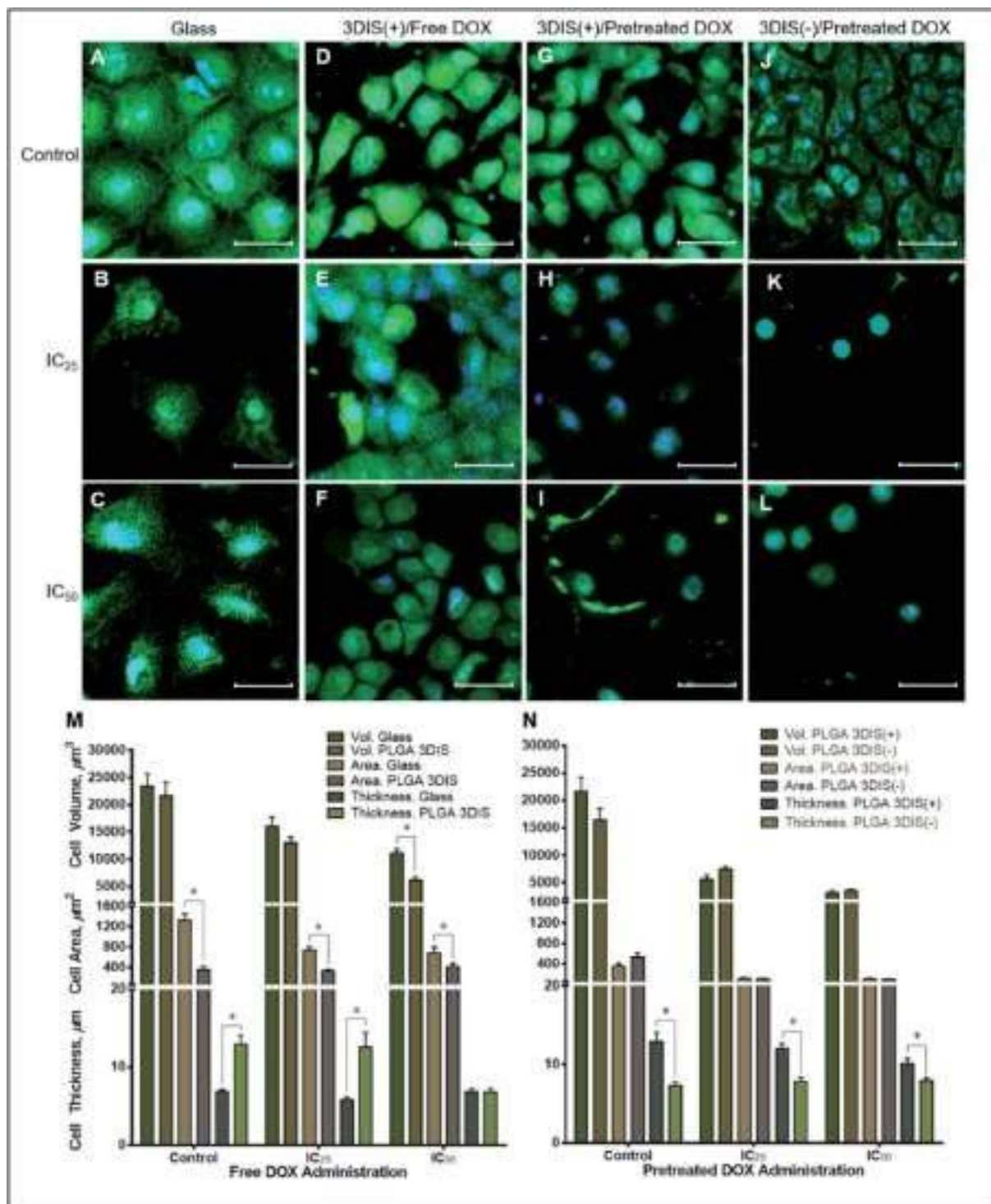


Fig. 5 Influence on DOX-cellular responses by A549 cell morphology alterations on glass and PLGA 3DIS. A549 cells cultured on (A) a glass surface (control) and further exposed to (B) an  $IC_{25}$  DOX dose and (C) an  $IC_{50}$  DOX dose. (D–F) Cells grown on PLGA 3DIS(+), (G–I) cells grown on a pre-existing DOX microenvironment, (J–L) cells grown on a 3DIS(–) control. All the confocal images were taken at the 48 h time point. FITC (green) stained the cytoplasm and DAPI (blue) stained the nucleus. Scale bar indicates 20  $\mu$ m. Comparison of (M) cell volume, cell area and cell thickness on glass and PLGA 3DIS surfaces upon treatment with  $IC_{25}$  and  $IC_{50}$  doses of DOX in PLGA 3DIS. \* represents statistical significance,  $p < 0.001$ . (N) 3DIS pore size influenced DOX-cell interaction. Cell volume, area and thickness are depicted for PLGA 3DIS(+) and PLGA 3DIS(–). \* indicates statistically significant difference,  $p$  value  $< 0.01$ .

utilize the experimentally determined  $IC_{50}$  value of 0.26 mM and the mathematically derived  $IC_{25}$  (0.13 mM) determined in a planar cell culture of A549 cells. For comparative purposes,

these concentrations have been kept constant across the different substrates. Based on the experimental results (Fig. S3†) the cell viability determined for the  $IC_{50}$  dose on



various substrates was found to be virtually similar, suggesting that the DOX  $IC_{50}$  dose determined for planar cultures was equivalent to the dose required to demonstrate  $IC_{50}$  lethality even in 3DIS substrates. Fig. 5A–L show the confocal images of A549 cells grown on glass substrates, PLGA 3DIS(+) and 3DIS(–), which were further subjected to DOX administration in cell media conforming to the  $IC_{50}$  and sub-lethal  $IC_{25}$  concentrations. Fig. 5A demonstrates the extensive spreading of A549 cells on the glass plane; the cells also showed evidence of cell projections connecting with the glass plane and neighboring cells as well. The cell viability assay showed 47% to 50% cell viability on PLGA 2D and 3DIS substrates when exposed to an  $IC_{50}$  concentration of DOX as determined on the glass-surface cell culture. The drug concentrations were used considering the cell viability established in the literature and by us (Fig. S3†).

During the course of treatment with DOX, the cells maintained a  $\Delta$  at pro  $IL_6$  (5.79  $\pm$  0.37 mm at  $IC_{25}$  and 6.88  $\pm$  0.34 mm at  $IC_{50}$ ) and demonstrated lateral spreading (Fig. 5M). When exposed to sub-lethal doses ( $IC_{25}$ ) of DOX, there appeared to be a mild decrease in the size of the cells (741.07  $\pm$  61.90  $\mu m^2$ ) with a general reduction in the number of cellular projections. A higher DOX concentration ( $IC_{50}$ ) in the cell media appeared to decrease the cell area further (679.83  $\pm$  117.68  $\mu m^2$ ) with a subtle shrinking effect on the nucleus.

Cell volume was reduced by about 30% in sub-lethal doses of DOX while  $IC_{50}$  caused a roughly 50% drop in cell volume. The cell area also significantly decreased due to DOX exposure compared to the control but not significantly between the two drug treatments (pretreated DOX,  $IC_{25}$  by  $\sim$ 44% and  $IC_{50}$  by  $\sim$ 48%) suggesting a near-maximal effect at  $IC_{25}$ . Interestingly, cells on PLGA 3DIS(+) dosed with a sub-lethal ( $IC_{25}$ ) DOX concentration did not demonstrate a significant change in cell area and cell thickness compared to the control. However, upon exposure to the  $IC_{50}$  dose of DOX the cells demonstrated a reduction in cell size such as volume (3548.57  $\pm$  220  $\mu m^3$ ) and height (7.927  $\pm$  0.37 mm). Additionally, the nuclei appeared to be proportionally shrunk.

Influence of 3DIS dimensions on cancer cell morphology and cell responses. The dependence upon pore size of the 3DIS system was also demonstrated for the cytotoxicity of the pretreated DOX (Fig. 5N). Interestingly, with pre-treatment of DOX for 48 h on 3DIS(–), the cells were unable to undergo significant size swelling (cell thickness  $\sim$ 7.83  $\pm$  4.90 mm and  $\sim$ 7.92  $\pm$  3.7 mm for  $IC_{25}$  and  $IC_{50}$  DOX treatments, respectively) and cell spreading (cell area  $\sim$ 116.50  $\pm$  8.71  $\mu m^2$  and 101.27  $\pm$  9.83  $\mu m^2$  for  $IC_{25}$  and  $IC_{50}$  DOX treatments, respectively). Fig. 5G–L depicts the morphological differences in cells within the two pre-treatment groups; while the volume and cell area parameters were comparable, there was a significant retention of lowered cell thickness over the drug course in the 3DIS(–) cells.

## Discussion

Enhanced adhesion along a single plane may not allow true spatial freedom for cell growth and the cell may likely compensate for the loss of 3D cell architecture by spreading

laterally. On the other hand, planar cell attachment substrates consequently may not mimic the physiological responses in the cancer cell microenvironment. Thus, the mechanism by which cells conform to available spaces and geometry and the specific role of the void spaces in enabling cell attachments and proliferation needed elucidation.

Spatial availability within tissues may likely result in tissue expansion *via* cell reorganization or multiplication; however, the availability may not be perceived in a similar fashion in conventional cell culture systems. As depicted in Fig. 1, the unrestricted space around the cells conforming to 180° for a glass surface and 360° spatial freedom for the illustrated 3D culture system respectively, appeared conducive for spatial growth; however, cells reliant on surface adhesion components were paradoxically bound to and spread along the available surface. However, restriction in 3DIS spaces with  $<180^\circ$  of spatial freedom provided cell adhesion opportunities across the available perimeter in 3DIS. Such spatial confinements prevented planar cell adhesion localization and allowed the cells to grow in 3D spaces and have a raised profile.

In consequence, the cell and its organelles such as the nucleus, remained free of the stress fiber mediated compression which in turn restored the *in vivo* physiological behavior of cells. 3DIS is thus an interesting and competent model to study *in vivo* cell growth patterns, and in addition, it was appropriate to interpret cell morphology behavior on exposure to cytotoxic drugs.

Subsequently, PS, PLA and PLGA polymer substrates were fabricated with 3DIS architecture and subjected to numerous physicochemical characterization experiments to determine their compatibility with A549 spatial cell growth. PLGA 3DIS substrates underwent SPM analysis and the depicted texture in Fig. 2A was hypothesized to span the substrate top surface and pore surface and provide adhesion support to adherent cells. The large protuberances were an indication of a potential cell adhesion site, with an average cell area of  $\sim$ 400  $\mu m^2$  (on PLGA 3DIS); it followed that a cell had access to a large number of adhesion-competent sites on PLGA substrates. However, SPM analysis of the glass surface demonstrated frequent outgrowths with greater height than in the PLGA topography. Thus, the glass surface promoted higher affinity of cells with abundant cell adhesion features and significantly increased the cell surface area, owing to the presence of highly uneven surface topography.

It was noted that PLGA and PS had lower contact angles in the pore size range of 12–18  $\mu m$ , which indicated higher wettability. Thus, PLGA and PS polymers were inferred to possess higher apparent affinity for cells compared to PLA which was evident for the measured cell surface area (Fig. 2). All cell studies on glass and polymer surfaces were reported *in vitro* 48 h incubation period for both morphology analysis and DOX treatment studies. An abundance of the hydrophilic surface area and compatible functional groups on the glass surface lead cells such as A549 and HeLa (data not shown) to demonstrate significant cellular spreading. Among the polymers, PS smooth substrates demonstrated cell attachment and spreading inferior to PLGA and glass surfaces.





The lower wettability of PLA likely reduced its utility in promoting cell adhesion and spreading making PLA the least favorable cell substrate among the materials under study. However, the greater hydrophilicity of PLGA, partially due to glycolic acid content (25%), resulted in the greater cell affinity of PLGA compared to PS or PLA. Owing to its superior selective cell adhesion trait, PLGA was identified in this study to further investigate 3DIS-cell behavior.

The ordering of spatial organization of the polymer substrate with regard to generation of 3DIS led to significant changes in cell morphology. In comparison to glass-bound A549 cells, cells cultured on PLGA substrates for 48 h displayed varied morphological signatures depending on the substrate geometry. Unlike glass, PLGA smooth substrates offered relatively less cell adhesive or retentive surface chemistry, leading to less dense cellular confluence. Indeed, a surface retraction of cells on PLGA smooth substrates was apparently compensated by increased cell thickness. For example, the orthogonal section in 3DIS(−) despite their restricted spatial confines allowed the cell to articulate with the adjoining pore walls and form adhesive junctions to act as anchors (Fig. 3). Conversely, since the cell adhesion features were distributed in 3D spaces within the 3DIS, there was conceivably a relaxation of the net-downward force, allowing the cell to grow while maintaining a tall profile, compared to a flattened profile seen on glass-bound cells.

Furthermore, the inter-pore substrate surface was limited in area, likely causing the cells to utilize the pores as additional cell adhesion surfaces. Specifically, as shown in Fig. 3, the cells were observed seated on the substrate surface (dotted line) while a portion of the cells appeared below the surface level. Thus in a controlled environment without drug pressure, cells demonstrate the ability to maintain a specific volume, comprising of both cytoplasmic and organelle volumes. While the volume of cells on glass, PLGA smooth and PLGA 3DIS(+) seemed invariable, cellular areas of cells on PLGA smooth and PLGA 3DIS(+) showed a marked decrease. In contrast, the cell height showed an opposing trend and showed increasing values when grown on PLGA smooth and PLGA 3DIS.

Besides allowing cells, in principle, to bear a more physiologically relevant phenotypical form, the 3DIS also generated a platform to explore cellular regeneration across simulated gaps (pores). The ability of the epithelial cells in wound closure was investigated by observing the cells adhere to the pore, spatially adapt or multiply, thereby filling the pore cavity (Fig. 4). PLGA 3DIS with tunable pore sizes presented an appropriate model of small tissue gaps or wounds which was exploited to determine the regenerative abilities of cells or co-cultures. The adhesion feature demonstrated here provided a platform upon which tumor models maybe developed as well. PLGA 3DIS demonstrated the ability to mimic cells in their near *in vivo* morphology; thus, further experiments involved comparison of the drug effect on cells on 3DIS and on standard 2D cultures to determine if the cells were altered with changes in their morphology and if these changes depicted *in vivo* outcomes.

On the other hand, we did not use collagen coating which may effectively nullify the polymeric 3DIS geometrical advantages seen in uncoated 3DIS substrates, presumably by enhanced cell attachment. Thus, we studied the interactions of A549 cells with the polymer substrate without the interfering influence of extra-cellular matrix (ECM) components. Furthermore, collagen and fibronectin may eliminate the localized surface charges of 3DIS polymer substrate structures, decrease the influence of 3D substrates and finally reduce the 3D inverse spaces milieu.

DOX was used in this study to contrast the difference in the drug effect on cells grown on different attachment substrates which manipulated cell morphology. The effect of DOX treatment on cells grown on glass and PLGA 3DIS revealed a complex interplay of the morphological features which were shown in the confocal microscopy images of cells depicted in Fig. 5; the cells cultured on glass serve as global controls. Various cell parameters such as thickness, surface area and volume were measured and the differences were depicted graphically. The parameters of cellular area (cytoplasmic area) and cell thickness (height) were considered distinct dimensions whereas cell volume was reliant on area as well as cell thickness. This phenomenon was restricted to the spatially-restored cells on 3DIS substrates and suggested a varied pharmacokinetics/pharmacodynamics balance as compared to control cells on 2D culture surfaces (glass). It may be inferred that the 3DIS(+) cells were more resistant to DOX than the results of DOX treatment on glass-bound cells suggested. The 3DIS platform exhibited cell adhesion and growth in the context of drug kinetics and activity in the cell microenvironment that was otherwise complicated to simulate in 2D cultures. The effect of altered cell morphology on the sensitivity to cytotoxic drugs was also explored; the greater surface area of cultured cancer cells on planar surfaces may likely enhance the capacity of xenobiotic uptake *via* multiple pathways including receptor mediated endocytosis *etc.*<sup>15</sup>

When considered in conjugation with upregulated drug efflux pumps in cancer cells, the 2D planar cell culture model presents a complex transport system which allows a rapid internalization and rapid efflux of the administered molecule.<sup>20,21</sup> However such models are not expected to provide a true kinetic profile for an administered compound in the given context. Consequently, cells with lesser deviation from their *in vivo* cell structure were preferred with limited surface area and a more elevated 3D profile. It was likely that 3DIS(+) allowed cells to briefly adapt spatially despite drug pressure due to the close proximity of the 3DIS walls leading to cell elongation in the vertical aspect. The behavior of cells in the pre-treated DOX context was explained by the slow release of DOX from the substrate as depicted in Fig. S2A.† The rapid release of DOX in the initial six hours was expected from rim-surface and surrounding area-accumulated DOX, whereas the slower release over 48 h was likely the result of DOX slowly diffusing out of pores (from the extended surface area as described earlier by eqn (1)). The slow drug release into the cell media retains the drug in the immediate substrate vicinity leading to a pronounced cytotoxic effect.



Indeed, the utility of optimized inhibitory anticancer drug concentrations at the local site produced a far more pronounced anticancer effect than that due to drug-infused media with comparable drug content. The phenomenon depicted a failure in attachment of cancer cells to the substrate in addition to cumulative drug pressure over time. It was conceivable that such a strategy might prevent the attachment and survival of cancer cells at a given tissue site; stated differently, it might imply prevention of metastasis at secondary sites if prophylactically treated in a site-specific manner. With a reduced cell surface area, it was likely that the drug uptake mechanisms were unable to counteract the activity of drug efflux pumps which resulted in reduced overall cytotoxicity. The results implied that reduced systemic DOX content in the body would result in potential failure of anticancer activity and allow cancer growth and even metastasis. Further, low blood drug concentrations might occur due to termination of chemotherapy.

In contrast, the presence of localized content of DOX, simulating  $IC_{50}$  drug content in the tissue as opposed to systemic circulation may generate a potent cytotoxic environment for cancer cells.  $IC_{50}$  and sub-lethal  $IC_{25}$  DOX concentrations were applied directly to PLGA 3DIS substrates instead of cell media dispersion and the pre-treated 3DIS was used to culture A549 cells. The presence of a localized, pre-existing drug environment strongly deterred the growth and spreading of cells in both sub-lethal and  $IC_{50}$  drug contents as evidenced in Fig. 5. The cells appeared to be shrunk with an apparently reduced cytoplasmic compartment.

The toxicity of the treatment resulted in a very small number of viable but near-apoptotic cells. Cell volumes were drastically affected for both drug treatments with a roughly 8-fold drop determined for  $IC_{50}$ -treated cells compared to the control. The cell height showed a modest drop for the sub-lethal dose and  $IC_{50}$  treatments, which resulted from the severe shrinkage of volume. It was likely that upon DOX treatment the freshly seeded cells on the PLGA 3DIS were unable to adapt to the substrate and consequently failed to adhere fully and spread. As a result, the cells retained their round shape and likely failed to deploy cytoskeletal scaffolding to attach and spread, in addition to undergoing cytotoxic damages, which were more pronounced for  $IC_{50}$  treated cells. It followed that localized  $IC_{50}$  and even the sub-lethal  $IC_{25}$  dose, administered as pretreatment upon the 3DIS, were far more effective in eliciting the cytotoxic activity of DOX in A549 cells than free DOX administration in the cell media. Overall, anticancer therapy often fails in achieving complete tumor regression due to sub-lethal dose concentrations and the cells that survive following the therapy continue to survive.<sup>22</sup> Here we demonstrated the *ex vivo* effect using polymeric 3DIS substrates.

## Conclusions

Upon comparison of PS, PLA and PLGA as 3DIS substrates, PLGA presented a viable 3DIS platform for the study of cancer cells in a near-*in vivo* morphological context. The ability of A549 cells to defend their cytoplasmic volume across glass and PLGA

substrates strongly suggested the biocompatibility of PLGA in the composition of 3DIS, which is supported by the viability assay comparing the substrates. The superior cellular affinity, as evidenced by cell spreading, allowed PLGA to support spatial growth in the confines of 3DIS. The results presented here highlighted the behavior of A549 cells in the 3DIS culture in mimicking physiological responses. While the 3DIS architecture was central to altering cell morphology, it also presented a discontinuous surface mimicking broken tissue membranes. PLGA 3DIS served as an appropriate tissue repair model to study epithelial cell growth and gap-bridging as an index of tissue repair/regeneration. The A549 cells were shown to grow rapidly to fill a larger pore thereby forming a continuous cell monolayer bridging the gap.

The evidence of morphological changes influencing cellular responses was demonstrated in the DOX study of cells grown on PLGA 3DIS. Compared to the PLGA 3DIS control, cells exposed to a sub-lethal  $IC_{25}$  DOX dose were undeterred. The study indicated a sustained  $IC_{50}$  dose strategy to elicit a noticeable anticancer (cytotoxic) effect. With its abnormal flattened morphology, cancer cells on glass lacked the physiological integrity to depict realistic *in vivo* responses to drugs. Similarly, the pre-treatment of DOX on the 3DIS illustrated its ability to mimic alternative drug dosing conditions which were more successful in tempering the cancerous growth of cells and in inhibiting their spread and survival altogether.

Advanced strategies can be adapted for use with 3DIS such as the use of flow-through analytical chambers with embedded PLGA 3DIS for real time monitoring of spatially restored cells, essentially mimicking entire tissues.

## Conflicts of interest

There are no conflicts to declare.

## Acknowledgements

Authors would like to acknowledge the financial support of DBT-Nano-Biotechnology, DST-FIST and DST-Nano Mission, Government of India.

## Note and references

- 1 P. X. Ma and J. W. Choi, *Tissue Eng.*, 2001, 7, 23–33.
- 2 S. Yang, K. F. Leong, Z. Duo and C. K. Chua, *Tissue Eng.*, 2001, 7, 679–689.
- 3 R. Zhang and P. X. Ma, *J. Biomed. Mater. Res.*, 1999, 45, 285–293.
- 4 C. C. Liang, A. Y. Park and J. L. Guan, *Nat. Protoc.*, 2007, 2, 329–333.
- 5 M. Mirbagheri, V. Adibnia, B. R. Hughes, S. D. Waldman, X. Banquy and D. K. Hwang, *Mater. Horiz.*, 2019, 6, 45–71.
- 6 Y. Xia, *Nat. Mater.*, 2008, 7, 758.
- 7 A. S. Curtis, J. V. Forrester, C. McInnes and F. Lawrie, *J. Cell Biol.*, 1983, 97, 1500–1506.



- 8 A. PrinaMello, N. Jain, B. Liu, J. I. Kilpatrick, M. A. Tutty, A. P. Bell, S. P. Jarvis, Y. Volkov and D. Movia, *Tissue Cell*, 2018, 50, 15–30.
- 9 H. J. Mulhall, M. P. Hughes, B. Kazmi, M. P. Lewis and F. H. Labeed, *Biochim. Biophys. Acta, Gen. Subj.*, 2013, 1830, 5136–5141.
- 10 R. Domura, R. Sasaki, Y. Ishikawa and M. Okamoto, *J. Funct. Biomater.*, 2017, 8, 18.
- 11 M. Ferrari, F. Cirisano and M. C. Morán, *Colloids Interfaces*, 2019, 3, 48.
- 12 J. Rosales-Leal, M. Rodríguez-Valverde, G. Mazzaglia, P. Ramón-Torregrosa, L. Díaz-Rodríguez, O. García-Martínez, M. Vallecillo-Capilla, C. Ruiz and M. Cabrerizo-Vílchez, *Colloids Surf., A*, 2010, 365, 222–229.
- 13 R. Fernandez-Gonzalez and J. A. Zallen, *Cell*, 2012, 149, 965–967.
- 14 K. Pietras and A. Östman, *Exp. Cell Res.*, 2010, 316, 1324–1331.
- 15 I. Levinger, Y. Ventura and R. Vago, *Advances in Cancer Research*, ed. K. D. Tew and P. B. Fisher, Academic Press, 2014, vol. 121 pp. 383–414.
- 16 B. Alberta, J. Lewis, K. Roberta, A. Johnson, M. Raff and P. Walter, *Molecular Biology of the Cell*, Garland Pub, USA, 2008.
- 17 B. Young, P. Woodford and G. O'Dowd, *Wheater's Functional Histology E-Book: A Text and Colour Atlas*, Elsevier Health Sciences, 2013.
- 18 H. Battenbo, R. Copley and S. Wilks, *Soft Matter*, 2011, 7, 10864–10873.
- 19 O. Karthaus, N. Maruyama, X. Cieren, M. Shimomura, H. Hasegawa and T. Hashimoto, *Langmuir*, 2000, 16(15), 6071–6076.
- 20 M. M. Gottesman, T. Fojo and S. E. Bates, *Nat. Rev. Cancer*, 2002, 2, 48–58.
- 21 J. P. Gillet and M. M. Gottesman, *Multi-Drug Resistance in Cancer*, ed. J. Zhou, Humana Press, Totowa, NJ, 2010, pp. 47–76.
- 22 S. Nandi, N. R. Kale, V. Takale, G. C. Chate, M. Bhave, S. S. Banerjee and J. J. Khandare, *J. Mater. Chem. B*, 2020, 8(9), 1852–1862.



OPEN

# Self-Propelling Targeted Magneto-Nanobots for Deep Tumor Penetration and pH-Responsive Intracellular Drug Delivery

Saloni S. Andhari<sup>1,4</sup>, Ravindra D. Wavhale<sup>2,4</sup>, Kshama D. Dhobale<sup>2</sup>, Bhausaheb V. Tawade<sup>2</sup>, Govind P. Chate<sup>2</sup>, Yuvraj N. Patil<sup>2</sup>, Jayant J. Khandare<sup>3\*</sup> & Shashwat S. Banerjee<sup>2\*</sup>

Self-propelling magnetic nanorobots capable of intrinsic-navigation in biological fluids with enhanced pharmacokinetics and deeper tissue penetration implicates promising strategy in targeted cancer therapy. Here, multi-component magnetic nanobot designed by chemically conjugating magnetic Fe<sub>3</sub>O<sub>4</sub> nanoparticles (NPs), anti-epithelial cell adhesion molecule antibody (anti-EpCAM mAb) to multi-walled carbon nanotubes (CNT) loaded with an anticancer drug, doxorubicin hydrochloride (DOX) is reported. Autonomous propulsion of the nanobots and their external magnetic guidance is enabled by enriching Fe<sub>3</sub>O<sub>4</sub> NPs with dual catalytic-magnetic functionality. The nanobots propel at high velocities even in complex biological fluids. In addition, the nanobots preferably release DOX in the intracellular lysosomal compartment of human colorectal carcinoma (HCT116) cells by the opening of Fe<sub>3</sub>O<sub>4</sub> NP gate. Further, nanobot reduce *ex vivo* HCT116 tumor spheroids more efficiently than free DOX. The multicomponent nanobot's design represents a more pronounced method in targeting tumors with self-assisted anticancer drug delivery for 'far-reaching' sites in treating cancers.

Designing miniaturized and versatile robots in the dimensional-range of a few micrometers or less offer potential for unprecedented biomedical applications, such as refinements in targeted drug delivery platforms<sup>1-7</sup>. Miniature robotic systems provide considerable benefits over conventional and micro/nanoparticle-based therapies<sup>8,9</sup>. Existing anticancer drug delivery systems demonstrate pharmacokinetic (PK) limitations as they are passive systems driven by the blood fluidics and lack intrinsic navigation for long circulation time, targeting, localized delivery, and tissue penetration<sup>10,11</sup>. Furthermore, despite surface functionalization with a specific ligand that allows nanocarriers to increase the active targeting ability; the nanocarriers are unable to guide themselves to a target. Hence, for targeted anticancer delivery of therapeutic payloads to disease sites, drug carriers are desired to possess some distinctive traits, including self-propelling force and velocity, navigational functions, precise cell targeting, drug cargo-towing and finally tissue penetration with the release of drug payload<sup>12-16</sup>.

Micro/nanomotors with efficient cargo towing and effective penetrating abilities make them excellent delivery vehicles that can meet the necessary features for targeted delivery of therapeutics<sup>6</sup>. Chemically propelled micro-/nanorobots have been widely explored for active drug delivery, and tremendous progresses has been made in the past few years<sup>17</sup>. However, designing nanobots for biological functionality is still a challenge as they have some inherent limitations, such as complex preparation technology, difficulty of surface modification, difficulty of motion in biological fluids and depending on the material, poor biocompatibility or biodegradability<sup>6,18,19</sup>. Furthermore, none of the reported micro/nanobot system has demonstrated practically useful speed high enough for biomedical applications due to high-speed blood flow in human arteries (dimensions from 4 to 25 mm) with a blood flow velocity from 100 to 400 mm/s<sup>20</sup>.

Herein, we report for the first time a smart H<sub>2</sub>O<sub>2</sub> and pH-responsive nanobot system to transport anticancer drug deep inside the three dimensional (3D) tumors by exploiting Fe<sub>3</sub>O<sub>4</sub> dependent decomposition of H<sub>2</sub>O<sub>2</sub>

<sup>1</sup>Maharashtra Academy of Engineering Education and Research's Maharashtra Institute of Pharmacy, Pune, 411038, India. <sup>2</sup>Maharashtra Institute of Medical Education and Research, Talegaon Dabhade, Pune, 410507, India. <sup>3</sup>School of Pharmacy, Dr. Vishwanath Karad MIT World Peace University, Pune, 411038, India. <sup>4</sup>These authors contributed equally: Saloni S. Andhari and Ravindra D. Wavhale. \*email: [jayant.khandare@mippune.edu.in](mailto:jayant.khandare@mippune.edu.in); [shashwatbanerjee@mitmimer.com](mailto:shashwatbanerjee@mitmimer.com)



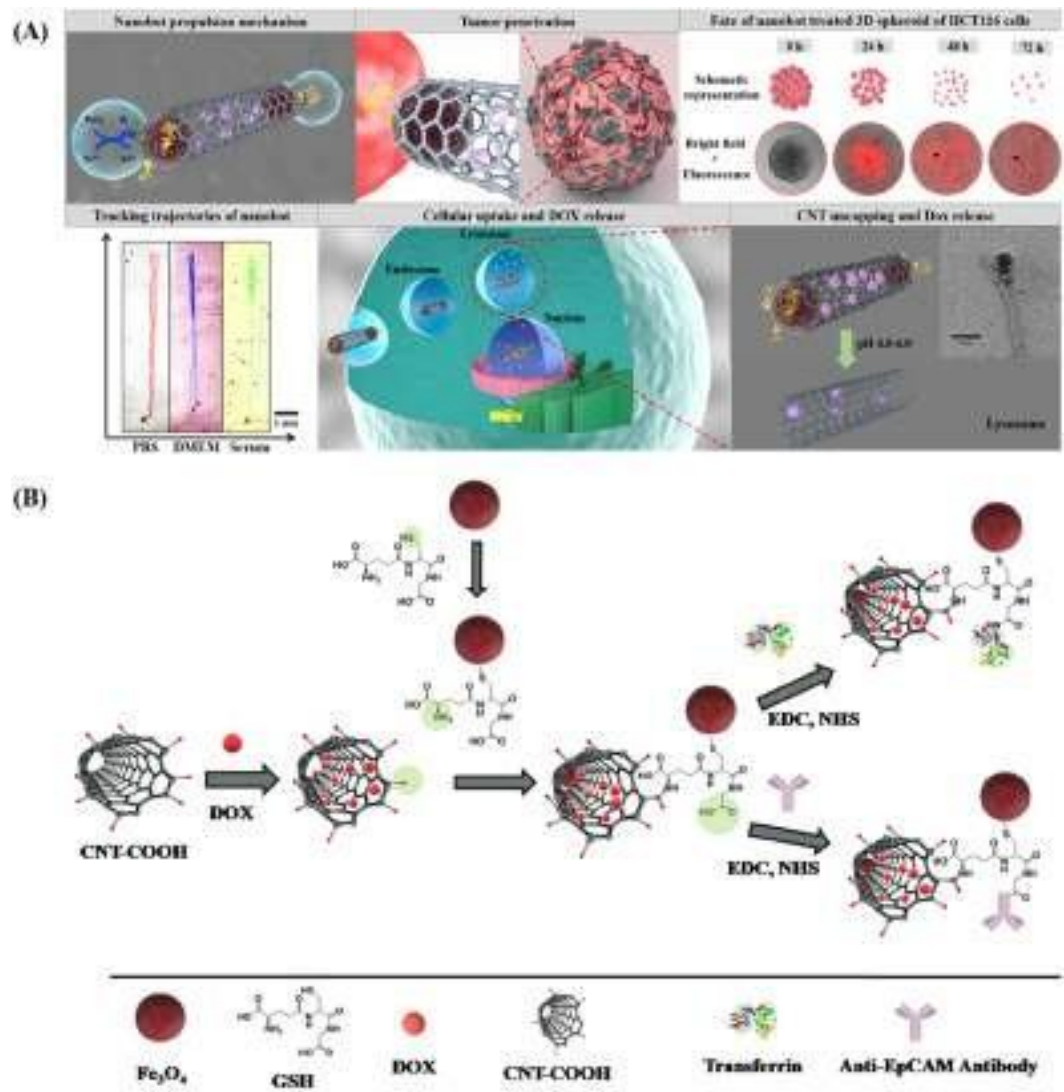


**Figure 1.** (A) Schematic representation of mechanism of oxygen bubble induced autonomous propulsion of nanobot and deep penetration in the tumor due to the generated thrust, fate of 3D spheroid treated with CNT-DOX-Fe<sub>3</sub>O<sub>4</sub>-Tf/CNT-DOX-Fe<sub>3</sub>O<sub>4</sub>-mAb nanobot, trajectories of nanobots in physiologically relevant media (trajectories obtained using Dino-Capture 2.0 v (<https://www.dino-lite.com/>), VirtualDub 1.10.4 v (<http://www.virtualdub.org/>) and MTrackJ plugin from ImageJ 1.8.0\_112v (<https://imagej.net/MTrackJ/>), followed by illustration of targeting DOX-loaded nanobot to transferrin/EpCAM receptor and entry in cancer cell, and finally, mechanism of triggered drug release under intracellular endo/lysosomal conditions. (B) Schematic illustration indicating the step-by-step synthesis of DOX loaded CNT-DOX-Fe<sub>3</sub>O<sub>4</sub>-Tf/ CNT-DOX-Fe<sub>3</sub>O<sub>4</sub>-mAb.

existing in the tumor microenvironment (TME) into water and oxygen. Tumor cells are known to produce H<sub>2</sub>O<sub>2</sub> at the rate of 0.5 nmol/10<sup>4</sup> cells/h<sup>21</sup>. The nanobot was designed by chemically coordinating Fe<sub>3</sub>O<sub>4</sub> NPs, conjugating anti-EpCAM mAb to carbon nanotubes (CNT) through reactive spacer glutathione (GSH) and loading of anticancer drug DOX. The unique advantages of anchoring Fe<sub>3</sub>O<sub>4</sub> NPs are, as they impart autonomous propulsion ability and superparamagnetic property to the nanobot system. Further they also impart mechanism of “on demand” intracellular release of the encapsulated DOX. Thus, the Fe<sub>3</sub>O<sub>4</sub> NP gates retard premature and non-specific release of DOX encapsulated in CNT thus minimizing therapy side effects. CNT platform was utilized as a carrier because it offers the benefit of chemical tunability, allowing integration of multiple component by conjugation chemistry including targeting moieties<sup>22</sup>. Importantly, functionalized CNTs have shown low toxicity and enhanced clearance, and even can be decomposed inside the human body<sup>23</sup>. CNTs with such advantages have been exploited to deliver various bioactive substances and contrasting agents. However, they have primarily been used as passive nanocarriers. Here, we have transformed passive CNTs into active autonomous nano-propelled-bots with controlled anticancer drug delivery platform, cellular specificity, targeting and deep 3D tumor penetration capability (Fig. 1A). Further, Fe<sub>3</sub>O<sub>4</sub>-catalyzed *in-situ* generation of oxygen from TME H<sub>2</sub>O<sub>2</sub> may also help in relieving tumor hypoxia with potential augmentation of antitumor influence.

The present work, demonstrates a nanobot drug delivery platform that facilitates propulsion in biological fluids, cellular targeting, modulates the intracellular release and enhanced penetration to TME for improved anti-cancer therapy.

## Results and discussion

**Antibody/Tf-targeted nanobot conjugation and characterization.** Tf and anti-EpCAM mAb conjugated nanobots were designed by multi-step chemical conjugation process (Fig. 1B). CNTs were first subjected to oxidation treatment to create abundant carboxylic groups mostly at the tips and defect sites of CNT surfaces. DOX was successfully encapsulated in the hollow CNTs (with inner diameter of ~11 nm) as the inner surface is hydrophilic, and aqueous solutions containing DOX can be loaded inside through the open ends. Here, we hypothesize that loading of DOX in CNTs will protect it from the early exposure to physiological milieu. Further, Fe<sub>3</sub>O<sub>4</sub> NP was conjugated to DOX loaded CNT through the GSH linker by the EDC coupling method. Thereafter, anti-EpCAM mAb was conjugated to the surfaces of CNT by EDC coupling reaction using the carboxyl groups on the CNT resulting in CNT-DOX-Fe<sub>3</sub>O<sub>4</sub>-mAb nanobots. Similarly, Tf was conjugated to the reactive surface of CNT resulting in CNT-DOX-Fe<sub>3</sub>O<sub>4</sub>-Tf nanobots. Tf protein has been used as a model targeting moiety to the cancer cells with overexpressed Tf receptors (TfR<sup>+</sup>).

Transmission electron microscope (TEM) images of CNT-DOX-Fe<sub>3</sub>O<sub>4</sub>-Tf nanobot revealed the presence of spherical Fe<sub>3</sub>O<sub>4</sub> NPs of average diameter ~16 nm at the tip ends of CNTs (Fig. 2A and Supplementary Fig. S1). Crystallographic structure of the Fe<sub>3</sub>O<sub>4</sub> NPs analyzed by high resolution TEM (HRTEM) showed magnetite crystalline nature (Fig. 2B). Furthermore, the identified lattice fringes co-related well to the structure of magnetite planes with a plane-to-plane separation of 0.486 nm. The Selected Area Electron Diffraction (SAED) pattern revealed spotty diffraction rings and well resolved spots thus confirming crystalline Fe<sub>3</sub>O<sub>4</sub> structure for the conjugated NPs (Fig. 2C).

The CNT-DOX-Fe<sub>3</sub>O<sub>4</sub>-Tf nanobot was also characterized by FTIR to verify the successful covalent conjugation between CNT, Fe<sub>3</sub>O<sub>4</sub> and Tf. Figure 2D shows the FTIR spectra of oxidized CNT, CNT-DOX, CNT-DOX-Fe<sub>3</sub>O<sub>4</sub> and CNT-DOX-Fe<sub>3</sub>O<sub>4</sub>-Tf, respectively. The IR spectrum of CNT showed characteristic peak at 1715 cm<sup>-1</sup> due to the presence of carbonyl groups. DOX loaded CNT showed characteristic peaks of DOX at 998 cm<sup>-1</sup> and 1213 cm<sup>-1</sup> indicating presence of DOX in CNT. The IR spectrum of CNT-DOX-Fe<sub>3</sub>O<sub>4</sub> showed prominent peaks at 575 cm<sup>-1</sup>, 629 cm<sup>-1</sup> due to Fe-O stretching thus confirming the conjugation of GSH-Fe<sub>3</sub>O<sub>4</sub> to the CNT<sup>21,24,25</sup>. Furthermore, the spectrum of CNT-DOX-Fe<sub>3</sub>O<sub>4</sub> conjugated with Tf showed new peaks at 3448 cm<sup>-1</sup> for free amine, and sharp peak at 1645 cm<sup>-1</sup> for amide linkage, providing clear evidence for conjugation of Tf with CNT-DOX-Fe<sub>3</sub>O<sub>4</sub>. We also evaluated the conjugation reaction with respect to the change in zeta potential of the individual step during the synthesis of CNT-DOX-Fe<sub>3</sub>O<sub>4</sub>-Tf (Fig. 2E). The zeta potentials of CNT-COOH, Fe<sub>3</sub>O<sub>4</sub>, CNT-DOX-Fe<sub>3</sub>O<sub>4</sub> and CNT-DOX-Fe<sub>3</sub>O<sub>4</sub>-Tf were determined to be -4.07, -18.6, -8.9, and -22.2 mV, respectively. The step-wise altered zeta potentials indicated successful conjugation of the multiple components with CNT. Tf conjugation quantified by a modified Bradford procedure was found to be ~326 mg per g of CNT-DOX-Fe<sub>3</sub>O<sub>4</sub>.

The drug loading and encapsulation efficiency of DOX was determined to be 63.8 µg/mg in CNT-DOX-Fe<sub>3</sub>O<sub>4</sub> nanobots using UV-visible spectrophotometry. DOX loading and Tf conjugation in CNT-DOX-Fe<sub>3</sub>O<sub>4</sub>-Tf was analyzed and confirmed by UV-visible and fluorescence spectroscopy methods. The UV-visible spectrum of CNT-DOX-Fe<sub>3</sub>O<sub>4</sub>-Tf was compared with the spectra of free DOX and Tf (Fig. 2F). The spectra revealed the presence of characteristic peaks of DOX ( $\lambda_{\text{max}} = 480$  nm) and Tf ( $\lambda_{\text{max}} = 280$  nm) in the CNT-DOX-Fe<sub>3</sub>O<sub>4</sub>-Tf nanobots. Furthermore, the fluorescence spectrum of the CNT-DOX-Fe<sub>3</sub>O<sub>4</sub>-Tf was compared to that of the free DOX under identical optical conditions (480 nm excitation). As depicted in Fig. 2G, typical DOX in PBS displayed  $\lambda_{\text{em}}$  at ~590 nm. The spectrum of CNT-DOX-Fe<sub>3</sub>O<sub>4</sub>-Tf also displayed the typical absorption band from DOX indicating loading of DOX. In addition, the presence of DOX in CNT was also confirmed using 2.5D fluorescence microscopy imaging of the CNT-DOX-Fe<sub>3</sub>O<sub>4</sub> nanobots. The image revealed presence of DOX (red) within the nanopores of the CNT carrier particle (gray) (Supplementary Fig. S2).

**Motion and position-kinetic analysis of nanobots.** The self-propelling abilities of the CNT-DOX-Fe<sub>3</sub>O<sub>4</sub>-Tf nanobot in different fluids simulating physiological environments such as in phosphate buffer saline (PBS; pH 7.4), Dulbecco's modified eagle medium (DMEM) cell media and serum were characterized to verify the compatibility in relevant biological fluids. Some organic and/or biological molecules are capable of quenching or inhibiting the H<sub>2</sub>O<sub>2</sub> decomposition reactions catalyzed by Fe<sub>3</sub>O<sub>4</sub> NPs and thus can significantly hamper the motion of the nanobot. NP tracking analysis was used to track in real-time the movement of the nanobots under a range of H<sub>2</sub>O<sub>2</sub> concentrations (Fig. 3A). The nanobots propelled upward instantaneously and gradually reverted in the downward direction. For the mechanism of motion, O<sub>2</sub> bubbles generated by Fe<sub>3</sub>O<sub>4</sub> NPs catalyzed decomposition of H<sub>2</sub>O<sub>2</sub> are responsible for propulsion in this system. The catalytic ability of Fe<sub>3</sub>O<sub>4</sub> evaluated in PBS comprising a range of H<sub>2</sub>O<sub>2</sub> (0.006 w/v% to 0.05 w/v%) concentrations revealed increased rate of reaction with increase in H<sub>2</sub>O<sub>2</sub> concentration (Supplementary Fig. S3). Supplementary Fig. S4 shows propelling CNT-DOX-Fe<sub>3</sub>O<sub>4</sub>-Tf nanobots in PBS buffer at pH 7.4 with 0.5% H<sub>2</sub>O<sub>2</sub> composition (Supplementary Fig. S4A) and its response when held next to a permanent magnet (Supplementary Fig. S4B). CNT-DOX-Fe<sub>3</sub>O<sub>4</sub>-Tf nanobots moving in vertical trajectory was acquired through the solution and got accumulated at the side of the tube where the magnetic field gradient was the strongest. Hence, the direction of the nanobots can be remotely controlled by a magnetic field and thus enabling it a cooperative propulsion mode under magnetic field in the presence of the chemical fuel.

Figure 3B shows images of the nanobot at different positions during its motion for a complete cycle. As evident from the images, the nanobot stayed away from the wall and moved through nearly the center of the liquid column during its flight. The average propulsion speed of the CNT-DOX-Fe<sub>3</sub>O<sub>4</sub>-Tf nanobot during its upward

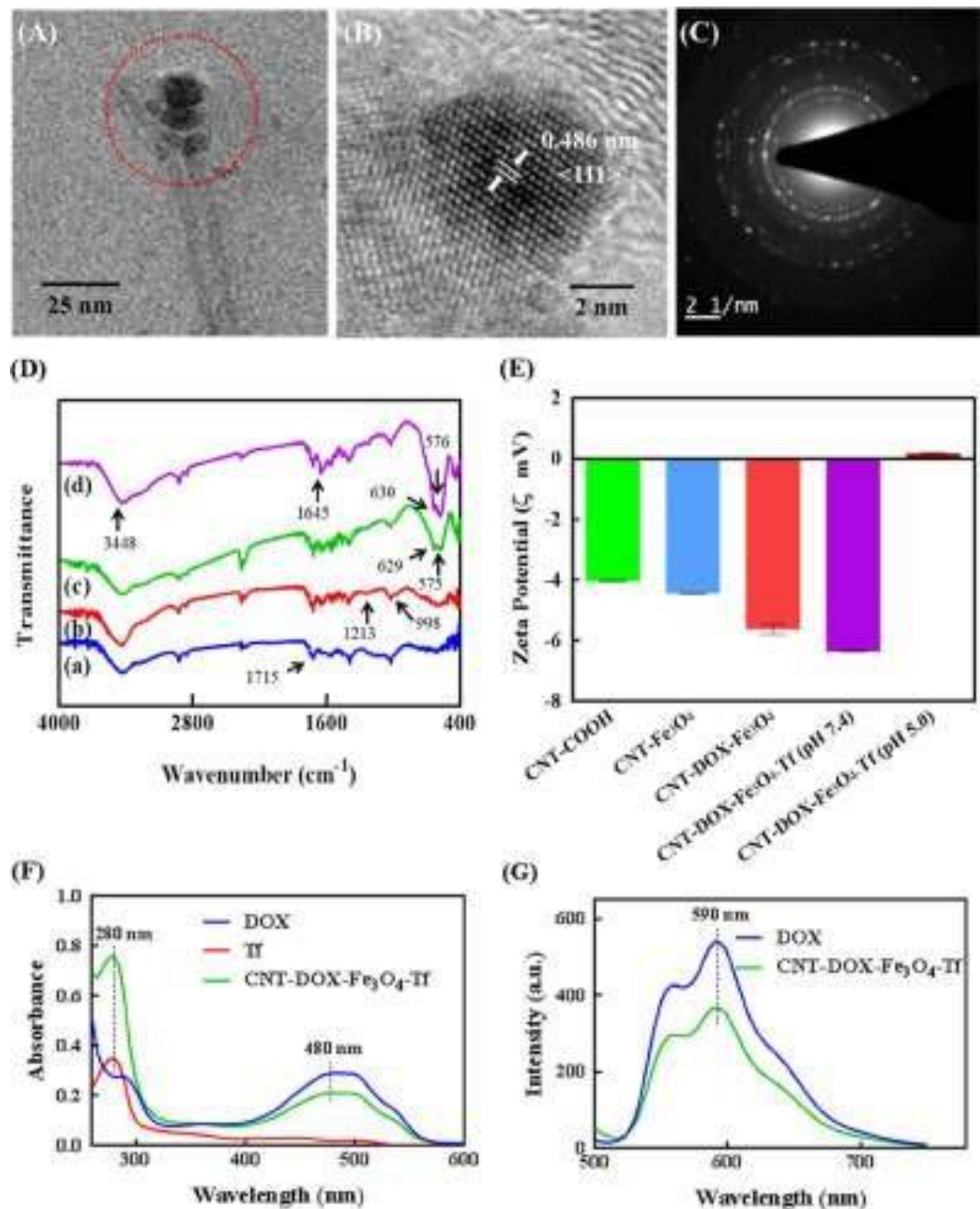


**Figure 2.** Characterization of CNT-DOX-Fe<sub>3</sub>O<sub>4</sub>-Tf and CNT modifications to obtain the multicomponent CNT-DOX-Fe<sub>3</sub>O<sub>4</sub>-Tf (nanobot). **(A)** TEM microscopy images of CNT-DOX-Fe<sub>3</sub>O<sub>4</sub>-Tf, **(B)** evidencing Fe<sub>3</sub>O<sub>4</sub> structure, and **(C)** crystalline features of the NPs. **(D)** FTIR spectra of (a) CNT-COOH, (b) CNT-DOX, (c) CNT-DOX-Fe<sub>3</sub>O<sub>4</sub> and (d) CNT-DOX-Fe<sub>3</sub>O<sub>4</sub>-Tf. **(E)** surface charge evolution upon loading of CNT with DOX and further conjugation of Fe<sub>3</sub>O<sub>4</sub> and Tf, **(F)** UV-visible spectra of DOX ( $\lambda_{\max} = 480$  nm) and Tf ( $\lambda_{\max} = 280$  nm) and CNT-DOX-Fe<sub>3</sub>O<sub>4</sub>-Tf (Tf peak at 280 nm and DOX peak at 480 nm). **(G)** Normalized fluorescence spectra of DOX and CNT-DOX-Fe<sub>3</sub>O<sub>4</sub>-Tf ( $\lambda_{\text{ex}} = 480$  nm,  $\lambda_{\text{em}} = 590$  nm).

movement velocity in PBS, DMEM, and the blood serum was 0.338, 0.831 and 1.011 mm s<sup>-1</sup> respectively, in 0.5% H<sub>2</sub>O<sub>2</sub>. On the other hand, the downward velocity of nanobots was measured to be 0.208, 0.221 and 0.502 mm s<sup>-1</sup>, respectively. The velocity and speed of nanobots was virtually stable without obvious deceleration for more than 5 cycles.

Interestingly, the upward and downward velocity of the nanobot in PBS, DMEM, and serum increased significantly to 0.972, 2.333, 8.026 mm s<sup>-1</sup> (equal to a relative speed of nearly 119 body length per second) and 0.535, 1.120, 1.120 mm s<sup>-1</sup> when the concentration of H<sub>2</sub>O<sub>2</sub> increased to 8% H<sub>2</sub>O<sub>2</sub> (Fig. 3C–E). This corresponds to a large driving force of 592, 1304 and 5435 pN in the upward direction, based on the drag force  $F = 6\pi\eta r v$ , where  $v$  is the speed,  $r$  is the radius of the nanobot and  $\eta$  is the viscosity of the medium (Fig. 3F). The increase in speed



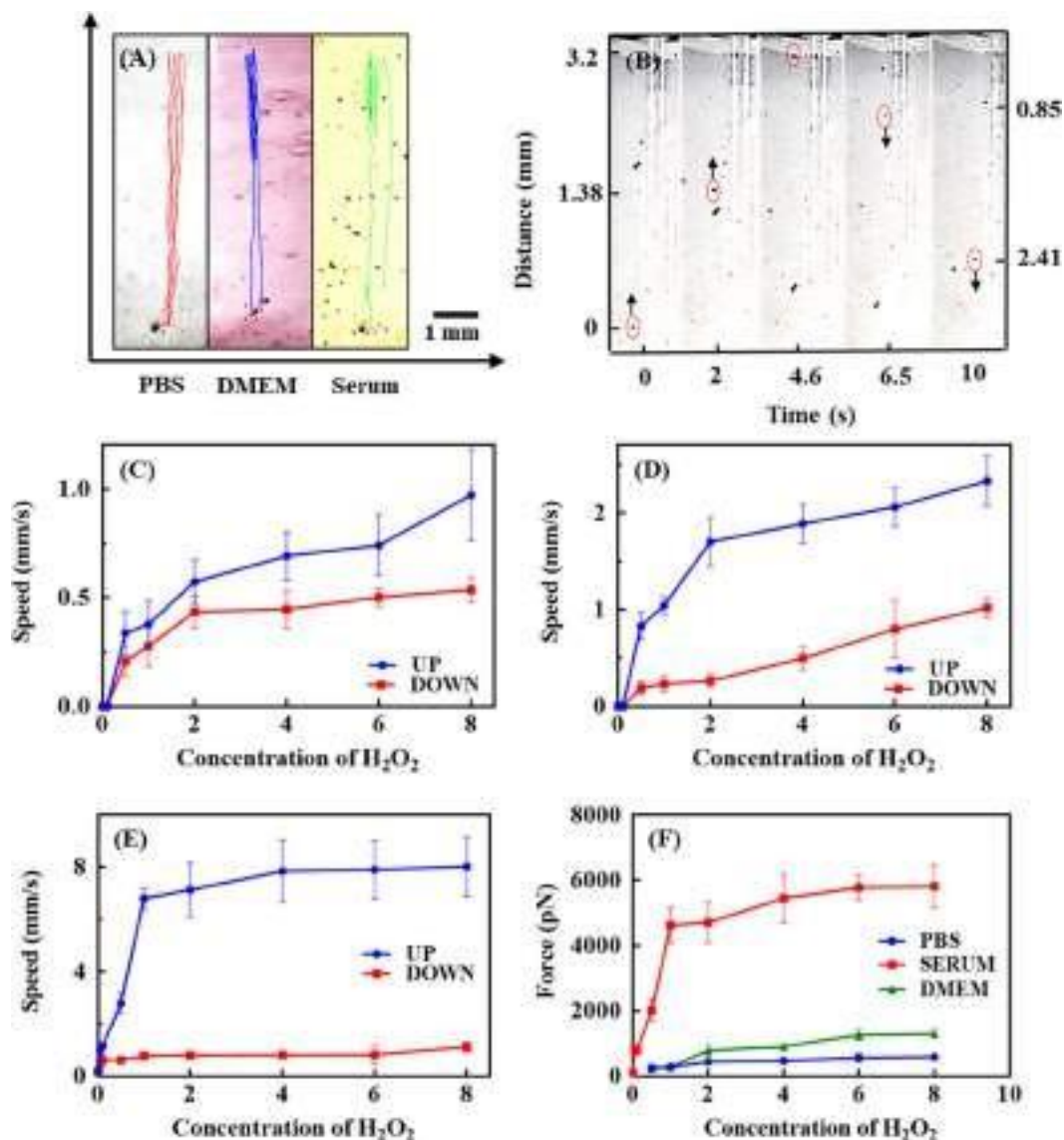


**Figure 3.** (A) Analysis of the motion behavior of CNT-DOX-Fe<sub>3</sub>O<sub>4</sub>-Tf nanobot. The videos were recorded with Dino-Lite digital microscope at 50× magnification, using the Dino-Capture 2.0 v (<https://www.dino-lite.com/>), best clip was chosen using VirtualDub 1.10.4 v (<http://www.virtualdub.org/>) and finally tracking and speed calculations were performed using MTrackJ plugin from ImageJ 1.8.0\_112v (<https://imagej.net/MTrackJ>). (a) Representative tracking trajectories of CNT-DOX-Fe<sub>3</sub>O<sub>4</sub>-Tf nanobots with different biologically relevant media. (B) Time-lapse images of the nanobot driven by oxygen bubble propulsion after time intervals of (a) 0, (b) 2.0, 4.6, 6.5 and 10 s. Speed of nanobot in the presence of different concentration of H<sub>2</sub>O<sub>2</sub> (0.5–8 w/v %) in (C) PBS, (D) DMEM and (E) serum, (F) Analysis of force of nanobot in PBS, DMEM and serum in presence of different concentration of H<sub>2</sub>O<sub>2</sub> (0.5–8 w/v %).

with increasing H<sub>2</sub>O<sub>2</sub> concentration is due to influence of surrounding H<sub>2</sub>O<sub>2</sub> concentration on the reduction rate of the Fe<sup>3+</sup> to Fe<sup>2+</sup>. Hence, with the presence of higher localized concentration of H<sub>2</sub>O<sub>2</sub> lead to an increased production of O<sub>2</sub> bubbles thus resulting in generation of strong thrust and buoyancy thereafter for the upward as well downward motion of the nanobots (Fig. 3F). Further, the speed of the nanobot in serum was ~8.3 and ~3.4 times the speed seen in PBS and DMEM. The distance travelled by the nanobot in serum changed with change in H<sub>2</sub>O<sub>2</sub> concentration. At low H<sub>2</sub>O<sub>2</sub> concentration (0.5%) the average distance travelled was low (19.069 mm), while it was high (63.543 mm) at higher concentration (8%). The three-fold enhancement of distance travelled by nanobots was influenced due to innate H<sub>2</sub>O<sub>2</sub> present in blood. H<sub>2</sub>O<sub>2</sub> has diverse roles in normal physiological context. It serves as a blood borne signaling molecule, while at the same time it is produced intra-mitochondrially in most live cells. While these sources produce small amount of H<sub>2</sub>O<sub>2</sub>, the circulatory system conceivably accumulates this product. Additionally, immune cells, endothelial, and unbound xanthine oxidase generate H<sub>2</sub>O<sub>2</sub> which also increase the cumulative H<sub>2</sub>O<sub>2</sub> serum levels<sup>26,27</sup>. Serum H<sub>2</sub>O<sub>2</sub> content varies between 0–5 μM depending on physiological conditions<sup>28</sup>. Significantly, tumor cells influence H<sub>2</sub>O<sub>2</sub> content locally and presumably systemically<sup>29–31</sup>.

Tumors are known to demonstrate the capability of exploiting  $H_2O_2$  in cell proliferation<sup>32</sup>. However, a restrained capacity to metabolize  $H_2O_2$  drives tumor masses to drain nascent  $H_2O_2$  in the surrounding tissue space which may ultimately reach systemic circulation and may increase systemic levels by up to  $10\ \mu M$  and higher<sup>33</sup>. Further, the catalase enzyme present in serum may also be imparting catalytic property by getting adsorbed on the surface of nanobots and thus greatly enhancing generating of oxygen bubbles. In addition, it is conceivable that as a result of localized protein oxidation in the presence of  $H_2O_2$ , the protein aggregation leads to the adsorption of serum proteins such as albumin and immunoglobulins on the surface of the NPs<sup>34,35</sup>. Aggregated proteins have a cascading effect which may further influence binding of other serum proteins including enzymes such as serum catalase onto the surface of the protein-masked NPs<sup>36</sup>. This synergistic effect may also be responsible for the rapid propulsion of nanobots in blood serum even at low  $H_2O_2$  concentration as compared to PBS and DMEM<sup>4,36–40</sup>. The results indicate an appropriate pairing of the propulsion mechanism pre-assumed for its physiological fate and subsequently for the clinical context. It may be possible to exploit the natural  $H_2O_2$  decomposition system in combination with limited exogenous  $H_2O_2$  and attain high propulsion resulting in significant driving force to nanobots for rapid transport of drug cargo followed by deep tumor penetrating capability.

**Drug release profiles of the nanobots.** To investigate the pH dependent control release of DOX, we performed drug release study at two different pH conditions, one representing the physiological pH i.e. 7.4 and the other cell lysosomal pH (~pH 5) in presence and absence of proteases enzyme-cathepsin B. As shown in Supplementary Fig. S5, CNT-DOX- $Fe_3O_4$ -Tf nanobot demonstrated low release of DOX (~26%) even after 48 h at pH 7.4, signifying efficient trapping of DOX in the CNT cavities by with  $Fe_3O_4$  NPs exterior cap. The observed small DOX release is probably of the loosely surface-bound DOX. Conversely at pH 5 and in presence of cathepsin B, a controlled DOX release pattern was observed. Around ~76% DOX got released till 4 h which then increased to ~94% at 48 h. This remarkable multi-order kinetics pattern of DOX release from the designed nanobot is due to the degradation of amide linkage resulting in time-dependent uncapping of CNT<sup>41</sup>. TEM images of nanobots after release study confirmed the uncapping of CNTs as no  $Fe_3O_4$  NPs were seen near the tip of the CNTs (Supplementary Fig. S6). However, in absence of cathepsin B ~75% DOX got released till 48 h in pH 5.0. The release of DOX is most likely due to the degradation of amide linkage in acidic pH<sup>42</sup>. Similarly, at pH 6.5 and in presence of cathepsin B, ~85% DOX got released till 48 h. However, in absence of cathepsin B only ~56% DOX got released. Further, to confirm the capping efficiency, release of DOX from CNT-DOX- $Fe_3O_4$ -Tf nanobot without the  $Fe_3O_4$  NP cap was also examined. Nanobot without cap demonstrated a predictable immediate burst-release of ~61% and ~18% of DOX within 30 min in pH 5.0 and 7.4, respectively. As mentioned earlier, the open-ended CNT allow cross-flow in the CNT cavity and consequently allow rapid release of the entrapped DOX. This pH-sensitive release behavior is of particular interest as it can reduce untimely drug release during systemic circulation and can specifically enhance intracellular (lysosomal) DOX release. This will be beneficial in cancer treatment as it will help in significantly lowering the dosage, few side effects and limited drug toxicity.

**Time dependent cell entry kinetics studies.** The cellular uptake and intracellular pH-dependent endo/lysosomal release of DOX from nanobots was studied over time by fluorescent cell imaging (Fig. 4). HCT116 colon cancer cells were cultured, and subsequently incubated with DOX, CNT-DOX- $Fe_3O_4$  and CNT-DOX- $Fe_3O_4$ -Tf at 37 °C before examination under fluorescence microscope at definite time intervals. The inherent fluorescence emissions of DOX were red, which were utilized as indicators for their corresponding distribution inside the cells (Fig. 5A). Figure 4 and Supplementary Fig. S7 depict the entry of free DOX influx, CNT-DOX- $Fe_3O_4$  and CNT-DOX- $Fe_3O_4$ -Tf into HCT116 cells, implied by rapid cytosolic DOX labeling followed by DOX importation into the nucleus. At the 1 h, CNT-DOX- $Fe_3O_4$  and CNT-DOX- $Fe_3O_4$ -Tf internalized into the cells by mechanisms including endocytosis and energy-independent, direct penetration and were localized mainly in the cytoplasm and subcellular vesicles. The (DAPI-stained) nucleus displayed a low DOX presence as compared to the cytosolic compartment (Supplementary Fig. S7A). Interestingly, the emission of DOX overlapped exactly with that of CNT-DOX- $Fe_3O_4$ -Tf. In contrast, cells treated with free DOX showed red fluorescence accumulation mainly in the cell nuclei. Exposure of the cancer cells to free DOX resulted in rapid influx owing to passive diffusion as well as carrier-mediated uptake of DOX<sup>43</sup>. The fluorescence intensity of free DOX in the cell was ~1.7 times higher than that of CNT-DOX- $Fe_3O_4$ -Tf. On the other hand, the intensity of DOX released from CNT-DOX- $Fe_3O_4$  was 3.3 times less than CNT-DOX- $Fe_3O_4$ -Tf. The influx of DOX into the nucleus is believed to be facilitated by binding to proteasomes<sup>44,45</sup>. On the other hand, energy-dependent drug efflux mechanisms such as ATP-binding cassette subfamily C member 1 (ABCC) are implicated in active efflux of DOX out of the cell<sup>46</sup>. The efflux machinery in turn contributes to the drug resistance of cancer cells. Furthermore, to understand how the TME affect the nanobot internalization process and intracellular delivery of DOX, the cellular entry kinetics was also studied at an acidic pH of 6.5. The pH of the media showed a clear influence on nanobot cell internalization and intracellular DOX release. While the CNT-DOX- $Fe_3O_4$  nanobot showed comparable DOX presence at 1 h in both pH environments, the CNT-DOX- $Fe_3O_4$ -Tf nanobot demonstrated ~1.7 fold increase in cellular DOX content in the acidic pH of 6.5, compared to the normal physiological pH 7.4 (Supplementary Fig. S7B, and Fig. 5A). The study clearly reveals higher cell entry of CNT-DOX- $Fe_3O_4$ -Tf nanobot at pH 6.5.

After incubation for 4 h, DOX released from CNT-DOX- $Fe_3O_4$  and CNT-DOX- $Fe_3O_4$ -Tf was observed to be localized in the nuclear region (Fig. 4A,B). The intracellular release of DOX can be attributed to the opening of pH-sensitive nanogates due to amide bond cleavage in the acidic lysosomal compartments (Fig. 1). Additionally, the release of DOX was studied using confocal laser scanning microscopy (CLSM). At 4 h the LysoTracker labeled acidic organelles appeared yellow-orange, owing to merging of the green (LysoTracker) and red (DOX) fluorescence, due to the release of DOX from CNT-DOX- $Fe_3O_4$ -Tf (Fig. 4E). Subsequently, to further confirm the uncapping of CNT-DOX- $Fe_3O_4$ -Tf nanobots,  $Fe_3O_4$  NPs in CNT-DOX- $Fe_3O_4$ -Cy5-Tf were labeled with a fluorescent dye, Cyanine 5 (Cy5). As depicted in Supplementary Fig. S8, a strong localization of Cy5 (purple signal,

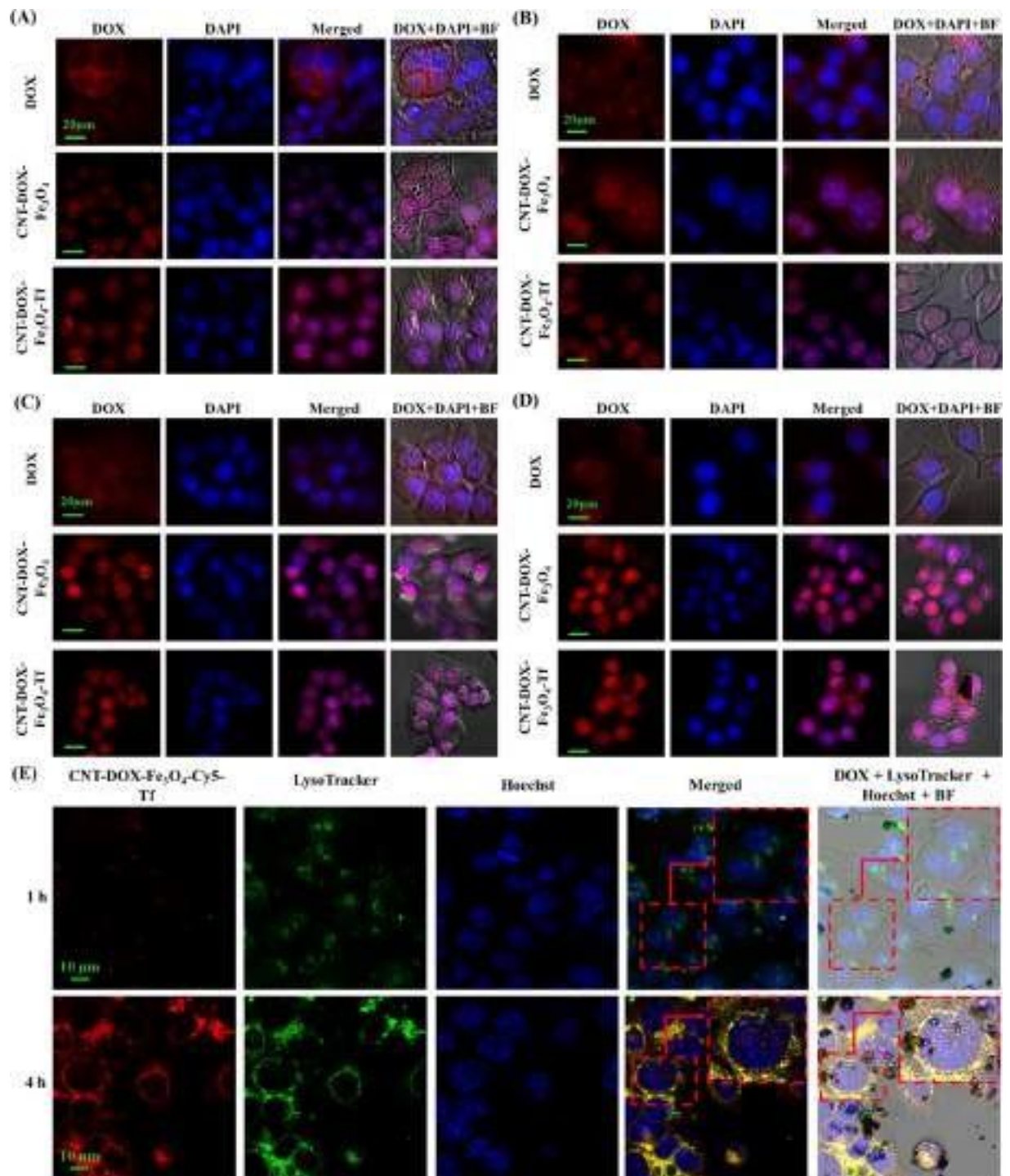


**Figure 4.** Fluorescent images of HCT116 cells treated with free DOX, CNT-DOX-Fe<sub>3</sub>O<sub>4</sub> and CNT-DOX-Fe<sub>3</sub>O<sub>4</sub>-Tf. **(A)** At 4 h exposure and at pH 7.4, DOX released from CNT-DOX-Fe<sub>3</sub>O<sub>4</sub> and CNT-DOX-Fe<sub>3</sub>O<sub>4</sub>-Tf was observed to be localized in the nuclear region **(A,B)**. The intracellular release of DOX can be attributed to the opening of pH-sensitive nanogates due to amide bond cleavage in the acidic lysosomal compartments. Cells incubated with free DOX showed efflux of DOX from the nucleus back into the cytoplasm, which is in contrast to the findings for CNT-DOX-Fe<sub>3</sub>O<sub>4</sub> and CNT-DOX-Fe<sub>3</sub>O<sub>4</sub>-Tf. **(B)** At 4 h exposure and at pH 6.5, the fluorescence intensity of DOX from CNT-DOX-Fe<sub>3</sub>O<sub>4</sub>-Tf nanobot was higher due to faster cellular internalization of CNT-DOX-Fe<sub>3</sub>O<sub>4</sub>-Tf. **(C)** At 24 h and at pH 7.4, most of the DOX was released from CNT-DOX-Fe<sub>3</sub>O<sub>4</sub>-Tf suggesting the efficient release of DOX from interior cavity of CNT after opening of Fe<sub>3</sub>O<sub>4</sub> nanogate in lysosomal conditions. **(D)** At 24 h and at pH 6.5, the fluorescence intensity of DOX in the cells was more pronounced suggesting enhanced cellular internalization of CNT-DOX-Fe<sub>3</sub>O<sub>4</sub>-Tf nanobot (Scale bars indicate 20 μm). **(E)** Kinetic study of Fe<sub>3</sub>O<sub>4</sub> NP uncapping and DOX release from CNT-DOX-Fe<sub>3</sub>O<sub>4</sub>-Cy5-Tf nanobots in cells using confocal microscopy. Time-dependant release of DOX (red) into the acidic lysosomal compartment (green, LysoTracker) over 4h, indicating -cleavage of CNT- Fe<sub>3</sub>O<sub>4</sub> amide-bond, subsequent



uncapping and DOX release. The merged image of the cells at 4 h shows a prominent yellow-orange signal indicating co-localization of DOX and lysosomes around the nucleus (blue), scale bars indicate 10  $\mu$ m.

Fe<sub>3</sub>O<sub>4</sub> NPs) with DOX (red) at 1 h was suggestive of site-restriction of DOX within CNT-DOX-Fe<sub>3</sub>O<sub>4</sub>-Cy5-Tf nanobots. However, in 4 h post-treatment images the whole LysoTracker labelled acidic organelles appeared orange indicating separation of Fe<sub>3</sub>O<sub>4</sub> and DOX signals, consistent with detachment of Fe<sub>3</sub>O<sub>4</sub> caps from CNT and subsequent release of DOX from CNT. This finding is consistent with the DOX release patterns from CNT-DOX-Fe<sub>3</sub>O<sub>4</sub> and CNT-DOX-Fe<sub>3</sub>O<sub>4</sub>-Tf at pH 5.0 (Supplementary Fig. S5). The fluorescence intensity of DOX for CNT-DOX-Fe<sub>3</sub>O<sub>4</sub>-Tf was ~8 times higher than that of free DOX (Fig. 5A). Cells incubated with free DOX showed efflux of DOX from the nucleus back into the cytoplasm, which is in contrast to the findings for CNT-DOX-Fe<sub>3</sub>O<sub>4</sub> and CNT-DOX-Fe<sub>3</sub>O<sub>4</sub>-Tf. Efflux of DOX prior to its activity in arresting topoisomerase is likely the reason for reduced efficacy of DOX. A rapid back-efflux phenomenon indicated an adaptive mechanism for drug resistance. It is conceivable that the efflux transport of free DOX occurs at a significantly higher velocity than that afforded by the DOX-proteasome nuclear import mechanism. On the other hand, the fluorescence intensity of DOX at pH 6.5 from CNT-DOX-Fe<sub>3</sub>O<sub>4</sub>-Tf nanobot was ~2.4 times higher than that observed in pH 7.4 (Figs. 4B and 5A). The presence of higher DOX could be attributed to faster cellular internalization of CNT-DOX-Fe<sub>3</sub>O<sub>4</sub>-Tf in pH 6.5 as compared to pH 7.4.

Tf is a vital protein for cellular uptake of systemic iron, consequently, the receptor mediated endocytosis which drives the import of exogenous CNT-DOX-Fe<sub>3</sub>O<sub>4</sub>-Tf nanobot ensures the capture, internalization, processing and release of DOX intracellularly. While diffusion of DOX and transporter mediated DOX import appears faster in the free DOX state, CNT-DOX-Fe<sub>3</sub>O<sub>4</sub>-Tf seemingly maintains molecular efficiency in DOX import<sup>47</sup>. Put differently, the deficiency of the Tf-conjugated nanobot in rapid initial diffusion velocity, as seen in free DOX, is compensated by the sustained import of Tf-nanobot-borne DOX. It is possible that the endosomal processing of nanobot-encapsulated DOX results in efficient presentation of liberated DOX to cellular proteasomes which in turn deliver it to the nucleus. In contrast, the CNT-DOX-Fe<sub>3</sub>O<sub>4</sub>-borne DOX is introduced within the cell in a diffusion and energy-independent membrane flipping manner. Presumably this exposes the DOX to cellular environment and therefore the efflux machinery resulting in poorer DOX nuclear import as compared to the CNT-DOX-Fe<sub>3</sub>O<sub>4</sub>-Tf nanobots.

At 24 h, DOX was almost exclusively present in the nucleus of the cells treated with the CNT-DOX-Fe<sub>3</sub>O<sub>4</sub> and CNT-DOX-Fe<sub>3</sub>O<sub>4</sub>-Tf nanobots (Fig. 4C,D). Post-endosomal and lysosomal processing and Fe<sub>3</sub>O<sub>4</sub> amide-bond cleavage, the released DOX undergoes the same nuclear entry pathway as free DOX, i.e. *via* proteasomes. However, the 24 h retention of DOX within the nuclear compartment is a significant improvement over free DOX. The nuclear efflux is apparently low or virtually non-existent in case of CNT-DOX-Fe<sub>3</sub>O<sub>4</sub> and CNT-DOX-Fe<sub>3</sub>O<sub>4</sub>-Tf, which is further evidenced by a virtual absence of DOX from the cytoplasm. Strongly contrasted with this nanobot-borne DOX behavior is the gradual disappearance of DOX from the cellular compartments in cells treated with free DOX. The fluorescence intensity of DOX for CNT-DOX-Fe<sub>3</sub>O<sub>4</sub>-Tf was ~35 times higher than free DOX (Figs. 4C and 5A). It is conceivable that the DOX, free from the influence of nanobot-mediated outcomes, is rapidly effluxed from the cell. ATP-dependent ABCC1 drug transporter is postulated to work even against the DOX concentration gradient across the cell membrane and achieve high DOX clearance. Interestingly, at pH 6.5, the fluorescence intensity of DOX in the cells exposed to CNT-DOX-Fe<sub>3</sub>O<sub>4</sub>-Tf nanobot was more pronounced than in pH 7.4. The intensity was ~1.3 times more in pH 6.5 suggesting enhanced cellular internalization of CNT-DOX-Fe<sub>3</sub>O<sub>4</sub>-Tf nanobot at pH 6.5 (Figs. 4B and 5A). The presence of higher DOX could be attributed to faster cellular internalization of CNT-DOX-Fe<sub>3</sub>O<sub>4</sub>-Tf in pH 6.5 as compared to pH 7.4.

At the 48 h, most of the DOX resided in the nuclei of the cells treated with CNT-DOX-Fe<sub>3</sub>O<sub>4</sub> and CNT-DOX-Fe<sub>3</sub>O<sub>4</sub>-Tf (Supplementary Fig. S7C,D), similar to the outcome seen at 24 h. While nuclear retention was apparent for both treatments, DOX intensity appeared greater for CNT-DOX-Fe<sub>3</sub>O<sub>4</sub>-Tf indicating efficient and steady release of DOX from the target-specific CNT-DOX-Fe<sub>3</sub>O<sub>4</sub>-Tf nanobot. The amount of DOX effluxed from the cell was as high as 93% as determined from the kinetic study for free DOX. While the efflux kinetics for the free DOX was similar in the both the pH conditions, CNT-DOX-Fe<sub>3</sub>O<sub>4</sub>-Tf nanobot demonstrated pH sensitivity even at 48 h. As shown in Supplementary Fig. S7C,D, DOX released from CNT-DOX-Fe<sub>3</sub>O<sub>4</sub>-Tf nanobot co-localized with DAPI concentrated in the nuclear region highlighting the nucleosome bodies, which contain the chromatin matter. The effect is more pronounced at pH 6.5 and the DOX accentuation in the nucleus suggests preferential binding of DOX to DNA and nucleosome-bound topoisomerases (Fig. 5B). The consequence of targeted delivery of DOX using the CNT-DOX-Fe<sub>3</sub>O<sub>4</sub>-Tf vehicle was the inversion of the net efflux kinetics seen in free drug to the net accumulation kinetics of DOX when administered *via* targeted nanobots (Supplementary Fig. S9).

As mentioned earlier, while the efflux velocity of the free DOX may overcome its nuclear entry, the proteasome-facilitated DOX nuclear import may be instrumental in enhanced DOX entry into the nucleus when cells are treated with DOX-nanobots. Moreover, the CNT-DOX-Fe<sub>3</sub>O<sub>4</sub> borne DOX may have secondary roles in enhanced nuclear delivery and nuclear retention which allow DOX to show nuclear presence past the clearance period for free DOX (Supplementary Fig. S7C,D). The proposed nanobot thus present a mechanism for evading drug efflux in cancerous cells and ensuring drug accumulation to achieve its cytotoxic goal.

To highlight the role of TME acidic milieu and H<sub>2</sub>O<sub>2</sub> in the uptake of nanobots, zeta potential of the cells exposed to CNT-DOX-Fe<sub>3</sub>O<sub>4</sub>-Tf nanobot was evaluated at two different pH conditions, physiological pH 7.4 and pH 6.5 which exists in TME in presence of H<sub>2</sub>O<sub>2</sub> as shown in Fig. 5C. The HCT116 cells demonstrated a negative surface charge in pH 7.4. However, at lower pH values (pH 6.5), the cells underwent surface charge modifications and exhibited a predominantly positive charge due to protonation of free fatty acid head groups in the outer



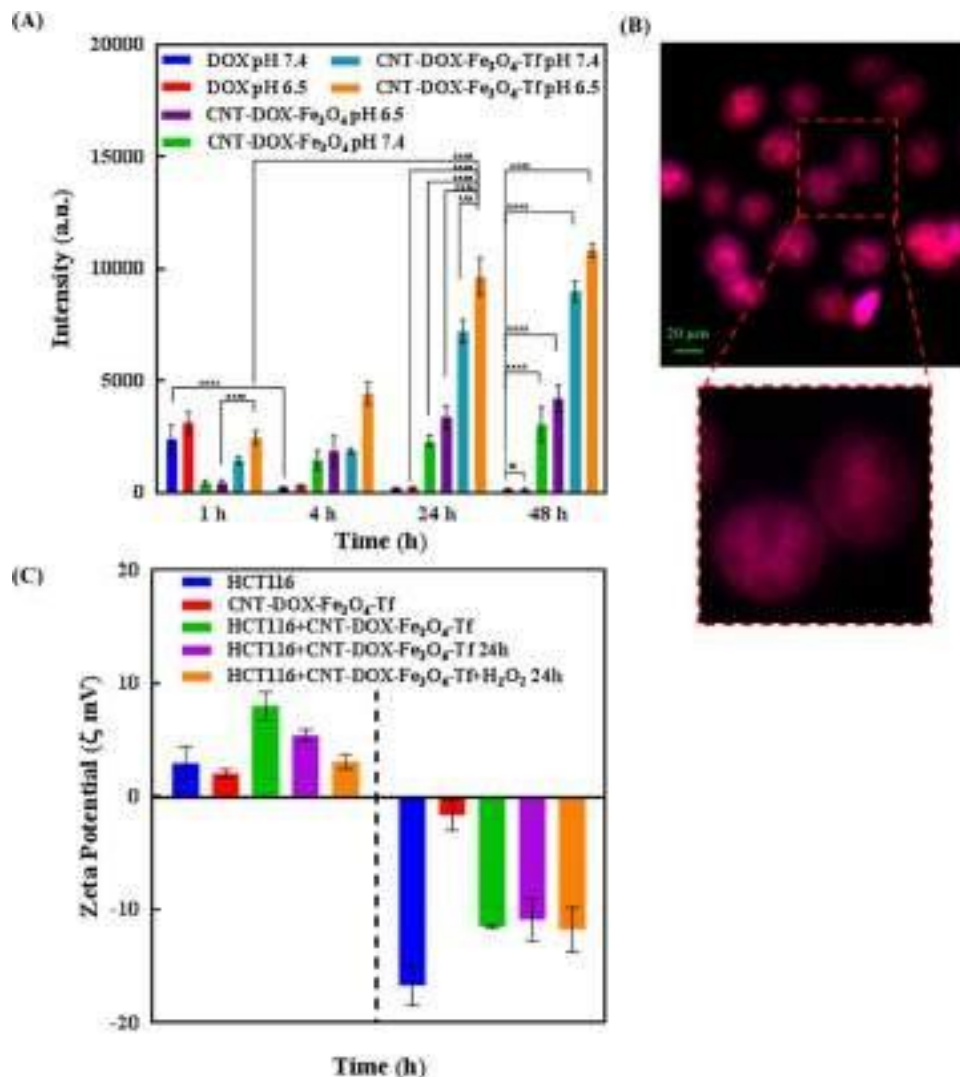


**Figure 5.** (A) Fluorescence intensity of intracellular DOX accumulation upon treatment with nanobots at varying pH. (B) DOX binding of nucleoli. The nucleolar enrichment of DOX post NP administration is suggestive of high-affinity binding of DOX to nucleoli. (C) Surface charge evolution upon exposing to CNT-DOX-Fe<sub>3</sub>O<sub>4</sub>-Tf in presence and absence of H<sub>2</sub>O<sub>2</sub>.

lipid<sup>48</sup>. Furthermore, cells exposed to CNT-DOX-Fe<sub>3</sub>O<sub>4</sub>-Tf nanobot resulted in a significant alteration of the cell's surface charge, regardless of the pH conditions. The zeta potential of the cells exposed to CNT-DOX-Fe<sub>3</sub>O<sub>4</sub>-Tf nanobot in pH 6.5 was roughly 3-times higher as compared to the cells alone. The increase in zeta potential of the cells can likely be attributed to surface-attachment of the nanobot which are also positively charged in acidic pH of 6.5. The increase in surface charge of the cells is shown to be reduced over time (24 h) and furthermore by co-incubation with H<sub>2</sub>O<sub>2</sub> in acidic media. This may be interpreted as a gradual reduction in surface charge due to internalization of the nanobots by receptor-mediated endocytosis. In the presence of H<sub>2</sub>O<sub>2</sub> at 24 h, the cells exposed to CNT-DOX-Fe<sub>3</sub>O<sub>4</sub>-Tf nanobot demonstrated a restoration to the initial zeta potential in acidic condition. It may be due to near-complete internalization of the attached CNT-DOX-Fe<sub>3</sub>O<sub>4</sub>-Tf nanobot in the cell. The acidic condition may have played a role in uptake of nanobots which is further accentuated in the presence of H<sub>2</sub>O<sub>2</sub> as shown in Fig. 5C. Interestingly, the cells exposed to the CNT-DOX-Fe<sub>3</sub>O<sub>4</sub>-Tf nanobot at physiological pH did not show any major change over time or by the presence of H<sub>2</sub>O<sub>2</sub> suggesting a slow internalization under physiological conditions. In accordance with the cell kinetics images (Fig. 4A–D), HCT116 cells do show greater DOX accumulation in acidic conditions.

**Nanobot's efficacy as a drug delivery vehicle.** Concurring with the microscopy data presented, cell viability assays were performed to compare the cytotoxic effects of DOX, CNT-Fe<sub>3</sub>O<sub>4</sub>, CNT-DOX-Fe<sub>3</sub>O<sub>4</sub>-Tf and CNT-DOX-Fe<sub>3</sub>O<sub>4</sub>-mAb nanobot, show anticancer effect of the targeted nanobots. The control treatment with CNT (CNT-COOH) showed no cytotoxicity in the treated HCT116 cells. CNT-Fe<sub>3</sub>O<sub>4</sub> nanobot showed a mild influence on decreasing viability of treated cells, however there was no statistical difference in the effects of

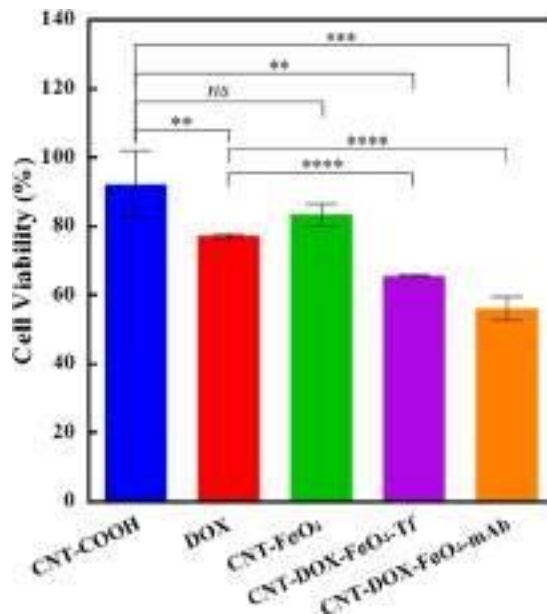


**Figure 6.** Cytotoxicity analysis of free DOX, CNT-DOX-Fe<sub>3</sub>O<sub>4</sub>, CNT-DOX-Fe<sub>3</sub>O<sub>4</sub>-Tf and CNT-DOX-Fe<sub>3</sub>O<sub>4</sub>-mAb nanobots incubated for 48 h with HCT116 cells. Cell viability study of treatments with free DOX and nanobots reveals a statistical improvement of CNT-DOX-Fe<sub>3</sub>O<sub>4</sub>-Tf and CNT-DOX-Fe<sub>3</sub>O<sub>4</sub>-mAb nanobots over free DOX treatment of HCT116 cells. The CNT-Fe<sub>3</sub>O<sub>4</sub> nanobot does not show greater cytotoxic effect as compared to the control-CNT treatment. The free DOX shows limited toxicity to the model cancer cells at the end of the treatment. In contrast, the CNT-DOX-Fe<sub>3</sub>O<sub>4</sub>-Tf and CNT-DOX-Fe<sub>3</sub>O<sub>4</sub>-mAb nanobot loaded with an equivalent dose of DOX shows statistically significant improvement in the toxicity induced, suggesting greater efficacy of the DOX delivery by nanobot.

control CNT and CNT-Fe<sub>3</sub>O<sub>4</sub> as shown in the Fig. 6. DOX on the other hand showed anticancer effect in HCT116 cells, based on the reduced viability of treated cells. The reduced cytotoxicity of the topoisomerase inhibitor *viz a viz* drug is attributed to the activity of the efflux pump which drive DOX out of the cell and decrease its intercalation with DNA<sup>33</sup>. As also seen in the cellular kinetics study (Fig. 4), DOX rapidly localizes to the nuclear region, however the energy-dependent efflux pumps are credited with effective removal of DOX from the nuclear compartment and eventually the cytoplasm as well. In contrast the targeted nanobots demonstrated superior nuclear DOX retention and maintained nuclear localization of the DOX for up to 48 h. The greater cytotoxicity of the targeted CNT-DOX-Fe<sub>3</sub>O<sub>4</sub>-Tf/mAb and CNT-DOX-Fe<sub>3</sub>O<sub>4</sub>-mAb nanobot maybe likely a result of the enhanced nuclear accumulation of DOX, as compared to the free DOX.

**Antitumor efficacy of drug loaded nanobots on 3D spheroidal tumors.** To verify the proposed enhanced tumor penetration of DOX loaded nanobots, multicellular cancer cell 3D spheroids were used to simulate *in vivo* tumors (Fig. 7)<sup>49</sup>. HCT116 spheroids were cultured for 3 days by hanging drop method which promoted 3D tumor formation. The spheroids cultured from single cell suspensions are known to mimic *in vivo* cell-cell interactions *via* formation of inter-cellular junctions contributing to their *in vitro* integrity. Spheroid tumors sustain a balance between cell proliferation and cell death depending on the nutrient supply, DNA replication machinery and death-inducing stimuli. Furthermore, the TME gradient produced due to cellular heterogeneity (outer proliferating layer, followed by a quiescent region and inner necrotic core) is also believed to mimic native tumor physiology, the primary difference being intra-tumor mass vascularization under *in vivo* physiological conditions. *In vivo* tumors are characterized by angiogenesis as a result of complex biochemical interplays to enable tumor survival *via* vascularization<sup>50,51</sup>. Lab-grown spheroids thus, have to rely on surrounding media for nutrient supply. Consequently, as a result of nutrient gradient, the spheroids develop cellular heterogeneity as described above. As the cells proliferate, the number of dead cells accumulates as well, especially in the necrotic core of the spheroid leading to the formation of a dense inner core and an outermost scattered mono layer of shed cells (Fig. 7A, control). Since free DOX can be rapidly taken up by the outer layer of the spheroid cells, a pronounced DOX effect was observed initially. However, DOX effect dissipated in the cell medium as a relatively dilute anti-neoplastic drug, DOX was apparently not sufficient to induce death of remaining cells even after 72 h (Fig. 7A). Note that the inner dense (darker) core is reduced, despite the apparent growth of the tumor area. The widening of the tumor base is attributed to the reduced cell-cell adhesions resulting from DOX treatment which consequently undermines the integrity of the spheroid mass causing it to settle downward and spread. CNT-DOX-Fe<sub>3</sub>O<sub>4</sub>-mAb and CNT-DOX-Fe<sub>3</sub>O<sub>4</sub>-Tf nanobots were significantly more efficacious in tumor reduction than free DOX and the CNT-DOX-Fe<sub>3</sub>O<sub>4</sub> nanobot. CNT-DOX-Fe<sub>3</sub>O<sub>4</sub>-mAb and CNT-DOX-Fe<sub>3</sub>O<sub>4</sub>-Tf nanobots were able to induce cell death resulting in tumor spheroid disintegration compared to control after 72 h of treatment, as shown in Fig. 7A. The lack in spheroid cohesion is apparent from 48 h for both treatments, while the inner dense cores were abolished completely by 72 h. On the

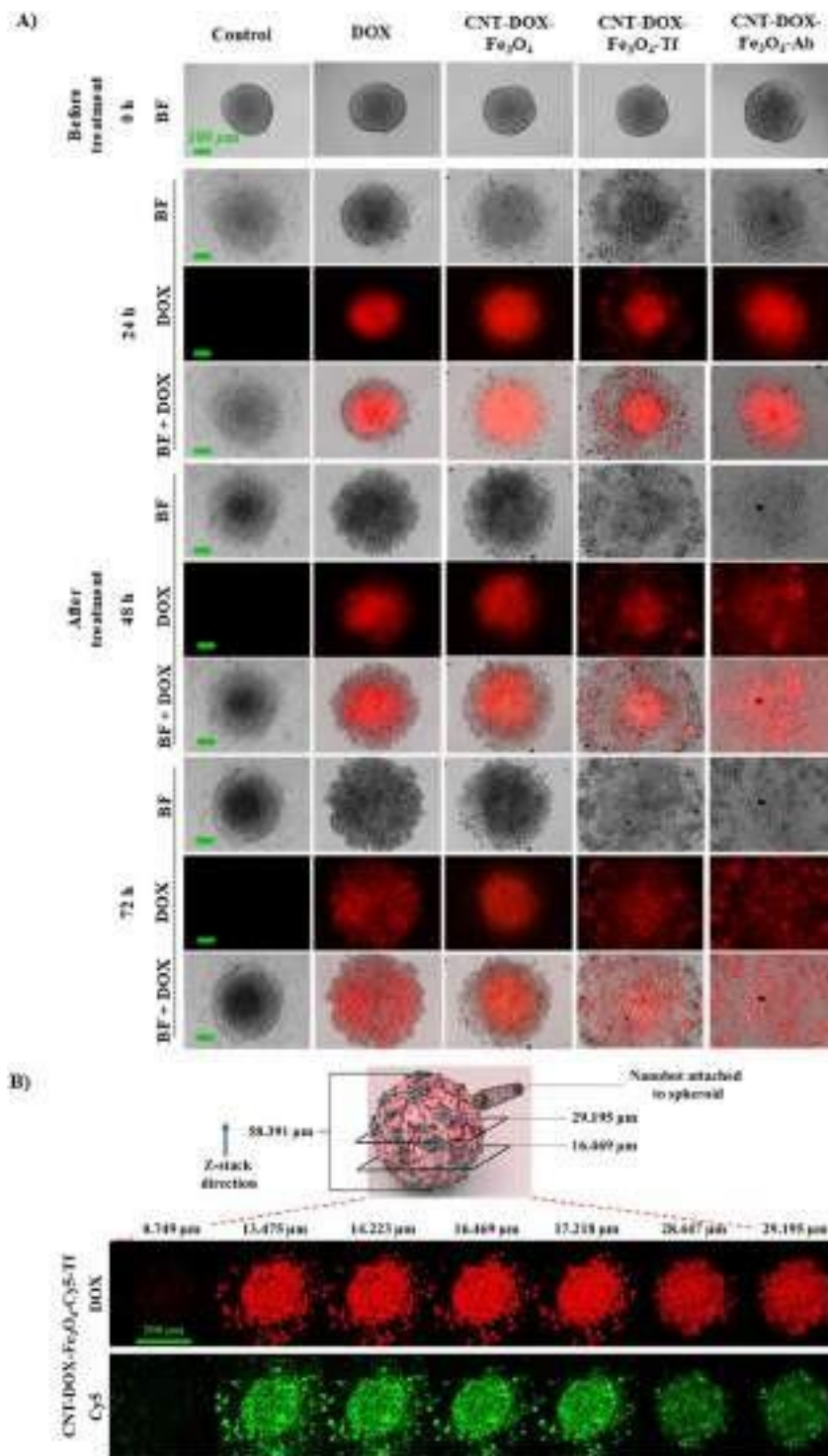


**Figure 7.** (A) Anti-tumor effect of free DOX, CNT-DOX-Fe<sub>3</sub>O<sub>4</sub> and CNT-DOX-Fe<sub>3</sub>O<sub>4</sub>-Tf on HCT116 spheroids. Red color shows the fluorescence of DOX under an excitation light with a wavelength of 488 nm. After 72 h exposure, CNT-DOX-Fe<sub>3</sub>O<sub>4</sub>-mAb and CNT-DOX-Fe<sub>3</sub>O<sub>4</sub>-Tf were efficacious in tumor-spheroid disintegration and were able to induce significant cell death due to enhanced tumor penetration compared to control (untreated tumor). Scale bar for panel represents 100 μm. (B) Deep penetration of CNT-DOX-Fe<sub>3</sub>O<sub>4</sub>-Cy5-Tf NPs into the tumor-spheroid core. Confocal microscopy of spheroid reveals co-localization of DOX (red) and Cy5 tagged CNT-DOX-Fe<sub>3</sub>O<sub>4</sub>-Cy5-Tf NPs (green) at various depths in the tumor mass suggesting deep penetration of the NPs. The schematic depicts the spheroid thickness (58 μm) and the representative planes shown in the confocal image panel below. Scale bar for panel represents 200 μm.

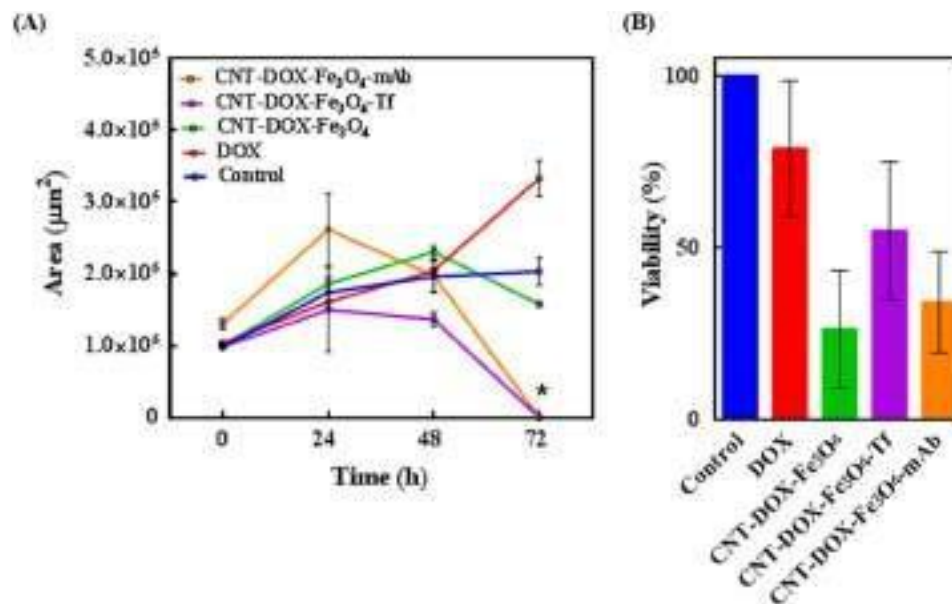


**Figure 8.** Anti-tumor efficacy of administered nanobots on HCT116 spheroids. **(A)** The tumor mass is expressed as area over a period of 72 h. Tumor disintegration (\*) is indicated by reduction in tumor area of spheroids treated with CNT-DOX-Fe<sub>3</sub>O<sub>4</sub>-mAb and CNT-DOX-Fe<sub>3</sub>O<sub>4</sub>-Tf. **(B)** Tumor viability under various treatments are depicted as percent survival, compared to control.

other hand, the control tumor after 72 h depicted an increase in core area by ~104% (from  $9.8 \times 10^4$  to  $20.3 \times 10^4 \mu\text{m}^2$ ) and CNT-DOX-Fe<sub>3</sub>O<sub>4</sub> nanobot treated tumor by ~62% (from  $9.9 \times 10^4$  to  $15.8 \times 10^4 \mu\text{m}^2$ ) compared to their respective before treatment area. One reason for the enhanced efficacy may be the deep tumor penetration ability of CNT-DOX-Fe<sub>3</sub>O<sub>4</sub>-Tf and CNT-DOX-Fe<sub>3</sub>O<sub>4</sub>-mAb due to the forward thrust obtained by nanobots and the delayed DOX clearance at the tumor site because of the retention property of the NPs. DOX is also responsible for inhibiting/blocking the transcriptome<sup>43</sup>, which may also affect the cancer cells ability to maintain the cell adhesion/cell contact machinery. It is conceivable that sustained DOX exposure may reduce the ability of spheroid cells to self-adhere/assemble and be subject to disaggregation and thus be increasingly more prone to the cytotoxic effects of DOX. The effects of CNT-DOX-Fe<sub>3</sub>O<sub>4</sub>-Tf and CNT-DOX-Fe<sub>3</sub>O<sub>4</sub>-mAb appear to manifest in a manner consistent with the above statement (Fig. 7A). Additionally, deep tumor penetration of CNT-DOX-Fe<sub>3</sub>O<sub>4</sub>-Cy5-Tf nanobots into the tumor-spheroid core was studied using confocal microscopy. Z-stack images of the spheroids revealed co-localization of DOX (red) and Fe<sub>3</sub>O<sub>4</sub>-Cy5 (green) signals at various planes, suggesting deep penetration of NPs as well as their internalization into individual tumor cells (Fig. 7B). The DOX and Fe<sub>3</sub>O<sub>4</sub>-Cy5 signals were visible with substantial intensity up to the core (~29  $\mu\text{m}$ ) of the entire tumor mass (~58  $\mu\text{m}$ ). The ablation of the dense tumor cores (Fig. 8A) are indicative of exposure to CNT-DOX-Fe<sub>3</sub>O<sub>4</sub>-Tf and CNT-DOX-Fe<sub>3</sub>O<sub>4</sub>-mAb particles. Furthermore, the protection of CNT-encapsulated DOX against rapid drug efflux prior to endocytosis and the subsequent intracellular release of DOX may contribute to the enhanced antitumor effect. In contrast, free DOX and CNT-DOX-Fe<sub>3</sub>O<sub>4</sub> were less effective in tumor regression possibly as a result of the small size of free DOX or extracellularly released DOX that would be rapidly diffused away from the tumor interstitium. Interestingly, tumor viability studies demonstrated a greater anticancer activity for CNT-DOX-Fe<sub>3</sub>O<sub>4</sub> particles (Fig. 8B), compared to the targeted NPs. This may result from sustained non-specific TME-acid triggered Fe<sub>3</sub>O<sub>4</sub> uncapping and DOX release in the immediate vicinity and interior of the spheroid. The resultant system is hypothesized to have generated a very high localized DOX concentration in the TME resulting in significant cell death, but insufficient impact to destroy the tumor integrity. Tf and anti-EpCAM mAb conjugated nanobots exhibited greater cell surface targeting, however this delayed the release of DOX payload intracellularly. The effect can be attributed to surface epitope interactions between Tf as well as anti-EpCAM mAb nanobot ligands and over-expressed cell surface receptors.

Finally, although Tf and anti-EpCAM mAb conjugated nanobots achieve greater targeting their cellular internalization mechanism, release from the overexpressed cell surface receptors, and the release of DOX inside the cells seems to be delayed. This can be attributed to the specific and tight interactions between over-expressed cell surface receptors and the Tf as well as anti-EpCAM mAb nanobots. However, the self-propulsion, cell surface specificity, cell kinetics, and finally the anticancer activity measurements makes these nanobots interesting to be further explored in anticancer therapy.

## Conclusions

We have demonstrated a novel self-powered multifunctional gated nanobot that offers promising alternative drug delivery system based on rapid autonomous motion for quicker and deeper delivery to the tumor site. The nanobots were fabricated by chemically coordinating and conjugating multiple components such as Fe<sub>3</sub>O<sub>4</sub> NPs and targeting moiety such as Tf or anti-EpCAM mAb to CNT. This nanobot system combines several intriguing



features, namely self-propulsion, high DOX loading, tumor targeting and profound penetration ability, *in situ* pH triggered release of the DOX, and improved drug availability. The CNT-DOX-Fe<sub>3</sub>O<sub>4</sub>-Tf nanobots demonstrated ultrafast self-propulsion (0.972 and 0.535 mm s<sup>-1</sup>) not only in high ionic media (PBS buffer) but also in biological media such as DMEM (2.333 and 1.120 mm s<sup>-1</sup>) and blood serum (8.026 and 1.120 mm s<sup>-1</sup>), a crucial ability necessary for its use in biomedical applications. The speed of the nanobot in serum was ~8.3 and ~3.4 times the speed seen in PBS and DMEM. The driving force of 592, 1304 and 5435 pN for the nanobot's upward propulsion was significantly higher. The high driving force and thus higher speed of CNT-DOX-Fe<sub>3</sub>O<sub>4</sub>-Tf nanobot in serum is maybe due to adsorbed serum catalase enzyme which may be imparting additional propulsion by catalytic property and thus enhancing generating of oxygen bubbles. Thus, propulsion of nanobot was also observed in serum with no external H<sub>2</sub>O<sub>2</sub> indicating ability of the nanobot to propel in blood and penetrate tumor by utilizing H<sub>2</sub>O<sub>2</sub> present in the TME. The cellular uptake study showed controlled release of DOX due to opening of pH-sensitive nanogates by cleavage of amide bond in the acidic lysosomal compartments. Further, higher intensity of DOX in nucleus for CNT-DOX-Fe<sub>3</sub>O<sub>4</sub>-Tf nanobot indicated not only efficient and steady release of DOX but also superior retentive property of the nanobot carriers. Upon administration to tumor spheroids, CNT-DOX-Fe<sub>3</sub>O<sub>4</sub>-Tf and CNT-DOX-Fe<sub>3</sub>O<sub>4</sub>-mAb nanobots were significantly more efficacious in tumor reduction at 72 h than the control groups including free DOX and CNT-DOX-Fe<sub>3</sub>O<sub>4</sub> nanobot. One reason for the enhanced efficacy might be the profound tumor penetration ability due to the propulsion of CNT-DOX-Fe<sub>3</sub>O<sub>4</sub>-Tf and CNT-DOX-Fe<sub>3</sub>O<sub>4</sub>-mAb nanobots, and the delayed clearance at the tumor site because of the retention property of the NPs. Thus, the synthesized CNT-DOX-Fe<sub>3</sub>O<sub>4</sub>-mAb and CNT-DOX-Fe<sub>3</sub>O<sub>4</sub>-Tf nanobots would be effective in smaller numbers, designed to selectively and efficaciously deliver the drug payload in targeted cancer cells alone within the TME.

## Materials and methods

**Reagents.** Multi-walled carbon nanotubes (CNTs) having outer diameter of 10–15 nm; length 1–5 μm; and purity >99%, were purchased from Ad-Nano Technologies, India. Ferric chloride tetrahydrate, ferrous chloride hexahydrate, transferrin (Tf), *N*-(3-Dimethylaminopropyl)-*N'*-ethylcarbodiimide (EDC.HCl), glutathione (GSH) and horseradish peroxidase (type VI) were purchased from Sigma-Aldrich, USA. Doxorubicin hydrochloride (DOX) was received as a gift from Naprod Life Sciences, India. Cy5 mono NHS ester was procured from GE Healthcare UK Limited, and LysoTracker Green DND-26 was procured from Invitrogen, Thermo Fisher Scientific. HCT116 cells were obtained from the National Centre for Cell Science, India. McCoy's 5A, fetal bovine serum (FBS), Penicillin and streptomycin were purchased from Sigma-Aldrich, USA. Ultrapure water (MilliQ) acquired from a Merck Millipore system, Germany, was used throughout. All other chemicals procured were of analytical grade and utilized without further purification.

**Functionalization of CNTs (CNT-COOH).** CNT was purified and oxidized using a modified literature procedure<sup>52</sup>. In brief, 85 mg of CNT was dispersed in 100 mL mixture of H<sub>2</sub>SO<sub>4</sub>/HNO<sub>3</sub> (3:1) and then sonicated for 6 h. The mixture was diluted with 100 mL ice cold water, concentrated by centrifugation and washed with 5% NaOH solution and ultra-pure water. Resulting functionalized CNT was dried at 80 °C (12 h).

**Synthesis of Fe<sub>3</sub>O<sub>4</sub>-GSH.** Fe<sub>3</sub>O<sub>4</sub> NPs were prepared by co-precipitation of ferric and ferrous ions (2:1) using aqueous ammonium hydroxide solution and then heated at 80 °C for 30 min, washed for several times with ultra-pure water and ethanol and finally dried at 70 °C (4–6 h)<sup>53</sup>. 5 mg of Fe<sub>3</sub>O<sub>4</sub> NPs were dispersed in 150 μl of ultra-pure water and 50 μl of methanol and sonicated for 15 min. 4 mg of GSH was dissolved in 50 μl of ultra-pure water, added in above solution and again sonicated for 2 h. The GSH functionalized NPs were then isolated by magnetic separation, washed repeatedly with ultra-pure water and dried well<sup>54</sup>.

**Loading of DOX in CNT-COOH (CNT-DOX).** Loading of DOX in CNT-COOH was carried using a modified procedure previously reported by us<sup>24</sup>. Briefly, 20 mg of CNT-COOH were suspended in 5 mL solution of DOX (8 mg/mL). The solution was sonicated for 6 h and was allowed to stand for further 12 h. The synthesized product, CNT-DOX was collected by centrifugation and dried well at room temperature.

**Synthesis of CNT-DOX-Fe<sub>3</sub>O<sub>4</sub>.** 20 mg of CNT-DOX and 5 mg of EDC were added in 5 mL of phosphate buffer (pH 7.4) and then agitated for 30 min. 20 mg of Fe<sub>3</sub>O<sub>4</sub>-GSH was added in the same mixture and agitated for another 1 h. The conjugated CNT-DOX-Fe<sub>3</sub>O<sub>4</sub> NPs were magnetically separated, washed extensively with phosphate buffer to remove externally adsorbed DOX and then dried well at 40 °C.

**Synthesis of CNT-DOX-Fe<sub>3</sub>O<sub>4</sub>-Tf.** 10 mg of CNT-DOX-Fe<sub>3</sub>O<sub>4</sub> were treated with 1 mL of EDC and NHS solution (50 mM each solution in phosphate buffer (pH 7.4)). After 30 min of agitation, CNT-DOX-Fe<sub>3</sub>O<sub>4</sub> NPs were separated with magnet and washed with PBS (3 times). 1 mL of Tf solution (5 mg/mL) was added. The reaction was then agitated for 4 h. The synthesized product, CNT-DOX-Fe<sub>3</sub>O<sub>4</sub>-Tf NPs were collected by magnetic separation and dried well at room temperature. Similarly, conjugation of anti-EpCAM mAb to CNT-DOX-Fe<sub>3</sub>O<sub>4</sub> NPs was carried out.

**Characterization.** TEM analysis was carried out using Tecnai FEI G2 (accelerating voltage of 300 kV). The samples were prepared by placing a drop of CNT-DOX-Fe<sub>3</sub>O<sub>4</sub>-Tf suspensions (in DI water) onto a Formvar-covered copper grid. The water was allowed to evaporate in air at room temperature before imaging. FTIR spectral studies were carried out using a Perkin Elmer Fourier Transform Infrared (FTIR) spectrometer, USA in the range between 4000 and 400 cm<sup>-1</sup>, with a resolution of 2 cm<sup>-1</sup>. The UV-Vis absorption spectra were recorded on Agilent Technologies Cary 60 UV spectrophotometer.

**Catalytic activity of Fe<sub>3</sub>O<sub>4</sub> in H<sub>2</sub>O<sub>2</sub>.** The catalytic activity of Fe<sub>3</sub>O<sub>4</sub> in H<sub>2</sub>O<sub>2</sub> was evaluated by incubating a 500 µg/mL dispersion of Fe<sub>3</sub>O<sub>4</sub> in PBS pH 7.4 with various concentrations of H<sub>2</sub>O<sub>2</sub> (0.006 w/v% to 0.05 w/v%) for 30 min. The difference in initial concentration of H<sub>2</sub>O<sub>2</sub> and the concentration of H<sub>2</sub>O<sub>2</sub> after 30 min was used to determine the rate of reaction. The concentration of H<sub>2</sub>O<sub>2</sub> in solution was determined using a modified horseradish peroxidase (HRP) based colorimetric assay<sup>55</sup>. Briefly, 10 µL of test sample (either standard H<sub>2</sub>O<sub>2</sub> solutions for calibration curve or reaction samples) was added to 990 µL of an enzyme mixture and incubated for 30 min in dark. The enzyme mixture comprised of 500 µL of 84 mM phosphate buffer pH 7, 350 µL of 12 mM phenol, 100 µL of 0.5 mM 4-aminoantipyrene and 40 µL of 1 U/mL of HRP in 84 mM phosphate buffer pH 7. The absorbance was read at 505 nm.

**Motion behavior of nanobot in different fluids.** The self-propulsion of the CNT-DOX-Fe<sub>3</sub>O<sub>4</sub>-Tf nanobot in PBS, DMEM and serum with different concentrations of H<sub>2</sub>O<sub>2</sub> (0, 0.05, 0.1, 0.5, 1, 2, 4, 6 and 8%), was recorded with Dino-Lite digital microscope at 50× magnification, using the Dino-Capture 2.0 v (<https://www.dino-lite.com/>). This was then processed to convert in to Avi format using Format Factory and chosen best clip using VirtualDub 1.10.4 v (<http://www.virtualdub.org/>). The propelling microparticles were tracked and calculated its speed using MTrackJ plugin from ImageJ 1.8.0\_112v (<https://imagej.net/MTrackJ>).

**Drug release profiles of the nanobot.** pH dependent *in vitro* release profile of DOX from CNT-DOX-Fe<sub>3</sub>O<sub>4</sub>-Tf was evaluated by suspending 10 mg of material in 20 ml of pH 5 and pH 7.4 phosphate buffer. The nano system was stirred continuously at ambient temperature. 1 ml of aliquot was withdrawn at different time intervals, centrifuged and was analyzed using UV spectroscopy at λ<sub>max</sub> of 484 nm. 1 ml of fresh phosphate buffer of same pH was replaced at every time point in the dissolution media. All the experiments were performed in triplicate.

**Cell culture.** HCT116 was procured from NCCS and cultured in McCoy's 5A, supplemented with 10% fetal bovine serum and 100 unit/ml penicillin, 100 mg/ml streptomycin and maintained in CO<sub>2</sub> incubator at 37 °C and 5% CO<sub>2</sub> saturation.

**Nanobot's efficacy as drug delivery vehicle.** The cytotoxic activity of compounds was quantitatively determined by a colorimetric assay utilizing (3-(4, 5-dimethylthiazol-2-yl)-2, 5- diphenyltetrazolium bromide) (MTT). HCT116 cells were seeded in 96-well plates (5000 cells/well) and maintained in CO<sub>2</sub> incubator for 24 h at 37 °C in McCoy's 5A medium supplemented with 10% FBS and 1% antibiotics. The free DOX, CNT-COOH, CNT-Fe<sub>3</sub>O<sub>4</sub>, CNT-DOX-Fe<sub>3</sub>O<sub>4</sub>-Tf and CNT-DOX-Fe<sub>3</sub>O<sub>4</sub>-mAb nanobots were added in the wells and incubated for 48 h. The DOX concentration in the study was 0.377 µg/ml (IC<sub>50</sub>). The cells were then incubated with MTT for 4 h at 37 °C. In the viable cells mitochondrial succinic dehydrogenase reduced MTT to an insoluble formazan precipitate. After removal of the media, dimethylsulfoxide (DMSO) was added to each well. After complete solubilization of the purple MTT formazan (approximately 10–15 min), the absorbance was measured at 570 nm with a microplate reader on Infinites F200 PRO (Tecan, Austria). Background readings (blank) were obtained from cell-free wells containing media also incubated with the MTT solution.

**Time dependent cellular entry studies using fluorescence microscopy.** 5000 cells of HCT116, were seeded in each well of 96 well plate. After 24 h, cells were treated with free DOX, CNT-DOX-Fe<sub>3</sub>O<sub>4</sub> and CNT-DOX-Fe<sub>3</sub>O<sub>4</sub>-Tf nanobots in a time dependent manner (1 h, 4 h, 24 h and 48 h). The concentration of DOX was 0.377 µg/ml (IC<sub>50</sub>). The free DOX and all the nanobots were added according to the IC<sub>50</sub> value of DOX and the DOX loading (60 µg/mg) in the nanobots. The media were removed and cells were washed with phosphate buffered saline (PBS) after consecutive time points and processed for fluorescence microscopy. Cells were fixed with 4.0% (w/v) paraformaldehyde for 15 min at room temperature, then washed with PBS and maintained in PBS. Cells were stained with 4,6-diamidino-2-phenylindole (DAPI) (Sigma) and examined under a fluorescence microscope (Carl Zeiss, AxioObserver A3, USA).

Additionally, the co-localization of DOX in acidic lysosomal compartments with LysoTracker green as a fluorescent probe was studied using confocal laser scanning microscopy (CLSM), Leica Microsystems.

**Time dependent cellular entry studies using zeta potential.** HCT116 cells were incubated with CNT-DOX-Fe<sub>3</sub>O<sub>4</sub>-Tf nanobots at pH 7.4 and 6.5 in presence or absence of H<sub>2</sub>O<sub>2</sub> (4.98 mM). The 5000 cell were re-suspended in 1 mL of 40 mM HEPES buffer pH 7.4 and 6.5. The zeta potential values of HCT116 cells and cells incubated with CNT-DOX-Fe<sub>3</sub>O<sub>4</sub>-Tf for different time duration *viz.* 0 min and 24 h, were measured using Zetasizer Nano ZS (Malvern Instruments, Worcestershire, UK). All the Zeta (ξ) potential measurements were carried out at room temperature using phase analysis light scattering mode.

**Culture of HCT116 cell 3D spheroidal tumor.** 3D tumor spheroids were formed by a modified method of the hanging drop technique<sup>49</sup>. In brief, the lid of sterile 12 well plates were coated with poly(dimethoxysiloxane) (PDMS) and Sylgard 184 in a 10:1 ratio and cured at 80 °C for around 45 min. The lids were then placed under UV for 30 min to ensure sterility of the PDMS coated surface. HCT116 cell suspension was prepared in complete McCoy's 5A medium. 20 µL drops of the cell suspension with a density of 2,500 cells/drop were placed at regular intervals on the PDMS coated lid. The wells were filled with sterile MilliQ water to ensure hydration of drops upon incubation. Thereafter, the cells were incubated at 37 °C in presence of 5% CO<sub>2</sub> for three days. Finally, the coherent mass of 3D tumor spheroids formed was selected for further studies.

**Antitumor efficacy of drug loaded nanobots.** Tumors generated by hanging drop method were transferred to 96 well plate for treatment with DOX and nanobots. The 3D tumor spheroids upon transfer to 96 well

plate were immediately treated with free DOX (5 µg/mL) and nanobots containing equivalent DOX for 72 h. The images of tumors were captured using Carl Zeiss, AxioObserver A3, USA, USA inverted fluorescence microscope. The exposure time while capturing bright field images was fixed at 100 ms and the exposure time while capturing fluorescence images was fixed at 400 ms.

Furthermore, the viability of tumors after 72 h was analyzed by MTT assay following similar protocol mentioned earlier. Similarly, for CLSM the 3D tumor spheroids were transferred to a glass bottom well plate before capturing z-stack images. The z-stack images were captured at intervals of 0.75 µm.

Received: 20 December 2019; Accepted: 24 February 2020;

© The Author(s) 2020

## References

- Tu, Y., Peng, F., White, P. B. & Wilson, D. A. Redox-Sensitive Stomatocyte Nanomotors: Destruction and Drug Release in the Presence of Glutathione. *Angew. Chemie Int. Ed.* **56**, 7620–7624 (2017).
- Li, J. *et al.* Micromotors Spontaneously Neutralize Gastric Acid for pH-Responsive Payload Release. *Angew. Chemie Int. Ed.* **56**, 2156–2161 (2017).
- de Ávila, B. E.-F. *et al.* Micromotor-enabled active drug delivery for *in vivo* treatment of stomach infection. *Nat. Commun.* **8**, 272 (2017).
- Hortelão, A. C., Patiño, T., Perez-Jiménez, A., Blanco, À. & Sánchez, S. Enzyme-Powered Nanobots Enhance Anticancer Drug Delivery. *Adv. Funct. Mater.* **28**, 1705086 (2018).
- Tu, Y. *et al.* Biodegradable Hybrid Stomatocyte Nanomotors for Drug Delivery. *ACS Nano* **11**, 1957–1963 (2017).
- Li, J., Esteban-Fernández de Ávila, B., Gao, W., Zhang, L. & Wang, J. Micro/nanorobots for biomedicine: Delivery, surgery, sensing, and detoxification. *Sci. Robot.* **2**, eaam6431 (2017).
- Yan, X. *et al.* Multifunctional biohybrid magnetite microrobots for imaging-guided therapy. *Sci. Robot.* **2**, eaag1155 (2017).
- Nelson, B. J., Kaliakatsos, I. K. & Abbott, J. J. Microrobots for Minimally Invasive Medicine. *Annu. Rev. Biomed. Eng.* **12**, 55–85 (2010).
- Wang, J. & Gao, W. Nano/Microscale Motors: Biomedical Opportunities and Challenges. *ACS Nano* **6**, 5745–5751 (2012).
- Gao, W. *et al.* Artificial Micromotors in the Mouse's Stomach: A Step toward *in Vivo* Use of Synthetic Motors. *ACS Nano* **9**, 117–123 (2015).
- Peng, F., Tu, Y., van Hest, J. C. M. & Wilson, D. A. Self-Guided Supramolecular Cargo-Loaded Nanomotors with Chemotactic Behavior towards. *Cells. Angew. Chemie* **127**, 11828–11831 (2015).
- Wang, H. & Pumera, M. Fabrication of Micro/Nanoscale Motors. *Chem. Rev.* **115**, 8704–8735 (2015).
- Sánchez, S., Soler, L. & Katuri, J. Chemically Powered Micro- and Nanomotors. *Angew. Chemie Int. Ed.* **54**, 1414–1444 (2015).
- Wang, H. & Pumera, M. Emerging materials for the fabrication of micro/nanomotors. *Nanoscale* **9**, 2109–2116 (2017).
- Zhang, Q., Wang, N., Ma, M., Luo, Y. & Chen, H. Transferrin Receptor-Mediated Sequential Intercellular Nanoparticles Relay for Tumor Deep Penetration and Sonodynamic Therapy. *Adv. Ther.* **2**, 1800152 (2019).
- Zhang, Q. *et al.* Inlaying radiosensitizer onto the polypeptide shell of drug-loaded ferritin for imaging and combinational chemoradiotherapy. *Theranostics* **9**, 2779–2790 (2019).
- Luo, M., Feng, Y., Wang, T. & Guan, J. Micro-/Nanorobots at Work in Active Drug Delivery. *Adv. Funct. Mater.* **28**, 1706100 (2018).
- Wu, Y., Wu, Z., Lin, X., He, Q. & Li, J. Autonomous Movement of Controllable Assembled Janus Capsule Motors. *ACS Nano* **6**, 10910–10916 (2012).
- Peng, F., Tu, Y. & Wilson, D. A. Micro/nanomotors towards *in vivo* application: cell, tissue and biofluid. *Chem. Soc. Rev.* **46**, 5289–5310 (2017).
- Sitti, M. *et al.* Biomedical Applications of Untethered Mobile Milli/Microrobots. *Proc. IEEE* **103**, 205–224 (2015).
- Szatrowski, T. P. & Nathan, C. F. Production of Large Amounts of Hydrogen Peroxide by Human Tumor Cells. *Cancer Res.* **51**, 794–798 (1991).
- Sun, Y.-P., Fu, K., Lin, Y. & Huang, W. Functionalized Carbon Nanotubes: Properties and Applications. *Acc. Chem. Res.* **35**, 1096–1104 (2002).
- Kostarelos, K. The long and short of carbon nanotube toxicity. *Nat. Biotechnol.* **26**, 774–776 (2008).
- Banerjee, S. S. *et al.* Calcium phosphate nanocapsule crowned multiwalled carbon nanotubes for pH triggered intracellular anticancer drug release. *J. Mater. Chem. B* **3**, 3931–3939 (2015).
- Sun, C. *et al.* PEG-mediated synthesis of highly dispersive multifunctional superparamagnetic nanoparticles: their physicochemical properties and function *in vivo*. *ACS Nano* **4**, 2402–10 (2010).
- Halliwell, B., Clement, M. V. & Long, L. H. Hydrogen peroxide in the human body. *FEBS Lett.* **486**, 10–3 (2000).
- Veal, E. A., Day, A. M. & Morgan, B. A. Hydrogen Peroxide Sensing and Signaling. *Mol. Cell* **26**, 1–14 (2007).
- Lacy, F., O'Connor, D. T. & Schmid-Schönbein, G. W. Plasma hydrogen peroxide production in hypertensives and normotensive subjects at genetic risk of hypertension. *J. Hypertens.* **16**, 291–303 (1998).
- Lisanti, M. P. *et al.* Hydrogen peroxide fuels aging, inflammation, cancer metabolism and metastasis. *Cell Cycle* **10**, 2440–2449 (2011).
- Vilema-Enríquez, G., Arroyo, A., Grijalva, M., Amador-Zafra, R. I. & Camacho, J. Molecular and Cellular Effects of Hydrogen Peroxide on Human Lung Cancer Cells. *Potential Therapeutic Implications. Oxid. Med. Cell. Longev.* **2016**, 1–12 (2016).
- Liu, S.-L. *et al.* Reactive oxygen species stimulated human hepatoma cell proliferation via cross-talk between PI3-K/PKB and JNK signaling pathways. *Arch. Biochem. Biophys.* **406**, 173–82 (2002).
- Park, I.-J., Hwang, J.-T., Kim, Y. M., Ha, J. & Park, O. J. Differential Modulation of AMPK Signaling Pathways by Low or High Levels of Exogenous Reactive Oxygen Species in Colon Cancer Cells. *Ann. N. Y. Acad. Sci.* **1091**, 102–109 (2006).
- Dartier, J. *et al.* ATP-dependent activity and mitochondrial localization of drug efflux pumps in doxorubicin-resistant breast cancer cells. *Biochim. Biophys. Acta - Gen. Subj.* **1861**, 1075–1084 (2017).
- Mirzaei, H. & Regnier, F. Protein:protein aggregation induced by protein oxidation. *J. Chromatogr. B* **873**, 8–14 (2008).
- Sabuncu, A. C. *et al.* Probing nanoparticle interactions in cell culture media. *Colloids Surfaces B Biointerfaces* **95**, 96–102 (2012).
- Weids, A. J., Ibstedt, S., Tamás, M. J. & Grant, C. M. Distinct stress conditions result in aggregation of proteins with similar properties. *Sci. Rep.* **6**, 24554 (2016).
- Khandare, J. J. *et al.* PEG-conjugated highly dispersive multifunctional magnetic multi-walled carbon nanotubes for cellular imaging. *Nanoscale* **4**, 837–844 (2012).
- Allen, B. L. *et al.* Mechanistic Investigations of Horseradish Peroxidase-Catalyzed Degradation of Single-Walled Carbon Nanotubes. *J. Am. Chem. Soc.* **131**, 17194–17205 (2009).
- Ma, X., Hortelão, A. C., Patiño, T. & Sánchez, S. Enzyme Catalysis To Power Micro/Nanomachines. *ACS Nano* **10**, 9111–9122 (2016).
- Orozco, J. *et al.* Artificial Enzyme-Powered Microfish for Water-Quality Testing. *ACS Nano* **7**, 818–824 (2013).
- Shankar, R. *et al.* Cathepsin B Degradable Star-Shaped Peptidic Macromolecules for Delivery of 2-Methoxyestradiol. *Mol. Pharm.* **10**, 3776–3788 (2013).



42. Chae, S. *et al.* Encapsulation and Enhanced Delivery of Topoisomerase I Inhibitors in Functionalized Carbon Nanotubes. *ACS Omega* **3**, 5938–5945 (2018).
43. Thorn, C. F. *et al.* Doxorubicin pathways. *Pharmacogenet. Genomics* **21**, 440–446 (2011).
44. Kiyomiya, K., Matsuo, S. & Kurebe, M. Proteasome is a carrier to translocate doxorubicin from cytoplasm into nucleus. *Life Sci.* **62**, 1853–1860 (1998).
45. Liu, J., Zheng, H., Tang, M., Ryu, Y.-C. & Wang, X. A therapeutic dose of doxorubicin activates ubiquitin-proteasome system-mediated proteolysis by acting on both the ubiquitination apparatus and proteasome. *Am. J. Physiol. Circ. Physiol.* **295**, H2541–H2550 (2008).
46. Munoz, M., Henderson, M., Haber, M. & Norris, M. Role of the MRP1/ABCC1 Multidrug Transporter Protein in Cancer. *IUBMB Life* **59**, 752–757 (2007).
47. Thorstensen, K. & Romslo, I. The role of transferrin in the mechanism of cellular iron uptake. *Biochem. J.* **271**, 1–9 (1990).
48. Lähdesmäki, K., Ollila, O. H. S., Koivuniemi, A., Kovanen, P. T. & Hyvönen, M. T. Membrane simulations mimicking acidic pH reveal increased thickness and negative curvature in a bilayer consisting of lysophosphatidylcholines and free fatty acids. *Biochim. Biophys. Acta - Biomembr.* **1798**, 938–946 (2010).
49. Kuo, C.-T. *et al.* Three-dimensional spheroid culture targeting versatile tissue bioassays using a PDMS-based hanging drop array. *Sci. Rep.* **7**, 4363 (2017).
50. Hillen, F. & Griffioen, A. W. Tumour vascularization: sprouting angiogenesis and beyond. *Cancer Metastasis Rev.* **26**, 489–502 (2007).
51. Liao, D. & Johnson, R. S. Hypoxia: A key regulator of angiogenesis in cancer. *Cancer Metastasis Rev.* **26**, 281–290 (2007).
52. Zhou, M. *et al.* Doxorubicin-Loaded Single Wall Nanotube Thermo-Sensitive Hydrogel for Gastric Cancer Chemo-Photothermal Therapy. *Adv. Funct. Mater.* **25**, 4730–4739 (2015).
53. Banerjee, S. S. & Chen, D.-H. Magnetic Nanoparticles Grafted with Cyclodextrin for Hydrophobic Drug Delivery. *Chem. Mater.* **19**, 6345–6349 (2007).
54. Polshettiwar, V., Baruwati, B. & Varma, R. S. Magnetic nanoparticle-supported glutathione: A conceptually sustainable organocatalyst. *Chem. Commun.* **14**, 1837–1839 (2009).
55. Fernando, C. D. & Soysa, P. Optimized enzymatic colorimetric assay for determination of hydrogen peroxide (H<sub>2</sub>O<sub>2</sub>) scavenging activity of plant extracts. *MethodsX* **2**, 283–291 (2015).

## Acknowledgements

We acknowledge financial support from Department of Biotechnology, Government of India and Department of Science and Technology, Government of India.

## Author contributions

S.S.B. and J.J.K. conceived the idea and designed the research. S.S.B., J.J.K., R.D.W., K.D.D. and Y.N.P. co-analyzed the experimental and calculated data. S.S.B., J.J.K., S.S.A., R.D.W., G.P.C. and Y.N.P. contributed to the writing and editing of the manuscript. R.D.W. prepared the nanobots and also performed the motion experiments. K.D.D. performed the *in vitro* cellular entry and cytotoxicity studies. B.V.T. supported the experiments on TEM characterization. S.S.A. supported all *in vitro* tumor experiments. S.S.B. directed the project. All authors reviewed the manuscript.

## Competing interests

The authors declare no competing interests.

## Additional information

**Supplementary information** is available for this paper at <https://doi.org/10.1038/s41598-020-61586-y>.

**Correspondence** and requests for materials should be addressed to J.J.K. or S.S.B.

**Reprints and permissions information** is available at [www.nature.com/reprints](http://www.nature.com/reprints).

**Publisher's note** Springer Nature remains neutral with regard to jurisdictional claims in published maps and institutional affiliations.



**Open Access** This article is licensed under a Creative Commons Attribution 4.0 International License, which permits use, sharing, adaptation, distribution and reproduction in any medium or format, as long as you give appropriate credit to the original author(s) and the source, provide a link to the Creative Commons license, and indicate if changes were made. The images or other third party material in this article are included in the article's Creative Commons license, unless indicated otherwise in a credit line to the material. If material is not included in the article's Creative Commons license and your intended use is not permitted by statutory regulation or exceeds the permitted use, you will need to obtain permission directly from the copyright holder. To view a copy of this license, visit <http://creativecommons.org/licenses/by/4.0/>.

© The Author(s) 2020

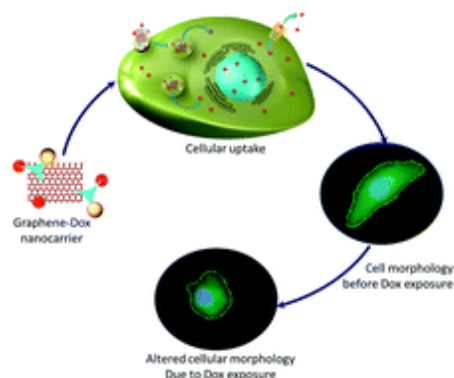
# Cell deformation and acquired drug resistance: elucidating the major influence of drug-nanocarrier delivery systems†

Semonti Nandi,<sup>‡a</sup> Narendra R. Kale,<sup>‡a</sup> Vijay Takale,<sup>a</sup> Govind C. Chate,<sup>a</sup> Madhura Bhawe,<sup>§a</sup> Shashwat S. Banerjee<sup>id</sup><sup>\*b</sup> and Jayant J. Khandare<sup>id</sup><sup>\*c</sup>

Author affiliations

## Abstract

Cancer diagnosis and its stage-wise assessment are determined through invasive solid tissue biopsies. Conversely, cancer imaging is enriched through emission tomography and longitudinal high-resolution analysis for the early detection of cancer through altered cell morphology and cell-deformation. Similarly, in post multiple chemo-cycle exposures, the tumor regression and progression thereafter are not well understood. Here, we report chemo-cycles of doxorubicin (Dox) carrying nanoparticles (NPs) to be highly indicative of cell deformation and a progressive indicator of phenotypic expressions of acquired drug resistance (ADR). We designed graphene (G) based nanocarriers by chemically conjugating multiple components: (i) G; (ii) iron oxide ( $\text{Fe}_3\text{O}_4$ ) NPs; and (iii) Dox through a cysteine (Cys) linker (G-Dox and G-Cys- $\text{Fe}_3\text{O}_4$ -Dox). Although Dox underwent cell diffusion, the G-based nanocarriers followed a receptor-mediated endocytosis which created a profound impact on the cell membrane integrity. ADR owing to Dox and G-based nanocarriers was analyzed through a cytotoxicity assay, cell morphology deformation parameters and cellular uptake kinetic patterns. Interestingly, after the third chemo-cycle, G-Dox incubated cells showed the greatest decrease in the alteration of the nuclear surface area (NSA) of  $\sim 28\%$ , a  $\sim 40\%$  reduction of the cell surface area (CSA) and a  $\sim 32\%$  increase in the cell roundness (CRd). Our results suggested that the G-based nanocarriers induced the cell deformation process, subsequently resulting in ADR. Although the G-based nanocarriers initiated ADR, G-Dox was most cytotoxic to cancer cells and induced the maximum cell morphology deformation within our scope of study. This outcome implies caution is needed when using G-based nanocarriers and other multi-component nanosystems for Dox delivery as they lead to possible phenotypic expressions of drug resistance in cancer cells.



# Does the Angle of Rigid Endoscope Makes a Difference in Videolaryngoscopy

Sapna Ramkrishna Parab<sup>1</sup> · Mubarak M. Khan<sup>2</sup>

Received: 3 May 2018 / Accepted: 18 June 2018 / Published online: 24 June 2018  
© Association of Otolaryngologists of India 2018

**Abstract** Authors describe the technique of office based rigid video laryngoscopy with 0° endoscope and compare with technique of 70° 4 mm videolaryngoscopy. (1) To compare and assess the efficacy of techniques of 0° and 70° office based video laryngoscopy for examining laryngopharyngeal disorders at Ear Nose Throat (ENT) Out Patient Department level. (2) To assess whether the degree of angle of the rigid endoscope makes any difference in the visualisation in videolaryngoscopy. Prospective non randomised double blinded study of direct videolaryngoscopies using 0° and 70° 4 mm rigid endoscope (Karl Storz, Germany) done at M.I.M.E.R. Medical College and Sushrut ENT Hospital, Talegaon-D, Pune, India, during the period of October 2016 to February 2017. Patients with predominant complaints of change of voice and foreign body sensation in throat were subjected for Videolaryngoscopy by 0° and 70° 4 mm Endoscope. 375 patients were examined with both the techniques. After the end of the procedure, the patient preference or discomfort with any of the techniques was enquired. The unlabelled endoscopic recording of both techniques was visualised by the second author to compare and evaluate the 0° videolaryngoscopy with 70° in terms of extent of visualisation. The time taken for each technique was recorded. The data of all patients has been analysed in terms of patient and surgeon grading. On statistical analysis, both the techniques with 0° as well as 70° rigid endoscope videolaryngoscopy were found to be

comparable. Our study concludes that both the endoscopes are equally efficient in comparable laryngeal visualization. Hence, the degree of angulation of the rigid endoscope makes no difference in videolaryngoscopy. With little practice, 0° videolaryngoscopy may be extended for routine use in laryngological examination.

*Level of Evidence* Level 4.

**Keywords** Laryngoscopy · 0° · 70° endoscope · Office procedure

## Introduction

Laryngoscopy or examination of the larynx is an essential part of the otolaryngologic examination. The 19th-century voice teacher Manuel Garcia was probably among the first to perform laryngoscopy in vivo [1]. Since introduction, the technique of indirect mirror laryngoscopy has been superseded by technologies that allow better visualization of the laryngeal structures through improved image resolution, improved light transfer, and greater patient comfort [2]. The first physician to directly visualise the larynx was the Berlin Laryngologist, Tobold [3, 4]. In the modern era of the endoscopy, the collaboration of Karl Storz and Harold Hopkins and the resulting in Hopkins rod telescope is a mainstay of otolaryngologic endoscopy. Indirect endoscopy through the rod-lens system provides not only excellent visualization but also stability of the light transmission system. In combination with 70 or 90 prisms, peroral laryngeal observations can be made in most patients [2].

Since last one decade, the senior author has been using the 0° rigid endoscope for laryngopharyngeal examination at office level as it gives end on direct visualisation of

✉ Sapna Ramkrishna Parab  
drsapnaparab@gmail.com

<sup>1</sup> Department of Otolaryngology, M.I.M.E.R. Medical College, Pune 410507, India

<sup>2</sup> Consultant Sushrut Hospital and Dr. Khan's ENT Research Center, Talegaon D, Pune, India

larynx and allows to look into the nooks and corners of larynx [5]. It is our opinion that the technique of 0° videolaryngoscopy is a useful technique for laryngeal examination with few additional advantages over 70°. This study was thus carried out to compare techniques of office based rigid video laryngoscopy with 0° and 70° endoscopes.

## Materials and Methods

A prospective study of videolaryngoscopies with 0° and 70° rigid endoscopes in consecutive 375 patients attending our Otolaryngology Out-Patient Department has been carried out from October 2016 to February 2017. The total number of males and females were 236 and 139 respectively. The patients ranged from 15 to 76 years with the mean age of the study group was  $37.23 \pm 11.54$  years. First author, skilled in both 0° and 70° videolaryngoscopies performed the examination.

The patients underwent videolaryngoscopies with both the techniques. Written consent was taken. Only one attempt was allowed with each technique. The throat was sprayed with 10% lidocaine. After completion of each procedure, the patient was asked to grade each technique from 1 to 10 (1 being poorest and 10 being the best) in terms of gagging and discomfort and to mention their preference for which of the two techniques. The recordings of the two techniques of laryngoscopic visualisation in each patient were evaluated by the second author (unaware of the sequence of the examination techniques) as to evaluate in terms of complete examination (graded from 1 to 10). All the videolaryngologic examinations were labelled with a coding system with no clue to the type of examination technique and the grading system for evaluation was done. Thus, bias or preference to a particular technique during grading was avoided.

We have developed a grading system for extent of the laryngopharyngeal visualisation:

- 1 = oropharyngeal examination
- 2 = 1 ? epiglottis seen
- 3 = 2 ? arytenoids seen
- 4 = 3 ? Aryepiglottic fold seen
- 5 = 4 ? pyriform fossa seen
- 6 = 5 ? partial view of True Vocal Cords and False Vocal Cords
- 7 = 5 ? total view of True Vocal Cords and False Vocal Cords and anterior commissure
- 8 = 7 ? ventricle ? vallecula visualised
- 9 = 8 ? subglottis visualised
- 10 = 9 ? tracheal rings (total view)

The time taken for each and every videolaryngoscopy by both the techniques was noted and documented.

The patient as well as the evaluator was blinded to the type of technique and sequence and hence the grading was done.

## Procedure of Videolaryngoscopy by 0° and 70° 4 mm rigid Endoscope

The office procedures are done with the patient sitting on chair and the otolaryngologist stands in front of the patient. The posterior pharyngeal wall is anaesthetized with 10% lidocaine spray to prevent the gag reflex.

### 0° Videolaryngoscopy: Figs. 1, 2, 3, 4, 5 and 6

0° 4 mm endoscope is connected to the light source and endoscopic camera recording facility, with the television monitor in front of the patient. The mouth of the patient is wide open and tongue protruding. The head of patient is partially extended posteriorly over the neck so that oral cavity axis and laryngeal axis will be aligned in one plane as far as possible. With the help of sterilized gauze piece, the anterior part of the tongue is gently held out with the left hand and 0° 4 mm endoscope with the right hand. Initially endoscope kept straight in horizontal position touching upper incisors to evaluate oropharynx completely. Then it is advanced into the oral cavity along the left angle of mouth using upper left first molar as a fulcrum which avoids the undue strain over the rod lens system of the endoscope. Without touching anterior one-third of the tongue, the oropharynx is visualised and the endoscope is progressed inwards toward the base of tongue to visualise the vallecula and posterior pharyngeal wall. The endoscope is then, given a downward inclination. This allows the visualization of the epiglottis and laryngeal inlet. The endoscope further advanced downwards into the interior of the larynx to allow visualisation of the false vocal cords, ventricle, true vocal cords, anterior commissure, arytenoids, aryepiglottic folds, pyriform fossae, subglottis and



Fig. 1 Oropharynx view with 0° sinuscope





Fig. 2 0° sinuscope view of epiglottis and vallecula



Fig. 5 End on view of vocal cords with 0° endoscope. 1: Anterior commissure, 2: false vocal cords, 3: right true vocal cord, 4: posterior commissure, 5: left true vocal cord, black arrow: right ventricle



Fig. 3 Larynx during phonation view with 0° sinuscope. 1: Closed glottis, 2: right arytenoid, 3: left aryepiglottic fold, 4: posterior pharyngeal wall, black arrows: pyriform fossa



Fig. 6 Subglottis view with 0° endoscope. 1: Right true vocal cord, 2: posterior commissure, 3: left true vocal cord, white arrows: subglottis



Fig. 4 Apex of right pyriform fossa view with 0° endoscope. 1: Right arytenoid, 2: right pyriform fossa, 3: posterior pharyngeal wall, black arrow: apex of right pyriform fossa



Fig. 7 Larynx view with 70° Endoscope. 1: Epiglottis, 2: right aryepiglottic fold, 3: right pyriform fossa, 4: right corniculate cartilage, 5: right arytenoid, 6: right false vocal cord, 7: left pyriform fossa, 8: posterior pharyngeal wall

trachea. The vocal cord mobility is assessed by asking the patient to say “ee” as in mirror laryngoscopy.

*70° videolaryngoscopy: Fig. 7*

The tongue is held with the left hand and the 70° endoscope with the right hand. Due to the 70° angulation of the

endoscope, base of the tongue and vallecula is seen immediately when lense is focused downward. With progress of the endoscope further, the interior of the larynx along with aryepiglottic fold and the pyriform fossa are visualised in one field view.

Patients are advised to avoid eating and drinking 30 min till the mucosal anaesthesia resolves.

## Results and Discussion

This study evaluates the videolaryngoscopy in 375 patients with 0° and 70° endoscopes in terms of the patient comfort, duration and the structures visualised. The completeness of the two techniques is assessed by viewing of the recordings of the two procedures by the second author. It was graded from 1 to 10 and was statistically analysed. The patient evaluation of the techniques was in terms of discomfort of the two procedures and their preference for any of the procedures. This was graded out of 10 for each of the procedure by the patient, 10 being the best and 0 being the least comfortable. This was documented and was statistically analysed.

The discomfort with the 0° and 70° videolaryngoscopy was experienced in 16 and 11 out of 375 which is 4.27 and 2.93% respectively. The mean scores of satisfaction with the 0° and 70° videolaryngoscopies was  $7.36 \pm 0.13$  and  $8.01 \pm 0.49$  respectively. The mean scores of the evaluation of the 2 techniques depending on the extent of the structures visualised was  $8.89 \pm 0.23$  and  $9.02 \pm 0.14$  respectively. With the exception of 2 patients with oral submucous fibrosis, in whom the 70° videolaryngoscopy fared better than 0°, the overall performance of 0° was comparable to the 70° videolaryngoscopy.

The mean time taken for the 0° and 70° videolaryngoscopy was  $37.24 \pm 1.28$  and  $29.31 \pm 1.01$  s respectively. On statistical analysis, there was no significant difference in the patient satisfaction level, laryngeal structures visualisation and time taken ( $p < 0.001$ ). Hence the two techniques are comparable in the parameters evaluated.

## Discussion

Laryngoscopy or laryngopharyngeal endoscopy can be performed with direct, rigid instrumentation or indirect instrumentation. Office-based laryngology is principally concerned with indirect laryngoscopy. Indirect endoscopy involves using mirrors, prisms, fiberoptic rods, or miniature chip cameras to bend or reflect the image of the pharynx and larynx back to the surgeon's eye. Direct endoscopy, in contrast, is currently most commonly performed in the

operating room under general anaesthesia. Indirect laryngoscopy allows the patient to maintain a relatively comfortable position while the examiner views the larynx and pharynx. This allows observations and procedures to be performed without general anaesthesia, and thus allows dynamic assessment of larynx and pharynx [2].

This is the first study to demonstrate the use of 0° office based laryngoscopy and compare with 70° videolaryngoscopy. We have been practicing this art of videolaryngoscopy since 2001 (last 13 years). Our previous non comparative study has been published [5]. Our technique of 0° videolaryngoscopy is an innovative one and in this study we attempt to demonstrate that in a single attempt examination of the larynx with a 4 mm zero endoscope with video monitoring was comparable to 70° in comfort, patient preference, and degree of laryngeal visualization.

The advantages of the 0° videolaryngoscopy [5]:

1. All the structures of the larynx are visualised with greater details as the endoscope can be kept very close to the structures without any trauma to the mucosal surfaces.
2. Ventricle, subglottis, anterior commissure and tracheal rings are better seen. Hence the associated pathologies can be appreciated with greater precision.
3. In depth, close end on view of each and every structure with 70°, all structures seen in one view.
4. As the structures can be visualised from near, can form the basis of contact endoscopy at office level.
5. Can be used for office based procedures: foreign body removal and biopsy with the endoscope in the non-dominant hand and the laryngeal forceps in the dominant hand and the patient grasping his tongue with sterilised gauze piece.
6. It is very economical technique as the 0° endoscope is available with every otolaryngologist and is used in routine nasal and ear endoscopy.
7. The videolaryngoscopic recording can be used for future comparison, documentation, and to share the visualization in cases of referral and is a very good teaching aid.

The other methods of videolaryngoscopies with 90° and 30° rigid endoscopes have been reported [6, 7]. The study by Barker and Dort with a 10 mm, 90° rigid endoscope in 1991 reported a success rate of 83% in topically anesthetized larynx compared to 52% success with laryngeal mirror examination [6]. Barker and Dort [6] recommended that VRLE be utilized in all university teaching programs. They noted that video documentation improves post treatment follow up, but that there was no proof that its routine use improved patient treatment. Whereas, Dunklebarger, has reported, success rate of 83.7% with 30° rigid videolaryngoscopy [7].

At present, the Voice Subspecialty in most of the institutions utilize video archiving of all laryngeal examinations with either rigid endoscopy, utilizing primarily the 10-mm 90 endoscope or video flexible fiberoptic laryngoscopy or both, frequently complemented with stroboscopic evaluation [6].

## Conclusion

In this non randomised double blinded study, we attempt to demonstrate the use of 0° videolaryngoscopy at office setup. Our study concludes that both the endoscopes were equally efficient in comparable laryngeal visualization. Though, learning the technique of 0° videolaryngoscopy requires effort, but definitely can be mastered with practice as any other art in clinical medicine. Hence it is evident that the degree of angulation of the rigid endoscope makes no difference in videolaryngoscopy. With little practice, 0° videolaryngoscopy use may be extended for routine use in the Out Patient Department. We believe that this technique may form the basis for further development of office based contact laryngoscopy and endoscopic laryngeal surgery with further study.

Compliance with Ethical Standards

Conflict of interest The authors declare that they have no conflict of interest.

## References

1. Merati AL, Rieder AA (2003) Normal endoscopic anatomy of the pharynx and larynx. *Am J Med* 115(3):10–14
2. Rosen CA, Amin MR, Sulica L et al (2009) Advances in office-based diagnosis and treatment in laryngology. *Laryngoscope* 119:S185–S212
3. Jahn A, Blitzer A (1996) A short history of laryngoscopy. *Logoped Phonatr Vocol* 21(3–4):181–185
4. Tobold A (1863) *Lehrbuch Der Laryngoskopie Und Des Localtherapeutischen Verfahrens Bei Kehlkopfkrankheiten*. Verlag von August Hirschwald, Berlin
5. Khan MM, Parab SR. Office based direct videolaryngoscopy using a 0° 4 mm sinuscope. *World articles in ENT*. <http://www.waent.org/archives/2011/Vol4-1/20110201-direct-laryngoscopy/fiberoptic-direct-largngoscopy.htm>
6. Barker M, Dort JC (1991) Laryngeal examination: a comparison of mirror examination with a rigid lens system. *J Otolaryngol* 20:100–103
7. Dunklebarger J, Rhee D, Kim S et al (2009) Video rigid laryngeal endoscopy compared to laryngeal mirror examination: an assessment of patient comfort and clinical visualization. *The Laryngoscope* 119:269–271

Research Article - Basic and Applied Anatomy

## Variability of small bowel length: Correlation with height, waist circumference, and gender

Sonali A. Khake<sup>1</sup>, Maitreyee M. Mutalik<sup>2,\*</sup>

<sup>1</sup> MIMER medical College, Talegaon 410507, India

<sup>2</sup> D Y Patil Medical College, D Y Patil Vidyapeeth, Pimpri, Pune 411018, India

### Abstract

First year medical students are always under impression that the small bowel length is almost 6 meters or more, as they have studied it in their textbooks; and when they try to measure, it does not always correspond with it. Knowledge of variable lengths of small bowel is important not just for an academic interest but it has implications in different surgical and other procedures related with small bowel length. In the present study, the height, waist circumference, and small bowel length was measured in 111 formalin-fixed cadavers (73 males and 38 females) from Indian population, and correlation of small bowel length to height, waist circumference and gender was searched, which showed small bowel length of 218-500 cm with a mean of 336.54 cm; the small bowel was significantly longer in males than that in females ( $p < 0.05$ ). Height and small bowel length showed moderately positive correlation with each other while waist circumference and small bowel length showed a strong positive reciprocal correlation. Linear regression analysis showed statistically significant relationship for both. Central obesity showed no correlation with small bowel length in males ( $R = 0.049$ ) and weak correlation in females ( $R = 0.281$ ). Small bowel length/height ratio as well as small bowel length/waist circumference ratio did not show statistically significant differences in either gender. Small bowel length in Indian population was found to be less than that reported in western studies or medical textbooks - a relevant finding - to be considered in application of different procedures and surgery of small intestine in Indian individuals.

### Key words

Intestine, small bowel length, height, waist circumference, bariatric surgery, resection.

### Introduction

Even though variability of small intestine has been known to researchers for many years, in traditional standard medical textbooks the small bowel length has been mentioned as around 6-7 meters (Williams and Warwick, 1980; Snell, 2012; Drake et al., 2015). First year medical students are always under impression that the small bowel length is almost 6 meters or more, and when they try to measure it the result does not always correspond with that expectation. In a research article of 1955, Underhill (1955) mentioned that the medical students had been unaware of such a deviation. This is also true even today.

The small bowel is a part of gastrointestinal tract from pyloric sphincter to the ileocecal junction, which comprises duodenum, jejunum and ileum. Duodenum is a

\* Corresponding author. E-mail: maitreyemadhav@gmail.com



fixed part with the length of 20-25 cm, while the remaining small bowel is free with total length of 3-7 meters in the living adults (Gabe, 2008). Research workers have considered many factors - like height, weight, obesity, age, gender etc. - that may have association with the variation in length of small bowel, but there is no uniformity of results in these studies (Guzman et al., 1977; Zhu et al., 2002; Hosseinpour and Behdad, 2008; Minko et al., 2014). In the present study the length of small bowel was measured in formalin-fixed adult cadavers of Indian origin. An attempt was made to correlate the small bowel length (SBL) with the height (H), waist circumference (WC) and sex of an individual. Knowledge of variable length of small bowel is not just for an academic interest but is important in massive resection of small bowel, intestinal bypass surgery, enteroscopy, magnetic resonance enterography, bariatric surgery or other types of surgery related to small bowel length. Studies of small bowel length (SBL) will provide a better approach for such procedures and surgery.

## Materials and methods

The present study was conducted during a period of 7 years on 120 formalin-fixed cadavers in three medical colleges in Maharashtra State of India between 2010 and 2017. Out of the total 120 cadavers, 111 (73 males, 38 females) were included. The reasons for exclusion were history of surgery on gastrointestinal tract, resected bowel, subhepatic cecum and adhesions of small bowel. Parameters like age or ethnicity were not considered for correlation with SBL because the age group was between 60-80 years and all individuals in the present study were from the Maharashtra State, a state located in central India, which is supposed to have individuals that have a mixture of Indo-Aryan, Dravidian, and Mongolian ethnicities (Mujumder, 2001).

The measurement of small bowel length (SBL) was taken from duodenojejunal junction to ileocecal junction along the antimesenteric border immediately after removing the duodenum and jejunum, and *in situ* for the duodenum. Body height (H) was taken from cranial vertex to heel and waist circumference (WC) was taken at the level of umbilicus (WHO, 2008) by a flexible measuring tape. All the parameters were recorded in centimeters.

Individuals with central obesity were defined as males with  $WC \geq 90$  and females with  $WC \geq 80$  (Martin et al., 2003; Misra et al., 2006; Ahmad et al., 2016).

Student's t-test for independent variables and Mann-Whitney U test were used to evaluate comparisons between males and females. Anova, Pearson's correlation coefficient and regression analysis were used to analyze differences and correlations regarding SBL, height and WC.

## Results

The mean SBL in 111 individuals was found to be 336.54 cm, with a mean of 345.45 cm in males and 319.42 in females (Figure 1, Table 1). The difference was significant ( $p < 0.05$ ; Mann-Whitney U test after t-test). In males the maximum SBL was 500 cm, while it was 450 cm in females. The minimum SBL in males was 218 cm in males and 271 cm in females.

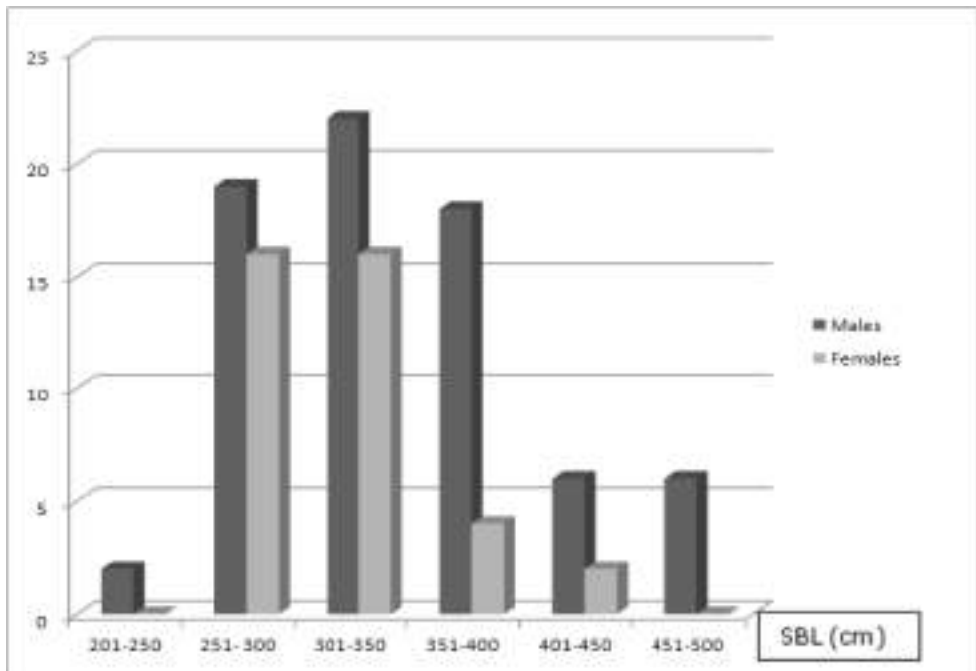


**Figure 1.** Comparison of SBL in males and females.

**Table 1.** SBL, SBL/H ratio and SBL/WC ratio in males and females.

Sex	SBL Mean (cm)	SBL/H	SBL/WC
Females (38)	319.42 ± 40.24	2.09±0.26	4.18±0.53
Males (73)	344.45 ± 63.20	2.07±0.36	4.28±0.61
p value	<0.05	not significant	not significant

Height and SBL showed a moderately positive reciprocal correlation with  $R=0.329$  (Figure 2, Table 2), while WC and SBL showed a strong positive reciprocal correlation with  $R=0.568$  (Figure 3, Table 2). Regression analysis showed coefficients of 2.312 and 4.379 for height and WC respectively, which was statistically significant. However, in individuals with central obesity SBL showed no correlation with WC in males ( $R=0.049$ ) and weak correlation in females ( $R=0.281$ ).

SBL/Height ratio in males was 2.07 and in females 2.09, while SBL/WC ratio was 4.28 in males and 4.18 in females, both with no statistically significant difference (Table 1).

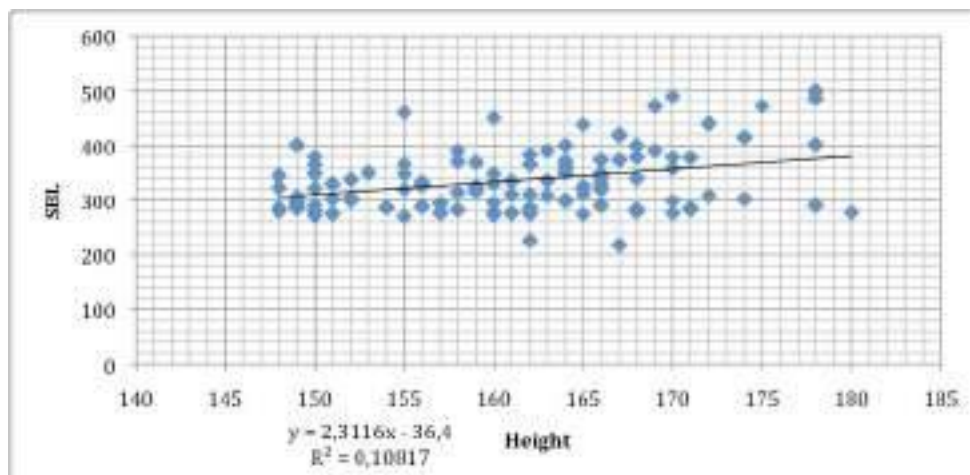


**Figure 2.** Correlation of height with small bowel length (SBL).

**Table 2.** Correlation of SBL with Height (H) and waist circumference (WC).

		H	WC
SBL	Pearson Correlation	0.329	0.568
	p-value	<0.05	<0.05
	N	111	111

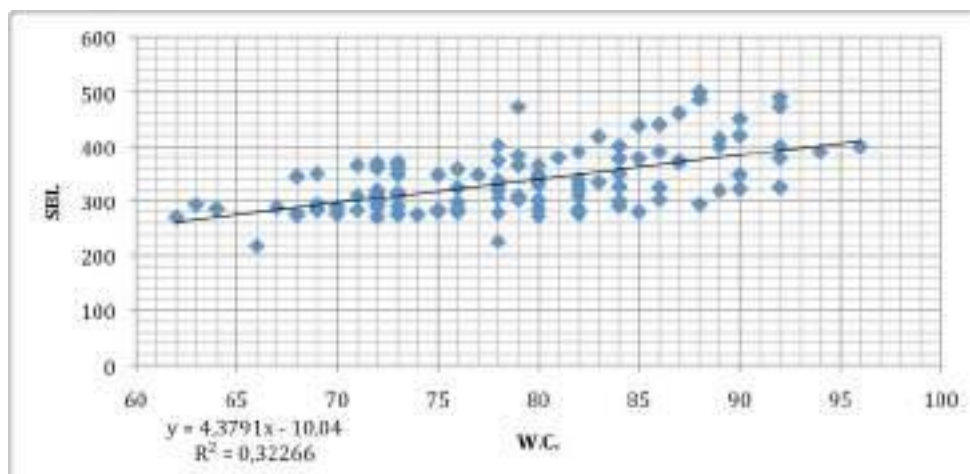


**Figure 3.** Correlation of waist circumference (WC) with small bowel length (SBL).

## Discussion

Gray's Anatomy, 40<sup>th</sup> edition, mentions small bowel length of 3-7 meters with an average of 5 meters in living adults (Gabe, 2008). Most of the European or American studies also showed average SBL to be around 6 meters or more e.g. 575 cm (Weaver et al., 1991), 609.6 cm (Underhill, 1955), 630-1510 cm (Raines et al., 2015),  $632.5 \pm 88.9$  (Hosseinpour and Behdad, 2008),  $690.1 \pm 93.7$  cm,  $795 \pm 129$  cm (Hounnou et al., 2005), 1193 cm (Tacchino 2015). These studies showed a wide range of variation in SBL length from a minimum of 201 cm to a maximum of 1510 cm, with a mean around 600 cm (Reiquam et al., 1965; Raines et al., 2015; Tacchino 2015). Such wide variations do not match with the description given in the standard textbooks. In the present study, we did not come across any measurement of small bowel length of more than 5 meters. Another study in Indian population also showed the SBL to be not more than 500 cm (Jadhav et al., 2015). The SBL in Indian population is less in comparison with the textbook figures as well as with the values of SBL mentioned in western studies. The present study in Indian population showed an SBL in the range of 218-500 cm, with an average of 336.54 cm.

Researchers have measured the SBL either in living, during laparotomy or by radiology or magnetic resonance imaging (Guzman et al., 1977; Fanucci et al., 1984; Hosseinpour and Behdad, 2008; Sinha et al., 2014; Raines et al., 2015; Tacchino, 2015), in brain dead (Gondolesi, 2012; Sinha et al., 2014; Tacchino, 2015), in cadavers which are not formalin-fixed (Underhill, 1955; Martin et al., 2003; Misra et al., 2006), or in formalin-fixed cadavers (Minko et al., 2014; Jadhav et al., 2015). It was reported that the bowel is longer in cadavers than the living due to decrease in the muscle tone after death (Gad, Gad 2007; Richards, 2018); however; Smyth (1988) found no significant increase in bowel length after death. In formalin-fixed cadavers, there is shrinkage due to hardening and dehydration of tissue (Coleman and Kogan, 1998; Clarke et al., 2014; Tran et al., 2015). The variable results may be due the measurements taken in different situations. However, as there is a wide variation in the small bowel length in living adults (Gabe, 2008), the same will be reflected during measurements in any particular situation mentioned above. In the present study, measurements of small bowel were taken in formalin-fixed cadavers.

There is no uniformity of results regarding the factors influencing SBL; however, height seems to be a relevant factor, as the higher bodies may need longer bowels.

However, some researchers found weak or no relationship of height with the SBL (Hosseinpour and Behdad, 2008; Minko et al, 2014) and some showed a decrease in SBL/height ratio as the age increases (in infants 4.24, in adults 2.12), as the bowel length does not significantly change after birth (Gondolesi et al., 2012). Some studies showed a significant height – SBL correlation (Raines et al., 2015; Tacchino, 2015; Ahmad et al., 2016). Mean SBL/height ratio in the present study was 2.09, and there was positive correlation between height and SBL.

Normal waist circumference in Indian males and females is 78 cm and 72 cm respectively. Higher WC (90 cm and more in males and 80 cm and more in females) indicates central obesity/abdominal obesity (Martin et al., 2003; Misra et al., 2006; Ahmad et al., 2016). There are studies showing strong positive correlation as well as no correlation between weight and SBL (Guzman et al, 1977; Zhu et al., 2001; Hounnou et al., 2002; Tacchino, 2015). One study mentions that jejunal length can be a



good predictor of weight (Tacchino, 2015). The present study tried to search the relation between WC (normal values) and SBL, and we found a positive correlation but only in subjects without central obesity. Regression analysis showed statistically significant coefficients for both height and WC.

Small bowel length is not just an issue of academic discussion. It is of concern for surgeons especially in the procedure of massive resection of small bowel, where large amount of the small bowel is to be resected and can lead to short bowel syndrome. It is reported that short bowel syndrome can occur following resection of small bowel if the remaining portion is less than 2 meters or 50% of the original length (Shonyo and Jackson, 1950; Robinson and Wilmore, 2001). If the original length of small bowel is around 3-4 meters, are there more chances of short bowel syndrome in massive resection? Same concern is shown by Tacchino in his research article (Tacchino, 2015). Knowledge of variable length of small bowel is important for intestinal bypass surgery, enteroscopy, magnetic resonance enterography, bariatric surgery and any surgery related to small bowel length (Gondolesi et al., 2012; Tacchino, 2015). Bowel length conditions its capacity to absorb micronutrients as well as its caloric absorptive capacity. The relationship between different bowel limb lengths and SBL is valuable for the success of bariatric surgery, which needs an accurate evaluation before surgery. The bypass done in bariatric surgery mimics resection of a major portion of proximal bowel (Tacchino, 2015). Studies of SBL will provide a better insight in above mentioned procedures and surgery, this study in particular for Indian population.

## Acknowledgments

The authors express their gratitude towards the body donors who donated their bodies to medical colleges, and provided the authors with the opportunity to carry out this research.

The authors have no conflict of interests to declare.

## References

- Ahmad N., Adam S.I., Nawi A. M., Hassan M. R., Ghazi H.F. (2016) Abdominal obesity Indicators: waist Circumference or waist-to-hip ratio in Malaysian adult population. *Int. J. Prev. Med.* 7: 82.
- Clarke B.S., Banks T.A., Findji L. (2014) Quantification of tissue shrinkage in canine small intestinal specimens after resection and fixation. *Can. J. Vet. Res.* 78(1): 46-49.
- Coleman R., Kogan I. (1998) An improved low-formaldehyde embalming fluid to preserve cadavers for anatomy teaching. *J Anat.* 192: 443-446.
- Drake R., Vogl A.W., Mitchell A.W.M., Veermani R., Holla S., Chand P., Chumber S. (Eds.) (2015) Small Intestine. Chapter 4. In: *Gray's Anatomy for Students*. South-east Asia Edition 1. Elsevier-Relx India New Delhi Pp. 346-347.
- Fanucci A., Cerro P., Fraracci L., Ietto F. (1984) Small bowel length measured by radiography. *Gastrointest. Radiol.* 9: 349-351.

- Gad S. (2007) Mechanism of digestion in small intestine. Introduction: The gastrointestinal tract as a barrier and as absorptive and metabolic organ. Chapter 1. In: Gad S.C.(Ed.) Toxicology of the Gastrointestinal Tract. Edition 1. CRC Press, London. Pp. 24-25.
- Gondolesi G., Ramisch D., Padin J., Almau H., Sandi M., Schelotto P.B., Fernandez A., Rumbo C., Solar H. (2012) What is the normal small bowel length in humans? First donor-based cohort analysis. *Am. J. Transplant.* 12: S49-S54.
- Guzman I.J., Fitch L.L., Varco R.L., Buchwald H. (1977) Small bowel length in hyperlipidemia and massive obesity. *Am. J. Clin. Nutr.* 30: 1006-1008.
- Hosseinpour M., Behdad A. (2008) Evaluation of small bowel measurement in alive patients. *Surg. Radiol. Anat.* 30: 653-655.
- Hounnou G., Destrieux C., Desme J., Bertrand P., Velut S. (2002) Anatomical study of the length of the human intestine. *Surg. Radiol. Anat.* 24: 290-294.
- Jadhav S.S., Wankhede H.A., Nimje D.A. (2015) Length of small intestine in formalin fixed adult human cadavers. *Int. J. Health Sci. Res.* 5: 135-139.
- Karasov W., Douglas A. (2013) Comparative digestive physiology. *Compr. Physiol.* 3: 741-783.
- Martin A.D., Daniel M., Clarys J.P., Marfell-Jones M.J. (2003) Cadaver-assessed validity of anthropometric indicators of adipose tissue distribution. *Int. J. Obes.* 27: 1052-1058.
- Minko E., Pagano A., Caceres N., Tony Adar T., Márquez S. (2014) Human intestinal tract length and relationship with body height. *FASEB J.* 28: 916.4.
- Misra A., Vikram N.K., Gupta R., Pandey R.M., Wasir J.S., Gupta V.P. (2006) Waist circumference cutoff points and action levels for Asian Indians for identification of abdominal obesity. *Int. J. Obes.* 30: 106-111.
- Mujumder P.P. (2001) Ethnic populations of India as seen from an evolutionary perspective. *J. Biosci.* 26: 533-545.
- Raines D., Arbour A., Thompson H.W., Figueroa-Bodine J., Joseph S. (2015) Variation in small bowel length: Factor in achieving total enteroscopy? *Dig. Endosc.* 27: 67-72.
- Reiquam C.W., Allen R.P., Akers D.R. (1965) Normal and abnormal small bowel lengths: An analysis of 389 autopsy cases in infants and children. *Am. J. Dis. Child.* 109: 447-451.
- Richards D. A. (2018) Introduction to the gastrointestinal system. Chapter 43. In: Pocock G., Richards C.D., Richards D.A. (Eds.) *Human Physiology*. Edition 5. Oxford University Press, Oxford. Pp. 674-675.
- Robinson M.K., Wilmore D. W. (2001) Short bowel syndrome. In: Holzheimer R.G., Mannick J.A. (Eds.) *Surgical Treatment: Evidence-based and Problem-oriented*. Munich, W. Zuckschwerdt. Pp. 140-145.
- Shonyo E. S., Jackson J. A. (1950) Massive resection of the small intestine; Report of a case. *Arch. Surg.* 61: 123-130.
- Sinha R., Trivedi D., Murphy P.D., Fallis S. (2014) Small intestinal length measurement on MR enterography: Comparison with in vivo surgical measurements. *AJR Am. J. Roentgenol.* 203: W274-W279.
- Smyth G.B. (1988) Effects of age, sex, and post mortem interval on intestinal lengths of horses during development. *Equine Vet. J.* 20: 104-108.
- Snell R.S. (2012) *Clinical Anatomy by Regions*. Chapter 5: The abdomen: Part II – The abdominal cavity. Edition 9. Lippincott, Williams and Wilkins Philadelphia. Pp.177-178.

- Standring S., Brown J. L., Moore L.A., Khan N. (2008) Small Intestine. Chapter 66. In: Standring S. (Ed.) *Gray's Anatomy Edition 40*. Churchill-Livingstone-Elsevier, Philadelphia. Pp.1125-1126.
- Tacchino R.M. (2015) Bowel length: measurement, predictors, and impact on bariatric and metabolic surgery. *Surg. Obes. Relat. Dis.* 11: 328-334.
- Tran T., Sundaram C.P., Bahler C.D., Eble J.N., Grignon D.J., Monn M.F., Simper N.B., Cheng L. (2015) Correcting the shrinkage effects of formalin fixation and tissue processing for renal tumors: toward standardization of pathological reporting of tumor size. *J. Cancer* 6: 759-766.
- Underhill B.M. (1955) Intestinal length in man. *Br. Med. J.* 2: 1243-1246.
- Weaver L.T., Austin S., Cole T.J. (1991) Small intestinal length: a factor essential for gut adaptation. *Gut* 32: 1321-1323.
- Gray H., Williams P., Warwick R. (1980) *Gray's Anatomy. The small intestine. Edition 36*. Churchill-Livingstone, Edinburgh. Pp. 1342-1343.
- World Health Organization (2011) Waist circumference and waist-hip ratio: report of a WHO expert consultation. Geneva, 8-11 December 2008. Geneva, WHO.
- Zhu S., Wang Z., Heshka S., Heo M., Faith M.S., Heymsfield S.B. (2002) Waist circumference and obesity-associated risk factors among whites in the third National Health and Nutrition Examination Survey: Clinical action thresholds. *Am. J. Clin. Nutr.* 76: 743-749.



## EFFECT OF PHYSICAL TRAINING ON PULMONARY FUNCTION TEST IN YOUNG ADULTS OF A PHYSICAL TRAINING ACADEMY

**Rupali S Baburdikar\***

Assistant Professor, Dept of Physiology, MIMER Medical College, Talegaon D, Pune.  
\*Corresponding Author

**Deepa Nair**

Professor and HOD, Dept of Physiology, MIMER Medical College, Talegaon D, Pune.

**Meena Agrawal**

Professor, Dept of Physiology, MIMER Medical College, Talegaon D, Pune.

### ABSTRACT

Physical inactivity and low cardio-respiratory fitness are recognized as important causes of morbidity and mortality. Pulmonary function tests help in monitoring the efficacy of physical training. It includes parameters like FEV1, FVC, MVV, PEFR, FEF 25-75. Cardio-pulmonary efficiency tests help to study aerobic conditioning, which includes lung ventilation. Lung ventilation, the most important parameter of physical fitness is controlled by skeletal muscle fitness. There are many studies carried out on defense personals, but very studies about young adults who aspire to take entry in the army, navy or police force. The present study was aimed to evaluate the importance of physical activity in improving strength and endurance of respiratory muscles. So we measured various spirometry parameters (PFT) to find out the cardio-respiratory response and blood pressure to study cardio-vascular response in the individuals who underwent rigorous physical training for 9 months. 30 healthy male subjects between age group of 18-23 years were selected randomly. Before and after training period of 9 months, spirometry and other parameters like height, weight, body surface area were recorded. We got statistically significant improvement in parameters like FEV1, FVC, MVV, PEFR and FEF 25-75. We observed statistically significant reduction in the mean systolic and diastolic resting blood pressure after training. From our results we conclude that physical training like regular aerobic exercise improves lung function parameters and cardiac efficiency. Regular aerobic exercise improves cardio-respiratory fitness.

**KEYWORDS** : Aerobic exercise, Physical training, FEV1, FVC, PEFR, MVV etc.

### INTRODUCTION:

Regular physical activity is an essential component of a healthy lifestyle that helps to keep fit.<sup>1</sup> Physical fitness is the ability to carry out daily tasks with vigor and alertness without undue fatigue. Physical inactivity and low cardio-respiratory fitness are recognized as important causes of morbidity and mortality.<sup>2</sup> Aerobic exercise is physical exercise of relatively low intensity that primarily depending on the aerobic energy-generating process.<sup>3</sup>

Pulmonary function tests help in monitoring the efficacy of physical training. It includes parameters like FEV1, FVC, MVV, PEFR, FEF 25-75. Various cardio-pulmonary efficiency tests help us to study aerobic conditioning which includes lung ventilation. Lung ventilation, the most important parameter of physical fitness is controlled by skeletal muscle fitness. Lung function is an important predictive tool of morbidity and mortality in medical practice. Pulmonary function is a long term predictor of overall survival rates in both genders and can be used as a tool for general health assessment.<sup>4</sup>

There have been many studies carried out on defense personals, but very negligible studies about the young adults who aspire to take entry in the army, navy or police force.

The present study was aimed to evaluate the importance of physical activity in improving strength and endurance of respiratory muscles. So we measured various spirometry parameters (PFT) to find out the cardio-respiratory responses and blood pressure to study cardio-vascular responses in the individuals who underwent rigorous physical training for duration of nine months.

### MATERIAL & METHODS:

This prospective study was done from January 2017 to January 2018 after approval from institutional ethics committee of the institute. The study was conducted in career training academy in Pune. The study participants were healthy young adults aspiring to gain entry in army, navy or police force.

The trainees included in the study were from different regions of Maharashtra.

The newly admitted candidates of the academy were screened for the inclusion and exclusion criteria. Those individuals who gave the

history of smoking, respiratory illness like bronchial asthma, COPD, pneumonia, history of tuberculosis in past and any cardiovascular disease or history of congenital heart disease, chest or spinal deformity, obesity (BMI > 32 kg/m<sup>2</sup>) were excluded. 30 healthy male subjects between age group of 18-23 years were finally selected randomly. The individuals who voluntarily agreed to participate in the study were enrolled. The detailed information of project was given and procedure was explained.

After taking written informed consent, general examination and spirometry was done. The parameters recorded were height (stadiometer), weight (standard scale weighing machine), Body Surface Area (Dubois nomogram).<sup>5</sup>

Spirometry was done on computerized spirometry machine Helios 401. It was done in sitting position and in the post-absorptive phase i.e. 4 hours after lunch. The test was simple, non-invasive easy to perform. It was done in two maneuvers. In First maneuver, Forced Vital Capacity (FVC), Forced Expiratory Volume in 1 second (FEV<sub>1</sub>), Peak Expiratory Flow Rate (PEFR), Forced mid Expiratory Flow Rate (FEF<sub>25-75</sub>) were recorded. Second maneuver included recording of Maximum Voluntary Ventilation (MVV). Two trials were given to each participant. For each test the best one out of three test readings were taken.

The participants in the study underwent vigorous physical training for duration of 9 months. During the training period, they performed various forms of exercises for 3 hours in the morning and 2 hours in the evening. The exercises were in the form of running, resistance exercises and other moderate to severe exercises.

Again after a period of 9 months, Spirometry readings and all the other parameters were recorded in the same group of subjects under similar conditions.

### Statistical

The results were given as Mean ± Standard Deviation. Comparisons were performed using paired student's t- test. A p-value of less than 0.05 was considered as statistically significant. Statistical software graph pad prism was used for the analysis of data. Microsoft word and Microsoft excel have been used to create text documents and tables etc.

### analysis:



**RESULT:****Table no 1: comparison of pre-training and post training baseline characteristics of subjects.**

Parameters	Pre-Training Mean $\pm$ SD	Post-Training Mean $\pm$ SD	P - Value
WEIGHT( Kg)	62.25 $\pm$ 10.13	58.21 $\pm$ 9.811	<0.0001**
BSA (m <sup>2</sup> )	1.749 $\pm$ 0.1463	1.738 $\pm$ 0.1425	0.3618ns
SBP(mm of Hg)	113.9 $\pm$ 11.90	112.6 $\pm$ 11.35	0.0103*
DBP(mm of Hg)	68.50 $\pm$ 9.053	67.3 $\pm$ 8.778	0.0107*

p values <0.05 : statistically significant\*, p values <0.0001: statistically highly significant\*\*, p values >0.05 : not significant  
SBP- systolic blood pressure, DBP- diastolic blood pressure, BSA- body surface area

**Table no 2: Comparison of pre-training and post training spirometry parameters.**

Parameters	Pre-training Mean $\pm$ SD	Post-training Mean SD	p-value
FEV1	3.29 $\pm$ 0.44	3.62 $\pm$ 0.31	0.0025*
FVC	3.43 $\pm$ 0.57	3.88 $\pm$ 0.57	0.0145*
PEFR	7.15 $\pm$ 1.89	8.35 $\pm$ 1.21	0.0100*
PEF 25-75	5.60 $\pm$ 1.42	6.27 $\pm$ 1.25	0.0462*
MVV	146 $\pm$ 12.75	151.5 $\pm$ 9.04	0.0286*

p values <0.05 : statistically significant\*, p values <0.0001: statistically highly significant\*\*, p values >0.05 : not significant

**DISCUSSION:**

The trainees in the career academy underwent vigorous physical training for duration of nine months. During training period, all the trainees were doing various forms of exercises mainly aerobic exercises like running, resistance exercises.

In the present study, improved respiratory performance was reflected in the spirometry parameters. The parameters like FEV1 and FVC are the hallmarks of respiratory performances. We got statistically significant improvement in FEV1 and FVC parameters after exercise training. This could be because of regular forceful inhalation and deflation of the lungs for prolonged period that leads to strengthening of respiratory muscles. As an effect of training, there must be an increase in the maximal shortening of the inspiratory muscles which has been shown to improve lung function parameters.<sup>1</sup>

We found statistically significant improvement in the mean values of PEFR and MVV before and after 9 months of physical training. The PEFR 25-75 also showed higher flow rates in post -training period. MVV which depends on strength of the voluntary muscles is an important parameter as it indicates physical work capacity.

The cardio-vascular changes were assessed by studying the blood pressure values before and after training period. We observed statistically significant reduction in the mean systolic and diastolic resting blood pressure after training the training period of nine months. The reduction of blood pressure indirectly indicates vasorelaxation, as regular exercise can restore the loss of endothelium-dependent vasodilation.<sup>6</sup> The mechanisms of physical training induced reduction in blood pressure are related to hemodynamic, humoral and neural factors like reduction in cardiac debt, a drop in total peripheral resistance due to increase in cross sectional area of vascular beds, particularly of skeletal muscles and vasodilatation caused by low levels of norepinephrine, plasma renin activity and a reduction in sympathetic activity.<sup>7,8</sup>

Training improves cardio-vascular, pulmonary and muscular adaptations to exercise by alterations in sympatho-adrenal acceleratory activity, vagally mediated deceleration. Training also leads to increased VO<sub>2</sub> max, increased muscle blood flow accompanied by elevated cardiac output, increased capillarization of muscle tissue and better substrate utilization.<sup>9,10</sup>

**CONCLUSION:**

From our results we conclude that physical training like regular

aerobic exercise improves lung function parameters and cardiac efficiency. Practice of aerobic exercise would benefit those who aim to be in defense, as this would prepare them in overcoming stress by modulating and optimizing sympathetic activities in stressful situations. It can be considered an important lifestyle modification to improve overall lung health and for prevention high blood pressure in healthy adolescents. Regular aerobic exercise improves cardio-respiratory fitness.

**REFERENCES:**

1. Jourkesh M, Sadri I, Ojagi A, Sharanavard A; Determination of fitness level in male and female college aged students. Archives of Applied Science Research, 2011; 3 (2): 326-333.
2. Twisk JW, Staal BJ, Brinkman MN, et al. Tracking of lung function parameters and the longitudinal relationship with lifestyle. Eur Respir J. 1998; 12: 627-34.
3. Plowman SA; Smith DL; Exercise Physiology for Health, Fitness, and Performance. Lippincott Williams & Wilkins. 2007: 61.
4. McArdle WD, Katch FI, Katch VL; Essentials of exercise physiology. Lippincott Williams & Wilkins, 2006: 204.
5. DuBois D, DuBois EF 1916. Clinical calorimetry: A formula to estimate the approximate surface area if height and weight be known. Arch Intern Med, 17: 863-870.
6. DcSouza CA, Shapiro LF, Clevenger CM; Regular aerobic exercise prevents and restores age related declines in endothelium-dependent vasodilation in healthy men. Circulation. 2000; 102(12): 1351-1357
7. Niranjan M, Bhagyalakshmi K, Ganaraja B, Adhikari P, Bhat R; Effects of yoga and supervised integrated exercise on heart rate variability and blood pressure in hypertensive patients. Journal of Chinese Clinical Medicine. 2009; 4(3):139-143.
8. Sormers VK, Conway J, Johnston J, Sleight P; Effects of endurance training on baroreflex sensitivity and blood pressure in borderline hypertensives. Lancet. 1991; 337(8754): 1363-1368.
9. Verma SK, Sidhu LS, Kansal DK; A study of maximum oxygen uptake and Heart rate during work and recovery as measured on cycle ergometer on National Indian sportsmen. Brit J Sports Med., 1979; 13(1): 24-28.
10. Buchhei M, Gindre C. Cardiac Parasympathetic regulation: respective associations with cardiorespiratory fitness and training load. Am J Physiol. 2006; 291 (1): H451458.



## MORPHOLOGIC AND CYTOMETRIC EVALUATION OF ANEMIA IN GERIATRIC PATIENTS

### Pathology

**Shruti S. Desale** Senior Resident Dept of Pathology, MIMER Medical College, Talegaon Dabhade

**Smita P. Bhide\*** Professor, Dept of Pathology, MIMER Medical College, Talegaon Dabhade  
\*Corresponding Author

**Sneha R. Joshi** Professor & Head, Dept of Pathology, MIMER Medical College, Talegaon Dabhade

### ABSTRACT

**BACKGROUND:** The UN agreed cut off to refer to older patients (i.e. geriatric age group) is 60+ years. Due to the rising tendency of the aging population in a modern society, the prevalence of anemia is also expected to rise in the future. Geriatric anemia is a unique anemia for several reasons. Its diagnosis poses a challenge. This is because there are several features of anemia which make it easy to overlook.

**OBJECTIVE:** To study types of anemia depending upon red cell morphology and red cell indices in geriatric patients.

**MATERIALS AND METHODS:** The present study was carried in department of pathology of the rural tertiary care hospital. All the geriatric patients coming to out patient as well as in patient department of the hospital with anemia satisfying the inclusion and exclusion criteria were included in the study. This study was conducted from October 2015 to August 2017.

**RESULTS:** Out of 690 total geriatric patients, 414 anemic patients fulfilling inclusion criteria were included in the study. Out of total 414 patients, 220 (67.4 %) were male and 194 (73.7%) were female patients. Majority of the patients were in 60-65 year age group, in both sexes. In present study, normocytic normochromic was the most common morphological pattern of anemia found on PBS and anemia of chronic disease was the most common cause of geriatric anemia, followed by nutritional deficiency.

**CONCLUSION:** Despite modern diagnostic methods, geriatric anemia still remains underreported and inadequately investigated. There is clearly a need for greater awareness of anemia in the elderly and of its significance in terms of poorer outcomes, prolonged hospital stay and increased mortality.

The present study underlines the importance of routine screening and individual assessment of the etiological factors of anemia in elderly allowing the timely initiation of optimal and appropriate therapy.

### KEYWORDS

Anaemia, Geriatric, Morphological

### INTRODUCTION

The UN agreed cut off to refer to older patients (i.e. geriatric age group) is 60+ years.<sup>1</sup> Due to the rising tendency of the aging population in a modern society, the prevalence of anemia is also expected to rise in the future. Anemia represents a sign of serious disease. Thus, if not treated properly, anemia can cause serious complications, especially among older population.<sup>2</sup> Geriatric anemia is a unique anemia for several reasons. Its diagnosis poses a challenge. This is because there are several features of anemia which make it easy to overlook.<sup>3</sup>

The onset of symptoms and signs is usually insidious and many elderly patients adjust their activities as their bodies make physiologic adaptations for the condition. Typical features of anemia are not specific and in elderly patients tend to be attributed to advancing age.<sup>3</sup> Anemia significantly increases the mortality and morbidity in the elderly. Thus, anemia needs thorough study of its pattern and profiles for proper evaluation and management.<sup>4</sup>

The present study is an attempt to study the pattern of anemia encountered in elderly and their association with clinical profile and possible etiological processes. Also it is undertaken to estimate the occurrence of anemia among elderly and to classify the anemia based on red cell morphology and indices.

### MATERIALS AND METHODS

The present study was carried in department of pathology of the rural tertiary care hospital. All the geriatric patients coming to outpatient as well as in patient department of the hospital with anemia satisfying the inclusion and exclusion criteria were included in the study. This study was conducted from October 2015 to August 2017.

#### 1) INCLUSION CRITERIA:

- Male patients aged 60 years and above with Hb % < 13 gm/dL.
- Female patients aged 60 years and above with Hb% < 12 gm/dL.

#### 2) EXCLUSION CRITERIA:

- Patients below 60 years of age.
- Male patients aged 60 years and above with Hb% > 13 gm/dl.
- Female patients aged 60 years and above with Hb% > 12 gm/dl.

A detailed clinical history was taken and a thorough physical examination was carried out in each patient. The following investigations were done.

A) Hematological Investigations : Venous blood was collected in EDTA bulb and all routine hematological investigations were carried out. The parameters like Hb, HCT, RBC count, RBC indices (MCV, MCH, MCHC) , RDW, TLC & Platelet count were obtained from automated hematology analyzer. We have used 3 part Automated SYSMEX XP-100 blood cell counter & 5 part Automated XS 800i blood cell counter.

PBS Findings were broadly classified into Microcytic hypochromic, Macrocytic, Normocytic normochromic & Dimorphic. Bone marrow aspiration study were done wherever necessary.

B) Non Hematological Investigations: Complete physical and chemical Urine examination were done for every patient. Examination of stool was done in patients wherever indicated. C) Special investigations: Serum Vit. B12/ Folic acid, Liver function test, Renal function test, Thyroid profile, Radiological studies & Endoscopic examination were done wherever indicated.

### RESULTS

The present study was carried out in a rural tertiary care hospital over a period of 1 year 11 months. Out of 690 total geriatric patients, 414 anemic patients fulfilling inclusion criteria were included in the study. Out of total 414 patients, 220 (67.4 %) were male and 194 (73.7%) were female patients.

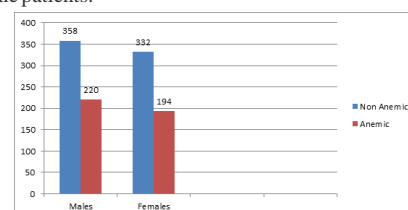


Fig 1: Occurrence of anemia

Out of total 358 male patients, 220 (61.45 %) were anemic. Out of total 332 female patients 194 (58.43 %) were having anemia.(Fig 1)

In the present study there were 220 (53.14 %) male patients and 194 (46.86%) were females.

Age range in present study was 60-92 years.Maximum patients belonged to age group of 60-65 years.(Table 1)

**Table 1: Distribution of patients according to age**

Age	Number	Percentage %
60-65	210	50.72 %
66-70	86	20.77 %
71-75	56	13.53 %
76-80	31	7.49 %
81-85	18	4.35 %
>85	13	3.14%
Total	414	100%

**Table 2: Grading of anemia amongst study subjects**

Grade	Number	Percentage
Mild	169	40.82 %
Moderate	195	47.10 %
Severe	50	12.08 %
Total	414	100%

The above table shows that moderate grade anemia was seen in maximum i.e. 47.1 % of patients, followed by mild (40.82%) and severe grade of anemia (12.08%). (Table 2)

Generalized weakness was the commonest presenting symptom (70%) in the study subjects, followed by fatigue (69.56%), breathlessness(41.78%) and palpitations(34.29%). Most common clinical sign in the present study was Pallor (90.01 %) followed by edema (35.99 %) and tachycardia (30.40 %).

In present study, normocytic normochromic (60%) was the most common morphological pattern of anemia found on PBS followed by Microcytic hypochromic (21%), Macrocytic (!%) and Dimorphic pattern (9%). (Fig 2)

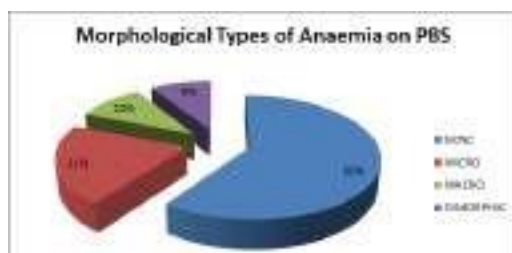


**Fig 2: Morphological types of anaemia on PBS**

**Table 3: Distribution of underlying major etiology of anemia in present study**

Cause of anemia	No. of cases	Percentage (%)
Anemia of chronic disease (ACD)	223	53.86%
Nutritional deficiency anemia	146	35.26 %
Bone marrow disorders	21	5.08%
Others	24	5.80 %
Total	414	100%

In the present study, anemia of chronic disease (53.86%) was the most common cause of geriatric anemia, followed by nutritional deficiency (35.26%).(Table3)

Out of total 223 cases of ACD, normocytic normochromic pattern was observed on PBS of 198 patients (88.78%) and in 25 (11.22%) cases PBS showed microcytic hypochromic pattern. In nutritional deficiency anemia, out of 146 patients, iron deficiency anemia was seen in 67 (45.90%) cases. Megaloblastic anemia was present in 4329.45%) cases, while 36 (24.65%) cases showed combined deficiency.

**Table 4: Distribution of hematological and non-hematological malignancies**

Type of malignancy	Number	Percentage
Hematological	17	26.15 %
Non-hematological	48	73.85 %
Total	65	100%

Out of total 414 patients, 65 cases were of malignancies. Out of these 65, 17 cases were of hematological malignancies and 48 were of Non-hematological malignancies.(Table 4)

In the present study, most common non-hematological malignancies found were related to female genital tract (33.34%). FGT was followed by carcinomas of oral cavity and GIT (29.17%)

CML was the commonest hematological malignancy found (35.29%), followed by CLL(29.41%) in the present study.

Bone marrow study was done in 66 (15.94%) cases. In nutritional deficiency anemia, bone marrow studies were done to confirm the diagnosis. In Chronic Lymphoid Leukemia, Chronic Myeloid leukemia, Multiple Myeloma, Aplastic Anaemia and Myelodysplastic Syndrome characteristic bone marrow findings of the disease were present.

## DISCUSSION

In elderly patients, anemia is highly prevalent. Earlier, it was considered as a consequence of physiological process of aging. Currently; anemia is considered as a pathological condition. However, many a time's exact etiology of anemia is difficult to find out.

Our study was aimed at analysis of the pattern of anemia encountered in elderly, their association with clinical profile and possible etiological processes. Also it was undertaken to estimate the occurrence of anemia among elderly and to classify the anemia based on red cell morphology and indices.

In present study, occurrence of anemia in elderly patients attending our tertiary care hospital was 60%. Similar findings were observed in the studies done by Bhasin et al<sup>5</sup>(60%), Shrivastav S et al<sup>6</sup> (68.5%) & Bisht N et al<sup>7</sup>(61.85%).

In present study, maximum numbers of patients (50.72 %) were found in the age group of 60-65 years. The finding was similar to the studies done by Tilak et al<sup>8</sup>, Prakash KG et al<sup>9</sup> & Aithal K et al<sup>10</sup>.

In our study, slight male predominance was noted which was consistent with the studies done by Tilak et al<sup>8</sup>, Raina et al<sup>11</sup>, Prakash KG et al<sup>9</sup> & Deshpande et al.<sup>12</sup>

In the present study, maximum number of patients had moderate grade anemia (47.10%). Similar findings were noted by Raina et al<sup>11</sup> (72.6%) and Mann et al<sup>13</sup>(46.67%)

In our study, it was observed that generalized weakness was the most common presenting symptom in 70.04% anemic study patients. Tilak et al<sup>8</sup> and Raina et al<sup>11</sup>, in their study have found weakness as a common symptom whereas studies done by Bhasin A et al<sup>5</sup> and Prakash KG et al<sup>9</sup>, showed fatigue as the most common presenting symptom.

Pallor (90.1%) was seen as a commonest sign of anemia in the present study In a study done by Tilak et al<sup>8</sup>, pallor was noted in 88.2 % patients whereas pallor was observed in all cases (100%) in a study by Raina et al.<sup>11</sup>

In the present study, normocytic normochromic picture (60.14 %) on peripheral blood smear was seen in majority of the patients.. This finding is in concordance with findings of Alwar et al<sup>14</sup> & Amarnel et al<sup>15</sup>

In the present study, anemia of chronic disease (53.86%) was the leading cause of geriatric cases. Similar findings were noted by Shrivastav S et al<sup>6</sup> & Tilak et al<sup>8</sup> whereas studies done by, Bhasin et al<sup>5</sup>, Alwar et al<sup>14</sup>, Bisht N et al<sup>7</sup> and Raina et al<sup>11</sup> nutritional deficiency was the leading cause of geriatric anemia.

In the present study, we observed 17 cases of hematological malignancies accounting to 4.10% anemic cases. Percentage reported by VanStaden et al<sup>16</sup> study was 7.1%.

In present study, 0.96 % of the patients (4/414), cause of anemia could not be detected. Similar findings were noted by Tilak et al<sup>8</sup>. However, in studies done by DeAmicis et al<sup>17</sup> & Prakash KG et al<sup>9</sup> unexplained anemia was significantly high. This could be attributed to an incomplete diagnostic evaluation.

## CONCLUSION

The incidence of anemia is quite high among elderly patients, more so when associated with chronic diseases and malignancies. Even mild anemia is associated with significant increase in morbidity irrespective of the underlying cause. Identifying and categorizing anemia is essential to direct the investigation towards the underlying etiology and to guide the clinicians for appropriate targeted treatment. Despite modern diagnostic advanced geriatric anemia still remains underreported and inadequately investigated. There is clearly a need for greater awareness of anemia in the elderly and of its significance in terms of poorer outcomes, prolonged hospital stay and increased mortality.

The present study underlines the importance of routine screening and individual assessment of the etiological factors of anemia in elderly allowing the timely initiation of optimal and appropriate therapy.

## REFERENCES

- 1 World Health Organization. Definition of an older or elderly person. Retrieved August 29, 2010. Available online: [www.who.int/healthinfo/survey/ageingdfolder/en/index.html](http://www.who.int/healthinfo/survey/ageingdfolder/en/index.html).
- 2 Kim H-S, Lee B-K. Cross-sectional study on the prevalence of anemia among rural elderly in Asan. *Nutrition Research and Practice*. 2008;2(1):8-12. doi:10.4162/nrp.2008.2.1.8
- 3 Smith D.L. Anemia in the elderly. *American Family Physician*. 2000, 62(7):1565-1574.
- 4 Duh MS, Mody SH, Lefebvre P, Woodman RC, Buteau S, Peich CT. Anemia and the risk of injurious falls in a community-dwelling elderly population. *Drugs Ageing* 2008,25(4): 325-334.
- 5 Bhasin A, Rao M.Y. Characteristics of anemia in Elderly: A Hospital based study in south India. *Indian Journal Of Hematology and Blood Transfusion* 2011; 27(1): 26-32.
- 6 Shrivastav S R, Hippargi S B, Ambali A P, Yelikar B R. Patterns of anemia in geriatric age group. *JKIMSU* 2013; 2(1): 77-81.
- 7 Bisht N, Sofia, Neki N.S. et al. Prevalence and pattern of anemia in elderly – a hospital based study. *International journal of current research in medical science* (2017), Vol.3, Issue 6, 27-35
- 8 Tilak V, Rani D, Gambhir IS. Characteristic of geriatric anemia in and around Varanasi: A hospital based study. *Indian J. Prev. Soc. Med.* Vol. 44 No1-2, 2013
- 9 Prakash KG, Devendrappa KR, Madhukumar MH, Priyashree R, Avinash B. Clinical Profile of Anemia in Elderly: A Cross Sectional Study from a Tertiary Care Center. *Sch J App Med.Sci*. 2015; 3(3C):1266-1270.
- 10 Aithal K, Meti K, Jain S et al. A study of pattern of anemia in elderly patients admitted at tertiary centre. *Sch. J. App. Med. Sci*. 2017; 5(4D) : 1483-1486
- 11 Raina A, Kumar A, Singh A, Gupta G, Malhotra P, Raina SK. A clinicohaematological profile of elderly patients being investigated for anaemia in a tertiary care centre in north-west India. *Egypt J Haematol* 2014;39:190-4
- 12 Deshpande N, Kakade H, Jathar M, Sangle SA, Deshpande N, Shinde A. Anemia in senior citizens. *MedPulse – International Medical Journal*, March 2017;4(3):349-350
- 13 Mann S, Kumar A, Singh SK, Katyal S, Chopra G, Varma SK. Clinical Evaluation of Anemia in Geriatric Patients - A Cross Sectional Study Conducted At Tertiary Care Hospital. *Natl J Community Med*. 2010; 5(3): 316-320.
- 14 Alwar v, Reethi K, Rameshkumar K. Geriatric Anemia: An Indian perspective. *Indian J Hematol Blood Transfus*. 2013; 29(2). 126-127
- 15 Amarnel S, Sheth N, Pattern of anemia in elderly age group. *USRR*. 2015; 4(2): 51-56.
- 16 VanStaden AM, Weich DJV. Retrospective analysis of the prevalence and causes of anaemia in hospitalised elderly patients. *S Afr Fam Pract*. 2015; 57(5): 297-299.
- 17 DeAmicis MM, Poggiali E, Motta I, Minonzio F, Fabio G, Hu C et al. Anemia in elderly hospitalized patients: prevalence and clinical impact. *Intern Emerg Med*. 2015;10(5): 581-586





## COMPARISON BETWEEN TAMSULOSIN VS TAMSULOSIN+ DEFLAZACORT IN EXPULSION OF LOWER URETERIC CALCULI

**Dr Shashikant Bhangre**

Associate Professor, Endourologist. Dept Of General Surgery Mimer Medical College. Pune. Maharashtra 410507

**Dr Dinesh Badarshahi\***

Senior Resident Dept Of General Surgery Mimer Medical College. Pune. Maharashtra 410507 \*Corresponding Author

**A STRACT** **BACKGROUND:** Medical Expulsive Therapy (MET) has become an established part of the protocol for treatment of ureteric stones of 5-10 mm size in the lower 1/3rd of the ureter.  $\alpha$ -1 adrenergic blockers with or without corticosteroid along with IV fluid therapy are in use to facilitate expulsion of stones. **AIMS & OBJECTIVE:** In this study comparison of  $\alpha$ -1 adrenergic blocker Tamsulosin alone and in combination with corticosteroid deflazacort have been compared. **MATERIALS AND METHODS:** Total of 50 symptomatic patients of lower ureteric stones, who presented in the OPD in MIMER Medical College Hospital were selected for our study. Patients were randomly divided in group 1 and group 2 viz. Group 1 (Tamsulosin Group) & Group 2 (Tamsulosin + deflazacort Group). **RESULTS:** It was found that with Tamsulosin + deflazacort offers better stone clearance rate with in shorter period. There was minimum discomfort to the patients during stone expulsion. Success rate was comparable in both groups up to 10 mm stone size. **CONCLUSION:** MET using Tamsulosin + Deflazacort has clear advantage over Tamsulosin alone therapy.

**KEYWORDS :** Ureteric Stones; Alpha Blockers; Corticosteroids

### INTRODUCTION

The patients of ureteric stones are increasing all over the world. This increase is seen across age, sex and race. Lifestyle changes in diet pattern and global warming seems to influence these trends.[1] Recent reviews of published papers suggest that 90% stones of less than 5mm and 15 % stones of sizes between 5 mm- 8 mm will pass spontaneously.[3] For stones less than 5mm size recommended management includes analgesics, antibiotics and hydration therapy. With medical expulsive therapy, in which Tamsulosin is the main stay, spontaneous passage of stone upto 10mm has been reported.[2]

The presence of stone in the ureter causes inflammation and edema, Corticosteroid decreases edema and when prescribed with  $\alpha$ -1 adrenergic receptor antagonists facilitates the early passage of stone.[6] Corticosteroids are used for short duration to avoid the side effects. Deflazacort is used because of lesser side effects. There is some evidence that Deflazacort in combination with alpha-blockers antagonist is more effective in expulsion of stones upto 10mm size.[8]

Among our patients ureteric colic account for 35% of urolithiasis and 75% of ureteral stones which are located in the lower third of the ureter. Similar results have been observed by other authors also.[1]

Since some decades ureteral stones treatment modalities have changed and MET is a standard protocol for treatment of small stones in the lower third of the ureter. It increases the expulsion rate and reduces the expulsion time, thereby reducing the cost and lost working days.[7] Stones up to 4mm size are expelled in almost all cases. Spontaneous expulsion rate for 4-6mm stones is about 25% and over 8mm size are rarely expelled.[7] Different procedures have been recommended for stone of greater than 5mm size. Stones upto 9.5mm have been successfully expelled with MET, the largest size stone being 1.4 cm.[5] The time required for stone expulsion depends on the size of the stone. Smaller the stone faster the expulsion and clearance.

Extra corporeal shock wave lithotripsy [ESWL] is the first line of management for ureteric stones of less than 20mm size. Success rate with ESWL in stones of over 8mm size in distal ureter varies from 49.9% to 91.1% and decreases as stones size increases.[5]

Few centres use ureteroscopy [URS] as first line treatment to achieve better stone free rate.[10]

MET is easy and cheap procedure and can be preferred as first line treatment before ESWL or URS.

Hancock reported presence of  $\alpha$  adrenergic and  $\beta$  adrenergic receptors

in human ureter.[13]

Additional studies showed that there is presence of  $\alpha$ -1d adrenergic receptors in the human ureter, and  $\alpha$ -1 blocker can facilitate the passage of ureteric stones in 80.4% of cases (Cervinakov et al.[2])

Tamsulosin- an alpha 1 antagonist, inhibits basal-tone and decreases peristaltic frequency resulting in increased fluid transport and decreased intra ureteral pressure and they also block the conduction of Visceral referred pain.[12]

Stone in ureter causes ureteral muscle spasm, infection leading to inflammation and oedema.

In the pioneering work of Borghi, methyl prednisolone with other drugs was shown to increase the rate of stone passage.[9] This has led to the aim of our study of MET. There is some evidence that a combination of  $\alpha$ -blocker and Corticosteroid might be more effective than treatment with  $\alpha$ -blocker alone. Among the Glucocorticoid's, Deflazacort, a synthetic Oxazoline derivative of prednisolone have shown equivalent anti-inflammatory potency with less side effect.

### MATERIALS AND METHODS

Total of 50 symptomatic patients of lower ureteric stones presenting in the OPD of MIMER Medical College and Hospital between Jan 2011 – May 2013, were selected for the study. There were 29 male and 21 female patients, Age was between 15-55 years. Renal function tests were normal in all patients.

Patients were randomly divided in two groups [group 1 & group 2]. Both groups had equal number of patients.

Antibiotics were prescribed based on culture and sensitivity.

Group 1 patients were given Tamsulosin 0.4 mg OD and Tab Deflazacort, till the 18 mg OD for 3 days 12 mg OD for 2 days and 6mg on the 6th day. stones are expelled or upto 30 days maximum.

Patient was advised to take at least 3 to 4 L of oral fluid daily.

Group 2 patients were given Tab Tamsulosin OD.

Treatment was considered successful when stone was expelled within 30 days and patients had fewer and milder symptoms.



**RESULT**

Stone size 6-7mm in group 1, out of 9 patients, stone clearance was achieved in 8 patients within 6 days, (SR-88%); and in group 2, out of 8 patients stone clearance was achieved in 6 patients within 5 days, (SR 75%).

Stone size 7-8mm in group 1, out of 7 patients, stone clearance was achieved in 7 patients within 6 days (SR-100%); and in group 2, out of 9 patients stone clearance was achieved in 8 patients within 8 days, (SR-88.8%).

Stone size 8-9mm size in group 1, out of 5 patients, stone clearance was achieved in 4 patients within 5 days (SR-80%); and in group 2, out of 5 patients stone clearance was achieved in 3 patients within 11 days, (SR-60%).

Stone size 9-10 mm size stone in group 1, out of 4 patients, stone clearance was achieved in 4 patients within 10 days (SR- 100%); and in group 2, out of 3 patients stone clearance was achieved in 1 patients within 14 days, (SR-33.3%).

**Table-1: Success rate of stone expulsion**

Size of the Stone	Group	Total Patients	stones cleared	Stone cleared in days	Success Rate
6-7 mm	1	9	8	6	88.8%
	2	8	6	5	75%
7-8 mm	1	7	7	6	100%
	2	9	8	8	88.8%
8-9 mm	1	5	4	5	80%
	2	5	3	11	60%
9-10 mm	1	4	4	10	100%
	2	3	1	14	33.3%

**DISCUSSION**

Nephrolithiasis is a very common problem. Patients often stones of different sizes. Small stones pass spontaneous usually but patients experience severe ureteric colic during passage of stone. Spontaneous passage of ureteric stone depends on stone size, site, anatomy of ureter and past history of stone passage.(11)

Median probability of stone passage is 68% for stone < 5 mm size and 47% for stones of 5 mm – 10 mm.(9)The MET aims at passage of stone with minimum discomfort to the patient.

Number of drugs have been used for the same purpose like corticosteroids, hormones, NSAIDs, calcium channel blockers and  $\alpha$ -1 adrenergic blockers. Corticosteroids decrease the inflammation around the ureter.[8] Calcium channel blockers suppress smooth muscle contraction and reduce ureteral spasm,  $\alpha$ -1 adrenergic blockers act by decreasing ureteral muscle tone and frequency and force of peristalsis.[7]

We have compared the effectiveness of  $\alpha$ -1 blockers with  $\alpha$ -1 blockers + corticosteroids. Group 1 was given only  $\alpha$ -1 blocker+corticosteroid and Group 2 was given  $\alpha$ -1 blocker alone.  $\alpha$ -1 blocker used was Tamsulosin and Corticosteroid used was Deflazacort. Deflazacort is a good anti edemic drug[10], well tolerated with limited side effects. In our study we consistently found better stone clearance rate and earlier passage of stone across all stone sizes in Group1 i.e Tamsulosin + Deflazacort group. Range of Stone size in our study varied from 6-10 mm.

**CONCLUSION**

MET using Tamsulosin has definite role in passage of smaller size

ureteric stone of less than 10mm size. It has acceptable success rate in bigger size stone in our study upto 17 mm size, when Tamsulosin was combined with Deflazacort.

**REFERENCE**

1. Sierakowski R, Finlayson B, Landes RR, Finlayson CD, Sierakowski N. The frequency of urolithiasis in hospital discharge diagnosis in the United States. Invest Urol 1978;15:438-41.
2. Cervenakov I, Fillo J, Mardiak J, Kopecky M, Smirala J, Lepies P. Speedy elimination of uretrolithiasis in lower part of ureters with the alpha 1-blocker-Tamsulosin. Int Urol Nephrol 2002;34:25-9.
3. Seitz C, Liatsikos E, Porpiglia F, Tiselius HG, Zwergel U. Medical therapy to facilitate the passage of stones: what is the evidence? Eur Urol 2009;56:455-71.
4. Gravas S, Tzortzis V, Karatzas A, Oeconomou A, Malekos MD. The use of Tamsulosin as adjunctive treatment after ESWL in patient with distal ureteral stones: do we really need? Result from a randomized study. Urol Res 2007;35:231-5.
5. Picozzi SC, Marengi C, Casellato S, Ricci C, Gaeta M, Carmignani L. Management of ureteral calculi and Medical Expulsive therapy in emergency department. J Emerg Trauma Shock 2011;4:70-6.
6. De Sio M, Autorino R, Di Lorenzo G, Damiano R, Giordano D, Cosentino L, et al. Medical expulsive treatment of distal-ureteral stones using Tamsulosin: a single – center experience. J Endourol 2006;20:12-6.
7. Cooper JT, Stack GM, and Cooper TM. Intensive medical management of ureteral calculi. Urology 2000;56:575-8.
8. Tilakv M, Bhamare N. Progesteron Hydrotherapy in Management of Small, Mid and Lower ureteric calculi; International Journal of Recent Trends in Science and Technology 2012;4:90-3.
9. 2007 AUA Guidelines for the management of Ueteral Calculi.
10. Francesco Porpiglia etal Corticostroids and Tamsulosin in the Medical Expulsive therapy for symptomatic distal ureter stones: Single drug or Association? European urology 50 (2006) 339-344.
11. Hubner, W. A., Irby, P. and Stoller, M. L.: Natural history and current concepts for the treatment of small ureteral calculi. EurUrol, 24: 172, 1993.
12. Tilakv M, Bhamare N. Progesteron Hydrotherapy in Management of Small, Mid and Lower ureteric calculi; International Journal of Recent Trends in Science and Technology 2012;4:90-3.
13. Hancock AA.  $\alpha$  1- adreno receptor sub types : a synopsis of their pharmacology & molecular biology. Drug Dev Res 1996;39:54-107.



## CLINICAL EXPERIENCE OF THE TUBELESS PCNL USING STANDARD EQUIPMENTS

**Dr Shashikant Bhangre**

Associate Professor, Endourologist., Dept Of General Surgery MIMER Medical College., Pune. Maharashtra 410507

**Dr Dinesh Badarshahi\***

Senior Resident, Dept Of General Surgery MIMER Medical College, Pune. Maharashtra 410507 \*Corresponding Author

### A STRACT

**INTRODUCTION:** The standard PCNL comprises nephrostomy tube and Double J stent placed in kidney after the procedure. But nowadays Tubeless PCNL is practised to reduce post-op morbidity and hospital stay. This leads to our study on tubeless PCNL.

**MATERIAL AND METHODS:** This study conducted in General Surgery Dept of MIMER Medical College, pune, where 22 patients were operated for tubeless PCNL. In the group of 3 patients, no nephrostomy tube or DJ Stent was inserted after removal of the stone fragments. In 19 patients DJ stent was kept. The duration of surgery, intra-op and post-op hematuria, complications, analgesic requirement and hospital stay were studied.

**RESULTS:** In this study, mean duration of surgery for Tubeless PCNL was observed around 60 minutes was found. The average hospital stay was found to be 4 days. The post-op morbidity was comparatively less with this procedure. However, there were no statistical difference in blood loss, no major complications or mortality.

**CONCLUSIONS:** Tubeless PCNL is a safe, economic and procedure, and it can markedly reduce the postoperative analgesic requirements and reduce the hospital stay and costs.

**KEYWORDS :** nephrostomy tube, DJ Stent, duration of surgery, analgesic requirement, complications

### INTRODUCTION

Percutaneous nephrolithotomy (PCNL) is the treatment of choice for renal stones more than 15mm. In current practice following PCNL DJ stent and nephrostomy tube is inserted.

A "Tubeless" percutaneous procedure-one that has no postoperative nephrostomy tube-was initially proposed by Wickham and colleagues.<sup>1</sup> The concept was revived by Bellman and colleagues<sup>2</sup>, with a ureteral stent left in place for a week or two.

### Tubeless PCNL is mainly two types

Tubeless PCNL with ureteral stent, where after completion of PCNL only double J stent placed, no nephrostomy tube inserted.

Totally tubeless PCNL i.e. no nephrostomy tube or DJ stent placed after the procedure.

Karami et al<sup>3</sup> reported their 5-year experience in 201 patients undergoing tubeless PCNL with only an externalized ureteral catheter, and concluded that it was a safe, effective, and economical option. Similar results were reported by Ashraf Abou- Elela et al.

### MATERIAL AND METHODS

This was a study, conducted in the Department of general surgery, MIMER Medical college, Pune, for a period of 6 months in 2018. A total number of 22 cases of tubeless PCNL were studied. pcnl was performed by single urologist using standard 20 fr nephroscope and stone fragmentation done using pneumatic lithotripter,

**Total patients:** 22 patients

**Age:** 25yrs to 65yrs

**Sex:** Male: 15 Female: 07

**Calculus size:** 15mm to 25mm

**Location:** Pelvis: 08

**Upper pole:** 03

**Mid pole:** 03

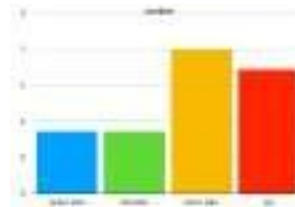
**Lower pole:** 07

### INCLUSION CRITERIA:

Patients with renal and/or upper uretric calculi of greater than 1.5cm amenable for PCNL.

### EXCLUSION CRITERIA:

- 1) Patient with significant intra-operative bleeding.
- 2) Patient with infected calculi.
- 3) Significant injury to the pelvic calyceal system.
- 4) Patient with stag horn calculus.



S No	Parametre	Values
1	Mean duration of procedure (minutes)	56.4±6.52
2	Bleeding requiring transfusion	0.0
3	Mean Length of hospitalization (days)	2.5±0.93
4	Mean analgesic requirement (tramadol iv)	62.4± 16.8 (mg)
5	Stone free rate	90.91%
6	Mean Procedure cost (rupees)	10000 to 15000
7	Time to return of daily life activities	5.2±0.18



### RESULTS

We studied 202cases undergoing tubeless PCNL in our hospital. We divided total cases in to 2 groups. There are 22 patients who underwent tubeless PCNL.

Mean stone burden is 2.0 cms with smallest stone of 1.5cm to largest stone of size 2.5cms. Single tract access was successful in most of the cases.

Mean duration of PCNL was 60 minutes.

No patient required blood transfusion intra or post operatively.

In addition, complications included high fever in 2 patients.

Post-op hematuria in 1 patient settled in 12 hrs.

DJ stent was not kept in 3 patients. Nephrostomy tube was not kept in any of the 22 patients.

## DISCUSSION

Since the introduction of PCNL about 30 years ago, continuous efforts have been made to improve the technique in order to decrease trauma to the kidney and the percutaneous tract, and reduce postoperative morbidity, hospital stay and costs. One of the clinically tested modifications is the mini-perc approach that was first reported in pediatric patients.<sup>6</sup> This version (mini perc) of PCNL uses 13-20 Fr working sheaths and was soon adapted for adults, resulting in reduced operative time, less postoperative morbidity and shorter hospital stay.<sup>7</sup> It did not, however, obviate the need for the placement of nephrostomy tubes. Pietrow et al used a narrower tube (10 Fr instead 22 Fr) and noted greater comfort in the immediate postoperative period without sacrificing safety.<sup>8</sup>

The concept of a tubeless technique represents a novel alternative in the search to miniaturize the procedure. Bellman et al. reported their initial experience with a series of 50 patients who underwent various percutaneous procedures. Later Limb and Bellman completed 112 successful tubeless procedures, representing almost one-third of all their percutaneous procedures.<sup>2</sup> Their Prospective randomized studies designed to compare tubeless vs. mini vs. standard PCNL confirmed the superiority of the tubeless PCNL.

Tubeless PCNL has been a successful procedure even in advanced aged patients. [13,14]

Shah et al. [14] documented superiority of percutaneous nephrolithotomy in terms of patient's satisfaction.

In Our present study, we studied the effectiveness and safety of tubeless PCNL for operative time, postoperative hematuria, hospital

stay, and stone-free rate. There was significant reduction in post operative pain, PCN site leakage and analgesic requirement. we used standard size nephroscope 20 fr , stone fragmented with pneumatic lithotripsy

The mean operative time in our study was shorter in the Tubeless PCNL group (59.4min) this difference was not statistically significant.

Ni et al. reported that tubeless PCNL had a reduced operative time versus standard PCNL.

In our study none of the patients required post op blood transfusion similar to the study of Khairy Salem et al. there.<sup>9</sup>

In studies conducted by Gupta et al and Crook et al there is no statistically significant difference in blood transfusion rates between two groups i.e standard PCNL and tubeless PCNL<sup>10</sup>

Hospital stay plays an important role in the evaluation of a technique, in our present study it was lower in Tubeless PCNL group was statistically significant. This result was similar to other published studies, such as in the study of Khairy Salem et al. in which the mean (range) hospital stay was 1.7 (1–4) days in the tubeless PCNL group and 2.8 (3–4) days in the Standard PCNL.<sup>9</sup>

In our present study, the postoperative analgesic requirement (tramadol) in the Tubeless PCNL group was less . This advantage of tubeless PCNL and has also been reported in other studies, such as that of Zhong et al. as their overall results indicated that the tubeless PCNL group had a lesser analgesic requirement.<sup>11</sup> In our study Average cost of the procedure for tubeless PCNL was less.

The mean time to return daily activities in our study for tubeless PCNL is 5 days and for standard PCNL it is 10.5 days. Zhong et al. reported that the time for return to normal activity in the totally tubeless group was significantly lower than the standard PCNL group.<sup>11</sup>

Reference study	N	Mean stone burden	Postoperative drainage	Analgesia requirement	Average Hb drop gm/dl	Stone free rates (%)
Agarwal et al <sup>12</sup>	101	3.8 cm <sup>2</sup>	JJs	81.7 mg MP	0.36 gm%	100
Desai et al	10	250	JJs	8.5 mg D	4.2 gm%	-
Feng et al	8	4.4 cm <sup>3</sup>	JJs	5.25 mg M	-	85.7
Singh et al	30	750mm	JJs	6 mg M, 415 mg D	1.2 gm%	100

## CONCLUSION

Our findings demonstrated that tubeless PCNLs can be safely and effectively performed by an experienced endourologist in selective patients.

Tubeless PCNL has an advantage of significantly reduced postoperative pain, cost of treatment and shorter hospital stay.

Complications rate are less with tubeless PCNL and blood transfusion is less when compared with traditional PCNL. We believe that this study will contribute to the further popularization of the tubeless technique for the benefit of the patient and the health care.

## REFERENCES

- Wickham JE, Kellett MJ. Percutaneous nephrolithotomy. *Br J Urol.* 1981;53:297–9. 4. Wickham JE, Kellett MJ. Percutaneous nephrolithotomy. *Br Med J.* 1981;283:1571–2. [PMCID: PMC1508044]
- Bellman GC, Davidoff R, Candela J, Gerspach J, Kurtz S, Stout L. Tubeless percutaneous renal surgery. *J Urol.* 1997;157:1578–82.
- Karami H, Jabbari M, Arbab AH. Tubeless percutaneous nephrolithotomy: 5 Years of experience in 201 patients. *J Endourol.* 2007;21:1411–3.
- Gupta NP, Kesarwani P, Goel R, Aron M. Tubeless percutaneous nephrolithotomy. A comparative study with standard percutaneous nephrolithotomy. *Urol Int.* 2005;74:58–61.
- Aghamir SM, Hosseini SR, Gooran S. Totally tubeless percutaneous nephrolithotomy. *J Endourol.* 2004;18:647–8.
- Desai MR, Kukreja RA, Desai MM, Mhaskar SS, Wani KA, Patel SH, et al. A prospective randomized comparison of type of nephrostomy drainage following percutaneous nephrolithotomy: Large bore versus small bore versus tubeless. *J Urol.* 2004;172:565–7.
- Chan DY, Jarrett TW. Mini-percutaneous nephrolithotomy. *J Endourol.* 2000;14:269–73.
- Pietrow PK, Auge BK, Lallas CD, Santa-Cruz RW, Newman GE, Albalá DM, et al. Pain after percutaneous nephrolithotomy: Impact of nephrostomy tube size. *J Endourol.* 2003;17:411–4.
- Feng MI, Tamaddon K, Mikhail A, et al: Prospective randomized study of various techniques of percutaneous nephrolithotomy. *Urology.* 2001;58:345–350.
- Gupta V, Sadasukhi TK, Sharma KK, Yadav RG, Mathur R. Tubeless and stentless percutaneous nephrolithotomy. *BJU Int.* 2005;95:905–6.
- Zhong Q, Zheng C, Mo J, Piao Y, Zhou Y, Jiang Q. Tubeless versus standard percutaneous nephrolithotomy: A meta-analysis. *BJU Int.* 2012;109:918-924.
- Ni S, Qiyin C, Tao W, Liu L, Jiang H, Hu H, et al. Tubeless percutaneous nephrolithotomy is associated with less pain and shorter hospitalization compared with

standard or small bore drainage: A meta-analysis of randomized, controlled trials. *Urology* 2011;77:1293-8. [CrossRef]

- Garofalo M, Pultrone CV, Schiavina R, Brunocilla E, Sanguedolce F, Borghesi M, et al. Tubeless procedure reduces hospitalization and pain after percutaneous nephrolithotomy: results of a multivariable analysis. *Urolithiasis* 2013;41:347-53.
- Shah H, Khandkar A, Sodha H, Kharodawala S, Hegde S, Bansal M. Tubeless percutaneous nephrolithotomy: 3 years experience with 454 patients. *BJU Int* 2009;104:840-6. [CrossRef]





## CLINICO PATHOLOGICAL STUDY OF OVARIAN TUMORS AT A TERTIARY CARE INSTITUTE

### Pathology

**Smita P. Bhide** Professor, Dept of Pathology MIMER Medical College Talegaon Dabhade.

**Janice Jaison\*** Assistant Professor, Dept of Pathology MIMER Medical College Talegaon Dabhade.  
\*Corresponding Author

**Sneha R. Joshi** Professor & HOD, Dept of Pathology MIMER Medical College Talegaon Dabhade.

### ABSTRACT

**Background:** Ovarian tumors are an increasing cause for morbidity and mortality world over due to late presentation. They have different cell origin and different histopathological picture.

**Objective:** To study the different histopathological types of ovarian tumors in the different age groups

**Materials and Methods:** This retrospective study included all histopathologically proven ovarian tumors reported in Department of Pathology MIMER Medical College Talegaon Dabhade Pune over 5 years period from January 2013 to December 2017. All the clinical and histopathological data was obtained from records and was analyzed.

**Results :** Out of 72 ovarian tumors included, 87.50% were benign, 2.78% were borderline and 9.72% were malignant. Surface epithelial tumors were most common (75%) followed by Germ cell tumors (20.83%) Benign surface epithelial tumors comprised 76.19% of all benign tumors whereas their malignant surface epithelial tumors comprised 57.14% of all malignant tumors.

**Conclusion :** Benign tumors are more common than malignant tumors in all age groups. Surface epithelial tumors are the most common of all tumors. Serous cystadenomas were most common benign tumors whereas Serous cystadenocarcinoma was the most common malignant tumor.

### KEYWORDS

Ovarian tumors, Histopathology, Benign, Malignant

### INTRODUCTION

The ovarian neoplasm is the most fascinating tumor of the women in terms of its histogenesis, clinical behaviour and malignant potentiality.<sup>1</sup>

Ovarian carcinomas represent 6<sup>th</sup> most common cancer in females and is 4<sup>th</sup> leading cause of cancer death in women.<sup>2</sup> The ovarian tumors manifest with a wide spectrum of clinical, morphological and histological features.<sup>3</sup> Many ovarian tumors are asymptomatic in the early stages and are unfortunately diagnosed late in the course of disease. The high mortality rate of ovarian cancer is due to its late detection, thus earning itself the term silent killer.<sup>4</sup>

Determining the histogenesis of the tumor by studying histological features is very important for effective treatment and predicting their behaviour and prognosis. Certain non neoplastic lesions of ovary frequently form a pelvic mass and potentially mimic an ovarian neoplasm. Proper recognition is therefore important to allow appropriate therapy.<sup>4</sup> Not only the primary tumors, the ovary is also the favourite site for the metastatic tumors.<sup>5</sup>

The present study was carried out with the aim to find out age related incidence and the different histopathological types of ovarian tumors and classify them according to WHO Classification of ovarian tumors.

### MATERIALS AND METHODS

This was a retrospective study comprising of 72 ovarian tumors diagnosed in Department of Pathology, MIMER Medical College Talegaon Dabhade Pune over a time period from January 2013 to December 2017. All cystectomy, oophorectomy, salpingo-oophorectomy and total abdominal hysterectomy with bilateral or unilateral oophorectomy specimens were included in this study. The relevant clinical details were obtained from the case files.

The specimens received in the department of pathology were grossly examined after fixing them in 10% formalin. Representative sections were taken and processed with paraffin embedding. Multiple sections were taken and stained with H&E. Special stains (PAS, Mucicarmine) and IHC were done wherever required. Histopathological diagnosis was given by using WHO Classification of Ovarian tumors.

### RESULTS

A total of 72 ovarian tumors were studied which were reported between January 2013– Dec 2017. Among 72 ovarian tumors

71 (98.61%) were primary ovarian tumors and remaining one (01.39%) was metastatic tumor. (Table no 1)

**Table No 1: Primary versus Secondary Ovarian tumors**

Tumour type	No. of cases	Percentage
Primary Ovarian Tumors	71	98.61%
Secondary Ovarian Tumors	01	01.39%
Total	72	100%

Out of 72 Ovarian tumors, majority were benign 63 (87.50%), followed by malignant ones 7 (9.72%). (Table no 2)

**Table No 2: Number of benign, borderline, malignant and metastatic ovarian tumors**

Nature of Tumour	No. of cases	Percentage
Benign	63	87.50%
Borderline	02	02.78%
Malignant	07	09.72%
Total	72	100%

**Table No 3: Age wise distribution of Ovarian tumors**

Age in years	Total no of tumors	Benign	Borderline	Malignant
0-10	0	0	00	00
11-20	02	02	00	00
21-30	22	22	00	00
31-40	21	20	01	00
41-50	14	12	00	02
51-60	07	06	00	01
61-70	05	01	01	03
>71	01	00	00	01
Total	72	63	02	07

The above table shows age wise distribution of benign and malignant tumors. Majority of the tumors occurred in the reproductive age group. The youngest patient was of 15 years of age whereas the oldest was 71 years old. Benign tumors showed a peak incidence between 21-50 years of age. Most of the malignant tumors occurred beyond 50 years of age. (Table no 3)



**Table No 4 :Clinical presentation of Ovarian tumors**

Clinical features	No. of benign tumors	No. of borderline tumors	No. of malignant tumors
Mass per abdomen	38	02	07
Pain in abdomen	31	02	04
Menstrual abnormality	07	00	02
Gastrointestinal disturbances	02	00	01
Ascites	00	01	02
Loss of appetite/ weight	00	00	01

Most common presenting symptom of ovarian tumors was mass per abdomen which was present in 38, 2 & 7 cases of benign, borderline & malignant tumors respectively. Next common symptom was pain in abdomen which was present in 31, 2 & 7 cases of benign, borderline & malignant tumors respectively. Ascites was present in 2 patients of malignant and 1 patient of borderline ovarian tumors. Many patients had more than one symptoms. (Table no 4)

**Table No 5 :Histological types of Ovarian tumors based on cell of origin**

Tumor type	No of Cases	Percentage
Surface epithelial tumors	54	75.00%
Germ cell tumors	15	20.83%
Sex cord stromal tumors	02	02.78%
Metastatic tumors	01	01.39%
Total	72	100%

Out of 72 ovarian tumors studied, 54 were surface epithelial tumors(75%), 15 were of germ cell origin (20.83%) and 2 were of sex cord stromal tumors(2.78%). 1 metastatic tumor studied was Krukenberg's tumor(1.39%). (Table no 5)

**Table No 6 : Histopathological subtypes of Ovarian tumors**

Tumor type	No. of cases	Percentage
<b>I.SURFACE EPITHELIAL TUMORS</b>		
<b>A.Serous Tumors</b>		
1.Serous Cystadenoma	38	52.78%
2.Serous cystadenofibromas	02	02.78%
3.Borderline Serous Tumor	02	02.78%
4.Serous Cystadenocarcinoma	03	04.16%
<b>B.Mucinous Tumors</b>		
1.Mucinous Cystadenoma	08	11.11%
2.Mucinous Cystadenocarcinoma	01	01.39%
<b>II GERM CELL TUMORS</b>		
1.Benign mature cystic teratoma	14	19.44%
2.Teratoma with malignant transformation (SCC)	01	01.39%
<b>III SEX CORD STROMAL TUMORS</b>		
1.Granulosa cell tumor	01	01.39%
2.Fibrothecoma	01	01.39%
<b>IV SECONDARY/METASTATIC TUMORS</b>		
Total	72	100%

On analysing the histologic subtypes of ovarian tumors, among the surface epithelial tumors serous tumors were more common constituting 83.33% . In benign serous tumors, serous cystadenoma was the most frequent (84.44%). 2 cases of borderline serous tumor were seen. Mucinous tumors comprised 16.66% of all surface epithelial tumors. Serous cystadenocarcinoma was the most common malignant tumor of all ovarian tumors. (4.16%)

Mature cystic teratoma comprised the majority of germ cell tumors.

(93.33% ). Among the sex chord stromal tumors 1 case each of granulosa cell tumor and fibrothecoma was seen. One case of metastatic tumor (Krukenberg's tumor) with primary arising from signet ring cell carcinoma of stomach was studied. (Table no 6)



**Figure No. 1 Photomicrograph showing Serous Cystadenoma (H&E 10X)**



**Figure No. 2 Photomicrograph showing Serous Cystadenocarcinoma (H&E 10X)**



**Figure No. 3 Photomicrograph showing Mature Cystic Teratoma (H&E 10X)**

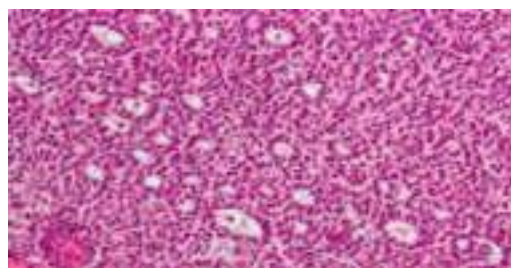


**Figure No. 4 Photomicrograph showing Adult granulosa cell tumor (H&E 10X)**



**Figure No. 5 Photomicrograph showing Krukenberg's tumor (H&E 40X)**

**DISCUSSION**

Ovarian tumors are one of the major health problems confronting the gynaecologists. Most of the ovarian tumors are detected incidentally on

imaging studies in patients who come to OPD for vague abdominal pain. In the early stages ovarian tumors remain silent. The symptoms are nonspecific like abdominal discomfort, dyspepsia and dull aching pain. The symptoms may remain vague till the patient has an acute emergency like torsion or rupture of ovarian tumor. There is marked variation in the clinical presentation as well as histopathological types of ovarian tumors.

Majority of the ovarian tumors occurred during reproductive age group. In the present study, the maximum number (59.72%) of benign tumors were observed between the age group 20-40 years which is the active reproductive life where as majority of malignant tumors (71.42%) occurred after 50 years of age. Similar findings were noted by Vissa Shanthi et al<sup>2</sup>, Monica Malli et al<sup>6</sup>, and Vinitha Wills & Rachel Mathew<sup>4</sup>.

Most of the benign and malignant ovarian tumors presented with mass per abdomen and pain in abdomen which is comparable with the studies done by Vissa Shanthi et al<sup>2</sup> & S Kayastha<sup>1</sup>.

Out of 72 Ovarian tumors, majority 63(87.50%) were benign, 02 (2.78%) were borderline and 7 (9.72%) were malignant. These findings are comparable with Vissa Shanthi et al<sup>2</sup>, Monica Malli et al<sup>6</sup>, Vinitha Wills & Rachel Mathew<sup>4</sup>, S Kayastha<sup>1</sup> and Ghosh A et al<sup>7</sup>. In all these studies majority of the ovarian tumors were benign.

Out of 72 ovarian tumors studied, 54 were surface epithelial tumors constituting the commonest type accounting for 75%. Studies done by Vissa Shanthi et al<sup>2</sup> (84.62%), Monica Malli et al<sup>6</sup> (78%), Vinitha Wills & Rachel Mathew<sup>4</sup> (71.42%), S Kayastha<sup>1</sup> (72.6%) and Ghosh A<sup>7</sup> (52.56%) also showed that surface epithelial tumors were the commonest among ovarian tumors.

In present study serous tumors constituted 83.33% of surface epithelial ovarian tumors which is in accordance with studies done by Vissa Shanthi et al<sup>2</sup> (78.78%), Monica Malli et al<sup>6</sup> (61.53%), Vinitha Wills & Rachel Mathew<sup>4</sup> (65%), S Kayastha<sup>1</sup> (55%) and Ghosh A et al<sup>7</sup> (67.44%). In serous tumors, serous cystadenoma was the most common tumor (84.44%). Studies done by Vissa Shanthi et al<sup>2</sup> (83.65%), Monica Malli et al<sup>6</sup> (72.91%), Vinitha Wills & Rachel Mathew<sup>4</sup> (96.15%) and Ghosh A et al<sup>7</sup> (76.77%) showed similar findings. Serous cyst adenocarcinoma constituted 6.66% of all serous tumors which is comparable with the studies done by Vissa Shanthi et al<sup>2</sup> (2.88%), Vinitha Wills & Rachel Mathew<sup>4</sup> (3.84%). Mucinous tumors were seen in 16.66% of surface epithelial ovarian tumors where as this figure was 20.45% & 25.58% in studies done by Vissa Shanthi et al<sup>2</sup> and Ghosh A et al<sup>7</sup> respectively.

In present study germ cell tumors constituted 20.83% of cases, and mature cystic teratoma was the most common germ cell tumor. Similar findings were noted by Vissa Shanthi et al<sup>2</sup> (10.90%), Monica Malli et al<sup>6</sup> (14%), Vinitha Wills & Rachel Mathew<sup>4</sup> (23.20%) and S Kayastha<sup>1</sup> (26.31%).

In present study, sex cord stromal tumors constituted 2.78% of cases where as metastatic tumors comprised 1.39% of cases. Vissa Shanthi et al<sup>2</sup> (3.84% & 0.64%), Monica Malli et al<sup>6</sup> (5% & 3%), and Ghosh A et al<sup>7</sup> (1.95% & 1.71%) showed similar findings.

## CONCLUSION

Benign ovarian tumors are more common than malignant tumors for all age groups. Most common histological types are Surface epithelial tumors constituting the bulk of both benign and malignant tumors followed by Germ cell tumors. Benign ovarian tumors occur more commonly in reproductive age group. Most of the malignant tumors occur beyond 50 years of age. Mass per abdomen and pain in abdomen are the most common clinical presentation. Though the imaging techniques and clinical examination help in detecting ovarian tumors, histopathological examination is the gold standard for the typing of ovarian tumor and its histogenesis which affects the treatment and prognosis of the tumor.

## REFERENCES

- 1 S Kayastha. Study of ovarian tumors in Nepal Medical College Teaching Hospital Nepal Med J 2009;11(3):200-02
- 2 Vissa Shanthi et al Clinico Pathological Study of Ovarian Tumors – A Retrospective and Prospective 5 Years Study. Journal Of Medical Science And Clinical Research. vol June 2016;4(6):10880-85
- 3 Shah PK, Shroff CP, Deodhar KP, Vaidya PR. Ovarian tumors in childhood and

- 4 Vinitha Wills, Rachel Mathew. A study on clinico-histopathological patterns of ovarian tumors. Int J Reprod Contracept Obstet and Gynecol. 2016 Aug;5(8):2666-71
- 5 Gupta N, Bishat D, Agarwal AK, Sharma VK. Retrospective and prospective study of ovarian tumors and tumor-like lesions. Indian J Pathol Microbiol 2007;50(3):525-7
- 6 Monika Malli, Bhavesh Vyas, Sunita Gupta, Hitendra Desai. A Histological Study of Ovarian Tumors in Different Age Groups. International Journal of Medical Science and adolescence. J Obstet & Gynaecol 1991;41(3):394-402

- 7 Public Health.2014;3(3):338-41  
Ghosh A,Ghartmagar D,Thapa S, Sathian B, Narasimhan R, Talwar op. Ovarian Tumors: Pattern of Histomorphological Types – 10 Years Study in a Tertiary Referral Center and Review of Literature. Kathmandu Univ Med J 2016;54(2):153-8

# Do Aesthetic Average Nasal Parameters Matter For Rhinoplasty in India?

Sapna Ramkrishna Parab<sup>1</sup> · Mubarak M. Khan<sup>2</sup>

Received: 3 June 2018 / Accepted: 29 June 2018 / Published online: 5 July 2018  
© Association of Otolaryngologists of India 2018

**Abstract** Nose morphology and facial features depend on ethnicity, gender and environmental conditions. Nasal parameters for rhinoplasty are well defined in the European and American population. Though rhinoplasty is a common cosmetic surgery in India, till now, there is no dedicated study delineating the parameters for the Indian Rhinoplasty. The aim of this study is to determine and delineate the anthropometric measurements of the Indian male and female noses and to propose the nasal parameters for Indian rhinoplasty. To determine the aesthetically pleasing nasal anthropometric parameters in Indian males and females and to put forth the parameters for Indian Rhinoplasty. This anthropometric study included a volunteer sample of 221 young, good-looking Indian males and females aged 18–25 years with Indian parents and no history of previous surgery or trauma to the nose. Standardized frontal, lateral and basal photographs of the noses along with the reference scale were taken, and 11 standard anthropometric measurements of the nose were determined. The sample size selected was such that it included representative population from the north south east and west zones of India. All the nasal measurements for the Indian women and men were found to be significantly different from the other European standards. In our study, we measured the nasal average values of the good looking, young Indian males and females and compared with the results of the nasal parameters of the other populations

found in the literature. This study is the first one to propose the aesthetic average nasal parameters for corrective rhinoplasty in Indian population. *Level of Evidence IV.*

**Keywords** Indian Nasal parameters · Anthropometry · Aesthetic average Indian nose · Indian rhinoplasty

## Introduction

The prose “Beauty Lies in the Eyes of the Beholder” is a paraphrase of a statement by Greek Philosopher Plato and was expressed by an Irish novelist in the nineteenth century. The connection of beauty to the eyes of the beholder is much deeper than what it looks. Each individual have different inclination and perception of what is beautiful. Beauty has always been the key to unlocking new doors to life and has played a major role on relationships. People undergo cosmetic correction to achieve the look that is thought and classified as beautiful. The concept of beauty has always been a very debatable topic. Whenever there is cosmetic correction for beautifying, there is a very important role of understanding the concept of beauty and aesthetics. And both beauty and aesthetics have a very close association with the knowledge of anthropometry.

Anthropometry has evolved due to increasing interest in determining the variations in human anatomy [1]. Anthropometry is a series of systematized techniques of measurement that express quantitatively the dimensions of the human body and skeleton. Anthropometry of face has become a useful tool used in genetic counselling, reconstructive surgery as well as in forensic investigation [2–4]. Nose is the most prominent feature of the face and makes an important contribution in the definition of a beautiful face. Anthropometry of facial symmetry and proportions

✉ Sapna Ramkrishna Parab  
drsapnaparab@gmail.com

<sup>1</sup> Department of Otorhinolaryngology, M.I.M.E.R. Medical College, Talegaon Dabhade, Pune, India

<sup>2</sup> Sushrut ENT Hospital and Dr. Khan’s ENT Research Center, Talegaon Dabhade, Pune, India

are considered determinants of beauty in a given population [5]. The nose is an individual's most determining feature of the face as it is at the centre [6]. The shape of the nose with regards to the nasal bridge, slope, tip broadness, septum and nares differs in races, tribes and in geographical areas. Thus the feature of the nose is a signature indicating the ethnicity, race, age and sex of the individual [7–10]. The differences in the nasal features in different parts of the world are partially the results of evolutionary adaptation to climate [11, 12]. The other determinants of the nasal features include genetic factors, race etc. Nose anthropometry is the measurement of the different nasal parameters. The nasal index has been correlated with average temperature and humidity [13, 14] and nasal size with oxygen consumption [15]. A low nasal index was associated with cold and dry climates, while a high nasal index was associated with hot and moist climates. It has not been confirmed whether differences in the size and the shape of the nose between different ethnic groups influences the different nasal physiology or predilection to sino-nasal pathology [16]. Since each racial group and ethnic population has their own nasal character and anatomic structure, mean nasal values of the nose should be comprehensively understood for each ethnic and racial group. Definitely, though beauty lies in the eyes of the beholder, it arises from harmonious proportions of the facial parts.

Direct anthropometry methods are time-consuming, problems like difficulty of patient adaptation, repeatability of measurements and archiving of data. Hence, indirect measurement methods like photograph, cephalogram, stereophotograph, laser scanning, and computerized tomography have increasingly become popular in recent years. The most frequent methods used clinically are photography. It is a fast and inexpensive method with better patient compliance [11]. In our study too, we have used the photographic method of anthropometric evaluation.

In the planning of rhinoplasty it is very important to take into consideration the type of nose characteristic for a particular race or ethnic group to suit the final outcome with the proportions of the face. Rhinoplasty surgeons require access to facial databases based on accurate anthropometric measurements to perform optimum correction in both sexes [11]. There are gender differences too in the nasal parameters and hence some points need to be considered during cosmetic nasal surgery for men because the expectations and anatomical differences exist. In the recent years, rhinoplasty is gaining popularity in the Indian population with the increasing number. To cater the ever increasing demands of the patients desiring cosmetic correction, it is of utmost importance that the rhinoplasty surgeon has thorough understanding and knowledge of the anthropometric measurements and ethnic variations of the

Indian population. A surgically corrected nose should blend harmoniously with the ethnic facial features of the individual [17]. India is a country of varied cultures and ethnic diversity. Till now, there is no single dedicated study that outlines the aesthetic anthropometric measurements to propose the guidelines for Indian Rhinoplasty. The nose is a person's most defining feature because it is at the centre of the face. The shape of the nose is a signature indicating the ethnicity, race, age and sex.

There are very few study in the literature mentioning the nasal parameters in males. This is the first study which is putting forward the concept of aesthetic nasal parameters representative of the whole of the Indian population for females as well as males. The aim of this study is to determine the nasal aesthetic anthropometric measurements in Indian male and female and to put forth the parameters for Indian Rhinoplasty.

## Methods and Materials

This is a descriptive Cross sectional anthropometric study carried out in MIMER Medical College and included a volunteer sample of 221 young good looking Indian male and female aged 18–25 years with Indian parents and no history of previous surgery or trauma to the nose or any congenital deformity of face. The mean age was  $20.45 \pm 1.42$  years. It included 110 males and 111 females. The written consent was obtained after explaining the study and its objectives to the participants. A special consent was taken with regards to the photography and identity revealing. The Institutional review Ethics Committee has approved the study. Among the other data, place of birth, and parental heritage was included. Standardized frontal, lateral, and basal photographs of the noses were taken, and 11 standard anthropometric measurements of the nose were determined. To minimise the error and to increase accuracy of measurement, each photograph was taken with a reference scale (Figs. 1, 2). The vertical scale was graduated with mm and was placed next to the face. The participants were seated in chair in a relaxed anatomical position (neutral position of the head) comfortably and the camera lens was aligned parallel to the front view of the face of the subject. Neutral head position is appropriate as it is easily reproducible and provides a natural orientation of face and helps in treatment planning. The photographs were captured using a digital Canon DSLR 550 D camera mounted on stand and maintaining a distance of 1 m between the subject and lens. The subject was advised not to change his/her position while photographs were being taken. Digital images were transferred to a computer. Calculations were done with Digimizer Image Measurement Software (Figs. 3, 4, 5, 6). All





Fig. 1 Measurements with the reference scale (female)



Fig. 2 Measurements with the reference scale (male)

measurements were performed three times to reduce error and the mean value was taken for further analysis. The

measurements were made with a permissible error of 1 mm. Data was fed into the IBM task (SPSS version) and

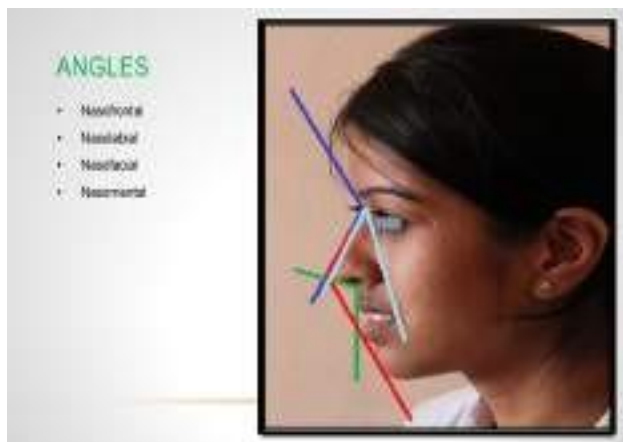


Fig. 3 Measurements of angles in female

descriptive statistical analysis was done using the SPSS version 16 (Illinois, Chicago, USA). Results were expressed in simple percentages, mean and standard deviation.

## Results

Our Medical College caters to a large population of students from different parts of the India with varied cultural diversity. It was thought that the nasal parameters may be grossly different in the different parts of the country. The study population thus selected was divided in such a way that the all the 4 zones of the country had its representative population. The sample size thus selected representative

population from the North, South, East and West zones of India. We the study population were divided primarily into 2 groups, Males and Females. Each subgroup was then subdivided into 4 zones. On subjecting to statistical analysis, there was no statistical difference in any of the parameters in the 4 zonal groups. Hence the sub-groups were again merged to form 2 larger groups; Indian Male and Female. The measurements of the nasal parameters calculated in the study are shown in Tables 1 and 2. The mean nasal height, basal width, dorsal height, radix height, nasal base, inter-canthal distance, angles (nasofrontal, nasofacial, nasolabial, nasomental) in males as well as females. On analysis of the results, it was observed that males had greater nasal parameter than females. The mean nasal length in males was 4.437 with SD 0.439 cm and in females was 4.1338 with SD 0.4569 cm. There was significant difference in the measurement between the two as the  $p$  value was  $\leq 0.05$ .

## Indian Female Nasal Parameters (Tables 1 and 2)

The mean nasal length in females was 4.1338 with SD 0.4569 cm. The other measurements were radix height 1.268 SD with 0.304 cm, dorsal height 2.0488 with SD 0.3046 cm, nasal tip projection 1.9494 with SD 0.265, Collumellar show 0.8045 with SD 0.204, nasal base 3.5748 with SD 0.412 cm and inter-canthal distance 2.949 with SD 0.391 cm. The Naso-frontal angle was 134.3269 with SD 8.8070°, Naso-labial angle 103.9878 with SD 12.659°, Naso-facial angle 37.6780 with SD.3062° and Naso-mental angle was 125.499 with SD 6.7892°.



Fig. 4 Measurements of angles in male

Fig. 5 Nasal measurements in females



Fig. 6 Nasal measurements in males

Table 1 NASAL angles: anthropometric measurements

Nasal parameters	Measurement in cm and SD	Measurement in cm and SD
	Female	Male
Nasofrontal angle	134.3269 (8.8070)	123.394 (10.7835)
Nasolabial angle	103.9878 (12.659)	100.619 (15.4805)
Nasofacial angle	37.6780 (5.3062)	41.721 (5.1924)
Nasomental angle	125.499 (6.7892)	124.483 (5.1830)

Indian Male Nasal Parameters (Tables 1 and 2)

The mean nasal length in males was 4.437 with SD 0.439 cm. The other measurements were radix height 1.421 with SD 0.336 cm, dorsal height 2.330 with SD 0.319 cm, nasal tip projection 2.0790 with SD 0.272, Collumellar show 0.836 with SD 0.161, nasal base 3.790 with SD 0.291 cm and inter-canthal distance 3.005 with SD 0.235 cm. The Naso-frontal angle was 123.394 with SD 10.7835°, Naso-labial angle 100.619 with SD 15.4805°, Naso-facial angle 41.721 with SD 5.1924° and Naso-mental angle was 124.483 with SD 5.1830°.

Table 2 Nasal anthropometric measurements

Nasal parameters	Measurements in cms with SD	Measurements in cms with SD
	Female	Male
Nasal length	4.1338 (0.4569)	4.437 (0.439)
Radix height	1.268 (0.304)	1.421 (0.336)
Dorsal height	2.0488 (0.3046)	2.330 (0.319)
Nasal tip projection	1.9494 (0.265)	2.0790 (0.272)
Collumellar show	0.8045 (0.204)	0.836 (0.161)
Nasal base	3.5748 (0.412)	3.790 (0.291)
Interanthal distance	2.949 (0.391)	3.005 (0.235)

## Discussion

Beauty arises from symmetric, balanced and harmonious proportions of facial parts. Nasal shape gives information about race, ethnicity, age and sex. The size, shape, and proportions of the nose provide a visual basis suggesting the character of the person. Moreover, it is an important key for a natural and aesthetically pleasing human face [18]. Definition of beauty and its concepts varies according to ethnicity. Anthropometric analysis is a method, aiming to achieve the most reliable comparison of the body forms by using specific landmarks determined in respect of anatomical prominences. Photogrammetry is an easier and more effective method for anthropometric analysis of the nose. Anthropometric analysis helps in enhancing the plans of the corrective surgery.

Recently, lot of people want to undergo rhinoplasty operations to improve the shape of nose and attractiveness of the face. India ranks 7th in the world for the maximum number of rhinoplasty in 2017 according to the world rhinoplasty statistics for the year 2017 with 878,180 rhinoplasties being operated with a 3.7% of the world population [19]. A successful outcome in rhinoplasty requires thorough and accurate preoperative planning, and this can only be made possible if one has a thorough preoperative planning in mind. Any surgeon who performs rhinoplasty must be keenly aware of the racial and ethnic differences in nasal anatomy between male and female of a particular population. Nasal parameters are well discussed in the Whites and African Americans. There is no study which comprehensively describes the whole of Indian Nose. Hence European and American standard cannot be applied for Indian population.

India is a country of cultural diversity, encompassing a large area. We expected Zonal Variations in the anthropometry of the noses. Hence sample size was selected in such a way so as to have representative population from all 4 zones– North, South, East and West. However on

statistical analysis, zonal variations were not statistically significant ( $p > 0.05$ ). Thus the 4 groups were combined to represent one population to calculate the anthropometric parameters.

Anthropometric analysis is a step to clarify these important points and basement for enhancing the plans of the corrective surgery. Nasal analysis is vital before performing rhinoplasty (plastic surgery). It is also important in forensic science. Hence research on the nasal parameters of various ethnic groups is very important. The normal values of nasal parameters are vital measurements in the evaluation and diagnosis of craniofacial deformities. The aim of this study is to determine the nasal parameters in male and female adults of the Indian population.

There are several anthropometric studies related with the nose, which are bringing forward other different methods. However we decide to review a landmark-based geometric morphometric technique which can be easily used to analyze the nasal shapes in any population.

The mean nasal length in males was 4.437 with SD 0.439 cm and in females was 4.1338 with SD 0.4569 cm. In the Chinese mean nose length [18] (53.50 mm), Caucasian [20] mean (53.00 mm), Afro-American mean values (52.4 mm), white northern Italian (54.33) [21], and Afro-Indian [22] mean (54.7 mm) values. In the Turkish population, the mean value was 56.92 mm [23].

### Nasal Width

In our study, the nasal width was 3.5748 with SD 0.412 cm in females and nasal base 3.790 with SD 0.291 cm in males. In Korean American [24] ( $35.5 \pm 3.4$ ) and white women ( $31.4 \pm 2.0$ ), Afro-American [20] (43.5 mm), Chinese [18] (39.20 mm), Japanese [9] (36.3 mm), Canadian-Caucasian [25] (36.9 mm), African [22] (45.9 mm), Afro-Caucasian (39.6 mm), Afro-Indian (42.7 mm) noses [22], and in young Turkish people [23] (33.63 mm).

### Nasofrontal and Nasolabial Angle

In the Turkish study [26], the nasofrontal angle in males was  $123.85 \pm 13.23^\circ$  and in females was  $133.16 \pm 8.88^\circ$ . Whereas the nasolabial angle in male was  $97.91 \pm 8.78^\circ$  and in female was  $98.91 \pm 10.01^\circ$ . In Korean female, the mean nasofrontal angle was  $136.8^\circ$ . In our study, the nasofrontal angle was (female) and (male) and nasolabial angle was (female) and (male).

### Nasofacial Angle

In Korean [27] female, the nasofacial angle was  $32.3^\circ$ , in Nigerian [28] Ibo ethnic group was  $36.3 \pm 0.37^\circ$  and Nigerian Yoruba group was  $35.5 \pm 0.38^\circ$ .

There are multiple Indian studies defining the nasal parameters [29, 30], but all of them describe the nasal parameters of state or region wise and not for the country as a whole. There is also study by Patil et al. [31], but it has described only the female average nasal parameters. The concept of average faces is different from that of the attractive and pleasing face. In other words, it means that the average nasal parameters are different aesthetically pleasing attractive nasal parameters for a particular region.

#### Advantages of Our Study

1. First study to propose the aesthetic average nasal parameters for Indian rhinoplasty.
2. These parameters can be used for Indians settled in foreign countries seeking rhinoplasty.
3. It aids in the preoperative plan of cosmetic correction of nose.
4. The photographic analysis used in this study is easier, repeatable in measurements unlike the manual measurements.
5. The parameters provided by our study can be used even in post-traumatic facial disfigurement.
6. It will help for enhancing the results of the corrective surgery in Indian Rhinoplasty.
7. It can also be used for genetic counselling and forensic investigation.
8. Our dedicated anthropometric study of the aesthetically pleasing Indian Nose would thus enable a better and accurate guidelines for performing cosmetic and reconstructive rhinoplasty.

**Limitations of the Study** Small study population.

#### Conclusion

In India, rhinoplasty is gaining popularity. But till now, there is no dedicated study with the nasal parameters for males and females in the Indian population. Our study shows that nasal measurements of the Indians are different from European, Chinese, American noses. Hence, the European and other international nasal parameters should not be applied for Indians seeking rhinoplasty. The concept of average faces is different from that of the attractive and pleasing face. Our study suggests the aesthetic average nasal parameters for the Indians based in India and those settled abroad seeking rhinoplasty. The nasal anthropometric norms proposed by our study will serve as a guide for cosmetic and reconstructive surgery, genetic counselling anthropology and forensic investigation.

In conclusion, we believe that aesthetic average values of the nose in this population may contribute to attractive results in Indian reconstructive nasal surgery.

**Acknowledgements** Dr. Mrs. Swati Rajee, Dept Of PSM, MIMER MC for the statistical analysis.

**Compliance with Ethical Standards**

**Conflict of interest** All authors declare that they have no conflict of interest.

**Ethical Approval** All procedures performed in studies involving human participants were in accordance with the ethical standards of the institutional committee and with the 1964 helsinki declaration and its later ammendments or comparable ethical standards Institutional Ethics Committee has approved the study.

**Informed Consent** Informed consent was obtained from all individual participants included in the study. Special consent was taken for photography and identity disclosure.

#### References

1. Eickstedt EV (1927) The race and types of the western Himalayas. *Man India* 6:237
2. Oladipo GS, Olabiyi AO, Oremosu AA, Noronha CC (2007) Nasal indices among major ethnic groups in Southern Nigeria. *Sci Res Essay* 2(1):20–22
3. Olotu JE, Eroje A, Oladipo GS, Ezon-Ebidor E (2009) Anthropometric study of the facial and nasal length of adult Igbo ethnic group in Nigeria. *Int J Biol Anthropol* 2(2):1–6
4. Krishan K (2008) Estimation of stature from cephalo-facial anthropometry in north Indian population. *Forensic Sci Int* 181(1–3):52e1–52e6
5. Carvalho B, Ballin AC, Becker RV, Berger CA, Hurtado JG, Mocellin M (2012) Rhinoplasty and facial asymmetry: analysis of subjective and anthropometric factors in the Caucasian nose. *Int Arch Otorhinolaryngol* 16(4):445–451
6. Romo T 3rd, Abraham MT (2003) The ethnic nose. *Fac Plast Surg* 19(3):269–278
7. Milgrim LM (1996) Anthropometric analysis of the female Latino nose: revised aesthetic concepts and their surgical implications. *Arch Otolaryngol Head Neck Surg* 122:1079–1086
8. Mishima K, Mori Y, Yamada T, Sugahara T (2002) Anthropometric analysis of the nose in the Japanese. *Cells Tiss Organs* 170:198–206
9. Ochi K, Ohashi T (2002) The effects of an external nasaldilator and nasal dimensions in Asians. *Otolaryngol Head Neck Surg* 126:160–163
10. Ofodile FA, Bokhari F (1995) The African–American nose: part II. *Ann Plast Surg* 34:123–129
11. Abdullah Etöz (2011). Anthropometric analysis of the nose. In: Brenner M (ed) *Rhinoplasty*. ISBN: 978-953-307-849-6, InTech. <http://www.intechopen.com/books/rhinoplasty/anthropometric-analysis-of-the-nose>
12. Davies A (1932) Man's nasal index in relation to climate. *J R Anthropol Inst GB Irel* 29:8–14
13. Balaesque PL, Ballereau SJ, Jobling MA (2007) Challenges in human genetic diversity: demographic history and adaptation. *Hum Mol Gen* 16:R134–R139



14. Thompson A, Dudley Buxton L (1923) Man's nasal index in relation to certain climatic conditions. *J R Anthropol Inst GB Irel* 53:99–122
15. Weiner JS (1954) Nose shape and climate. *Am J Phys Anthropol* 12:615–618
16. Hall RL (2005) Energetics of nose and mouth breathing, body size, bod composition and nose volume in young adult males and females. *Am J Hum Biol* 17:321–330
17. Trenite' GJN (2003) The ethnic nose. *Facial Plast Surg* 19(3):237–238
18. Aung SC, Liam FC, Teik LS (2000) Three dimensional laser scan assessment of the Oriental nose with a new classification of Oriental nasal types. *Br J Plast Surg* 53(2):109–116
19. <https://globenewswire.com/news-release/2017/06/27/1029348/0/en/Demand-for-Cosmetic-Surgery-Procedures-Around-the-World-Continues-to-Skyrocket-USA-Brazil-Japan-Italy-and-Mexico-Ranked-in-the-Top-Five-Countries.html>
20. Ofodile FA, Bokhari F (1995) The African–American nose Part II. *Ann Plast Surg* 34:123–129
21. Ferrario VF, Sforza C, Poggio C, Schmitz JH (1997) Three-dimensional study of growth and development of the nose. *Cleft Palate-Craniof J* 34:309–317
22. Ofodile FA, Bokhari F, Ellis C (1993) The black American nose. *Ann Plast Surg* 31:209–218
23. Uzun A, Akbas H, Bilgic S, Emirzeoglu M, Bostanc O, Sahin B, Bek Y (2006) The average values of the nasal anthropometric measurements in 108 young Turkish males. *Auris Nasus Larynx* 33:31–35
24. Choe KS, Yalamanchili HR, Litner JA, Sclafani AP, Quatela VC (2006) The Korean American woman's nose: an in-depth nasal photogrammatic analysis. *Arch Facial Plast Surg* 8:319–323
25. Farkas LG, Phillips JH, Katic M (1998) Anthropometric anatomical and morphological nose widths in Canadian-Caucasian adults. *Can J Plast Surg* 6:149–151
26. Ahmet Uzun, Fikri Ozdemir (2014) Morphometric analysis of nasal shapes and angles in young adults. *Braz J Otorhinolaryngol.* 80(5):397–402
27. Choe KS, Sclafani AP, Litner JA, Yu G, Romo T (2004) The Korean American woman's face anthropometric measurements and quantitative analysis of facial aesthetics. *Arch Fac Plast Surg* 6(4):244–252
28. Eliakim-Ikechukwu CF, Ekpo AS, Etika M, Ihentuge C, Mesembe OE (2013) Facial aesthetic angles of the Ibo and Yoruba ethnic groups of Nigeria. *IOSR J Pharm Biol Sci (IOSR-JPBS)* 5(5):14–17. e-ISSN: 2278-3008. <http://www.iosrjournals.org/iosr-jpbs/papers/Vol5-issue5/C0551417.pdf>
29. Choudhary A, Choudhary DS (2012) Comparative anthropometric study of nasal parameters between two ethnic groups of Rajasthan State. *Int J Med Public health* 2(2):46–48
30. Chhabra DN, Bedi DM, Patnaik DVVG (2012) Anthropometric study of the nose of 600 North Indian Adults (a study done for forensic identification). *NJIRM* 3(5):62–68
31. Patil SB, Kale SM, Jaiswal S, Khare N, Math M (2011) The average Indian female nose. *Aesthetic Plast Surg* 35(6):1036–1042

# Minimal Invasive Endoscopic Ear Surgery: A Two Handed Technique

Sapna Ramkrishna Parab<sup>1</sup> · Mubarak Muhamed Khan<sup>2</sup>

Received: 7 May 2018 / Accepted: 22 May 2018 / Published online: 29 May 2018  
© Association of Otolaryngologists of India 2018

**Abstract** To evaluate the surgical outcome of two handed technique of endoscopic ear surgery with endoscope holder. Retrospective Non Randomized Clinical Study. A total of 547 endoscope holder (Justtach) assisted ear surgeries (331 cartilage tympanoplasties and 216 cholesteatoma surgeries) were operated with Justtach from July 2013 to April 2016 with a follow up period ranging from 12 to 45 months to evaluate its feasibility and results with the technique. The design of the endoscope holder, Justtach is described along with its functioning and maneuvering techniques. In the endoscopic tympanoplasty group, at 1 year follow up, the graft uptake was seen in 323 ears with three residual perforation and 5 recurrent perforations giving a success rate of 97.58%. At the 2 years follow up, the graft uptake was in 322 ears with 6 recurrent perforations and 3 residual perforations with a success rate of 97.28%. Whereas in case of endoscopic cholesteatoma surgery, there was residual cholesteatoma in 5 and recurrent in 6 out of 216 cases. The study reports the successful application and use of endoscope holder in two handed technique of endoscopic ear surgery.

*Level of Evidence* Level 4.

**Keywords** Endoscope holder · Justtach · Two handed endoscopic ear surgery · Endoscopic cartilage tympanoplasty · Endoscopic cholesteatoma surgery

## Introduction

Minimal invasive surgery has influenced the techniques in every specialty of surgical medicine. This has led to the replacement of conventional procedures with minimally invasive ones, stimulated surgeons to re-evaluate conventional approaches. However, two major drawbacks of the minimal invasive surgery include the prolonged learning curve for most surgeons, and secondly, increased costs due to investment in the equipment required as well as longer operating times. Since the introduction of microscope in middle ear surgery, all the well-established techniques in ear surgery have evolved. However since last decade, endoscopes have been introduced into ear surgery. Endoscopic ear surgery is an evolving science in the field of otology and provides minimally invasive transcanal approach to the middle ear. Though endoscopic techniques are similar to the standard well known microscopic ear surgery techniques, it differs in its approach to the middle ear and adds a new perspectives and dimensions to the understanding of middle ear anatomy and pathology. The advantages of endoscopes in ear surgery include (1) visualization of the whole tympanic membrane and the ear canal without manipulation of the patient's head or the microscope, (2) extension of the operative field in transcanal procedures into structures usually hidden from the microscope (anterior tympanic perforation, posterior retraction pocket, facial recess, and hypotympanum) and (3) visualization of structures from multiple angles as

Electronic supplementary material The online version of this article (<https://doi.org/10.1007/s12070-018-1411-7>) contains supplementary material, which is available to authorized users.

✉ Sapna Ramkrishna Parab  
drsapnaparab@gmail.com

<sup>1</sup> Department of Otorhinolaryngology, M.I.M.E.R. Medical College, Pune 410507, India

<sup>2</sup> Sushrut ENT Hospital, Dr. Khan's Creations, Talegaon D, Pune, India

opposed to the microscope's single axis along the ear canal [1, 2]. In cholesteatoma surgery, the use of endoscopes has reduced the incidence of residual disease [3].

The only disadvantage of endoscopic ear surgeries as compared to microscopic ear surgery is that it is single handed surgical technique in which the non-dominant left hand of the surgeon is utilized for holding and manipulating the endoscope. The problem of one handed endoscopic ear surgery is more evident during drilling (in which simultaneous suction and drilling is not possible) hemorrhage (simultaneous suctioning and instrumentation is not possible), during fogging of the endoscope (one needs to remove endoscope again and again for lens cleaning), during prosthesis fitting in ossiculoplasty (manipulation may be difficult with one hand). In these situations, one feels the immense need for the two handed technique as in the microscopic ear surgery. Development of the endoscope holder would solve the single handed difficulties. Hence, the first endoscope holder, EndoHold [4] (Patent Application No. 2313-Mum-2013) was developed. The first endoscope holder is a modification of the microscopic stand. Endoscopic ear surgery (EES) is still in its developing stage. Though endoscope offers lot of advantages in middle ear surgery, but many a times, the surgeon, in the initial days of endoscopic ear surgery, may be compelled to shift to the microscope to visualize the magnified middle ear structures or for drilling. This necessitated the development of the second patented endoscope holder attachment to microscope which would allow both hands of the surgeon to be free for surgical manipulation during EES and allow alternate use of microscope whenever needed during ear surgery [1, 4, 5]. Operating Microscopes have range of motion in space during otological surgeries for focusing the desired object for magnification. This whole range of motions can be applied for driving the endoscope smoothly in any biological cavities once an endoscope holding attachment is fixed to optical system of any operating microscope (Patent Application No. 3300-Mum-2013) [5]. The purpose of this study was to report our experience of our minimally invasive two handed technique of endoscopic ear surgery with the second endoscope holder, Justtach.

## Methods and Materials

From 2010 to 2013, we operated with the single handed technique of Endoscopic Ear Surgery. However, due to the technical difficulties of the single handed surgery, we developed two endoscope holders; Patent Application No. 2313-Mum-2013 or EndoHold [4] and Patent Application No. 3300-Mum-2013 or Justtach [5]. This study includes exclusively the endoscopic ear surgeries operated with the

second endoscope holder, Justtach [5]. A total of 331 endoscope holder assisted endoscopic cartilage tympanoplasties and 216 primary cholesteatoma surgeries were operated from July 2013 to April 2016 in M.I.M.E.R Medical College and Sushrut ENT Hospital with a follow up period ranging from 12 to 45 months. There were 281 males and 266 females in the study group. The mean age of the study group was  $29.32 \pm 4.31$  years. The youngest patient was 9 years of age and the oldest was 56 years of age. Written consent was taken in all the patients. The details of the operative procedure was explained to the patients. The Institutional review Ethics Committee has approved the study. The average preoperative Air–Bone–Gap in the study group was  $31.32 \pm 3.76$  dB in the pars tensa perforation group. Part of the study has been already published [5]. In the cholesteatoma group, the average preoperative Air–Bone–Gap was  $35.68 \pm 5.69$  dB.

### Design of Endoscope Holder (Justtach-Patent Application No. 3300-Mum-2013) [5]

It is a metallic plate of 170 × 70 × 12 mm in dimensions with a circular slot measuring 16 × 16 mm in diameter to hold rigid endoscope and square slot to hold onto the microscope (Fig. 1). It has to be fixed to the optical system of any operating ENT microscope with the built in tightening screws (Fig. 2).

### Operating Theatre Requirements and Preparation of the Patient

Zero degree 4 mm endoscope with triple charge coupled device Camera (Karl Storz, Germany) is firmly fixed to optical system of microscope just above objective lens.

The ear canal is infiltrated with 2% lidocaine with 1 in 2,00,000 adrenaline. All patients of cholesteatoma surgery were operated under general anaesthesia and in the cartilage tympanoplasty group all, except 32, were operated under local anaesthesia. Preoperatively, all the patients were explained about the endoscopic procedure. Intraoperatively, the head of the patient is steadied by the assistant by placing the hand over the head of the patient to avoid any accidental head movement [4, 5].



Fig. 1 Justtach



Fig. 2 Justtach attached to microscope for two handed EES

#### Procedure [5] of Endoscopic ear Surgery with Justtach™ (Figs. 3, 4, 5, 6, 7, 8)

Instruments used in two handed endoscopic ear surgery are the same as in microscopic ear surgery. Using all aseptic precautions, the hair in the ear canal are trimmed with the 15 number surgical blade. The ear canal is irrigated with normal saline solution to clean any debris.



Fig. 3 Tragal cartilage graft harvest



Fig. 4 Transcanal zero degree middle ear endoscopy



Fig. 5 Ventilation pathway check

#### Incision and Approach

In endoscopic cartilage tympanoplasty, permeal (transcanal) incision is taken. In cholesteatoma cases, either transcanal (for limited attic cholesteatoma) or an endaural incision (in extensive cholesteatoma surgery) is taken.

#### Tragal Cartilage Harvest and Graft Preparation

Tragal cartilage is the graft of choice. It is harvested via the horizontal incision on the tragus in case of transcanal incision (Fig. 3). When endaural incision is taken, the tragal cartilage is harvested via the vertical limb of the Lempert's endaural incision. The tragal cartilage



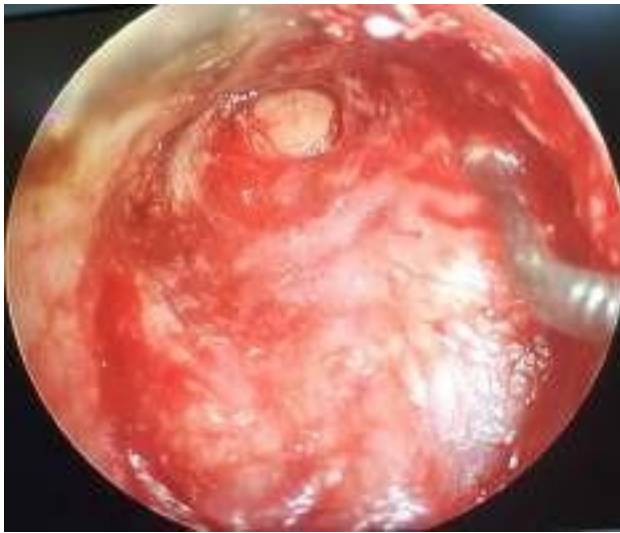


Fig. 6 Sliced cartilage graft view after the tympanomeatal flap reposition

perichondrium graft is sliced [1, 5–11] with *Slice It*® (Dr. Khan's Creations, India) to 0.5 mm thickness.

#### Middle ear Disease Clearance and Function Restoration

Intraoperative evaluation of middle ear anatomy during endoscopic surgery for inflammatory pathology allows to clearly visualize the presence of an anatomic blockage of ventilation pathway. The middle ear is evaluated (Fig. 4) for any presence of glue, cholesteatoma, granulation or block in the ventilation pathway (Fig. 5). The sliced cartilage graft is then placed by underlay technique (Fig. 6). In cholesteatoma surgery, the inside out technique of mastoidectomy is used to chase the cholesteatoma (Fig. 7a–c) and to excise the cholesteatoma. The atelectatic tympanic membrane or cholesteatoma matrix is elevated. The squamous epithelium loosely adherent to the neck of the malleus and scutum allows for a good starting point for surgical dissection. In the two handed technique of EES, the suction is held in left hand to avoid the fogging and also to achieve cooling of endoscope. Intermittent irrigation is done for cleaning and cooling of endoscope [1, 4, 5]. The stability rendered to the endoscope with the endoscope holder aids and augments the technical usage of endoscope in ear surgery during all steps of the routine tympanoplasty. With endoscope holder, Justtack, the simultaneous drilling and suctioning is possible. The panoramic view of the endoscope allows the visualization of the pathology beyond the corners without much bone removal. The angled endoscopic view allows complete removal of cholesteatoma from hidden areas like aditus, facial recess, or sinus tympani without much bone removal. The





Fig. 7 a Drilling with the two handed technique of ear surgery. b Atticoantrostomy and clearance of cholesteatoma with only stapes superstructure present. c Atticoantrostomy and clearance of cholesteatoma with no ossicles

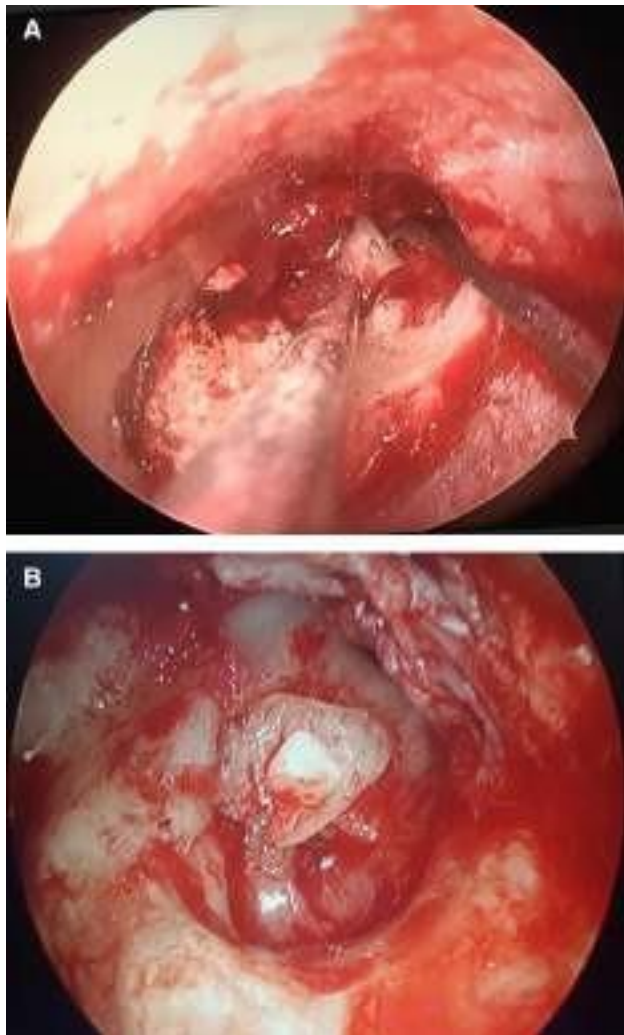


Fig. 8 a Sliced cartilage graft placed over stapes superstructure after atticoantrostomy. b Tragal cartilage graft for ossiculoplasty

ossiculoplasty with cartilage graft is done in patients with ossicular erosion (Fig. 8a, b). Soft wall reconstruction is done in atticoantrostomy canal wall defect. In case of narrow canal, we used 3 mm zero degree designed Karl Storz endoscope of 14 cm length [1, 4, 5].

## Results

A total of 547 two handed endoscopic ear surgeries were operated with Justtach (331 cartilage tympanoplasties and 216 cholesteatoma surgeries have been operated from July 2013 to April 2016 with follow up period ranging from 12 to 45 months (Table 1). No middle ear injury is reported in

Table 1 Age gender distribution of the study population

Operation performed	Number of ears		
	Male	Female	Total
Cartilage tympanoplasty	170	161	331
Cholesteatoma surgery	111	105	216
Total	281	266	547

our series. In all cases of endoscopic cartilage tympanoplasties, a transcanal incision was taken. In endoscopic cholesteatoma surgery, transcanal incision was taken in 173 ears and endaural incision was used in 43 ears. The extent of the disease dictated the amount of drilling and bone removal. In our series of endoscopic cholesteatoma surgery with Justtach, cholesteatoma was limited to the attic in 72 ears (33.33%), beyond antrum in 107 ears (49.54%) and extensive cholesteatoma up to tip was seen in 37 cases (17.13%). Hence in our study of endoscopic cholesteatoma surgery with two handed technique, atticoantrostomy was performed in 72 ears, atticoantrostomy in 107 ears and endoscopic inside out mastoidectomy in 37 ears. At 1 year follow up, the graft uptake was seen in 323 ears with three residual perforations and 5 recurrent perforations giving a success rate of 97.58%. At the 2 years follow up, the graft uptake was in 322 ears with 6 recurrent perforations and 3 residual perforations with a success rate of 97.28% (Table 2). The average preoperative Air–Bone–Gap in the study group was  $31.32 \pm 3.76$  dB and postoperative AB gap closed to  $9.34 \pm 3.32$  dB at 2 years (Table 3). Part of the study [6] has been already published. The results of our endoscopic cartilage tympanoplasty was comparable to our published microscopic primary cartilage tympanoplasty [6] outcome. Whereas in case of endoscopic cholesteatoma surgery (Figs. 9 and 10), there was residual cholesteatoma in 5 and recurrent cholesteatoma in 6 cases out of 216 cases. The average preoperative Air–Bone–Gap

Table 2 Graft uptake of endoscopic cartilage tympanoplasty

Cartilage tympanoplasty	1 year	2 years
Graft uptake	323	322
Recurrent	5	6
Residual	3	3
Success rate (in percent)	97.58	97.28

Table 3 Pre and postoperative airborne gap in endoscopic cartilage tympanoplasty for pars tensa perforations

Avg preop AB Gap (dB)	Postop ABG 6 months	Postop ABG 1 year	Postop ABG 2 years
$31.32 \pm 3.76$	$9.75 \pm 4.67$	$9.04 \pm 3.17$	$9.34 \pm 3.32$



Fig. 9 Preoperative patient of cholesteatoma



Fig. 10 Postoperative view after reconstruction with cartilage

in the cholesteatoma study group was  $35.68 \pm 5.69$  dB and post-operative AB gap closed to  $26.76 \pm 5.39$  dB (Table 4).

Table 4 Pre and postoperative airborne gap in cholesteatoma operated by endoscopic atticotomy

Avg preop AB gap (dB)	Postop ABG 6 months	Postop ABG 1 year	Postop ABG 2 years
$35.68 \pm 5.69$	$25.65 \pm 5.65$	$25.14 \pm 5.27$	$26.76 \pm 5.39$

## Discussion

The middle ear surgical techniques have evolved and developed after the introduction of the operating microscope. Since last few decades, endoscopic ear surgery also has started gaining popularity. In the initial years, the use of endoscope in ear was limited only for photography, documentation and for diagnostic purposes. Nomura [12, 13] and Takahashi [12, 14] reported first trans-tympanic middle ear endoscopy. Diagnosis of perilymphatic fistulae by transtympanic endoscopy was reported by Poe and Bottrill [12, 15]. The value of endoscopy as an adjunct in cholesteatoma surgery was documented by Badr-el-Dine [12, 16] and El-Messlaty [12, 17] to reduce the risk of recurrence of cholesteatoma. Yung [12, 18] and Ayache [12, 19] confirmed reduction of residual cholesteatoma by use of endoscope in middle ear surgery. Baki [12, 20] used endoscope to evaluate sinus tympani pathology. Endoscopic assisted surgery of the petrous apex was reported by Mattox [12, 21].

Minimal invasive endoscopic and endoscope assisted otologic surgeries are increasingly being performed. The introduction of endoscopes in middle ear surgery has not only changed the surgical approach but also has distinctly reduced the occurrence of residual cholesteatoma due to better visualization of the sinus tympani, facial recess and epitympanic recesses [1, 2, 4–6].

At present, the scenario of the endoscopic ear surgery is a single handed procedure with the endoscope being held in the non-dominant hand of the surgeon and the instrumentation in the dominant hand. We have been operating with the two handed technique of ear surgery using Justtach [1, 4, 5] due to its obvious benefits. In our study, we did not have any trauma to the middle ear structures due to any jerky movements of the endoscope. Neither was there any reported case of middle ear trauma or damage to endoscope tip.

The use of Justtach allows: [4, 5]

1. Allows two handed Endoscopic ear surgery (EES) similar to micro ear surgery as both the hands are available for surgical manipulation.
2. All movements (not functions) of the microscope optical body for endoscope movement can be applied to endoscope holder.
3. With Justtach, the endoscope can be moved more or less similar to the pattern of working of the left hand.
4. Every ENT surgeon owns microscope for ear surgery. With Justtach™, the microscope can be converted into endoscope holder. (At present nobody in the world is doing this) with simply fixing one endoscope holding metallic plate.

5. One can shift to microscopic ear surgery as and when needed with Justtach.
6. As ENT surgeons are well versed with the two handed technique of microscopic ear surgery, hence incorporating the Justtach for two handed EES will not be difficult.

#### Advantages of our Justtach [4, 5]

1. Due to endoscope holder there is stability of the endoscope, camera and image on the monitor is ensured throughout.
2. No surgeon fatigue in holding the endoscope (as compared with single handed endoscopic ear surgery).
3. When angled endoscope (30, 45, 70 degree) is used with the endoscope holders, it allows better visualization of sinus tympani, facial recess, anterior tympanic cavity and hypotympanum with just rotation of the endoscope within the Holder.
4. All the steps of the ear surgery are similar to Microscopic ear surgery as the left hand holds the suction cannula continuously and the instruments in the right hand.
5. Justtach can be used effectively without compromising the surgical field.
6. As an effective alternative for documentation and a useful teaching aid.
7. Minimizes the need for assistance.
8. As Justtach™ is designed on the Microscopic Stand, the fine focus of the microscopic stand can be utilized for additional advancing into the external auditory canal.
9. No retro auricular incision.
10. No Mastoid bandage is not required.
11. Lesser duration of surgery as the time required for the retro auricular incision and suturing is avoided.
12. Fogging of the endoscope is avoided by use of suction cannula and by irrigation.
13. Canalplasty can be done with the drill in the right hand and suction in the left hand.

#### Disadvantages and Our Solutions to It [1, 4, 5]

1. In narrow canal, either 3 mm zero degree endoscope or canalplasty may be performed.
2. Simple techniques used by us to avoid thermal damage.
  - a. The endoscope is kept at the isthmus of external auditory canal.
  - b. Continuous suction is held in left hand during the procedure as suggested in previous study [22].

- c. Intermittent irrigation helps in the cooling effect and cleaning of the tip of the endoscope. It also avoids frequent taking out of the endoscope for defogging (as in single handed endoscopic ear surgery) [22].
3. Additional cost of the endoscope holder in addition to the routine ear instruments.
4. Care is to be taken to avoid accidental injury due to head movement to the tip of the endoscope. For cases operated under local anesthesia with intravenous sedation, the assistant steadies the head of the patient.

Endoscopic techniques permit transcanal exploration of disease-containing area without opening areas that are not involved by cholesteatoma. The transcanal endoscopic approach opens only diseased areas, preserves many healthy air cells, and leaves the cortical bone intact. It also allows one to create two separate cavities; a small reconstructed tympanic cavity that conducts sound through the middle ear and is small enough to be serviced by the (usually dysfunctional) eustachian tube, and a larger attic, antrum, and mastoid cavity, which is joined to the ear canal and exteriorized [2, 12].

Study by Harugop et al. [23] has compared results of single handed endoscopic tympanoplasty with microscopic tympanoplasty with successful outcome in the 82% in the endoscope group 86% in the microscopic group. The surgical outcome was comparable in both the groups, however in terms of cosmesis and post-operative recovery, the endoscope group fared better. In a study by Furukawa et al. [24], endoscopic and microscopic view was analysed. The endoscopic view had clear advantages in terms of entire tympanic membrane visualization in a single field with clear visualization of the perforation edges even when the ear canal was curved. This facilitated reliable refreshing of the perforation edges and grafting. The anterior edge of the perforation was not visible under microscopy in 5 of 25 ears. They performed transcanal endoscopic myringoplasty successfully with a simple underlay technique or with an intracanal incision in cases of marginal perforation. Till now, all the studies mentioned in the literature are those of single handed endoscopic ear surgery. This is the first study which describes the role of endoscope holder, Justtach in two handed endoscopic ear surgery.

The learning curve for endoscope holder aided endoscopic ear surgery may not as steep as that for routine endoscopic or microscopic surgery. All of us are trained in microscopic ear surgery during the post-graduation course of otolaryngology. The microscopic ear surgery is a two handed technique in which one holds the suction in the left hand and the micro ear instruments in the right hand. Our two handed technique also is similar to the microscopic ear surgery with the added advantages of the endoscope. With



sufficient training and practice the technique may be adopted by all. Many experienced with endoscopic surgeries will find the technique easy to master, but surgeons who have limited themselves to an entirely microscopic otology practice are likely to find endoscope holder aided endoscopic surgery more difficult or unnecessary to perform or master. Before starting the endoscopic ear surgery, we insist that the surgeon should perform, at least 5 cadaveric endoscopic temporal bone dissection [1, 4, 5].

In the early days of endoscopic ear surgery, the case selection plays a very important role to develop confidence and to master the skills. The initial cases should be endoscopic ventilation tube insertion (grommet), myringotomy and then gradually progress and proceed to endoscopic tympanoplasty for small pars tensa perforations. After the comfort level with the technique increases, one may proceed to performing endoscopic tympanoplasty for large pars tensa perforations and later on to endoscopic cholesteatoma surgery. In cholesteatoma surgery too, one should start with limited cholesteatomas and then extensive cholesteatoma surgery. In two handed endoscopic cholesteatoma surgery, endoscope holder adds to the advantages as compared to traditional mastoidectomy. It is a minimally invasive surgical approach in terms of incision, bleeding, drilling, postoperative pain and healing, and it is curative in terms of the radical eradication of the pathology including hidden areas poorly accessible and thus overlooked by a microscope. As compared to the single handed technique, drilling simultaneously along with suctioning is possible with the endoscope holder.

## Conclusion

In the era of minimally invasive surgery, we have designed and developed the endoscope holder, Justtack for overcoming the disadvantages of the single handed endoscopic ear surgery. The advantages and disadvantages of the endoscope holder for two handed endoscopic ear surgery are well highlighted.

The minimally invasive two handed endoscopic ear surgery (EES) allows better and panoramic view of the middle ear structures without much bone removal, no retroauricular incision and suturing. There is also no fatigue involved in long duration surgery as in single handed EES with the surgeon holding the endoscope in left hand.

Endoscopic cartilage tympanoplasty is operated by using the sliced tragal cartilage. Whereas for cholesteatoma surgery, the inside out technique of atticotomy is used with reconstruction of the attic defect.

Use of the endoholder requires the training to acquire the skills.

## Compliance with Ethical Standards

**Conflict of interest** The authors declare that they have no conflict of interests.

**Ethical Approval** All procedures performed in this study involved human participants and was in accordance with the ethical standards of the institutional committee and with the 1964 helsinki declaration and its later amendments or comparable ethical standards. Institutional Ethics Committee has approved the study.

**Informed Consent** Informed consent was obtained from all individual participants included in the study.

## References

1. Khan MM, Parab SR (2016) Endoscopic cartilage tympanoplasty: a two-handed technique using an endoscope holder. *Laryngoscope* 126:1893–1898. <https://doi.org/10.1002/lary.25760>
2. Tarabichi M (1999) Endoscopic middle ear surgery. *Ann Otol Rhinol Laryngol* 108(1):39–46
3. Migirov L, Wolf M (2015) Minimally invasive transcanal endoscopic ear surgery. In: *Endoscopy-innovative uses and emerging technologies* 2015. <https://doi.org/10.5772/60551> (InTech)
4. Khan MM, Parab SR (2015) Concept, design and development of innovative endoscope holder system for endoscopic otolaryngological surgeries. *Indian J Otolaryngol Head Neck Surg* 67(2):113–119
5. Khan MM, Parab SR (2016) Novel concept of attaching endoscope holder to microscope for two handed endoscopic tympanoplasty. *Indian J Otolaryngol Head Neck Surg* 68(2):230–240
6. Khan MM, Parab SR (2011) Primary cartilage tympanoplasty: our technique and results. *Am J Otolaryngol* 32(5):381–387
7. Khan MM, Parab SR (2013) Reinforcement of sliced tragal cartilage perichondrium composite graft with temporalis fascia in Type I tympanoplasty: our techniques and results. *J Rhinolaryng Otol* 1:57–62
8. Khan MM, Parab SR (2012) Day care ear surgery: our experience of 4 years. *Indian J Otolaryngol Head Neck Surg* 64(3):280–284
9. Khan MM, Parab SR (2014) Sliced Island tragal cartilage perichondrial composite graft: early results and experience. *J Rhinolaryng Otol* 2:4–9
10. Khan MM, Parab SR (2015) Comparative study of sliced tragal cartilage and temporalis fascia in type I tympanoplasty. *J Laryngol Otol* 129(1):16–22
11. Khan MM, Parab SR (2015) Average thickness of tragal cartilage for slicing techniques in tympanoplasty. *J Laryngol Otol* 129(05):435–439
12. Tarabichi M. Endoscopic Cholesteatoma, Tympanoplasty And Middle Ear Surgery. Open access atlas of otolaryngology, head & neck operative surgery. <http://www.endoscopic-earsurgery.com/wp-content/uploads/2016/07/Endoscopic-cholesteatoma-tympanoplasty-and-middle-ear-surgery.pdf>
13. Nomura Y (1982) Effective photography in otolaryngology-head and neck surgery: endoscopic photography of the middle ear. *Otolaryngol Head Neck Surg* 90:395–398
14. Takahashi H, Honjo I, Fujita A, Kurata K (1990) Transtympanic endoscopic findings in patients with otitis media with effusion. *Arch Otolaryngol Head Neck Surg* 116:1186–1189
15. Poe DS, Bottrill ID (1994) Comparison of endoscopic and surgical explorations for perilymphatic fistulas. *Am J Otol* 15:735–738

16. Badr-el-Dine M (2002) Value of ear endoscopy in cholesteatoma surgery. *Otol Neurotol* 23:631–635
17. El-Meselaty K, Badr-El-Dine M, Mandour M, Mourad M, Darweesh R (2003) Endoscope affects decision making in cholesteatoma surgery. *Otolaryngol Head Neck Surg* 129:490–496
18. Yung MW (2001) The use of middle ear endoscopy: has residual cholesteatoma been eliminated? *J Laryngol Otol* 115:958–961
19. Ayache S, Tramier B, Strunski V (2008) Otoendoscopy in cholesteatoma surgery of the middle ear. What benefits can be expected? *Otol Neurotol* 29(8):1085–1090
20. Abdel Baki F, Badr-El-Dine M, El Saiid I, Bakry M (2002) Sinus tympani endoscopic anatomy. *Otolaryngol Head Neck Surg* 127:158–162
21. Mattox DE (2004) Endoscopy-assisted surgery of the petrous apex. *Otolaryngol Head Neck Surg* 130:229–241
22. Kozin ED, Lehman A, Carter M et al (2014) Thermal effects of endoscopy in a human temporal bone model: implications for endoscopic ear surgery. *Laryngoscope* 124(8):E332–E339
23. Harugop AS, Mudhol RS, Godhi RA (2008) A comparative study of endoscope assisted myringoplasty and microscope assisted myringoplasty. *Indian J Otolaryngol Head Neck Surg* 60:298–302
24. Furukawa T, Watanabe T, Ito T, Kubota T, Kakehata S (2014) Feasibility and advantages of transcanal endoscopic myringoplasty. *Otol Neurotol* 35(4):e140–e145





## Novel horizontal and vertical integrated bioethics curriculum for medical courses

Russell F. D'Souza, Mary Mathew, Derek S. J. D'Souza & Princy Palatty

**To cite this article:** Russell F. D'Souza, Mary Mathew, Derek S. J. D'Souza & Princy Palatty (2018): Novel horizontal and vertical integrated bioethics curriculum for medical courses, Medical Teacher

**To link to this article:** <https://doi.org/10.1080/0142159X.2018.1442921>



Published online: 28 Feb 2018.



Submit your article to this journal



View related articles



View Crossmark data



## Novel horizontal and vertical integrated bioethics curriculum for medical courses

Russell F. D'Souza<sup>a</sup> , Mary Mathew<sup>b</sup> , Derek S. J. D'Souza<sup>c</sup>  and Princy Palatty<sup>d</sup> 

<sup>a</sup>International Institute of Organizational Psychological Medicine, Dandenong, Australia; <sup>b</sup>Department of Pathology, Kasturba Medical College, Manipal Academy of Higher Education, Manipal, India; <sup>c</sup>Department of Dental Surgery, Maharashtra Institute of Medical Sciences, Pune, India; <sup>d</sup>Department of Pharmacology, Father Muller Medical College, Mangalore, India

### ABSTRACT

Studies conducted by the University of Haifa, Israel in 2001, evaluating the effectiveness of bioethics being taught in medical colleges, suggested that there was a significant lack of translation in clinical care. Analysis also revealed, ineffectiveness with the teaching methodology used, lack of longitudinal integration of bioethics into the undergraduate medical curriculum, and the limited exposure to the technology in decision making when confronting ethical dilemmas. A modern novel bioethics curriculum and innovative methodology for teaching bioethics for the medical course was developed by the UNESCO Chair in Bioethics, Haifa. The horizontal (subject-wise) curriculum was vertically integrated seamlessly through the entire course. An innovative bioethics teaching methodology was employed to implement the curriculum. This new curriculum was piloted in a few medical colleges in India from 2011 to 2015 and the outcomes were evaluated. The evaluation confirmed gains over the earlier identified translation gap with added high student acceptability and satisfaction. This integrated curriculum is now formally implemented in the Indian program's Health Science Universities which is affiliated with over 200 medical schools in India. This article offers insights from the evaluated novel integrated bioethics curriculum and the innovative bioethics teaching methodology that was used in the pilot program.

### Introduction

In recent decades, medical education curricula have undergone many modifications for a variety of reasons (Du Bois and Burkemper 1994). Despite these changes, ethics education has not received adequate attention in medical schools throughout the world. There is an emerging need for the introduction of teaching medical ethics as a consequence of several social transitions and scientific advancement.

Scientists, healthcare providers, and members of institutional review board find themselves confronting bioethical issues without sufficient expertise to address them. In response to this, academic bioethics programs have proliferated and specialized to meet the needs of diverse professionals and scholars (Eckles et al. 2005).

In this article, we articulate the general pedagogical goals for ethics education in undergraduate medical education (Dsouza and Mathew 2016) reformed integrated curriculum and innovative tested teaching methodology proposed for the medical training at universities in the International program of the UNESCO Chair in Bioethics (Haifa, Israel). These goals have been influenced by debates in bioethics literature, scholarly presentations, publications, and insights gained from designing and piloting curriculum at medical colleges and universities in the Asia Pacific division of the UNESCO Chair in Bioethics (Haifa, Israel).

### Bioethics education

Bioethics education in the medical training is linked to various competencies, i.e. behaviors and skills that can be demonstrated and measured. The emphasis on

### Practice points

- Bioethics should not be taught by traditional teaching methods as they are considered ineffective.
- Case-based Learning used for the initiation of the discussion is one of the most effective means of teaching bioethics.
- Advanced interactive learning methodology such as drama and role play should be used.
- Undergraduate medical bioethics curriculum should be integrated throughout the years of medical education.

measurement can seem to diminish the importance of education designed to enrich moral sensibilities.

All bioethics programs must attend to character development, knowledge, and skills. Bioethics is taught both in educational programs and in what might be considered the as the "hidden curriculum" (Hafferty and Franks 1992). For example observation of mentors and colleagues undoubtedly shapes moral behavior; however, the focus of this article is on the novel innovative horizontal and vertical integration of bioethics curriculum in medical training in which bioethics education occurs by design. The settings go beyond classrooms and include clinical, research arenas, and professional contexts. Academic bioethics programs involve curricula and pedagogical objectives (Dsouza and Mathew 2016). Further, there is evidence that

undergraduate medical education that is not assessed is not learned (Mattick and Bligh 2006). Curriculum development is an iterative dynamic process. Program evaluation must be built in as it gives an impetus to curriculum designers and other stakeholders. Ethics curriculum must be seamlessly integrated in a longitudinal manner. The goals should reflect achieving not only what is right and wrong but also nurturing the right attitude in medical and healthcare students. Sowing the ethical seeds early in their training when they are moldable “like wet clay” would result in imprinting in early years of their course. The horizontal and vertical integrated bioethics curriculum based on the UNESCO core curriculum principles, designed, piloted, and tested at the Indian Program of the UNESCO Chair in Bioethics (Haifa), and was introduced by the Association of Indian Health Science Universities (AIHSU) which accounts for over 200 medical colleges, as a joint program with the UNESCO Chair in Bioethics. Similarly, a number of private universities who are part of the international program of the UNESCO Chair in Bioethics Haifa have introduced the novel integrated bioethics curriculum in their medical schools. This is a reference to the seamlessly integrated bioethics that traverse through four and half years of medical training and offering the longitudinal perspective with evidence of translation of learned ethical principles being applied to the clinical settings and beyond.

## Background

Two international researches were carried by The International Centre for Health, Law, and Ethics at the University of Haifa in 1996 and 2001 (unesco-chair-bioethics.org). The aim of the study was to evaluate the teaching of ethics in medical schools in the world, where ethics teaching was an accreditation requirement. The findings were that teaching ethics did not result in its application at the doctor-patient clinical interphase. It was found that there was a lack of translation of bioethics taught to it being applied to the clinical settings and beyond. Further, the translation gap was identified to be one of the reasons for the deterioration of the doctor-patient relationship. This study was the catalyst to the International Centre for Health, Law, and Ethics at the University of Haifa program to advocate for a reformed method for ethics education and a new modern integrated curriculum of medical ethics to be taught in medical schools all over the world. The UNESCO Chair in Bioethics (Haifa, Israel) adopted and established this program in UNESCO Bioethics (2001) (unesco-chair-bioethics.org). They established a network of bioethics units within universities and research centers in the world committed to disseminating, improving, and monitoring education of ethics in medical schools. The modern curriculum reflects the need for integration of ethics in daily practice, increasing interest and respect to values involved in health care delivery, ethical decision making, and raising awareness of the competing interests that the modern health care delivery has to contend with UNESCO Bioethics Core Curriculum (2008).

## The horizontal curriculum

The horizontal arm of the medical ethics education starts with student learning of medicine's long history. The students are introduced to the codes and oaths that have influenced medical ethics, the common morality, and areas that distinguished the commitments of physicians from those of other professions. Areas included in the horizontal arm are exercises to influence the need to be compassionate, caring, respectful, autonomy, informed consent, and informed refusal. The exposure and learning of the challenges to professionalism, ethical decision making, research ethics, and the reflection on practice dilemmas are introduced in this domain. Further concepts addressed include the realities of commercially-driven healthcare ethics vs. ethics of healthcare, morality of healthcare providers, academic integrity, sexual harassment, boundary issues, standards of care, malpractice, confidentiality, breaking bad news, errors in healthcare management, truth-telling, cultural issues, and ethical conflicts. Students are introduced to ethical issues in recordkeeping and documentation, ethical issues in treatment planning, and state law (Fox et al. 1990). The Bioethics Core Curriculum of UNESCO ([www.unesco.org/shs/ethics/eep](http://www.unesco.org/shs/ethics/eep)- Bioethics Core Curriculum)) which is based on the 15 principles of the Universal Declaration on Bioethics and Human Rights encompasses almost all of these issues and concerns addressed and is used as the framework to integrate ethics into the medical curriculum.

The horizontal arm of the novel curriculum moreover, addresses the interpersonal and cognitive skills that are crucial tools for physicians. Students are taught the importance of demonstrating the ethics of caring, compassion, and respect in their interactions with patients, families, and colleagues. Exercises are designed to encourage the practice and mastering of skills of critical reflection and clinical moral reasoning. The curriculum further validates the appropriateness to discuss ethical issues in clinical practice with other health professionals, who cooperate in implementing ethical decisions. In addition to these, the curriculum overall supports the development of the distinctive character of an exemplary physician in order that they mature into competent professionals with the appropriate dispositions and attitudes (i.e. the character and virtues) essential to be a good physician.

## Vertical (subject-wise) curriculum

The vertical curriculum consists of ethical principles of the core curriculum, as they relate to all the undergraduate medical subjects in the preclinical, paraclinical, and clinical phases. This subject ethics curriculum was specially designed by subject expert committees comprising senior subject faculty from various medical colleges. This curriculum was further validated through several workshops where respective subject faculty members assembled in break-out rooms, to review, refine, and offer practical methods to integrate subject-related ethics principles, into the teaching and assessing methodology in use. A pertinent example of the integrated curriculum in ethics is the cadaveric oath in anatomy at the beginning of the placement, which emphasizes human dignity, respect to the human body and respect for the dead. The integrated bioethics

curriculum is thus incorporated into every undergraduate medical subject as the student moves through the course.

### Integration of bioethics in medical curriculum

This integrated bioethics curriculum is seamlessly incorporated into the teaching and assessment (both formative and summative) of the undergraduate subjects.

The students are assessed periodically throughout the course trajectory in the form of a log book. The summative component includes a written 3 h paper and viva on a case discussion. In addition, students are formatively assessed in feedback for case-based learning. Interest indicators, such as participation and organizing bioethics programs earn credit points that translate into grades for the summative assessment. Although no foolproof mechanism of assessment in affective domain is available as yet, the present multitude of assessments could bring out a reasonable outcome. Long-term assessment of the effectiveness of this program has not yet been fully undertaken and few of the program effectiveness was drawn from patient comparative satisfaction indices. It is envisaged to monitor the critical incident report, future career graph, and personal success.

While this will transcend the challenges of a packed curriculum in the undergraduate teaching program, this approach further has the advantage of demonstrating that ethical considerations are important aspects of medicine and that they need to be considered along with the scientific and clinical decisions that are made. Medical students are thus open to developing a clear understanding of their distinctive professional responsibilities, as well as the basic vocabulary of bioethics. This methodology offers avenues to master the skill of identifying ethical concerns and applying ethical concepts to clinical cases. The integrated approach offers skills in dealing with common moral dilemmas that arise in clinical practice and in collaborating with fellow healthcare providers in moral deliberation and conflict resolution. Thus, beyond mastering the basic ethical concepts that are embedded in the practice of medicine, students will also need to learn the local and federal laws that govern their practice, as well as the institutional policies with which they are required to comply. This may be especially important because during training, residents and fellows often work in multiple settings that are governed by varied laws and policies. This curriculum is vertically integrated across the longitudinal medical curriculum, including carrying it over into the clinical years, clinical seminars, bed-side, and other formal hands-on aspects of the medical training.

This horizontally and vertically integrated curriculum design effortlessly integrates the concepts of bioethics into every undergraduate medical subject in the pre-clinical, para-clinical, and clinical levels. It makes the graduating doctor, suitably sensitized and equipped to confront, and address most of the ethical issues in their subsequent clinical practice.

### Innovative teaching-learning methodology for teaching faculty

In this reformed curriculum and teaching methodology, all medical teaching faculties are qualified to be teachers of

bioethics in their respective subject specialties. The medical teaching faculty undergoes the accredited specialized training course for medical teachers – the 3 T-IBHSc Course (Train, Teach, and Transfer-Integrated Bioethics in Health Sciences) developed and evaluated by the Department of education of the UNESCO Chair in Bioethics, Haifa, Israel. The course uses innovative teaching methodology and has three components. These are the Principles of Bioethics and Human Rights, Bioethics knowledge transfer technology and Integration of discipline-specific bioethics curriculum in the teaching and assessment of individual subjects of the medical undergraduate training. At the end of the 30 h contact period of the course, the teaching faculty is required to participate in a simulated teaching exercise that is assessed and followed by feedback. Medical teaching faculty is invited and encouraged to register for an ongoing 12-week international webinar which consists of 12 modules on the principles of the Universal Declaration on Bioethics and Human Rights. This course is conducted and accredited by the Department of Education of the UNESCO Chair in Bioethics, Haifa, Israel.

### Role of workshops, small groups, case-based learning, and role play in teaching

Teaching bioethics by traditional teaching methods is not recommended as they have been shown to be ineffective. Use of workshops, small group discussions is a proven means of facilitating sustained and effective student interaction and engagement. It also encourages active research, reading and is ideal for a discussion of ethical real-life case scenarios (Christakis and Feudtner 1993). Such interactions allow the student's adequate opportunity to introspect, examine, and defend their own ethical belief systems, while being open to the ethical perspectives of their fellow learners. The role of the faculty is to be role models for their students with respect to demonstrating ethical standards and behavior.

Role-playing has proved to be another, successful teaching tool in teaching ethics and professionalism. Case-based learning (CBL) likewise has been effectively used to introduce the concepts of bioethics to medical students. This is an excellent means of assessment and evaluation of the students' understanding by observing their reactions and responses (Mattick and Bligh 2006).

### Case-based learning

A case-based approach to teaching-learning methodology in the medical field has been shown to improve student-instructor interaction, make the learning outcomes more effective and can be used to assess student learning (Thistlethwaite et al. 2012). The use of Case-Based Learning in which real patient cases are used for initiation of the discussion is one of the most effective means of teaching bioethics. Teachers who have adopted this methodology have reported that it supports student engagement and enhances the clinical relevance of the bioethics lesson (Mattick and Bligh 2006).



## Innovative teaching methodology

Innovative teaching methodologies that are successfully employed are the screening of movies, and video clips that encourage ethical debates on the situation or issue in the video clip. The use of seminars and debates on a specific ethical situation or principle that the students are likely to encounter in the future is effective teaching methodology. Real-life stories, vignettes, or small narratives are used effectively to stimulate student reflection. Students are taught to reflect on the overall context of ethical situations rather than just considering ethical issues as mere concepts.

The use of taped and live video of both real patients and “simulated patients” are found to be effective in maximizing learning. After the session, the students are asked to write down their reactions or answer subjective questions which can also be used for assessment of learning outcomes (Mattick and Bligh 2006).

Innovative knowledge transfer methodology used for example in teaching Autonomy and Consent will have a scripted role play, where a scene of a wrong procedure of consenting is acted out for a case of appendectomy. This is followed by a second scene where the correct way of consenting is demonstrated which includes the three elements of the informed consent process. This is followed by a discussion and an assigned activity. Similarly, to teach vulnerability, the film “My Sister’s Keeper” is screened or a scripted role-play of a family attempting to donate the kidney of their child with mental retardation to the brother who is the only earning member of the family. This is followed by a discussion and an assigned activity for eliciting types of vulnerable population.

## Feedback and reflection

Feedback and personal reflection are incorporated into the formal teaching of bioethics. These ensure the ability to utilize both positive and negative feedback for personal growth and development. Additionally, the students are encouraged to introspect and intuitively learn from their clinical experiences on how to be ethically inclined professionals and to approach ethical dilemmas with confidence and moral courage (Branch and Paranjape 2002).

## Multidisciplinary faculty teaching

Ethical dilemmas are very often of diverse nature involving many disciplines. Therefore, an interdisciplinary approach that invites faculty from varied disciplines, such as ethics, psychology, and law may be used to ensure comprehensive teaching–learning outcomes in the realm of bioethics. The application of interdisciplinary consultation and knowledge bases encourages clinicians to understand the need and respect the values of other professionals and is an effective model to emphasize inter-professional consultation in clinical practice.

## The evaluation of the pilot reformed bioethics curriculum

Medical students who had completed the modern bioethics curriculum that was integrated over four and half years of

their undergraduate medical training, when assessed were found to be competent in medical ethics. They demonstrated a deep understanding of the basic principles of ethics applied in medicine, were able to recognize ethical issues in clinical scenarios with ethical dilemmas and understand how they might apply these within a clinical context. They were further able to describe and employ the basic concepts of medical ethics, identify moral issues and conflicts that arose in medical practice and formulate the dilemma as a question.

A noticeable outcome was the ability to convey compassion, caring, respect, and professionalism, besides demonstrating skills to deliberate about ethical issues with their fellow students. They were capable of resolving ethical dilemmas with supporting reasons.

Further, it was found they were proficient in recognizing moral conflicts when they arose and had reasonable knowledge to navigate their way through an ethical dilemma to a resolution.

## Conclusions

Over the past 30 years, bioethics education has become an integral part of undergraduate medical education in North American, Australia, United Kingdom medical schools, and indeed medical schools around the world. Medical education organizations have officially endorsed the incorporation of bioethics into the required medical school curriculum.

The curriculum should provide ample opportunities for students to practice their interpersonal, communication, and moral reasoning skills (Dsouza and Mathew 2015). An ideal curriculum should, therefore, help medical students to understand their professional responsibilities and the distinctive ethics of medicine, nurture them to become trustworthy and exemplary physicians, and provide the tools required to do what patients and society reasonably expect of them (Eckles et al. 2005). These requirements suggest that medical school ethics education should address issues that physicians are most likely to encounter during their medical careers. Most bioethics educators agree that the undergraduate medical course’s bioethics curriculum should be vertically and horizontally integrated throughout the medical training program, with ethics teaching included in both the preclinical years and the clinical years.

This novel horizontal and vertical integrated bioethics curriculum for undergraduate medical training have been found to mitigate the gaps that had been identified with conventional bioethics teaching in medical education and offers the required competencies to graduating doctors to provide ethical, value-based quality medical care.

## Disclosure statement

The authors report no conflicts of interest. The authors alone are responsible for the content and writing of the article.

## Notes on contributors

*Russell F. D'Souza*, MD, DSc, DPM, FIOPM (Australia), MUCB (Haifa, Israel), is the Head of the Asia Pacific Division and Director of Education International Network of the UNESCO Chair in Bioethics Haifa, Israel.



*Mary Mathew*, MD, DCH, PGDMLE is a Professor of Pathology at Kasturba Medical College, Manipal, Karnataka, India and the Head of the Indian program of International Network of the UNESCO Chair in Bioethics, Haifa, Israel.

*Derek S. J. D'Souza*, MDS, MBA, is the Director, National Bioethics Curriculum. Implementation Centre & Professor, Department of Dental Surgery at Maharashtra. Institute of Medical Education and Research, Pune.

*Princy Palatty*, MD, is the National Chair Curriculum & Professor, Department of Pharmacology, Father Muller Medical College, Mangalore, Karnataka.

## ORCID

Russell F. D'Souza  <http://orcid.org/0000-0002-0125-7161>  
 Mary Mathew  <http://orcid.org/0000-0002-4048-3567>  
 Derek S. J. D'Souza  <http://orcid.org/0000-0002-3970-8546>  
 Princy Palatty  <http://orcid.org/0000-0003-4147-0482>

## References

- Branch WT Jr, Paranjape A. 2002. Feedback and reflection: teaching methods for clinical settings. *Acad Med.* 77:1185–1188.
- Christakis DA, Feudtner C. 1993. Ethics in a short white coat: the ethical dilemmas that medical students confront. *Acad Med.* 68:249–254.
- Du Bois JM, Burkemper J. 1994. Ethics education in US. Medical schools study of syllabi. *Acad Med.* 69:861–871.
- Dsouza R, Mathew M. 2016. Pedagogical goals for Bioethics Programs of Health Science Universities, *Global Bioethics Enquiry.* Vol. 4. Hershey (PA): IGI Global; p. 5–10.
- Dsouza R, Mathew M. 2015. Medical education and ethics, *Global Bioethics Enquiry.* Vol. 3. Hershey (PA): IGI Global; p. 5–8.
- Eckles RE, Meslin EM, Gaffney M, Helft PR. 2005. Medical ethics education: where are we? Where should we be going? A review. *Acad Med.* 80:1143–1152.
- Fox E, Arnold RM, Brody B. 1990. Medical ethics education: past, present, future. *Acad Med.* 70:761–769.
- Hafferty FW, Franks R. 1992. The hidden curriculum, ethics teaching, and the structure of medical education. *Acad Med.* 69:861–871.
- Mattick K, Bligh J. 2006. Teaching and assessing medical ethics: where are we now? *J Med Ethics.* 32:181–185.
- Thistlethwaite HE, Davies D, Ekeocha S, Kidd JM, MacDougall C, Matthews P, Purkis J, Clay D. 2012. The effectiveness of case-based learning in health professional education. A BEME systematic review: BEME Guide No. 23. *Med Teach.* 34: e421–e444.
- UNESCO Bioethics. 2001. International network of the UNESCO Chair in Bioethics Haifa. [www.unesco-chair-bioethics.org/](http://www.unesco-chair-bioethics.org/)
- UNESCO Bioethics Core Curriculum. 2008. Section 1: Syllabus Ethics Education Programme, Sector for Social and Human Sciences; Division of Ethics of Science and Technology. Haifa: UNESCO. [www.unesco.org/shs/ethics/eep](http://www.unesco.org/shs/ethics/eep)

# Neonatal Screening for Prevalence of Hearing Impairment in Rural Areas

Sapna R. Parab<sup>1</sup> · Mubarak M. Khan<sup>1</sup> · Sneha Kulkarni<sup>1</sup> · Virendra Ghaisas<sup>2</sup> · Prakash Kulkarni<sup>2</sup>

Received: 14 May 2017 / Accepted: 28 April 2018 / Published online: 4 May 2018  
© Association of Otolaryngologists of India 2018

**Abstract** Hearing is one of the most important sense organs for man. Hearing loss is often associated with delayed speech and language development in young children. Early identification and intervention improves the chance a child gets to lesser delays in development and improving the overall quality of life. To find out the prevalence of hearing loss in neonates in the rural taluka of Maval, Pune, Maharashtra, India. Prospective Non Randomized Clinical Study. The study was carried out between April 2012 and April 2015. A total of 8192 babies were screened across various centers around the Maval area. The babies who had some high risk factors were 1683 in number and babies who had no high risk factors i.e. well babies were 6509. In our study, the overall prevalence of hearing loss in neonates in Maval taluka of Maharashtra was found to be 3.54 per 1000 live births, in normal born neonates (well babies) was 1.689 per 1000 births, in high risk babies was 10.69 per 1000 high risk births. The prevalence of low birth weight neonates, hyperbilirubinaemia neonates and neonates with craniofacial abnormalities developing hearing impairment was found to be 5.9, 3.56 and 1.18 per 1000 high risk births respectively. India is the second most populated country in the world with nearly a fifth of the world's population. There is a need for the universal neonatal screening for deafness for earlier detection of deafness and rehabilitation.

*Level of Evidence:* Level IV.

**Keywords** Neonatal screening · Deafness · Otoacoustic emission · Brainstem evoked response audiometry

## Introduction

Hearing is one of the most important sense organs for man important for normal speech and language acquisition. Hearing loss is often associated with delayed speech and language development. This often cause children with hearing impairment to fall behind their peers in aspects of literacy, academics and overall social wellbeing. This indirectly leads to lower educational and employment levels in adults. It is estimated that 50% of children with hearing impairment in school dropout at the age of 13 years. The rural areas of India lack in health care facilities as compared to the urban areas. In a recent survey, 4 out of every 1000 children born in India were found to have severe, to profound hearing loss. The incidence of hearing loss could be alarmingly in rural areas where neither study is done to detect the incidence/prevalence of hearing loss in infants nor audiological rehabilitation is provided. This could be either due to lack of awareness among parents, health care professionals and the society as a whole. With no dedicated National Health Program to detect neonatal hearing loss, it becomes all the more important to us to detect these unfortunate infants with congenital hearing loss in our rural area of Maval.

Neonatal hearing loss has a prevalence that is more than twice that of other newborn disorders amenable to screening such as congenital hypothyroidism and phenylketonuria [1, 2].

✉ Sapna R. Parab  
drsapnaparab@gmail.com

<sup>1</sup> Department of Otorhinolaryngology, M.I.M.E.R. Medical College, Talegaon-D, Pune 410507, India

<sup>2</sup> M.I.M.E.R. Medical College, Talegaon-D, Pune, India

## World Problem Statement

World Health Organization (WHO) estimates that 5.3% of the world's population, 360 million, suffers from disabling hearing loss with 91% adults and 9% children. Disabling Hearing Loss is defined as hearing loss greater than 40 dB in the better hearing ear in adults (15 years or older) and greater than 30 dB in the better hearing ear in children (0–14 years). The prevalence of hearing loss in children is highest in South Asia, Asia Pacific and Sub-Saharan Africa. India is one of the countries in South Asia [3].

## Problem Statement in India

As per National Sample Survey Organization survey, currently there are 291 persons per one lakh population who are suffering from severe to profound hearing loss [4]. Out of this population, a large percentage is children between the ages of 0–14 years.

Congenital bilateral hearing impairment occurs in approximately in 1–5 per 1000 live births and when permanent unilateral hearing loss is included, the incidence increases to 8 per 1000 live births [5, 6]. Studies done in India using different hearing screening protocols have estimated the neonatal hearing loss to vary between 1 and 8 per 1000 babies screened [7–9]. Early identification and intervention for hearing loss by 6 months of age provides better prognosis in language development, academic success, social integration and successful participation in the society [5].

The statistics indicate a huge number of children suffer from hearing loss which must be detected at an early age to integrate the children in society. The Joint Committee on Infant Hearing (JCIH) was established with such points in mind. The JCIH was established in late 1969 and composed of representatives from audiology, otolaryngology, pediatrics, and nursing. It was the American Speech Language Hearing Association (ASHA), the then American Academy of Ophthalmology and Otolaryngology (AAOO) and the American Academy of Pediatrics (AAP) who were the founders. The Committee was charged with a two-fold responsibility: first, to make recommendations concerning the early identification of children with, or at-risk for hearing loss and second, newborn hearing screening. The first statement issued by the JCIH in 1971 [10], stated that mass hearing screening could not be justified at that time because of lack of appropriate test procedures. The statement encouraged ongoing research and acknowledged the need to detect hearing loss early in life.

The first attempts at hearing screening were behavioural observation techniques in mid 1960s using the auro-palpebral response, startle response and limb and head movements to judge a response to high frequency narrow band

noise at about 90–100 dB SPL. The drawbacks of this method were that the method was time consuming identified only infants with bilateral severe to profound high frequency hearing loss. The method also did not provide ear and frequency specific information and had a high false negative rate [11].

The 1971 statement given by JCIH defined the first high-risk factors for hearing loss and recommended following infants with these high risk factors: history of hereditary childhood hearing impairment, congenital perinatal infection such as rubella or other nonbacterial fetal infection like cytomegalovirus, and herpes; craniofacial anomalies, birth weight less than 1500 g and a bilirubin level greater than 20. In 1982, bacterial meningitis and severe asphyxia were added. Additional risk indicators were added between 1982 and 1994.

JCIH in 1994 [12] endorsed universal detection of hearing loss in newborns and infants and stated that all infants with hearing loss be identified before 3 months of age and receive intervention by 6 months. In 2000, the focus was given on quality of the care provided for each infant. JCIH endorsed the development of early hearing detection and identification with use of state or universal hearing screening

protocols. JCIH in 2000 provided guidelines for early hearing detection and identification programs. Recently

JCIH in 2007 issued another position statement which updated the principles from the 2000 statement. The changes made were—updating the definition of targeted hearing loss, issue separate protocols for well-baby nursery and NICU babies, tests included in diagnostic audiological evaluation, medical evaluation, early intervention and monitoring and surveillance of developmental milestones. The position statement made clear each role and responsibility of each team member in the early detection and intervention program and also the protocol to be followed.

The effectiveness and need for universal hearing screening in neonates has previously been well proven [12, 13]. Although hearing screening programs using different screening protocols have been setup in some centers, procedures for systematic identification and rehabilitation on a large scale are yet to be tested and implemented in the Indian setting.

This study was undertaken with the primary objective of detecting hearing impairment in Maval Taluka with two stage sequential screening protocol with otoacoustic emission (OAE) and brainstem evoked response audiometry (BERA).

## Materials and Methods

This descriptive study was carried out between April 2012 and April 2015 around the Maval area. The project was approved by the MIMER ethical committee. Various

centers which catered to neonates were selected. A two tier screening protocol was followed.

All normal new born babies delivered in MIMER Medical College, Nursing homes around Talegaon, PHC and private hospitals were screened by the Audiologist using TEOAE between 24 and 72 h after birth. Newborns admitted in the Neonatal Intensive Care unit (NICU) were screened prior to discharge from NICU (once their general condition was stable). A quiet area was chosen for screening. The OAE probe was introduced in the neonate's ear after examination of the externa ear for debris, wax etc. The results were saved on the device and later transferred to a computer for analysis. Mothers of all babies were counselled regarding the benefits of hearing screening, procedure of the test, need for follow up and further tests if neonate failed the screening test, and the interventions available if hearing loss was confirmed. The first screening test was done in the post-natal wards or NICU after obtaining informed consent from the mother. Parents of babies who failed ("refer") screening test once were counselled and asked to return after 2 weeks for second screening. These babies underwent a second testing in a quiet room. Those who passed on the second screening were discharged from the study while those who failed second time were called after 2 weeks for ABR testing.

A detailed case history, which included questions relating to mother's history, pre, peri and post-natal birth history and family history was obtained. In addition to this, a detailed history regarding the high risk factors was also taken. The high risk factors taken into consideration, on the basis of JCIH, 1994 position statement were—family history of hearing loss, maternal infections like TORCH, craniofacial anomalies, birth weight less than 1500 g, hyperbilirubinemia at serum level requiring exchange transfusion, ototoxic medications taken by the mother, bacterial meningitis, APGAR scores of 0–4 at 1 min or 0–6 at 5 min, mechanical ventilation lasting for 5 days or longer and syndromes associated with sensorineural or conductive hearing loss. The neonate underwent an examination by the ENT surgeon for outer, middle ear anomalies. Next step of the protocol was TEOAE screening using LABAT Ecolab-Screener. The protocol set was as follows:

- Type of stimuli: clicks
- SNR: 3–6 dB
- Frequency: 1–4 kHz.

The Auditory Brainstem Response (ABR) was carried out using LABAT Epic Plus-ABR system, either under sedated sleep or natural sleep. The following protocol was used.

- Type of stimuli: clicks
- Intensity: varying intensity (threshold estimation)

- Polarity: alternating
- Number of clicks: 2000
- Time window: 15 ms
- Filter settings: 30–3000 Hz
- Electrode montage: FPz—M1–M2.

The impedance was kept as low as possible and the electrical activity was kept at a minimum. The least intensity at which a replicable and robust wave V was seen was considered as the threshold. The babies who were detected with hearing loss with ABR were considered for hearing rehabilitation either with hearing aids or cochlear implants.

The data collected was tabulated and analyzed.

## Results

The study was carried out between April 2012 and April 2015. The aim of the study was to find out the incidence of hearing loss in neonates in rural areas of Maval taluka of Maharashtra. A total of 8192 babies were screened across various centers around the Maval area. The babies who had some high risk factors were 1683 in number and babies who had no high risk factors i.e. well babies were 6509.

In the well-baby group, 4926 passed in the first tier of screening. The 1583 who were referred in the first phase underwent another screening after two weeks. At the second visit, 1454 passed the screening, 105 failed the screening and 24 were lost to follow up. In the high risk group, 1406 passed in the first tier of screening. The 277 who were referred in the first phase underwent another screening after two weeks. At the second visit, 184 passed the screening, 72 failed the screening and 21 were lost to follow up.

A total of 18 out of 72 referred neonates for ABR were detected with hearing impairment, whereas 54 out of 72 neonates were having hearing sensitivity within normal limits on ABR. Among the well-baby group, 105 well babies who were referred for ABR 11 were detected with hearing impairment, 67 had hearing sensitivity within normal limits and 27 were lost to follow up. Among the 18 high risk babies detected with hearing loss, 10 had low birth weight, 6 had hyperbilirubinemia and 2 had craniofacial abnormalities (Table 1 and Fig. 1).

In our study, the overall prevalence of hearing loss in neonates in Maval taluka of Maharashtra was found to be 3.54 per 1000 live births, in normal born neonates (well babies) was 1.689 per 1000 births, in high risk babies was 10.69 per 1000 high risk births. The prevalence of low birth weight neonates, hyperbilirubinemia neonates and neonates with craniofacial abnormalities developing hearing impairment was found to be 5.9, 3.56 and 1.18 per 1000 high risk births respectively.



Table 1 Table showing the number of babies screened and referred at both stages

	No. of babies screened	Babies referred on 1st screen	Babies who underwent 2nd screen	Babies referred on 2nd screen	Babies who underwent ABR	Babies with confirmed hearing loss
Normal	6509	1583	1559	105	78	11
High risk	1683	277	256	72	72	18
Total	8192	1860	1815	177	150	29

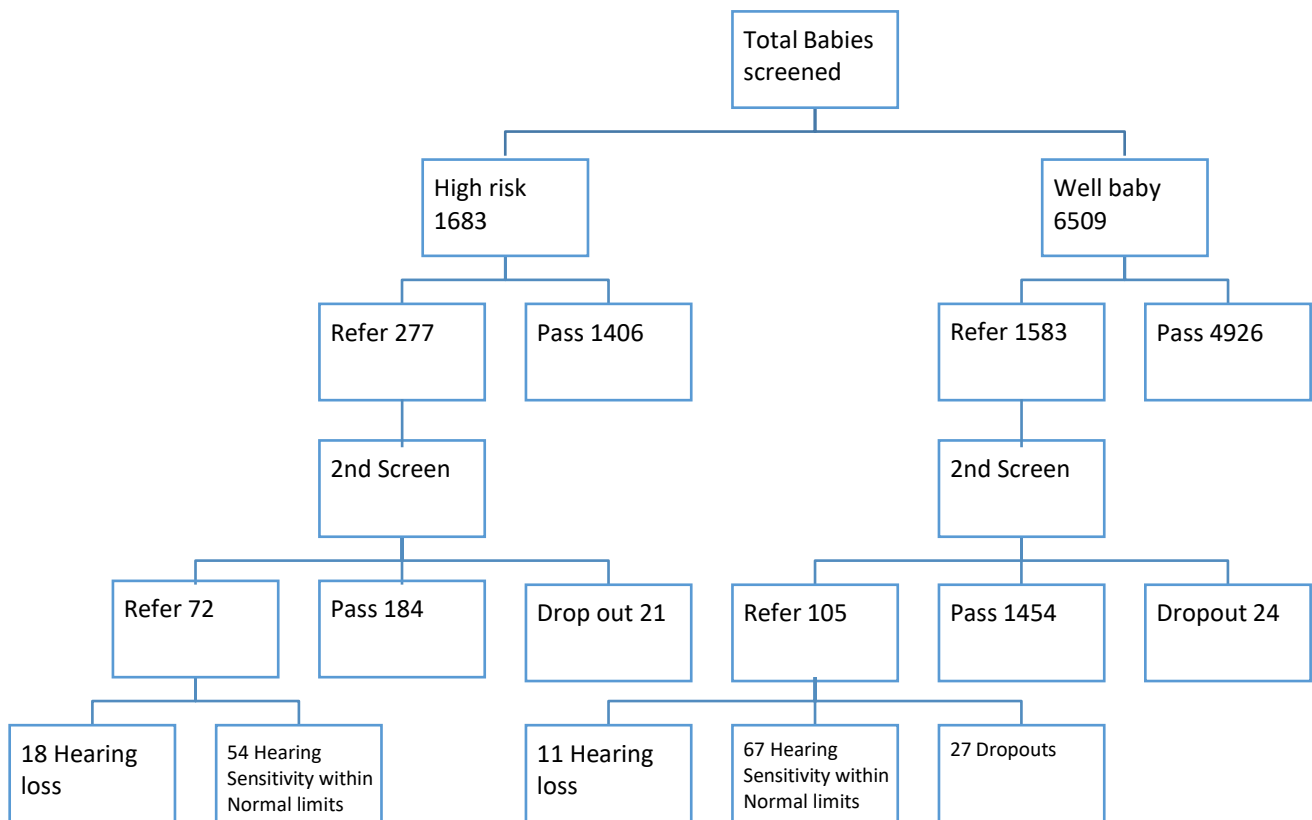


Fig. 1 Flow chart depicting the screening protocol and results obtained

**Discussion**

Many universal screening programs use a two-step protocol consisting of OAE and Automated ABR (AABR). In developed nations, testing with either OAE or AABR is mandatory, or at least encouraged, prior to discharge from maternity hospital. In the US and UK, it is mandatory for the newborn to undergo hearing screening either before leaving the hospital or shortly after discharge from hospital. However, the scenario in developing nations is different. There are often barriers like expensive equipment, scarcity of trained and skilled personnel, and shortage of skilled maternal and newborn health workers especially in rural areas [14]. Additionally, the births may not take place

in a hospital setting where the screening resources are available. Many infants are also lost for follow up [15].

The Government of India initiated the National Programme for Prevention and Control of Deafness (NPPCD) in 2006 [16]. It was initially started as a pilot project and was implemented in 25 districts in 10 states and 1 union territory. The project aims to cover three levels of prevention and care: primary, secondary and tertiary ear care. It aims at preventing avoidable hearing loss which is due to disease or injury, early identification and treatment either medically or by rehabilitation. The programme has four main components—manpower training and development; building infrastructure at district hospitals, community health centers and primary health centers; early detection

and management of hearing and speech impaired cases at different levels of health care system and fourth component is the creation of awareness among levels of health care system. In developing nations particularly where limited resources are available, use of low cost calibrated mechanical noisemakers to conduct hearing screening was studied [17]. They trained six health workers who were supervised by a qualified audiologist to observe behavioral responses of neonates using calibrated noisemakers. Twenty out of 425 neonates with confirmed severe to profound hearing loss by ABR testing were included. The mechanical calibrated noisemakers of 50, 60, 70 and 80 dB (A) were used to elicit behavioral responses. Neonates were in state of light sleep when the test was performed. The observer was blinded to the stimulus. The tester presented the stimulus at a distance of 1 m from the testing ear which was not in the visual field of observer. The stimuli was presented 3 times with a 1 min interval. The tester noted the time at which the stimulus was presented. The observer noted the response and the time at which it was observed. A qualified audiologist observed if the health worker correctly identified the response. The authors found that the sensitivity and specificity was high for 70 and 80 dB (A) noisemakers with least false positive referrals. The authors, thus concluded that in controlled settings, health workers with primary education can be trained by qualified audiologists to use calibrated noisemakers to conduct screening for severe to profound hearing loss.

Our study carried out between April 2012 and April 2015 in the Maval taluka of Maharashtra included total of 8192 babies with 1683 neonates having high risk factors and 6509 well babies. This is the first study in the state of Maharashtra for screening of deafness in neonates. The overall prevalence of hearing loss in neonates of Maval taluka in our study was found to be 3.54 per 1000 live births; in normal born neonates (well babies) was 1.689 per 1000 births and in high risk babies was 10.69 per 1000 high risk births. The prevalence of low birth weight neonates, hyperbilirubinemia neonates and neonates with craniofacial abnormalities developing hearing impairment was found to be 5.9, 3.56 and 1.18 per 1000 high risk births respectively.

Tests used for screening newborns for hearing loss include Otoacoustic Emissions (OAE) and Automated Auditory Brainstem Evoked Response (aABR). While OAE is cheap, quick, simple and reliable with a sensitivity of 100% and specificity of 99% [18–20], ABR has the additional advantage of identifying neonates with auditory neuropathy.

The advent of Otoacoustic Emissions (OAE) and Auditory Brainstem Evoked Response (ABR) has provided noninvasive recordings of physiologic activity underlying normal auditory function and both are easily performed in

neonates and infants. Otoacoustic emissions (OAEs) are sounds given off by the inner ear when the cochlea is stimulated by a sound. When sound stimulates the cochlea, the outer hair cells vibrate. The vibration produces a nearly inaudible sound that echoes back into the middle ear. The sound can be measured with a small probe inserted into the ear canal. The auditory brainstem response (ABR) test gives information about the inner ear (cochlea) and brain pathways for hearing.

Various studies are published which are constrained to a particular center usually tertiary care centers [7, 15, 21–23]. These studies follow different protocols, screening of at risk versus well baby clinic, difference in times between re screening and different use of instruments and tests.

Nagapoornima et al. [20], studied a total of 1769 neonates from a total of 8192 out of which 6509 were not at risk babies and 1683 were at risk babies. The babies underwent Transient evoked Oto Acoustic Emissions (OAE) as the first level of screening by 6 weeks. The neonates who failed at the first screening underwent re screening within 3 weeks of first screening. If neonates failed a second screening, they underwent an Auditory Brainstem Response and behavioral audiometry to confirm the hearing loss. Results in the study reported an incidence of 10 per 1769 infants screened which is 5.65 per 1000 screened. Out of 1769 infants, 279 were at risk neonates 3 out of which were detected to have hearing loss. This puts the incidence to 10.75 per 1000 neonates. Out of the 1490 who are not at risk, 7 had hearing loss, which makes the incidence 4.70 per 1000 screened. The authors extrapolated the findings and found an incidence of 5.60 per 1000 neonates in a tertiary care center. The study also showed that hearing screening of only high risk neonates can miss the detection up to 70% of children with hearing impairment.

John et al. [7] screened 500 neonates with automated distortion product otoacoustic emission (aDPOAE) followed by automated Auditory Brainstem Response (aABR) on neonates who failed a repeat DPOAE. On the first screening, 32 failed the screening. On repeat OAE only 8 failed the test, out of which 3 did not pass the aABR test. The authors thus concluded that the incidence of moderate to moderately severe sensorineural hearing loss in their study was 0.6%.

A two tier centralized screening programme which consisted of otoacoustic emission as first screen followed by auditory brainstem response for those who failed the first screen was initiated for all newborns in Cochin. A total of 10,165 babies were screened using this program which brought together twenty major hospitals with maternity units. The incidence of hearing loss in the high risk group was found to be 10.3 per 1000 and 0.98 per 1000 in the well-baby group [8].

A similar programme was started at Ludhiana [21]. The screening initially was done by using TOAE after 48 h of birth. Neonates who failed the initial screen were screened again after 1 month and those who failed this screening were referred to Audiologist. Among the 1000 neonates who were screened initially, 6% failed the initial screen. Four failed the next screening out of the 42 who reported for the rescreening out of which 3 had risk factors. Two babies had severe sensorineural hearing loss and two had moderate to severe hearing loss.

In spite of the individual regional studies of neonatal screening for deafness, till now, there is an absence of large scale studies which target hearing screening of neonates.

Auditory neuropathy is defined as an abnormal or absent auditory brainstem response but intact OAE or cochlear microphonics. In our screening protocol like most other universal screening programs [13, 16–21], OAE was performed first and ABR was performed only when OAE failed twice. Neonates who undergo automated ABR with OAE can be screened successfully for auditory neuropathy. The screening protocols [24, 25], in which ABR is done in patients with passed OAE in NICU can detect early auditory neuropathy. We did not detect cases of auditory neuropathy in our study.

## Conclusion

In our study, the overall prevalence of hearing loss in neonates in Maval taluka of Maharashtra was found to be 3.54 per 1000 live births, in normal born neonates (well babies) was 1.689 per 1000 births, in high risk babies was 10.69 per 1000 high risk births.

India is the second most populated country in the world with nearly a fifth of the world's population. Rural areas lack in medical and health care facilities as compared to urban areas. There is a need for the implementation of the National Health Programme for neonatal deafness screening for earlier detection and rehabilitation of these unfortunate neonates so as to allow less delay in development and to improve the overall quality of life.

Funding ICMR funded.

Compliance with Ethical Standards

Conflict of interest The authors declare that they have no conflict of interest.

Ethical Approval All procedures performed in studies involving human participants were in accordance with the ethical standards of the institutional committee and with the 1964 helsinki declaration and its later amendments or comparable ethical standards. Institutional Ethics Committee has approved the study.

Informed Consent Informed consent was obtained from all individual participants included in the study.

## References

1. Augustine AM, Jana AK, Kuruvilla KA, Danda S, Lepcha A, Ebenzer J, Paul RR, Tyagi A, Balraj A (2014) Neonatal hearing screening—experience from a tertiary care hospital in Southern India. *Indian J Pediatr* 51:179–183
2. Bickel H, Bachmann C, Beckers R et al (1981) Neonatal mass screening for metabolic disorders. *Eur J Pediatr* 137:133. <https://doi.org/10.1007/BF00441305>
3. De Capua B, De Felice C, Costantini D, Bagnoli F, Passali D (2003) Newborn hearing screening by transient evoked otoacoustic emissions: analysis of response as a function of risk factors. *Acta Otorhinolaryngol Ital* 23:16–20
4. Directorate General of Health Services. Ministry of Health and Family Welfare, National Program for Prevention and Control of Deafness, Project Proposal. New Delhi (2006). [https://mohfw.gov.in/sites/default/files/51892751619025258383Operational%20Guidelines%20for%2012th%20Plan\\_0.pdf](https://mohfw.gov.in/sites/default/files/51892751619025258383Operational%20Guidelines%20for%2012th%20Plan_0.pdf)
5. Fisher DA, Dussault JH, Foley TP, Klein AH, LaFranchi S, Larsen PR et al (1979) Screening for congenital hypothyroidism: results of screening one million North American infants. *J Pediatr* 94:700–705
6. Jewel J, Varghese P, Singh T, Varghese A (2013) Newborn hearing screening—experience at a tertiary hospital in northwest India. *Int J Otolaryngol Head Neck Surg* 2(5):211–214. <https://doi.org/10.4236/ijohns.2013.25044>
7. John M, Balraj A, Kurien M (2009) Neonatal screening for hearing loss: pilot study from a tertiary care center. *Indian J Otolaryngol Head Neck Surg* 61:23–26
8. Joint Committee on Infant Hearing (1994) 1994 position statement. *AAO-HNS Bull.* 12:13
9. Joint Committee on Infant Hearing (1994) 1994 position statement. *ASHA* 36(12):38–41
10. Joint Committee on Infant Hearing (1994) Joint Committee on Infant Hearing (JICH) 1994 position statement. *Pediatrics* 95:152
11. Joint Committee on Infant Hearing (2007) Year 2007 position statement: principles and guidelines for early hearing detection and intervention programs. *Pediatrics* 120:898–921
12. Joint Committee on Infant Hearing, American Academy of Audiology, American Academy of Pediatrics, American Speech-Language-Hearing Association, Directors of Speech and Hearing Programs in State Health and Welfare Agencies (2000) Year 2000 position statement: principles and guidelines for early hearing detection and intervention programs. *Pediatrics* 2000(106):798–817
13. Judith A, Mason MS, Kenneth R, Herrmann MD (1998) Universal infant hearing screening by automated auditory brainstem response measurement. *Pediatrics* 101:221–228
14. National Sample Survey Organization (2003) Disabled persons in India, NSS 58th round (July–December 2002) Report no. 485 (58/26/1). New Delhi: National Sample Survey Organization, Ministry of Statistics and Programme Implementation, Government of India
15. Paul AK (2011) Early identification of hearing loss and centralized newborn hearing screening facility—the Cochin experience. *Indian Pediatr* 48:355–359
16. Rai N, Thakur N (2013) Universal screening of newborns to detect hearing impairment—is it necessary? *Int J Pediatr Otorhinolaryngol* 77:1036–1041
17. Ramesh A, Jagdish C, Nagapoorinima M, Suman Rao PN, Ramakrishnan AG, Thomas GC, Dominic M, Swarnarekha A

- (2012) Low cost calibrated mechanical noise maker for hearing screening of neonates in resource constrained settings. *Indian J Med Res* 135:170–176
18. Maxon AB, White KR, Behrens TR, Vohr BR (1995) Referral rates and cost efficiency in a universal newborn hearing screening program using transient evoked otoacoustic emissions. *J Am Acad Audiol* 6:271–277
  19. Maxon AB, White KR, Vohr BR, Behrens TR (1993) Using transient evoked otoacoustic emissions for neonatal hearing screening. *Br J Audiol* 27:149–153
  20. Nagapoomima P, Ramesh A, Rao S, Patricia PL, Gore M et al (2007) Universal hearing screening. *Indian J Pediatr* 74:545–549
  21. Sanders R, Durieux-Smith A, Hyde M, Jacobson J, Kileny P, Murnane O (1985) Incidence of hearing loss in high risk and intensive care nursery infants. *J Otolaryngol* 14:28–33
  22. World Health Organization. Fact sheet. Deafness and hearing impairment. <http://www.who.int/mediacentre/factsheets/fs300/en/index.html>. Accessed on 10 Jan 2009
  23. World Health Organization. State of hearing and ear care in the South East Asia Region. WHO Regional Office for South East Asia. WHO-SEARO. SEA/Deaf/9. [http://www.searo.who.int/LinkFiles/Publications\\_HEARING\\_&\\_EAR\\_CARE.pdf](http://www.searo.who.int/LinkFiles/Publications_HEARING_&_EAR_CARE.pdf). Accessed on 10 Jan 2009
  24. Berg AL, Spitzer JB, Towers HM, Bartosiewicz C, Diamond BE (2005) Newborn hearing screening in the NICU: profile of failed auditory brainstem response/passed otoacoustic emission. *Pediatrics* 116:933–938
  25. Kirkim G, Serbetcioglu B, Erdag TK, Ceryan K (2008) The frequency of auditory neuropathy detected by universal newborn hearing screening program. *Int J Pediatr Otorhinolaryngol* 72:1461–1469

# Selective Cell Isolation by Transferrin Functionalized Silane–Carbon Soot Mediated Superhydrophobic Micropatterns

Govind P. Chate, Narendra R. Kale, Vrushali Khobragade, Chinmay Rahane, Marcelo Calderón, Shashwat S. Banerjee,\* and Jayant J. Khandare\*

Surfaces that facilitate selective cell adhesion using specific targeting moieties have great implications in diagnostics, tissue engineering, and high throughput screenings. However, designing robust and spatially confined micropatterns for selective cell isolation on portable platform is highly challenging. Here, wettable, silane (Si) micropatterns holding covalently attached transferrin (Tf) for targeting Tf overexpressing cancer cells are reported. These micropatterns are separated by carbon soot based superhydrophobic regions that turn these targeting sites into surface tension confined “microwells.” These microwells facilitate capture of human colorectal carcinoma cells (HCT 116) and human cervical adenocarcinoma cells (HeLa) by confining their attachment to wettable region, thereby making isolation and spotting of the targeted cells more efficient. In addition, owing to its transparent trait, the Tf conjugated wettability based patterned chip offer real time optical monitoring of cell adhesion, cell growth, and cell behavior. The specific cell isolation using such surface has applications in devising cancer recurrence monitoring tests.

Designing patterned superhydrophobic (SH) surfaces is highly challenging, since the fabrication of wettable and biologically imperative surfaces with functionalized patterns necessitates control for fluid handling in confined space.<sup>[1–7]</sup> However, imparting chemical functionality to wettable microframes surrounded by SH regions is highly challenging. This is because, few techniques have been proposed to obtain wettable patterned surfaces by using surface modification techniques namely “ink” printing. Furthermore, functional groups have been generated using UV irradiation.<sup>[8,9]</sup> However, the targeting moieties have not been conjugated covalently on wettable patterns surrounded by SH region. Therefore, a novel chemical approach is envisioned to design functionalized micrometer-sized patterns

embedded with targeting moieties for selective cell isolation.

We report design and synthesis of functionalized patterns by covalently conjugating transferrin (Tf) on silanized glass surfaces bordered by CS regions. We hypothesize that the covalently conjugated Tf on wettable silanized glass surfaces will demonstrate specific capture of Tf overexpressing cells. Tf is a serum glycoprotein that is widely used as a targeting moiety in cancer therapeutics. Cancer cells overexpress Tf receptors (TfRs) when compared with normal cells. The reason behind overexpressing TfRs by malignant cells is because they are rapidly dividing and growing. This property of malignant cells proves to be their Achilles’ heel.<sup>[10]</sup> Recently, we reported the use of Tf as cell targeting moiety to isolate and capture cancer cells from cancer patients blood

samples though 3D matrix substrates.<sup>[11–14]</sup> Similarly, the targeted drug delivery systems designed by Tf-decorated nanoparticles (NPs) demonstrate its cell specific accumulation in tumor, highlighting the enhanced targeting ability after conjugation with Tf.<sup>[15–19]</sup> It is envisioned that Tf targeting moiety covalently attached on wettable patterns will target TfRs overexpressing cells and shall offer several advantages over surfaces that have no confined space limited by boundary layer. Therefore, the uniqueness of such surfaces is fourfold: (a) Tf-mediated wettable cell adhesion sites, (b) nonwetable Cassie–Baxter state inducing SH regions surrounding adhesion sites for preventing cell attachment, (c) high media holding capacity of patterned wells, and (d) ease of monitoring the cell growth studies due to translucent surface.

To demonstrate the efficiency of Tf silane (Si-Tf) functionalized chip, HCT 116 and HeLa cells were used to evaluate the cell isolation efficiency from cell enriching medium. Earlier, Si-Tf chip was prepared by a multistep process as depicted in **Figure 1**. Number of wettable patterns per Si-Tf chip can be increased, depending on the size of the glass substrate used and the volume of cell suspension from which cell isolation has to be carried out. The process for preparation of Si-Tf chip with multiple wettable sites (**Figure 1**) and Si-Tf chip with single wettable pattern (**Figure 2a**) is similar, except the number of masking beads used. Glass cover slips were silanized to impart  $\square$ NH<sub>2</sub> functional groups for further chemical conjugation. Each glass slip was estimated to contain  $\approx$ 19 amine groups per nm<sup>2</sup>.<sup>[20]</sup> Quantitation of the number of amine groups per nm<sup>2</sup>

G. P. Chate, N. R. Kale, V. Khobragade, C. Rahane, Prof. J. J. Khandare  
MAEER’s Maharashtra Institute of Pharmacy  
Kothrud, Pune 411038, India

E-mail: jayant.khandare@mippune.edu.in

Prof. M. Calderón  
Freie Universität Berlin  
Institut für Chemie und Biochemie  
Organische Chemie  
Takustrasse 3, 14195 Berlin, Germany

Dr. S. S. Banerjee  
Maharashtra Institute of Medical Education and Research Medical  
College  
Talegaon Dabhade, Pune 410507, India  
E-mail: shashwatbanerjee@mitmimer.com

DOI: 10.1002/admi.201701581



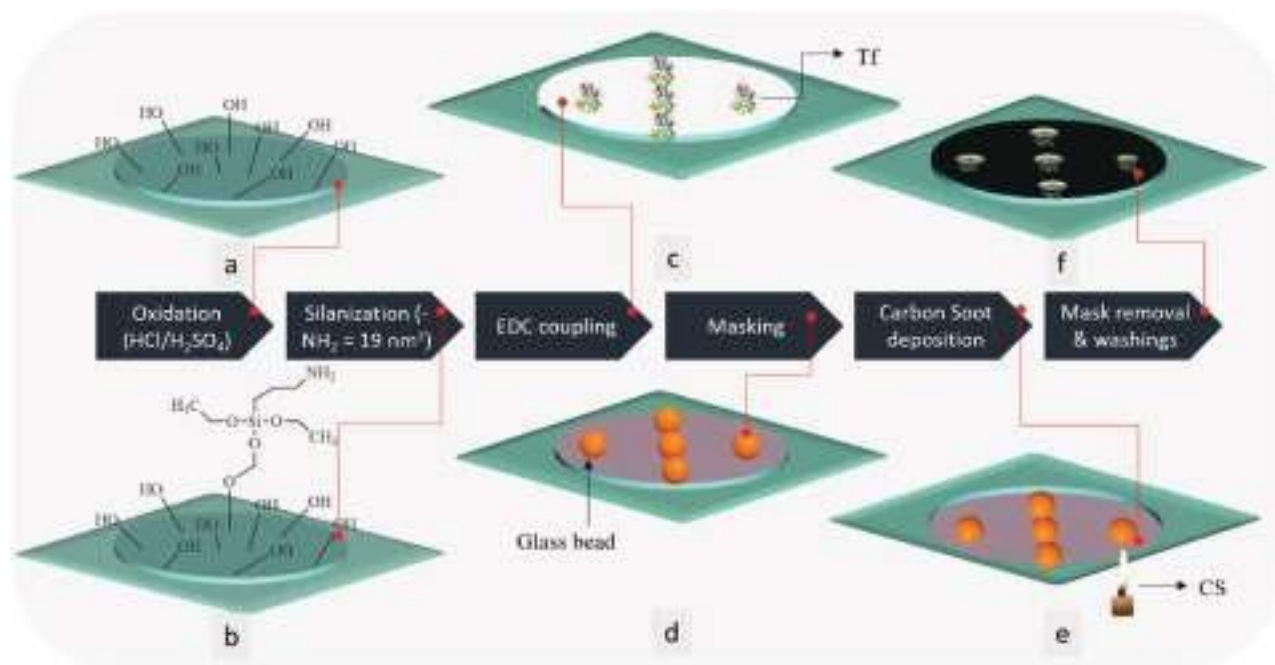


**Figure 1.** Scheme of events leading to formation of spatially controlled Tf-conjugated patterns on a glass substrate. a,b) Glass cover slips were used as substrate and were oxidized using piranha solution and subsequently silanized. c) Tf was covalently conjugated on the silanized surface using EDC·HCl as coupling agent. d) Functionalized spots were masked with glass beads of 2 mm diameter to avoid CS deposition. Rest of the silanized glass was covered with PDMS layer (PDMS:curing agent 10:1). e,f) CS was deposited on PDMS layer as well as on glass beads and non-SH patterns were carved out by removing CS-covered glass beads.

area was performed using orange II dye method. This amine group quantitation method was used to confirm silanization. Consequently, silane-functionalized glass slips were then subjected to Tf conjugation at marked sites where patterns

were developed. Tf was chemically immobilized with amine-functionalized silanated glass using *N*-(3-dimethylaminopropyl)-*N*-ethylcarbodiimide HCl (EDC · HCl) coupling reaction. The silanization provides the necessary amine groups to be

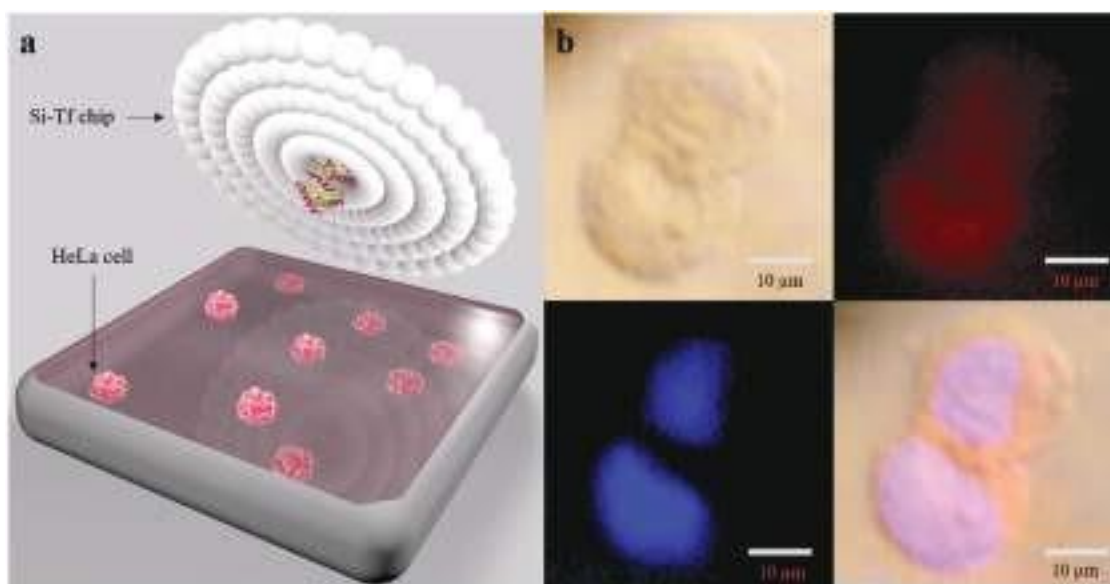


**Figure 2.** Cell isolation in 3D nanostructured patterns. a) Schematic representation of Si-Tf chip and artificial cell suspension. Si-Tf chip is dropped in the cell suspension where wettable target sites allow target cells to get adhered along with some cell media. The presence of nonwetable CS NPs layer around wettable spots prevents cell suspension attachment to the surface except target site. b) Fluorescence microscope images of HeLa cells isolated in wettable patterns 24 h after their isolation were acquired using fluorescence microscopy. Brightfield, Eosin, DAPI, and multichannel overlay images demonstrate the wettability assisted cell isolation from cell suspension. Scale bar is 10 μm.

introduced on the acidified glass substrate. EDC coupling facilitates covalent conjugation of Tf in wettable silanized patterns without formation of any intermediate byproducts. This results in excellent coupling of Tf to wettable patterns as evident from its quantitation. The amount of Tf conjugation was quantitated to be  $\approx 12 \mu\text{g}$  on each pattern using Bradford assay. On the other hand, nonwetable regions were fabricated by depositing CS over semicured polydimethylsiloxane (PDMS) mixed with curing agent and mapped around conjugation site. The semicured PDMS allows more firm attachment of CS as compared to completely cured PDMS as evident from the CA measured for  $10 \mu\text{L}$  water droplet on surfaces prepared by semicured and completely cured PDMS. CA for  $10 \mu\text{L}$  water droplet on semicured PDMS turned SHS was  $162^\circ$  while SHS resulting from completely cured PDMS was  $138^\circ$ . Glass beads were used as covers to mask the conjugation site and to prevent CS deposition on conjugated Tf. Finally, glass beads covered on Si surface were removed to form the wettability tuned Si-Tf chip.

Scanning electron microscopy (SEM) images of CS NPs deposited on PDMS surface are shown in **Figure 3a**. The image indicates, CS NPs of  $\approx 40 \text{ nm}$  size were formed at uppermost layer. Interestingly, the static contact angle ( $\theta$ ) for a  $5 \mu\text{L}$  sessile water droplet on nonwetable region was observed to be  $162^\circ$  (Figure 3d) showing the SH nature of the nonwetable region. This is expected to assist the cell media droplet to assume Cassie–Baxter state by trapping air pockets beneath the contact line of cell media drops. The robustness of nonwetable region of Si-Tf chip was evaluated by examining change in CA for  $10 \mu\text{L}$  water droplet on nonwetable region after washing. The washing process involved passing  $50 \text{ mL}$  distilled water over  $30 \text{ s}$  as water current and repeating the process three times. Superhydrophobicity of the nonwetable section of the Si-Tf chip is maintained even after repeated washings as evident from the  $< 2^\circ$  change in CA for a  $10 \mu\text{L}$  water droplet measured before and after washings.

Notably, cell adhesion molecules (CAMs) do not find adhesion sites when the cell suspension drop comes in contact with nonwetable region, thereby preventing the cell attachment.<sup>[21]</sup> Furthermore, the surface tension induced by CS layer with very low surface energy allows the water droplet to roll off from the surface even at  $2^\circ$  inclination (Figure S2, Supporting Information). As evident from atomic force microscopy (AFM) images, the height of CS aggregates in top layer was below  $500 \text{ nm}$  formed by individual CS particles of  $40\text{--}50 \text{ nm}$  size that were attached to the PDMS during the curing process (Figure 3a). While, AFM studies showed nanoscale roughness on PDMS template resulting from CS deposition (Figure 3b). CS NPs were deposited as uneven patterns resulting into nanoscale roughness. This arrangement of CS aggregates allowed the formation of pillars of varying heights that prevented the water droplets and polar solvents from wetting the surface. Further, the arrangement of CS aggregates at the interface of wettable and nonwetable pattern resulted in cell media droplet confinement only to wettable region (Figure 3e).<sup>[22]</sup> Cell media drops adhered to the wettable patterns could be easily transferred from Si-Tf chip to 6-well plate by using micropipette for cell incubation and microscopy studies. Interestingly, cell media drops remain in these patterns even when the Si-Tf chip was rotated at  $180^\circ$  owing to its adhesive force enabled attachment to the wettable pattern (Figure S1, Supporting Information).

Cell targeting and cell isolation efficiency was studied by seeding HCT 116 and HeLa cells using wettable pattern on Si-Tf surface that was initially immersed in cell suspension for  $30 \text{ s}$  and later repeatedly washed with excess amount of cell media. The droplets were then observed under fluorescence microscope and total number of cells attached per pattern was accounted. The surface area (SA) of each pattern was calculated to correlate the number of cells attached in each wettable pattern (Table S1, Supporting Information). The number of cells captured for Si-Tf was found to be  $\approx 7$  times higher than

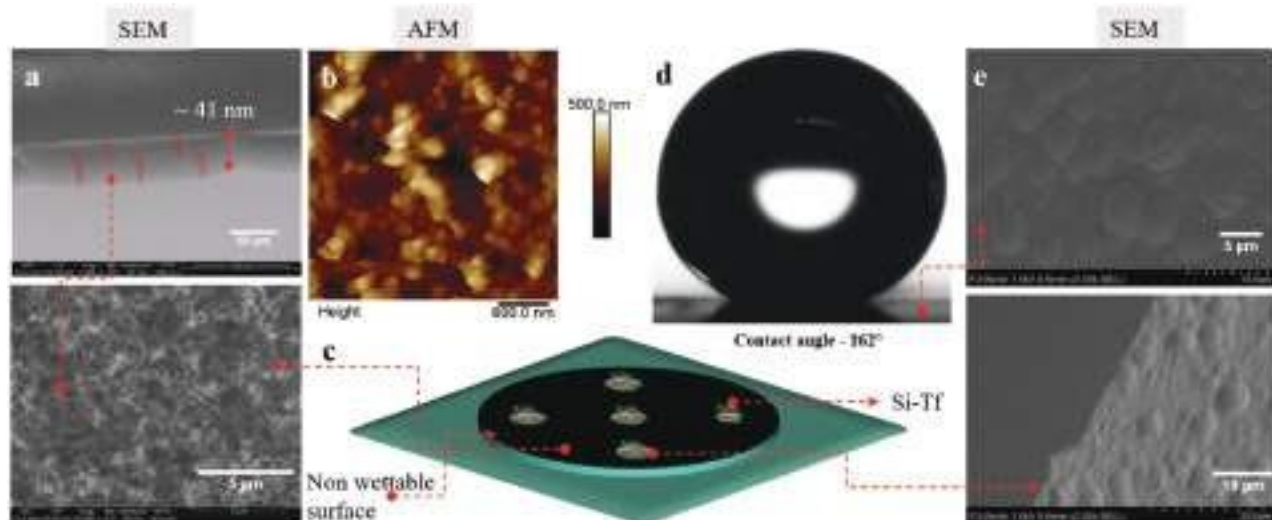


**Figure 3.** Characterization of Si-Tf chip. a) SEM micrographs of CS particles deposited on PDMS layer by combustion of carnauba wax candle flame. b) AFM micrograph indicating surface geometry of nonwetable region depicting arrangement of CS particles. c) Schematic representation of concentric patterns of Tf-functionalized Si-Tf chip. d) Static contact angle of  $5 \mu\text{L}$  water drop on nonwetable region. e) SEM microscopy images of interface of functionalized wettable pattern and surrounding SH region.

nonfunctionalized surface indicating the role of Tf moiety. In order to compare the efficiency of Tf functionalized Si-Tf versus nonfunctionalized pattern, the SA required to isolate cells was considered as a prudent parameter. Area required to isolate a single cell in Si-Tf patterns was found to be  $177.25 \mu\text{m}^2$ . On the other hand, the Tf negative patterns required  $1256.16 \mu\text{m}^2$  area to isolate a single cell. This significantly lower area required for cell isolation by functionalized patterns can be attributed to the presence of Tf and its cell specificity. TfRs overexpressing HCT 116 colorectal cancer cell isolation enhancement is in line with our hypothesis and supported by earlier reports.<sup>[23,24]</sup>

To further investigate the influence of Tf on cell capture efficiency, we employed wettable patterns of Tf conjugated (SHS-Tf), silanized glass (SHS-Sil), and plain oxidized glass (SHS-glass) for capturing HeLa and HCT 116 (Figure 4). Silanized glass surface isolated more number of cells ( $1256.16 \mu\text{m}^2$  surface area required for single isolated cell) over untreated glass patterns ( $2235.15 \mu\text{m}^2$  surface area for single cell) indicating the significance of surface functionalization induced by silanization. The linear chains created on the surface after silanization have amide groups at the terminal that enables Tf attachment to this surface through EDC coupling reaction. Rough silanized surface isolated more cells as compared to its untreated glass counterpart highlighting the importance of surface roughness for CAM attachment. Tf conjugated to silanized surface further enhances the capturing ability of Si-Tf for Tf overexpressing tumor cells. Our results further showed that SHS-Tf surface isolated highest number of cells ( $\approx 7$  times) per unit area indicating the enhanced efficiency of surface after conjugation with Tf. Enhanced cell isolation after covalent conjugation of Tf to silanized wettable surface proves the need for chemically attaching targeting moieties on wettable spots as hypothesized by us. It was noted that no fraction of cell suspension remained attached to the nonwetable region highlighting the Cassie–Baxter state attained by media droplet, resulting from the air entrapped in upper layer of surface beneath the droplet. Further, no fraction of CS was observed in the wettable pattern proving the robust attachment of CS

to PDMS, thereby maintaining nonwettability throughout the experiment.

Tf conjugated in patterns of Si-Tf chip act as favored as well as enhanced interacting sites for cancer cells and thereby a high number of cancer cells are attached on these patterns. Thus, the surface tension confined system enables cell attachment in wettable patterns, whereas nonwettability induced by superhydrophobicity assisted in directing the cell suspension droplets to wettable patterns. Importantly, cell adhesion and cell growth is facilitated in Si-Tf patterns that provide nanorough wettable surface for enhanced cell interactions with CAMs. Si-Tf pattern (Figure S3b, Supporting Information) accounts  $\approx 1 \text{ mm}^2$  surface area that could hold  $330 \mu\text{L}$  cell media inside individual pattern (Figure S3a, Supporting Information). Cell growth in the Si-Tf pattern is uniform, as evident from cell growth at boundary region of the pattern indicating uniformity of Tf conjugation in Si-Tf chip functionalized wettable spots (Figure S4, Supporting Information).

In order to assess the feasibility of Si-Tf to be used for monitoring cell growth, study of its cell media holding capability was essential. Moreover, the cell media held in wettable patterns should be sufficient enough to provide the necessary nutrients to cells during cell growth phase. In addition, we studied the rate of evaporation of cell media, i.e.,  $\approx 50 \mu\text{L}$  McCoy's 5A (modified) medium droplet was used at room temperature. After 24 h, 45% reduction in droplet volume was observed. Likewise  $\approx 48\%$  droplet size reduction was observed for Dulbecco's Modified Eagle Medium (DMEM) after 48 h. When compared with the amount of media required for cell growth observation in case of 96-well plate ( $300 \mu\text{L}$ ), there was a sixfold decrease in cell media requirement. This makes the cell isolation and growth studies fairly economical as compared to conventional techniques. Toward this, cell growth studies were carried out on Si-Tf patterns for 72 h with periodic replenishment of cell media. Cell growth images were taken after regular time intervals of 4, 12, and 24 h. The cell growth images taken after 24 h are as shown in Figure S4 (Supporting Information). These results underline the potential of Si-Tf patterns to monitor cell growth parameters in real time.

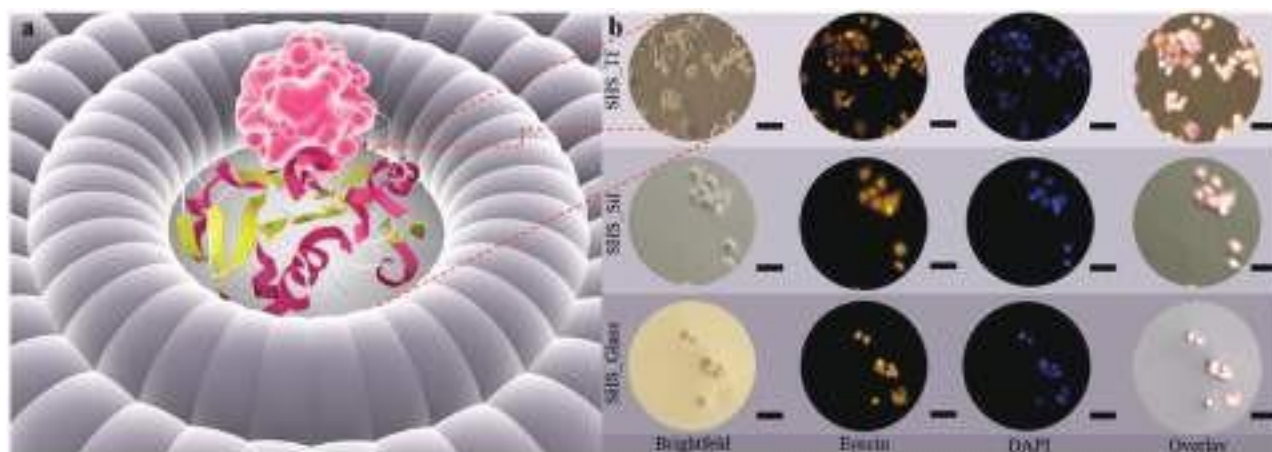


**Figure 4.** HCT 116 cell isolation using Si-Tf chip. a) Images of schematic representation depicting cell attachment to conjugated Tf in wettable pattern of Si-Tf chip. The Si-Tf chip is shown containing Tf covalently attached to wettable pattern, thereby making it a substrate that acts as a trap for targeted cells. The cancer cell attachment to Tf is shown in these schematics with marked reference to actual cells isolated in Si-Tf chip. b) HCT 116 cell growth over a period of 48 h in patterns functionalized with Tf, without Tf conjugation, and without silanization. Scale bar is  $20 \mu\text{m}$ .



In another set of experiments, we evaluated the cell media evaporation rate in Si-Tf patterns to be used as prospective platform for cell aggregation studies (Figure S5, Supporting Information). Cell suspension droplet adhered to Si-Tf pattern has fixed contact line spanning across the diameter of wettable pattern. 10–50  $\mu\text{L}$  cell suspension droplets when placed on the wettable patterns assume a convex shape with their boundaries lying completely within the wettable region. But as the volume of droplets is increased, although the contact line remains fixed, the droplet starts spreading over to the nonwettable region. The nonwettable region has low surface energy, which in combination with surface tension of water makes the droplet assume semispherical shape (Figure S3, Supporting Information). When cell suspension droplet is placed in wettable pattern, the cells start settling at the bottom under the influence of gravitational pull. Meanwhile, the droplet starts shrinking as the evaporation starts, bringing the cells settled on the concave portion of the droplet toward the fixed contact line. This ultimately resulted into aggregation of cells specifically limited to area of contact line. The shape of the sediment changed with the number of cells present in the droplet. In this study, we observed the shrinking pattern of the droplet as well as the reduction in its area. 100  $\mu\text{L}$  cell suspension droplet shrinks 70% in volume after 80 min. The contact line of the droplet remains fixed during evaporation (Figure S5, Supporting Information). In order to carry out cell growth of the aggregated cells, it is necessary that cell media volume is maintained which changes during evaporation. Si-Tf chip facilitates compensation of loss of media through evaporation by manually adding fresh cell media during cell growth studies. These results indicate the feasibility of using Si-Tf as a platform for cell aggregation studies for prolonged duration. Cell media droplet can be held in inverted state as shown in Figure S1a (Supporting Information). This makes the Si-Tf chip, a prospective platform for studying 3D tumor spheroid formation. Cell aggregate formation studied by us yielded clustered cells in wettable patterns (Figure S1b, Supporting Information), but further studies are needed to be carried out using the Si-Tf chip in inverted state holding cells suspended in anchored droplet.

In summary, we have prepared a novel Si-Tf cell targeting and isolation chip where wettable patterns are formed by functionalization of glass substrates to covalently attach a targeting moiety, Tf. This covalent attachment binds the Tf in targeting spots, allows selective capturing of Tf overexpressing cancer cells when Si-Tf is exposed to cell suspension. We demonstrated that Tf can be covalently conjugated to functionalized wettable patterns through EDC coupling reaction carried out on silanized glass pattern surrounded by CS NPs induced superhydrophobicity. CS-based SH layer surrounding the wettable pattern facilitates surface tension induced confinement of cell suspension drop. We effectively isolated 55 HCT 116 cells in Si-Tf patterns spanning cumulative area of 9749  $\mu\text{m}^2$  spread over four wettable spots. In comparison, number of cells isolated in Si-Tf wettable patterns without Tf, was 9 in 4 spots with cumulative area of 11305  $\mu\text{m}^2$ . Ease of cell media transfer to and from the wettable spot allows cell growth studies to be conducted for 48 h. The cell suspension droplet evaporation studies revealed that the droplet shrinking takes place along

the fixed contact line, thereby facilitating the cell aggregation in wettable spot.

We conclude that transferrin functionalized silane-carbon soot mediated superhydrophobic micropattern is a potential platform for cell targeting which can be developed into a diagnostic tool to isolate cells of interest in confined space. Various other biologically implicated targeting moieties can be conjugated to the functionalized glass substrates by altering the functionality imparted to wettable spots, which provide confined sites for cell growth parameter studies. In addition, results presented here also highlight that designing wettability controlled patterns can prove to be a choice of surface patterning for containment and confinement of fluids and their motion, which will act as guiding template for bio-functionalized materials. Overall, this study present the feasibility of chemically attaching targeting moieties with spatial conformities coupled with prospect of selecting targeting moiety for specific cell isolation.

## Experimental Section

**Preparation of Functionalized Glass Substrates:** Glass cover slips were procured from a local supplier and treated with Piranha solution (conc.  $\text{H}_2\text{SO}_4$  and  $\text{H}_2\text{O}_2$  in 3:1 proportion) at 80  $^\circ\text{C}$  for 2 h with constant stirring. Treated cover slips were washed thoroughly by double distilled water and dried in oven at 40  $^\circ\text{C}$ . The oxidized cover slips were further functionalized with 3% (3-aminopropyl) trimethoxysilane in toluene. After overnight stirring, silanized glass substrates were washed with double distilled water and dried at room temperature.

**Attaching Tf to Silanized Glass:** EDC.HCl and Tf (30  $\mu\text{g mL}^{-1}$ ) were mixed at pH 6.0 for 30 min. 500  $\mu\text{L}$  of Tf and EDC.HCl solution were placed on the sites of pattern formation and incubated at room temperature for 3 h. The glass substrate was washed with DI water to remove any unattached Tf from the sites and subsequently dried at room temperature. These Tf functionalized wettable patterned cover slips were UV sterilized for 15 min and stored in sterile conditions to be used for cell capture studies.

**PDMS-Glass Bead Mask Formation:** Sylgard 184 elastomer base and curing agent were mixed in a proportion of 10:1. Silanized glass slips were covered with thin layer PDMS except for the sites of Tf conjugation. Tf conjugated sites were masked with glass beads surrounded by PDMS layer. Uniformly spread PDMS layer is allowed to cure at 80  $^\circ\text{C}$  for 30 min and cooled to room temperature.

**Wettability Controlled Confined Pattern Formation on Silanized Glass:** Masked silanized glass was deposited with nonwettable CS layer using carnauba wax candle flame. CS started emitting from candle flame during wax combustion in oxygen-deprived state resulting from glass slip capping the flame tip. After CS deposition, the glass slip was exposed to water current to remove excess and unbound CS. Glass beads were removed leaving behind Tf spots surrounded by CS layer.

**Evaluation of Contact Angle of Silanized Glass and Patterned Surface:** Contact angle Goniometer was used to evaluate the static contact angle of silanized glass as well as functionalized glass substrate. A 5  $\mu\text{L}$  water drop was placed on the nonwettable region and the angle at the three-phase contact line was measured by the software interface. Captured images were further processed with image processing freeware ImageJ using Low Bond Axisymmetrical Drop Shape Analysis (LB-ADSA) plugin of ImageJ.

**Cell Suspension Preparation:** HCT 116 colorectal cancer cell line and HeLa cervical cancer cell line were used to evaluate Si-Tf chip. HCT 116 cell line was maintained in 90% McCoy's 5A medium in addition to 9% fetal bovine serum and 1% antibiotic in cell culture flask. HeLa cell line was maintained in DMEM supplemented with 9% fetal bovine serum and 1% antibiotic; incubated at 37  $^\circ\text{C}$  and 5%  $\text{CO}_2$  concentration. These cell lines were periodically inspected for contamination. Cells in

suspension were maintained in a suspended state by transferring to multiwell plates prior to isolation process using Si-Tf.

**Evaluation of Cell Targeting and Isolation:** HCT 116 cell suspension with cell concentration of  $2 \times 10^6$  cells mL<sup>-1</sup> and HeLa cell suspension with  $4 \times 10^5$  cells mL<sup>-1</sup> were maintained separately in a 35 mL disposable petri dish in a biosafety cabinet as shown using schematics in Si-Tf chips were dipped in both cell suspensions with wettable functionalized patterns facing the suspension (Figure 4a). Si-Tf chip was moved through the suspension for 30 s and taken out using tweezers. PBS was used to remove the unattached cells. Adhered cell suspension droplets were stained with 1  $\mu$ L nuclear staining dye 4',6-diamidino-2-phenylindole (DAPI) (0.5 mg mL<sup>-1</sup>) and 1  $\mu$ L cytoplasm staining dye Eosin (5 mg mL<sup>-1</sup>) and incubated for 30 min. After washing with PBS, the number of attached cells in each pattern was observed under fluorescence microscope (Carl Zeiss Axio Observer A1) as shown in Figure 4b.

**Comparison of Cell Adhesion on Silanized Glass versus Tf Functionalized Glass:** HCT 116 and HeLa cells adhered on Si-Tf chip patterns were observed under fluorescence microscope. Number of cells adhered in patterns with conjugated Tf and non-Tf conjugated patterns were compared. Area of each pattern was measured using Zeiss Core (blue edition) software to calculate the number of cells adhered per pattern on Si-Tf chip and control surface. Efficiency of Si-Tf chip patterns was calculated by measuring the area of each pattern and comparing the number of cells per pattern.

**Observation of Cell Growth in Wettable, Functionalized Patterns:** Si-Tf chip and control surface with adhered cell suspension drops were transferred to a 6-well plate. 50  $\mu$ L McCoy's 5A medium was added to HCT 116 cell suspension drops and 50  $\mu$ L Dulbecco's Modified Eagle's medium was added to HeLa cell suspension drops. The 6-well plate containing the patterns was transferred to a bioincubator maintained at 37 °C and 5% CO<sub>2</sub> concentration. Cell growth was observed at every 3 h interval.

**Attachment of Cells on Nonwettable Region:** In a control experiment, cell attachment to nonwettable CS layer was observed by placing 10  $\mu$ L of HCT 116 cell suspension with  $2 \times 10^6$  cells mL<sup>-1</sup> concentration on CS layer for 2 h. 1  $\mu$ L nuclear staining dye DAPI (0.5 mg mL<sup>-1</sup>) and 1  $\mu$ L cytoplasm staining dye Eosin (5 mg mL<sup>-1</sup>) were added to the drop and incubated for 30 min and subsequently washed with phosphate buffer. Cell suspension drop was removed from the surface to observe the number of cells attached to CS layer. CS pattern was observed under fluorescence microscope for detection of attached cells.

**SEM Characterization of Nonwettable and Boundary Regions on Si-Tf Chip:** The morphology of CS particles forming the nonwettable part of the chip was characterized by SEM (FEI, Quanta 200-USA). The functionalized patterned wells and CS particles present at the interface were also observed. The morphology of the CS particles attached to PDMS that form the nanoaggregates to accommodate the air pockets imparting nonwettability was observed.

**AFM Characterization of CS Layer:** Patterned Tf nonwettable surfaces were characterized using the Park XE 150 Atomic Force Microscope attached to a Labram high-resolution spectrometer. CS NPs attached to the PDMS layer on the silanized glass were evaluated for their attachment to assess the formation of air pockets which imparts superhydrophobicity through their arrangement.

## Supporting Information

Supporting Information is available from the Wiley Online Library or from the author.

## Acknowledgements

The authors acknowledge the financial support of the Department of Science and Technology, Government of India for the Fund for Improvement of Science and Technology infrastructure (FIST-DST)

and the Department of Biotechnology (DBT) grant. The authors also appreciate Freie Universitat, Berlin, Alumni research grant and Prof. Marcelo Calderón Group's support for SEM and AFM studies.

## Conflict of Interest

The authors declare no conflict of interest.

## Keywords

cell isolation, conjugation, superhydrophobic, transferrin, wettability

Received: December 3, 2017

Published online:

- [1] L. Wen, Y. Tian, L. Jiang, *Angew. Chem., Int. Ed.* **2015**, *54*, 3387.
- [2] I. You, N. Yun, H. Lee, *ChemPhysChem* **2013**, *14*, 471.
- [3] J. Ziauddin, D. M. Sabatini, *Nature* **2001**, *411*, 107.
- [4] H. Erfle, B. Neumann, U. Liebel, P. Rogers, M. Held, T. Walter, J. Ellenberg, R. Pepperkok, *Nat. Protoc.* **2007**, *2*, 392.
- [5] E. Palmer, *Cell-Based Microarrays: Methods and Protocols*, (Eds: E. Palmer) Humana Press, Springer Science, LLC New York, US, **2011**, p. 1.
- [6] J. H. Butler, M. Cronin, K. M. Anderson, G. M. Biddison, F. Chatelain, M. Cummer, D. J. Davi, L. Fisher, A. W. Fraundorf, F. W. Frueh, *J. Am. Chem. Soc.* **2001**, *123*, 8887.
- [7] F. L. Geyer, E. Ueda, U. Liebel, N. Grau, P. A. Levkin, *Angew. Chem., Int. Ed.* **2011**, *50*, 8424.
- [8] L. Zhang, J. Wu, M. N. Hedhili, X. Yang, P. Wang, *J. Mater. Chem. A* **2015**, *3*, 2844.
- [9] Y. Liu, K. Ai, L. Lu, *Chem. Rev.* **2014**, *114*, 5057.
- [10] S. Banerjee, K. Todkar, G. Chate, J. Khandare, in *Targeted Drug Delivery: Concepts and Design* (Eds: P. V. Devarajan, S. Jain), Springer Cham, Switzerland **2015**, p. 367.
- [11] S. S. Banerjee, A. Jalota-Badwar, S. D. Satavalekar, S. G. Bhansali, N. D. Aher, R. R. Mascarenhas, D. Paul, S. Sharma, J. J. Khandare, *Adv. Healthcare Mater.* **2013**, *2*, 800.
- [12] S. S. Banerjee, G. V. Khutale, V. Khobragade, N. R. Kale, M. Pore, G. P. Chate, A. Jalota-Badwar, M. Dongare, J. J. Khandare, *Adv. Mater. Int.* **2017**, *4*, 1600934.
- [13] S. S. Banerjee, D. Paul, S. G. Bhansali, N. D. Aher, A. Jalota-Badwar, J. Khandare, *Small* **2012**, *8*, 1657.
- [14] M. Asadian-Birjand, C. Biglione, J. Bergueiro, A. Cappelletti, C. Rahane, G. Chate, J. Khandare, B. Klemke, M. C. Strumia, M. Calderón, *Macromol. Rapid Commun.* **2016**, *37*, 439.
- [15] W. Faulk, C. Taylor, C. Yeh, J. McIntyre, *Mol. Biother.* **1990**, *2*, 57.
- [16] J. F. Head, F. Wang, R. L. Elliott, *Adv. Enzyme Regul.* **1997**, *37*, 147.
- [17] N. G. Rainov, A. Söling, *Curr. Opin. Mol. Ther.* **2005**, *7*, 483.
- [18] N. C. Bellocoq, S. H. Pun, G. S. Jensen, M. E. Davis, *Bioconjugate Chem.* **2003**, *14*, 1122.
- [19] S. H. Pun, F. Tack, N. C. Bellocoq, J. Cheng, B. H. Grubbs, G. S. Jensen, M. E. Davis, M. Brewster, M. Janicot, B. Janssens, *Cancer Biol. Ther.* **2004**, *3*, 641.
- [20] S. Noel, B. Liberelle, L. Robitaille, G. De Crescenzo, *Bioconjugate Chem.* **2011**, *22*, 1690.
- [21] L. Shapiro, A. M. Fannon, P. D. Kwong, A. Thompson, *Nature* **1995**, *374*, 327.
- [22] W. M. Sigmund, S.-H. Hsu, in *Encyclopedia of Membranes* (Eds: E. Drioli, L. Giorno), Springer-Verlag, Berlin Heidelberg **2016**, p. 310.
- [23] J. Wu, Y. Lu, A. Lee, X. Pan, X. Yang, X. Zhao, R. J. Lee, *J. Pharm. Pharm. Sci.* **2007**, *10*, 350.
- [24] C. H. J. Choi, C. A. Alabi, P. Webster, M. E. Davis, *Proc. Natl. Acad. Sci. USA* **2010**, *107*, 1235.



## SHORT ARTICLE

# An insight into hardiness status of medical undergraduates

Sanjeev Vasanttrao Chincholikar<sup>1</sup>, Surendra Kulkarni<sup>2</sup>

<sup>1</sup>Professor, Department of Community Medicine, Maharashtra Institute of Medical Education and Research Medical College, Pune, India

<sup>2</sup>Assistant Professor, Department of Community Medicine, Maharashtra Institute of Medical Education and Research Medical College, Pune

<a href="#">Abstract</a>	<a href="#">Introduction</a>	<a href="#">Methodology</a>	<a href="#">Results</a>	<a href="#">Conclusion</a>	<a href="#">References</a>	<a href="#">Citation</a>	<a href="#">Tables / Figures</a>
--------------------------	------------------------------	-----------------------------	-------------------------	----------------------------	----------------------------	--------------------------	----------------------------------

## Corresponding Author

Address for Correspondence: Dr Sanjeev Vasanttrao Chincholikar, Professor, Community Medicine, MIMER Medical College, Talegaon Dabhade, Dist Pune 410507  
E Mail ID: [aruna@mitmimer.com](mailto:aruna@mitmimer.com)



## Citation

Chincholikar SV, Kulkarni S. An insight into hardiness status of medical undergraduates. Indian J Comm Health. 2017; 29, 2: 191 – 193.

Source of Funding: Nil Conflict of Interest: None declared

## Article Cycle

Received: 30/04/2017; Revision: 10/05/2017; Accepted: 31/05/2017; Published: 30/06/2017

This work is licensed under a [Creative Commons Attribution 4.0 International License](https://creativecommons.org/licenses/by/4.0/).

## Abstract

**Background:** The construct of hardiness was first introduced by Kobasa and Maddi, who defined it as a resistance resource in encounter with stressful situations. Hardiness is related to three mutually related dispositions—commitment, control, and challenge. **Aims and objectives:** To explore hardiness status in medical undergraduates and to study the relationship between hardiness and psychological distress. **Material and Methods:** A cross-sectional study was carried out among medical students of a private medical college in Maharashtra. A validated Hardiness Questionnaire of Kobasa was administered. Scores on control, commitment and challenge were calculated and then summed up to calculate total hardiness score. Psychological distress was measured by SRQ tool, as designed by Mari J. and Williams. **Results:** The study population comprised of 331 students out of which 39 medical undergraduates had hardiness score less than zero indicating that 12% of study subjects were non-hardy. Significant negative association was observed between hardiness level and psychological distress. **Conclusion:** It was observed that 12% medical undergraduates were non-hardy. From the analysis of the data, it has been found that there is a fair negative association in hardiness and psychological distress.

## Keywords

Hardiness; Medical Students; Prevalence; Psychological Distress.

## Introduction

The construct of hardiness was first introduced by Kobasa (1,2,3) who defined it as a resistance resource in the encounter with stressful situations. It is considered as a pattern of personality characteristics comprising three mutually related dispositions—commitment, control, and challenge. Commitment refers to the tendency to involve oneself in the activities in life and have a genuine interest in and curiosity about the activities, things and other people. Dimension of control is defined as a tendency to believe and act as if one can influence

the life events through one's own effort, while challenge refers to the belief that changes in life are opportunities for personal growth.

Limited evidence about the probable mental health morbidities, which exist in medical students, depend upon hardiness status. The present study was inspired from the fact that psychosocial aspects, particularly, hardiness status of medical undergraduates need due attention.

## Aims & Objectives

To explore hardiness level in medical undergraduates.

To study the association between hardiness and psychological distress

## Material & Methods

A cross-sectional study was carried out in a private medical college in Maharashtra. The participants in the study were, medical students enrolled in a private medical college. There are no studies available regarding prevalence of hardiness status in medical students in India. Therefore, all the medical students present in the class were included as study population. A total of 331 medical undergraduates participated in the study; all returned the filled questionnaire.

A validated Hardiness Questionnaire of Kobasa was administered. The original scale developed by Bartone<sup>5</sup>, (1995) The Dispositional Resilience Scale (DRS-15). Hardiness was measured using the 15-item scale developed by Bartone (1995) consisting of three dimensions including commitment, control and challenge. For this instrument participants respond on a 4-point scale indicating the level at which each of the 15 statements apply to them as follows: 0 (not at all true); 1 (a little true); 2 (quite true); & 3 (completely true). Scores were obtained by reverse coding the appropriate and summing items for each dimension. The overall hardiness score was obtained by summing all 15 items. For the present study, three negatively oriented items originally aimed at measuring challenge were excluded. Finally, a 12 question scale was used. (The Dispositional Resilience Scale, DRS-12). This scale was well validated in a study conducted by Kobasa<sup>5</sup> and Igor Kardum, Jasna Hudek-Knežević, Nada Krapić. (6) Scores on control, commitment and challenge were calculated and then summed up to calculate total hardiness score. Hardiness score are classified as follows. Less than 0 are non-hardy while score 0-9 are moderately hardy and above nine are considered hardy. For convenience, they were categorized in to hardy (score equal to or more than zero) and non-hardy. (score less than zero) Mental morbidity was measured by using SRQ test.

Self-reporting questionnaire (SRQ-20) is designed as an instrument to screen for mental health disorder and found to be a reliable tool for use in different countries and cultures. In a study conducted in Pune, India, this tool was validated and found that a score of 10 or more was the most sensitive and specific cut of point to consider as mental morbidity. (7) Cutoff point of 10 was taken to consider mental morbidity.

Experience for scientific utilization of SRQ was obtained under a qualified psychiatrist.

Information on socio demographic and other variables was collected separately. Written consent was taken from the students and they were asked to fill the questionnaires with an open mind. Reasons for the study were explained.

Socioeconomic status was assessed by using modified Prasad classification. (8) The study design was approved by the ethics and research committee of the institute. Analysis was done by using appropriate statistical test.

## Results

A total of 331 medical undergraduates participated in the study; all returned the filled questionnaire. The study population comprised 41 % females and 59% males. The study population comprised of first-year MBBS students -75; second year MBBS students -111; third-year MBBS students -145. It is mentioned that in some tables total is not 331 indicating some students have not responded to that part of question. Hardiness score was calculated among blind subjects and subjects were classified as hardy and non-hardy. It can be observed from the [figure 1](#), that 12% of study participants were non-hardy.

[Figure 2](#) reveals relation between hardiness and psychological distress. 31 non-hardy are SRQ negative. When chi-square test of significance was applied to the data as shown in [Figure 2](#), results were statistically highly significant meaning that there is a significant negative association between hardiness and psychological distress among medical students.  $\chi^2 = 4.618$  d.f. =1,  $p > 0.05$ .

## Discussion

The study examined the hardiness score among medical students. As mentioned in table 1, there were 12% medical students having hardiness score less than zero. This would mean, that 12% of participants were unable to cope up with stressful conditions of life and were more prone to develop psychological maladjustments. These participants would need intervention in the form of psychological counseling for improving their hardiness for successful psychological rehabilitation.

There is a significant negative association between hardiness and psychological distress among college students as revealed in [figure 2](#). Similar findings are observed in other studies. (9,10). There is no single study that produced the opposite results that there is positive relation between hardiness and

psychological distress. The reason may be that variables used in the study, hardiness and psychological distress are opposite in nature. So, these constraints produced negative results in almost every condition. However, from the [figure 2](#), it is also observed that 8 SRQ positive people are hardy and 31 SRQ negative people are less hardy creating a dilemma whether the two tests supplement or oppose each other.

**Conclusion**

It was observed that 12% medical undergraduates were non-hardy. From the analysis of the data, it has been found that there is a fair negative association in hardiness and psychological distress. As it has been already mentioned in discussion, that the reasons may be, because these two variables are opposite in nature. It can be concluded that the medical undergraduates who have higher levels of hardiness are inclined to report lower levels of psychological distress and vice versa. It was also observed that other parameters are not associated with hardiness like gender, sports activity, year of MBBS study of the subject details of which are not mentioned in the study.

**Recommendation**

Findings suggest that there is a need of hardiness training program in a medical institute which will be effective in increasing hardiness, decreasing perceived stress levels in the students and may have positive impact on them. Counseling services, as an integral part of routine clinical services, may be provided to the medical undergraduates. Early detection of low hardiness may shorten the sufferings. This study could be used as marker for future studies.

**Limitation of the study**

Sample was not representative as the study was conducted in a private medical school. Therefore, the study results cannot be generalized. Entire study is

based on verbal response of the students. Longitudinal studies on a representative sample, involving more medical schools are needed to substantiate the findings.

**Relevance of the study**

Hardiness of medical students is a neglected domain it needs due attention to create worthy IMG.

**Authors Contribution**

CSV: Idea, data collection, paper writing; KS: data analysis.

**References**

1. Kobasa SC. Stressful life events, personality, and health: an inquiry into hardiness. *J Pers Soc Psychol.* 1979 Jan;37(1):1-11. PubMed PMID: 458548.[PubMed].
2. Kobasa S.C. and Maddi S.R.: Existential personality theory in R Corsini (ed), *current personality theory itasca,1977.*
3. Kobasa SC, Maddi SR, Kahn S. Hardiness and health: a prospective study. *J Pers Soc Psychol.* 1982 Jan;42(1):168-77. PubMed PMID: 7057354.[PubMed].
4. Kobasa , “How Hardy Are You?” (*American Health Magazine* September 1984, p 64-77).
5. Bartone, P. T. (1995, July). A short hardiness scale. Paper presented at the annual convention of the American Psychological Society, New York.
6. Igor Kardum, Jasna Hudek-Knežević, Nada Krapić The Structure of Hardiness, its Measurement Invariance across Gender and Relationships with Personality Traits and Mental Health Outcomes, *Psychological Topics* 21 (2012), 3, 487-507 Original scientific paper – UDC – 159.923.3.072 159.944.072.
7. Chincholikar SV. Use of SRQ in psychiatric epidemiology. *Indian J Community Med* 2004;29;190-1.
8. Mangal A, Kumar V, Panesar S, Talwar R, Raut D, Singh S. Updated BG Prasad socioeconomic classification, 2014: a commentary. *Indian J Public Health.* 2015 Jan-Mar;59(1):42-4. doi: 10.4103/0019-557X.152859. PubMed PMID: 25758730.[PubMed]
9. Jaya Jotwani. Hardiness and Psychological Distress among University Students Studying in Madhya Pradesh The *International Journal of Indian Psychology* ISSN 2348-5396 (e) | ISSN: 2349-3429 (p) Volume 3, Issue 2, No.6, DIP: 18.01.100/2016 0302.
10. Kenneth, M. N. (1986). Type A, hardiness and psychological distress. *Journal of Behavioral Medicine*, Vol. 9, Issue 6, pp. 537-548.

**Figures**

**FIGURE 1 HARDINESS AMONG STUDENTS**

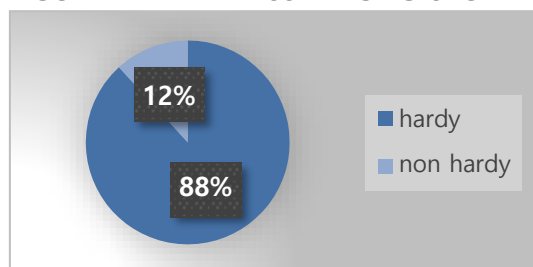
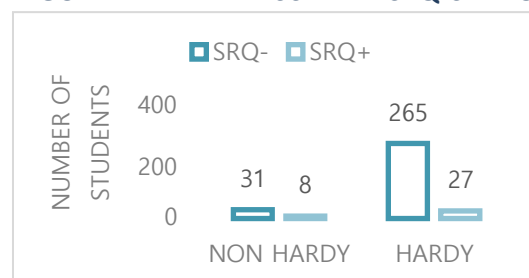


**FIGURE 2 HARDINESS AND SRQ STATUS**



# Biofunctionalized Capillary Flow Channel Platform Integrated with 3D Nanostructured Matrix to Capture Circulating Tumor Cells

Shashwat S. Banerjee,\* Ganesh V. Khutale, Vrushali Khobragade, Narendra R. Kale, Milind Pore, Govind P. Chate, Archana Jalota-Badhwar, Manoj Dongare, and Jayant J. Khandare\*

Circulating tumor cells (CTCs) from peripheral blood account genetic information for cancer diagnosis and overall disease monitoring. Analysis of “liquid biopsy” holds immense promise as it may lead to new approaches for cancer treatment. The study reports effective and continuous flow microchannel system for isolating CTCs using transferrin conjugated 3D matrix synthesized by crosslinking polyethylene glycol-Fe<sub>3</sub>O<sub>4</sub> nanostructures for rapid and efficient capturing of CTCs. The platform provides option of using multiple microchannel units in series that can influence higher cell-capture efficiency due to increasing cell-substrate contact frequency. CTCs are captured with high efficiency even at low concentration of target cells (~90% at 25 cells per mL blood). Furthermore, the study demonstrates that the cell-capture performance is influenced by topographic interactions between nanostructure based matrix and cancer cells of interest. In addition, this study demonstrates the “proof of concept” using 3D microchannel system having capacity of simultaneously capturing and permanently eliminating CTCs from peripheral blood samples. Further, the study evaluates clinical samples of colon and breast cancer patients for rapid isolation of CTCs. Conclusively, the present platform demonstrates inordinate capacity for cancer cell sorting, biological studies of CTCs, and cancer metastasis, potentially benefiting the real time liquid biopsy and early prognosis of cancer.

## 1. Introduction

Circulating tumor cells (CTCs) disseminate from the primary tumor and migrate in peripheral blood of cancer patients.<sup>[1–4]</sup> CTCs play an important role in metastases and are primarily responsible for the growth of secondary tumors and spread of cancer in distant part of the body.<sup>[5–7]</sup> Besides conventional diagnostic approaches (e.g., tumor biopsy, anatomical/molecular imaging, and serum marker detection), detecting CTCs in peripheral blood is of prognostic value to predict disease progression, response to treatment, relapse, and overall survival.<sup>[8–10]</sup> However, the detection and characterization of CTCs have been technically challenging due to their extremely low occurrence (10–100 mL<sup>-1</sup>) among a high number (10<sup>9</sup> cells mL<sup>-1</sup>) of hematologic cells in blood.<sup>[7,8]</sup> In recent years, a diversity of diagnostic methods have been developed for CTC detection and enrichment that principally include immunomagnetic separation,<sup>[2,11]</sup> microfluidic platforms,<sup>[8,12,13]</sup> and microfilter devices.<sup>[14]</sup>

Microfluidic approaches require precise control over operational parameters and often involve complex designs besides being slow due to lower fluid transfer rates, thus limiting them in time efficiency and high throughput analysis. On the other hand, immunomagnetic methods for separation of CTCs are simple to use but suffer relatively low separation efficiency and require pretreatment of blood to remove hematogenic cells.<sup>[15]</sup> Food and Drug Administration-approved CellSearch Technology uses markers with immunomagnetic beads to isolate CTCs. To enhance CTC capturing efficiency and to reduce cost, researchers have been exploring new platforms including microrockets.<sup>[2,5,8,16,17]</sup>

Here, we report the use of glass capillary-flow channel functionalized with 3D antibody matrix impinged with magnetic nanoparticles for simultaneous isolation and detection of CTCs from clinical samples. Nanostructure materials such as nanopillars, graphene sheets, and nanoparticles enhance biomolecule

Dr. S. S. Banerjee,<sup>[†]</sup> G. V. Khutale,<sup>[††]</sup> V. Khobragade, M. Pore, Dr. A. Jalota-Badhwar  
Actorius Innovations and Research (AIR)  
100 NCL Innovation Park, Pune 411 008, India  
E-mail: shashwatbanerjee@mitmimer.com  
N. R. Kale, G. P. Chate, Prof. J. J. Khandare  
Maharashtra Institute of Pharmacy  
MIT Campus  
Paud Road, Pune 411 038, India  
E-mail: jayant.khandare@mippune.edu.in  
M. Dongare  
Manik Hospital and Research Center  
Aurangabad 431001, India



<sup>[†]</sup>Present address: Maharashtra Institute of Medical Education and Research Medical College, Talegaon Dabhade, Pune 410 507, India

<sup>[††]</sup>Present address: Nanolab Focas Research Institute, Dublin Institute of Technology, Dublin, 8, Ireland

DOI: 10.1002/admi.201600934



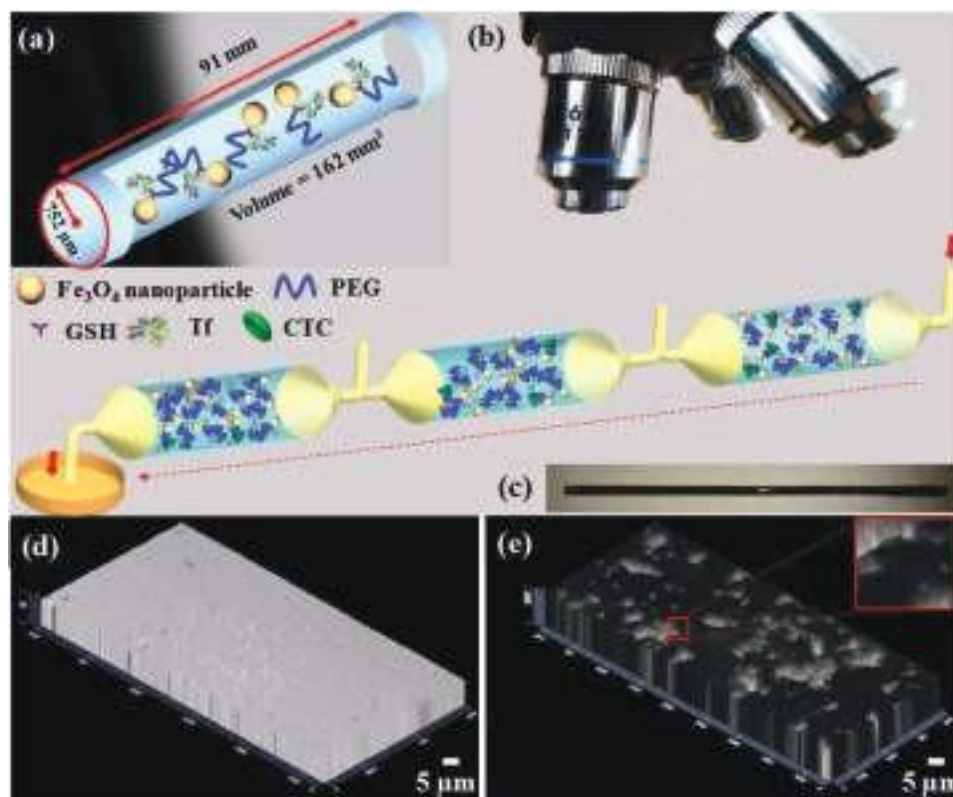


**Figure 1.** Schematic representation of the configuration and operational mechanism of multi-unit microchannel system for capturing circulating tumor cells (CTCs). a) 3D  $\text{Fe}_3\text{O}_4$ -GSH-PEG-Tf matrix conjugated microchannel glass substrate with 91 mm of length, 1.55 mm of diameter, and  $162 \text{ mm}^3$  volume. b) Cancer patient's blood sample is fed in the first 3D microchannel capillary to capture CTCs. Subsequently, blood with the uncaptured cells from the first microchannel is then fed to the second microchannel capillary and similarly to the third microchannel capillary. Finally, the CTC capturing efficiency is calculated using the set of three cycles. Intermediate outlets between microchannels enable cell capture efficiency estimation of individual microchannels. c)  $\text{Fe}_3\text{O}_4$ -GSH-PEG-Tf matrix conjugated glass capillary image. d) Pseudo-3D electron microscopy images of glass capillary and e)  $\text{Fe}_3\text{O}_4$ -GSH-PEG-Tf conjugated glass capillary demonstrating 3D surface on CTC substrate using Zeiss Zen software.

recognition.<sup>[18]</sup> Most of these CTC capturing platforms are limited by single unit operations. Therefore, we hypothesized that integrating a flow-channel unit system such as glass capillary with a patterned 3D matrix based on nanostructured materials will offer unique advantages such as (i) better cell–substrate contact frequency leading to enhanced CTC capture due to the 3D matrix and high surface to volume ratio of glass capillary, (ii) opportunity of using multiple units in series for higher cell capture efficiency and sensitivity, (iii) user flexibility to adjust the number of capillary units that best fit his particular assay, and (iv) also the capillaries with different coatings and targeting moieties can be applied simultaneously for isolating CTCs based on specific affinity as well as to sort them as they often exist with many subtypes by multiple isolation steps. Glass-based materials have been widely accepted in applications such as cell fixing substrates and as promising biocompatible materials.<sup>[19,20]</sup> However, the glass-based materials suffer from other disadvantages such as low cell affinity. To overcome this, most existing technologies rely on chemical modification to render the inert surfaces bioactive.<sup>[20]</sup>

In study we principally employed HCT116 colon cancer cells overexpressing transferrin-receptors (TfRs) to probe the capture efficiency of capillary flow-cell platform. Thus advantages of our platform are: (1) nanoprotusions generated by Poly(ethylene

glycol)-iron oxide (PEG- $\text{Fe}_3\text{O}_4$ ) functionalized “Transferrin-conjugated Nanostructured Matrix on Silane-Functionalized Glass Capillary” (Tf-NMSFGC) increases the topographic interactions between cancer cells and substrate as depicted in **Figure 1**. (2) The dimensions of the platform mediate high density packing of PEG- $\text{Fe}_3\text{O}_4$ -Tf on NMSFGC, which results in increased local concentration of Tf, and (3) optimized multi-component 3D matrix with tunable architecture by application of PEG to cross-link  $\text{Fe}_3\text{O}_4$  nanoparticles. The length of the capillary flow channel was 91 mm while the volume was  $162 \text{ mm}^3$ . These aspects of capillary flow channel 3D system synergistically contribute to enhance capture of cancer cells.

## 2. Results and Discussion

The 3D nanostructured matrix was synthesized through a multistep process (**Figure 2**). First, the cross-linked matrix of PEG- $\text{Fe}_3\text{O}_4$  was obtained according to our recent procedure.<sup>[17]</sup> Second, the resulting PEG- $\text{Fe}_3\text{O}_4$  was functionalized with specific targeting ligand Tf and then chemically immobilized to the amine-functionalized silanated glass through the reactive carboxyl group of the glutathione (GSH) linker using *N*-(3-dimethylaminopropyl)-*N*-ethylcarbodiimide HCl

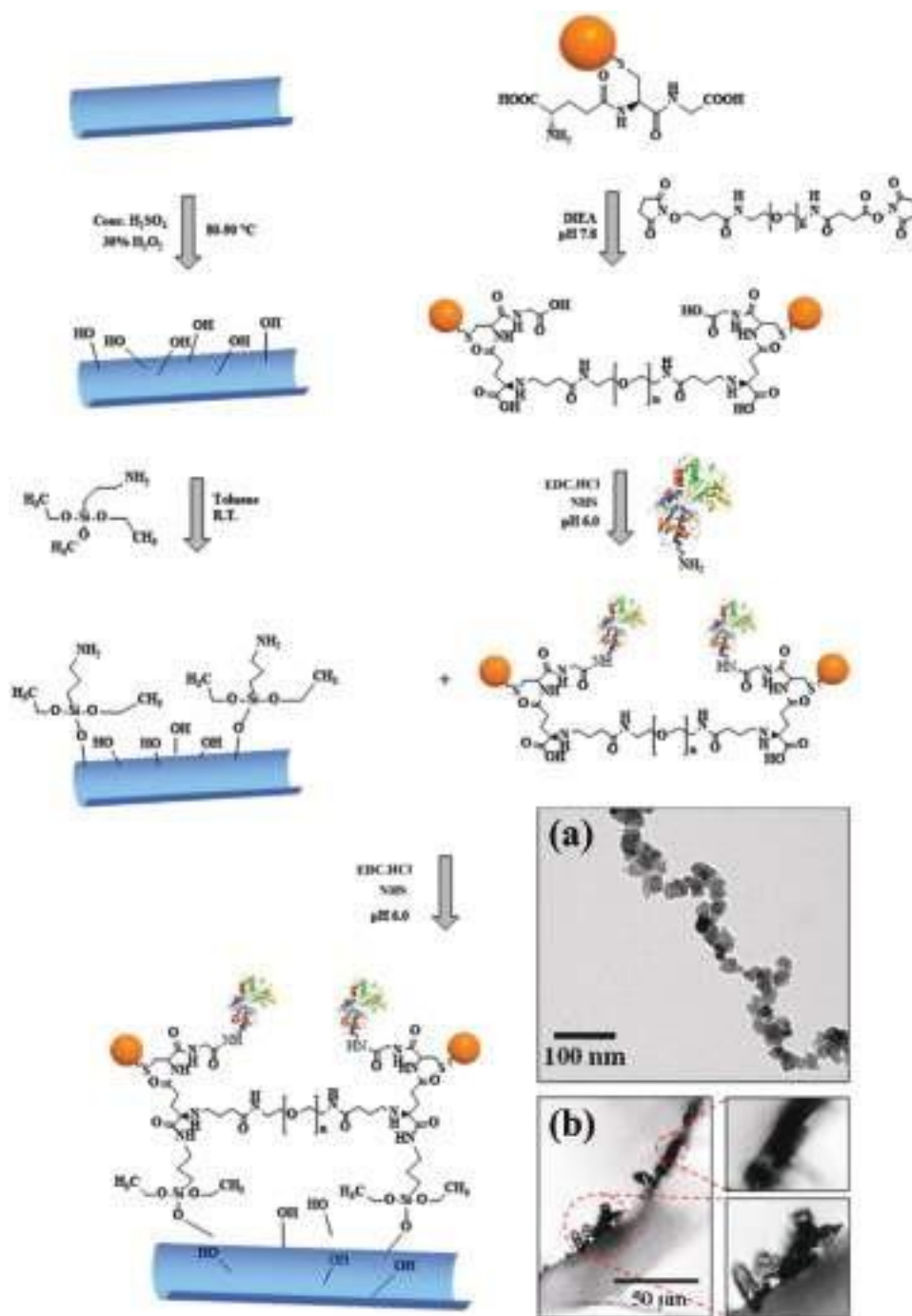


**Figure 2.** Synthetic scheme of Tf-NMSFGC microchannel system. a) TEM image of the branched structure where multiple  $\text{Fe}_3\text{O}_4$  nanoparticles are cross-linked by PEG chains forming a 3D matrix. b) Optical image of a cross-section of Tf-NMSFGC substrate. The average thickness of the matrix (shown by a dotted red circle) estimated from the images was  $11 \pm 1 \mu\text{m}$  and few isolated aggregates with thickness  $\sim 34 \pm 1 \mu\text{m}$  were also present.

(EDC·HCl) coupling reaction. An amide linkage was formed between the carboxyl group of PEG- $\text{Fe}_3\text{O}_4$  and the amine group of silane. Finally, the unreacted components on the glass substrate were removed by a series of washings with Milli-Q water. It was noted that  $\approx 2.0 \text{ mg}$   $\text{Fe}_3\text{O}_4$ -GSH-PEG-Tf was chemically deposited on the glass substrate. Consequently, a flow-channel system with  $\text{Fe}_3\text{O}_4$ -GSH-PEG-Tf 3D matrix of  $\approx 91 \text{ mm}$  long

chaotic mixing channel ( $od = 1.82$  and  $id = 1.55 \text{ mm}$ ) was produced. The amount of amine groups on the silanized glass surface was estimated to be  $\approx 16 \text{ nm}^{-2}$ . The anchoring of the  $\text{Fe}_3\text{O}_4$ -GSH-PEG-Tf matrix on the silane-functionalized glass was found to be strong, as the Tf-NMSFGC platform could survive multiple cycles of washings and drying. Figure 2 (inset) shows a typical transmission electron microscopy (TEM)

image of the PEG-Fe<sub>3</sub>O<sub>4</sub> matrix, which confirms the cross-linking of the Fe<sub>3</sub>O<sub>4</sub> nanoparticles through the PEG chains, thereby leading to 3D nanoscale architecture. The darker parts in the image result from the Fe<sub>3</sub>O<sub>4</sub> particles as they are more electron-dense than the PEG chains. The mean size of Fe<sub>3</sub>O<sub>4</sub> nanoparticles in the matrix was estimated to be  $\approx 24 \pm 8$  nm, which corroborates well with their starting size. It also suggests that the conjugation reaction did not alter the morphology of the particles. Furthermore, the nanosystem was characterized by Fourier Transform Infrared (FTIR) spectroscopy to verify successful conjugation of PEG and Tf to Fe<sub>3</sub>O<sub>4</sub>-GSH (Figure S1, Supporting Information). The IR spectrum of Fe<sub>3</sub>O<sub>4</sub>-GSH showed peaks at 1630, 1542, 1390, and 890 cm<sup>-1</sup> corresponding to C=N and Fe-O bonds, respectively. The IR spectrum of Fe<sub>3</sub>O<sub>4</sub>-GSH-PEG and Fe<sub>3</sub>O<sub>4</sub>-GSH-PEG-Tf showed additional peak at 1262 cm<sup>-1</sup> due to C=O stretch and resulted from the presence of PEG. The IR spectrum of Fe<sub>3</sub>O<sub>4</sub>-GSH-PEG-Tf showed new peak at 1542 cm<sup>-1</sup> confirming conjugation of Tf with Fe<sub>3</sub>O<sub>4</sub>-GSH-PEG.<sup>[17]</sup>

The flow-channel substrate was evaluated by analyzing the cross-section of the NMSFGC substrate (Figure 2, inset). The average thickness of the matrix (shown by the dotted red circle) was estimated to be  $\approx 11 \pm 1$   $\mu$ m from the TEM image. A few isolated aggregates with thickness  $\approx 34 \pm 1$   $\mu$ m were also present. The amount of matrix covering the flow-channel surface was estimated to be  $\approx 2.0 \pm 0.2$  mg. Furthermore, the matrix was found to cover 90% of the surface when evaluated using optical microscopy and ImageJ software (Figure 3). On the other hand, the density of Tf on the Tf-NMSFGC matrix was estimated to be  $\approx 285$  mg g<sup>-1</sup> by a modified Bradford procedure.

The performance of this integrated flow-channel glass substrate system was evaluated at first using TfR-positive HCT116



**Figure 3.** Optical microscopy image of microchannel system coated with Fe<sub>3</sub>O<sub>4</sub>-GSH-PEG-Tf matrix (2.0 mg).

cells. As shown in Figure 4, a 15 min incubation using the Tf-NMSFGC flow-channel system showed excellent cell-capture efficiency of >95% (Figure 5a). Two control experiments based on identical design features (1) without Fe<sub>3</sub>O<sub>4</sub>-GSH-PEG-Tf matrix on flow-channel device surface and (2) NMSFGC without Tf were also evaluated. As shown in Figure 5a, the flow-channel system without Fe<sub>3</sub>O<sub>4</sub>-GSH-PEG-Tf matrix and NMSFGC showed significantly less cell attachment of 5% and 52%, respectively. Thus, the (complete) Tf-NMSFGC flow-channel system showed  $\approx 19$  times and times higher cancer cell-capture efficiency as compared with flow-channel systems without Fe<sub>3</sub>O<sub>4</sub>-GSH-PEG-Tf matrix and NMSFGC without Tf, respectively. The results clearly confirm that the cancer cell-capture efficiency of the system without Fe<sub>3</sub>O<sub>4</sub>-GSH-PEG-Tf matrix was significantly less, suggesting that both Fe<sub>3</sub>O<sub>4</sub>-GSH-PEG matrix and Tf were crucial for enhanced performance. The capture efficiency of Tf-NMSFGC was further investigated with increasing order of cell concentrations of 25, 50, and 100 cells mL<sup>-1</sup> (Figure 5b). Tf-NMSFGC was found to

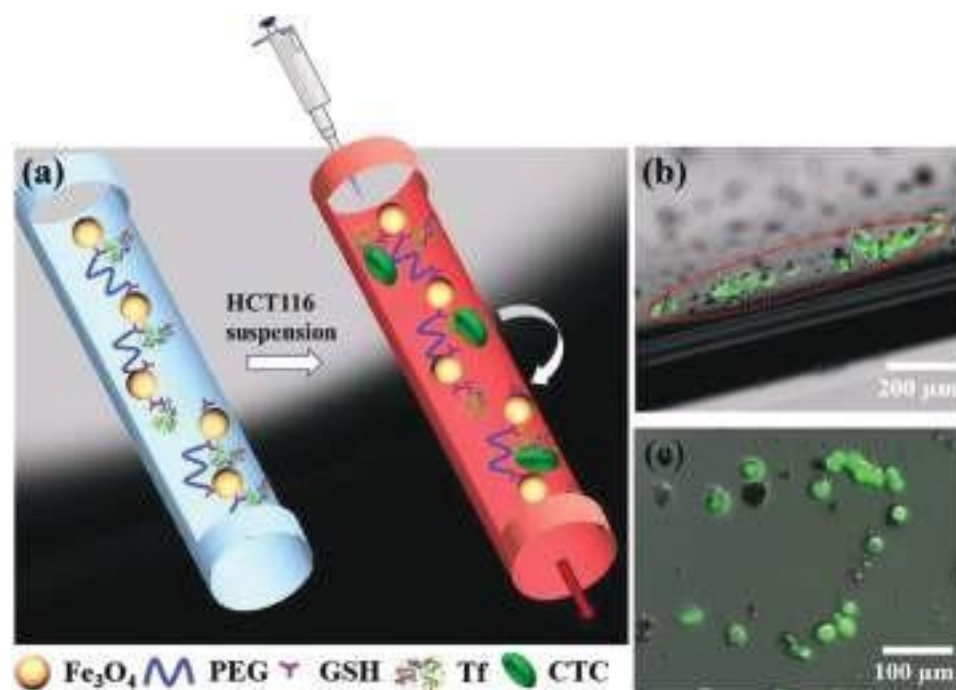


**Figure 4.** a) Schematic representation of HCT116 cells captured from cell medium on 3D Tf-NMSFGC microchannel system. b,c) Fluorescence images of HCT116 cells captured from cell medium on 3D Tf-NMSFGC microchannel system after 15 min incubation.



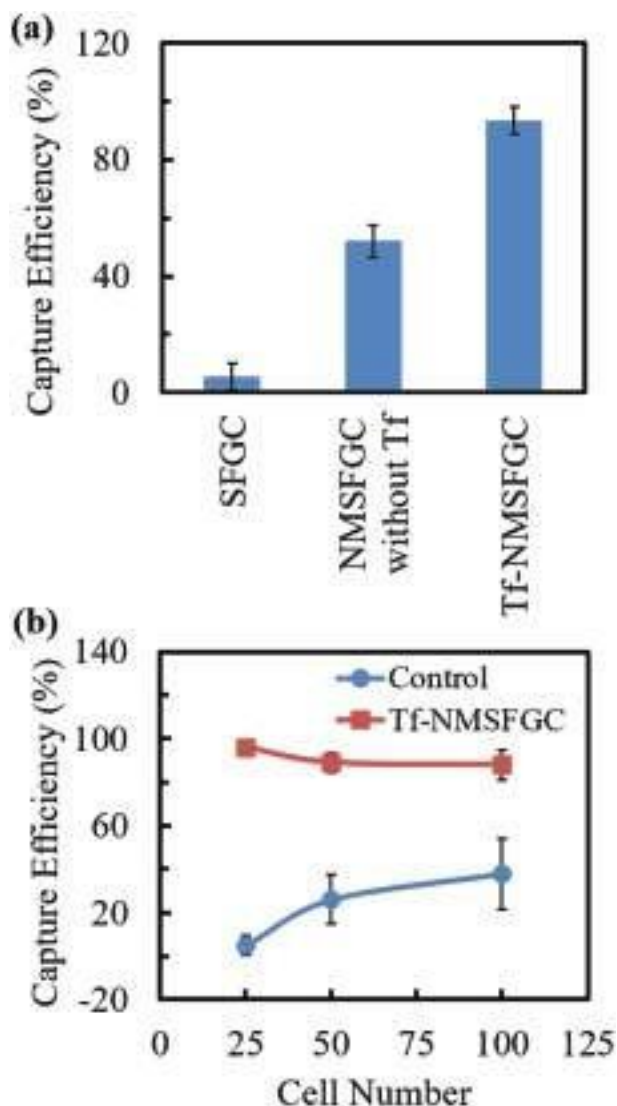


**Figure 5.** a) CTC capture efficiency of  $\text{Fe}_3\text{O}_4$ -GSH-PEG-Tf coated microchannel system in cell medium ( $n = 3$ ). b) CTC capture efficiency of  $\text{Fe}_3\text{O}_4$ -GSH-PEG-Tf and  $\text{Fe}_3\text{O}_4$ -GSH-PEG (control) coated microchannel system in cell medium having different cell concentration ( $n = 3$ ).

capture 96%, 89%, and 88% cells, respectively, demonstrating that the cell-capture efficiency showed a similar trend even at higher cell concentrations. Interestingly, the highest CTC efficiency was achieved with the lower number of cells (i.e., for 25 cells concentration  $\text{mL}^{-1}$ ). This might be due to the optimal cell number and the optimized available surface area in flow-channel substrate. Furthermore, it was found that the captured cells remained intact for  $\approx 24$  h and could be used for further studies (Figure 6).

To further investigate the influence of  $\text{Fe}_3\text{O}_4$ -GSH-PEG-Tf matrix on cell capture efficiency, the flow-channel system was functionalized with different amounts of matrix (0.7–2.0 mg per glass capillary) and then evaluated for capturing HCT116 cancer cells. The study showed that the cell capture efficiency increased with increasing amount of 3D matrix (Figure 7). The capture efficiency increased from 48% to 96% when the matrix

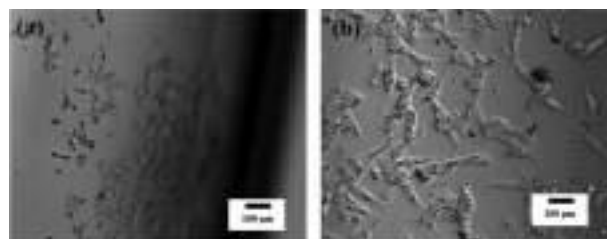


**Figure 6.** Images of HCT116 cells captured on Tf-NMSFGC microchannel system after 24 h. a) 10 $\times$  magnification and b) 20 $\times$  magnification.

amount increased from 0.7 to 2.0 mg. Thus, the flow-channel system with higher matrix amount (2.0 mg) showed two fold increase in capture efficiency for HCT116 cells as compared to the system with lower amount (0.7 mg). This difference further verified the contribution of the matrix in improving cell anchorage due to enhanced topographic interactions between the  $\text{Fe}_3\text{O}_4$ -GSH-PEG-Tf matrix and the surface of the cancer cells, leading to the enhanced cell capture.

Furthermore, capability of the flow-channel system to capture rare tumor cells was validated using bio-simulated CTC samples. The sample was prepared by spiking Green Fluorescent Protein (GFP) labeled HCT116 cells into whole (human) blood with concentrations of about 25 cells  $\text{mL}^{-1}$ . For comparison, capture efficiency was also evaluated in lysed blood spiked with similar concentrations of HCT116 cells. After 15 min incubation of the bio-simulated CTC sample in Tf-NMSFGC flow-channel system, HCT116 cells were found to be attached to the  $\text{Fe}_3\text{O}_4$ -GSH-PEG-Tf matrix as shown in Figure 8a–c. The 3D images of the flow-channel system incubated with spiked blood sample clearly revealed immobilization of the HCT116 cells on  $\text{Fe}_3\text{O}_4$ -GSH-PEG-Tf matrix, thus confirming the cell capture due to the presence of nanostructure-based matrix (Figure 8d). The CTC capture efficiency in Red Blood Cell (RBC) lysed blood was 92%, and in intact peripheral blood was 88% (Figure 8e), comparable to the capture efficiency in McCoy medium (96%). It can be observed that Tf-NMSFGC flow-channel system could efficiently capture HCT116 cells in all cases. The capture efficiencies were comparable and did not have significant differences regardless of whether the red blood cells were lysed or intact. These results clearly suggest that complex conditions had no significant effects on the cancer cell

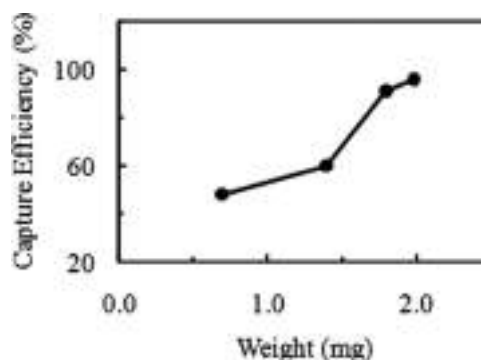


**Figure 7.** Effect of  $\text{Fe}_3\text{O}_4$ -GSH-PEG-Tf matrix concentration on cell capture efficiency from medium having 25 cells  $\text{mL}^{-1}$ .



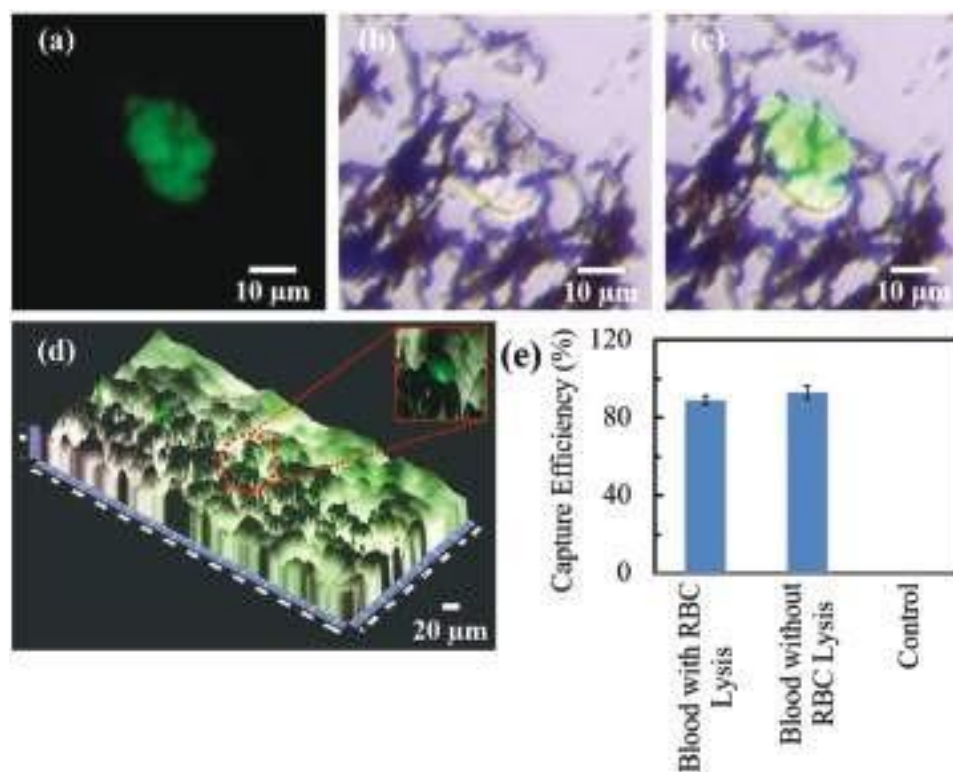


**Figure 8.** a–c) Bright field and fluorescent images of HCT116 cells captured from spiked blood on 3D Tf-NMSFGC microchannel system after 15 min incubation. d) Pseudo-3D image of CTCs captured on Fe<sub>3</sub>O<sub>4</sub>-GSH-PEG-Tf coated capillary. e) CTC capture efficiency of Fe<sub>3</sub>O<sub>4</sub>-GSH-PEG-Tf coated capillary in whole blood with RBC lysis, without RBC lysis, and in culture media ( $n = 3$ ).

capturing ability and Tf-NMSFGC flow-channel system can be directly used in whole blood.

After confirming that the Tf-NMSFGC flow-channel system with the matrix can rapidly and efficiently capture tumor cells, we translated the system to study clinical samples from three cancer patients' peripheral blood (including colon and breast cancer patients). As in control, blood was also processed from healthy individuals. Cells were identified as CTCs when stained positive for tumor markers cyokeratin (CK18) and DNA interacting probe (4,6-diamidino-2-phenylindole i.e. DAPI) and negative for leukocyte markers (CD45). The images of CTCs captured from clinical samples with our method from 0.1 mL of blood are shown in **Figure 9**. As shown in the image, CTCs exhibited strong CK staining and DAPI staining confirming intact nuclei in the captured cells. Conversely, no CTC was found in any healthy samples, suggesting that the Tf-NMSFGC flow-channel system can be successfully applied to real patient blood samples. We anticipate the capture of CTCs from cancer patients having anti-epithelial cell adhesion molecules (EpcAM). Further study in this direction with greater numbers of clinical samples is currently in progress. Our system exhibited excellent capacity in capturing CTCs as it offers flexibility of using 3D flow-channel system units in series for cancer cell capture, which is otherwise not easy to be captured from one cycle. A continuous microflow-system in controlling the feed and output using patient's sample is currently being designed and evaluated.

### 3. Conclusions

We developed a new-generation flow-channel system by synergistically incorporating Fe<sub>3</sub>O<sub>4</sub>-GSH-PEG-Tf nanostructured 3D matrix by chemical conjugation. This unique flow-channel system combines simple flow-channel system with a 3D nanostructured matrix to produce a synergistic effect of enhanced cell–substrate contact frequency as well as affinity. The resulting flow-channel system exhibited efficient and rapid (within 15 min) CTC-capturing ability in both cell medium and in spiked blood samples. Furthermore, the system was successfully employed for detecting cancer patient's clinical peripheral blood samples, endorsing their clinical potential in CTC studies. We envision that the novel flow-channel will open new opportunities for early diagnosis of cancer metastasis as well as recovery of other rare cells, proteins, DNA, and from biological specimens.

### 4. Experimental Section

**Reagents:** Bis-NHS-PEG, EDC-HCl, *N,N*-diisopropyl ethylamine (DIPEA), ferric chloride tetrahydrate, ferrous chloride hexahydrate, and transferrin (Tf) were purchased from Sigma-Aldrich (St. Louis, MO). GSH and *N*-hydroxysuccinimide (NHS) were procured from Sigma-Aldrich Chemical Co. (Germany). Milli-Q water, obtained from a Millipore water purification system (Merck Millipore, India), was used throughout the study. All chemicals were of the analytical grade and were used without further purification.

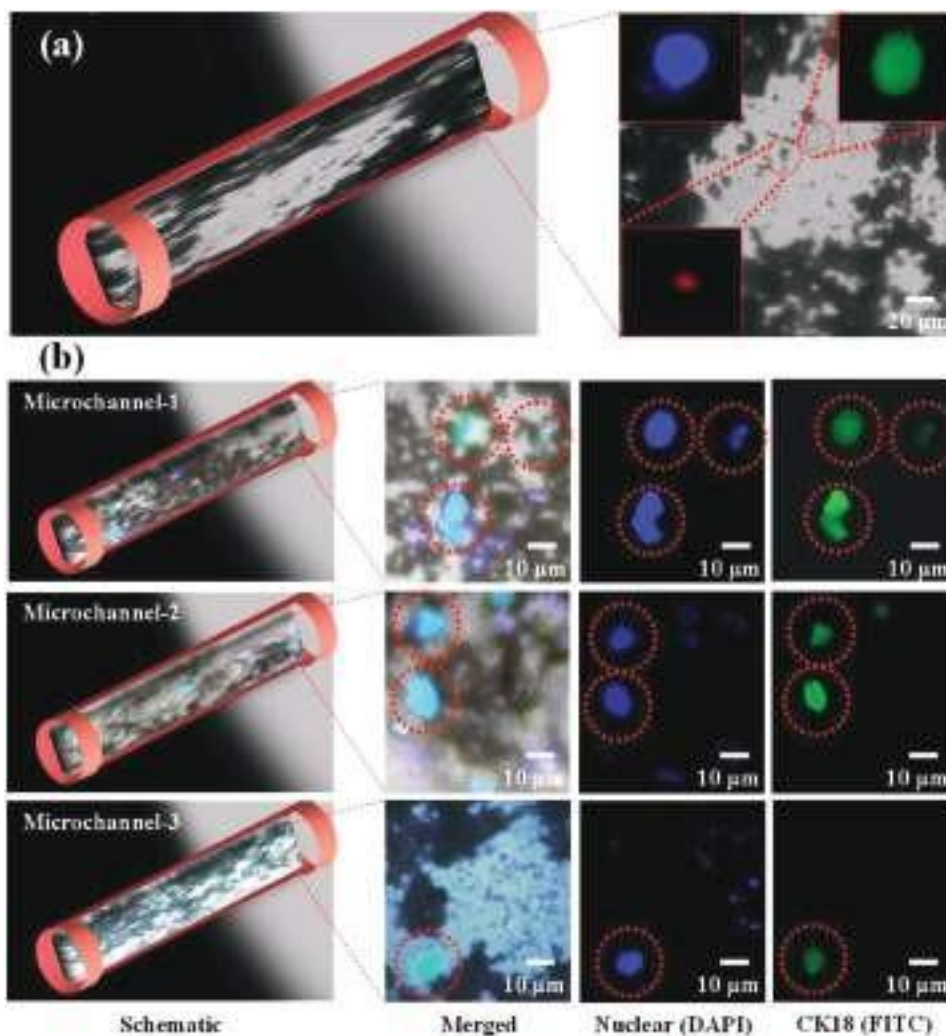


**Figure 9.** Bright field and fluorescent images of CTCs captured from blood samples of a colon cancer patient. a) Immunocytochemistry method based on Fluorescein Isothiocyanate-labeled anti-cytokeratin (green), PE-labeled anti-CD45 (red), and DAPI (blue) nuclear staining was applied to identify and enumerate CTCs on  $\text{Fe}_3\text{O}_4$ -GSH-PEG-Tf coated capillary. The fluorescence images were acquired in 3D capillary at different planar positions with highest intensity. b) Bright field and fluorescent merged images of CTCs captured on 3D microchannel system in series.

**Synthesis of  $\text{Fe}_3\text{O}_4$ -GSH Conjugate:**  $\text{Fe}_3\text{O}_4$  nanoparticles were synthesized by co-precipitation of  $\text{Fe}^{2+}$  and  $\text{Fe}^{3+}$  ions using ammonia base followed by hydrothermal ripening of nanoparticles.<sup>[21]</sup> For typical nanoparticle functionalization reaction, 500 mg of  $\text{Fe}_3\text{O}_4$  was dispersed in 15 mL Milli-Q water and 5 mL methanol by sonication for 15 min. 400 mg of GSH was dissolved in Milli-Q water and mixed with  $\text{Fe}_3\text{O}_4$  solution. The mixture was then re-sonicated for 2 h.  $\text{Fe}_3\text{O}_4$ -GSH was then isolated by magnetic separation, washed with repeated cycles of excess Milli-Q water, and dried under vacuum.

**Synthesis of  $\text{Fe}_3\text{O}_4$ -GSH-PEG Conjugate:** 120 mg of bis[2-(N-succinimidyl-succinylamino)ethyl]polyethylene glycol (Bis-NHS-PEG; 3 kDa) was dissolved in 6 mL of Milli-Q water and was allowed to react with 30 mg of  $\text{Fe}_3\text{O}_4$ -GSH in the presence of 100  $\mu\text{L}$  of 1000 ppm DIPEA at a final solution pH of 7.8. The reaction mixture was continuously stirred at room temperature for 24 h.  $\text{Fe}_3\text{O}_4$ -GSH-PEG was then isolated by magnetic separation, washed with repeated cycles of excess Milli-Q water, and dried under vacuum.

**Synthesis of Tf-PEG-GSH- $\text{Fe}_3\text{O}_4$ :** 40 mg of PEG-GSH- $\text{Fe}_3\text{O}_4$  was first gently stirred in the presence of  $200 \times 10^{-3}$  M EDC·HCl and  $200 \times 10^{-3}$  M NHS at pH ~6.0 for 15 min to activate the carboxyl groups at room temperature. Next, 10 mg of Tf was incubated with activated

PEG-GSH- $\text{Fe}_3\text{O}_4$  for 4 h at room temperature, then washed with Milli-Q water, and finally dried.

**Functionalization of Glass Capillary:** Commercially available glass capillaries were activated in hot (80–90 °C) piranha solution ( $\text{H}_2\text{O}_2$  (30%): $\text{H}_2\text{SO}_4$ ) (1:3) for 2 h. The treated glass capillaries were then rinsed thoroughly with Milli-Q water and dried under vacuum at room temperature. Silanization of the glass capillary surface was carried out by treating the glass with (3-aminopropyl) triethoxysilane in toluene (3% solution) at room temperature for 24 h. The glass substrates were rinsed with toluene and Milli-Q water, respectively, and the density of the amine groups on the silanized glass surface was estimated by a colorimetric assay reported by Noel et al.<sup>[22]</sup> Five different silanized substrates were measured to estimate the average density of amine groups on the silanized surfaces.

**Anchoring  $\text{Fe}_3\text{O}_4$ -GSH-PEG-Tf Matrix on Silane-Functionalized Glass Capillary:** First, the carboxyl group in the GSH linker of  $\text{Fe}_3\text{O}_4$ -GSH-PEG-Tf (10 mg) was activated in 3 mL solution of  $200 \times 10^{-3}$  M EDC·HCl and  $200 \times 10^{-3}$  M NHS with gentle shaking for 15 min. 10  $\mu\text{L}$  of  $\text{Fe}_3\text{O}_4$ -GSH-PEG-Tf solution was passed through the inert part of silanized glass capillary and the capillary was rolled for 2 min for uniform coating. This step was repeated twice and finally the film was

dried under vacuum at room temperature. The coated glass capillary (NMSFGC) was then repeatedly washed with Milli-Q water to remove any noncovalently attached material and again re-dried under vacuum at room temperature.

**Cell Culture and Patients:** HCT116 cells (ATCC) were cultured in McCoy's cell culture medium (Invitrogen) supplemented with 10% fetal calf serum (Invitrogen), 100 units penicillin (Invitrogen), and 100  $\mu\text{g mL}^{-1}$  streptomycin (Invitrogen) in 25  $\text{cm}^2$  flask. After incubation for 4 d at 37  $^{\circ}\text{C}$  and 5%  $\text{CO}_2$ , cells were trypsinized, stained with 1 $\times$  Trypan blue, and counted using Neubauer chamber. Blood from healthy volunteer was obtained by strictly following protocols and guidelines of the ethics committee. All cancer patient samples included in this study were collected at Manik Hospital and Research Center, Aurangabad, India with their informed consent. The Manik Hospital and Research Center ethics committee approved the study and consent forms. The conducted study strictly adhered to the approved protocols and the guidelines of the ethics committee.

**Capture of Cancer Cells in McCoy Medium:** Preliminary studies revealed that the optimal volume of the glass capillary to hold cell medium was 100  $\mu\text{L}$ . This optimal condition was employed in further studies for CTC capture and isolation from McCoy medium. 100  $\mu\text{L}$  of McCoy medium containing low concentration of HCT116 cells (25 cells  $\text{mL}^{-1}$ ) was introduced in Tf-NMSFGC using micropipette and then rolled inside the capillary for 5 min in order to initiate the interaction between the cells and  $\text{Fe}_3\text{O}_4$ -GSH-PEG-Tf. After 5 min the sample was collected from the capillary using micropipette and transferred to another Tf-NMSFGC and again rolled inside it for another 5 min. This procedure was repeated one more time. The sample was then collected in 96-well plates using micropipette. The capillaries were rinsed with PBS at least three times in order to remove unattached cells. The number of uncaptured cells was counted using the Zeiss Axio Observer A1 fluorescence microscope. Also, the capture efficiency in medium with different cell concentrations of  $\approx 25$ , 50, and 100 cells  $100 \mu\text{L}^{-1}$  was also evaluated.

**Capture of Cancer Cells from Cancer Cell-Spiked Blood Samples:** 25 dual fluorescent HCT116 cells were spiked in 100  $\mu\text{L}$  of blood from healthy person. Then the blood was lysed using RBC lysis buffer using 1:3 blood:RBC lysis buffer proportion. The sample was incubated at room temperature on rotator at 50 rpm for 5 min, followed by centrifugation at 2000 rpm for 3 min. The supernatant was discarded and pellet was re-suspended in 100  $\mu\text{L}$  PBS. This PBS was inserted in Tf-NMSFGC and rolled inside the capillary for 5 min in order to initiate the artificial CTC sample and  $\text{Fe}_3\text{O}_4$ -GSH-PEG-Tf interaction. After 5 min the sample was collected from the capillary using micropipette and transferred to another Tf-NMSFGC and rolled inside it for another 5 min. This procedure was repeated one more time. The sample was then collected in 96-well plates using micropipette followed by rinsing of the capillaries with PBS at least three times. The number of uncaptured cells was counted using the Zeiss Axio Observer A1 fluorescence microscope.

**Capture of CTC Cells from Clinical Colon Cancer Patient Sample:** Peripheral blood obtained from clinically advanced cancer patients (including colon and breast cancer patients) in the age group of 45–60 years was used for the experiment. 1 mL of the blood was lysed in 3 mL RBC lysis buffer at room temperature for 15 min on rotator at 50 rpm. The sample was centrifuged at 2000 rpm for 15 min at room temperature. The supernatant was discarded and pellet was resuspended in 500  $\mu\text{L}$  PBS. This was followed by fixation of the sample by incubating with 4% paraformaldehyde (500  $\mu\text{L}$ ) for 10 min on rotator at 50 rpm. The sample was then centrifuged at 2000 rpm for 15 min at room temperature. The supernatant was discarded and pellet was resuspended in 300  $\mu\text{L}$  PBS. Finally, the sample was stained with anitcytokeratin18 (Abcam) and anti CD45 antibodies (Santa Cruz Biotechnology) for 1 h at room temperature and DAPI (0.5  $\text{mg mL}^{-1}$ ) for 10 min at room temperature and visualized in 96-well plates under the fluorescence microscope (Zeiss Axio Observer A1 fluorescence microscope). After confirming that the stained/tested blood fraction contains cancer cell, the blood was inserted in the Tf-NMSFGC flow channel and rolled inside the capillary for 5 min in order to initiate the blood and  $\text{Fe}_3\text{O}_4$ -GSH-PEG-Tf interaction. After 5 min the sample

was collected from the capillary using micropipette and transferred to another Tf-NMSFGC and again rolled inside it for another 5 min. This procedure was repeated one more time. The blood sample was then collected in 96-well plates using micropipette. The capillaries were rinsed with PBS at least three times to get rid of unattached cells. The number of uncaptured cells was counted using the fluorescence microscope.

**Characterization:** TEM analysis was performed using a Philips (CM 200) TEM machine set at an accelerating voltage of 200 kV. Samples for TEM were prepared by placing a drop of the  $\text{Fe}_3\text{O}_4$ -GSH-PEG-Tf suspension in deionized water on a Formvar-covered copper grid and then evaporating the water at room temperature. Conjugation of protein (Tf) to  $\text{Fe}_3\text{O}_4$ -GSH-PEG was confirmed by a modified Bradford assay. Fluorescence imaging and counting of cells were performed using Zeiss Axio Observer A1 microscope (Carl Zeiss, Jena, Germany).

## Supporting Information

Supporting Information is available from the Wiley Online Library or from the author.

## Acknowledgements

The authors would like to acknowledge the financial support from the Biotechnology Ignition Grant (BIG), Biotechnology Industry Research Assistance Council (BIRAC), Department of Biotechnology (DBT). J.J.K. acknowledges nanobiotechnology research grant from the Department of Biotechnology and funds for improvement of science and technology infrastructure from the Department of Science and Technology (FIST-DST).

Received: September 29, 2016

Revised: November 15, 2016

Published online:

- [1] K. Pantel, R. H. Brakenhoff, B. Brandt, *Nat. Rev. Cancer* **2008**, *8*, 329.
- [2] S. S. Banerjee, A. Jalota-Badwar, S. D. Satavalekar, S. G. Bhansali, N. D. Aher, R. R. Mascarenhas, D. Paul, S. Sharma, J. J. Khandare, *Adv. Healthcare Mater.* **2013**, *2*, 800.
- [3] J. Kaiser, *Science* **2010**, *327*, 1074.
- [4] S. S. Banerjee, A. Jalota-Badwar, K. R. Zope, K. J. Todkar, R. R. Mascarenhas, G. P. Chate, G. V. Khutale, A. Bharde, M. Calderon, J. J. Khandare, *Nanoscale* **2015**, *7*, 8684.
- [5] K. Pantel, R. H. Brakenhoff, *Nat. Rev. Cancer* **2004**, *4*, 448.
- [6] A. H. Kuo, M. F. Clarke, *Nat. Biotechnol.* **2013**, *31*, 504.
- [7] C. A. Klein, *Science* **2008**, *321*, 1785.
- [8] S. Nagrath, L. V. Sequist, S. Maheswaran, D. W. Bell, D. Irimia, L. Utkus, M. R. Smith, E. L. Kwak, S. Digumarthy, A. Muzikansky, P. Ryan, U. J. Balis, R. G. Tompkins, D. A. Haber, M. Toner, *Nature* **2007**, *450*, 1235.
- [9] E. I. Galanza, E. V. Shashkov, T. Kelly, J. W. Kim, L. Yang, V. P. Zharov, *Nat. Nanotechnol.* **2009**, *4*, 855.
- [10] Q. Shen, L. Xu, L. Zhao, D. Wu, Y. Fan, Y. Zhou, W. H. OuYang, X. Xu, Z. Zhang, M. Song, T. Lee, M. A. Garcia, B. Xiong, S. Hou, H. R. Tseng, X. Fang, *Adv. Mater.* **2013**, *25*, 2368.
- [11] A. H. Talasaz, A. A. Powell, D. E. Huber, J. G. Berbee, K. H. Roh, W. Yu, W. Xiao, M. M. Davis, R. F. Pease, M. N. Mindrinos, S. S. Jeffrey, R. W. Davis, *Proc. Natl. Acad. Sci. USA* **2009**, *106*, 3970.
- [12] A. Adams, P. I. Okagbare, J. Feng, M. L. Hupert, D. Patterson, J. Gttert, R. L. McCarley, D. Nikitopoulos, M. C. Murphy, S. A. Soper, *J. Am. Chem. Soc.* **2008**, *130*, 8633.
- [13] S. Wang, K. Liu, J. Liu, Z. T. F. Yu, X. Xu, L. Zhao, T. Lee, E. K. Lee, J. Reiss, Y. K. Lee, L. W. K. Chung, J. Huang, M. Rettig, D. Seligson,



- K. N. Duraiswamy, C. K. F. Shen, H. R. Tseng, *Angew. Chem. Int. Ed.* **2011**, *50*, 3084.
- [14] S. Zheng, H. Lin, J. Q. Liu, M. Balic, R. Datar, R. J. Cote, Y. C. Tai, *J. Chromatogr. A* **2007**, *1162*, 154.
- [15] Z. A. Nima, M. Mahmood, Y. Xu, T. Mustafa, F. Watanabe, D. A. Nedosekin, M. A. Juratli, T. Fahmi, E. I. Galanzha, J. P. Nolan, A. G. Basnakian, V. P. Zharov, A. S. Biris, *Sci. Rep.* **2014**, *4*, 4752.
- [16] G. Vona, A. Sabile, M. Louha, V. Sitruk, S. Romana, K. Schutze, F. Capron, D. Franco, M. Pazzagli, M. Vekemans, B. Lacour, C. Brechot, P. Paterlini-Brechot, *Am. J. Pathol.* **2000**, *156*, 57.
- [17] S. S. Banerjee, D. Paul, S. G. Bhansali, N. D. Aher, A. Jalota-Badhwar, J. Khandare, *Small* **2012**, *8*, 1657.
- [18] E. Reátegui, N. Aceto, E. J. Lim, J. P. Sullivan, A. E. Jensen, M. Zeinali, J. M. Martel, A. J. Aranyosi, W. Li, S. Castleberry, A. Bardia, L. V. Sequist, D. A. Haber, S. Maheswaran, P. T. Hammond, M. Toner, S. L. Stott, *Adv. Mater.* **2015**, *27*, 1593.
- [19] J. S. Miller, K. R. Stevens, M. T. Yang, B. M. Baker, D. H. T. Nguyen, D. M. Cohen, E. Toro, A. A. Chen, P. A. Galie, X. Yu, R. Chaturvedi, S. N. Bhatia, C. S. Chen, *Nat. Mater.* **2012**, *11*, 768.
- [20] G. Yang, Y. Cao, J. Fan, H. Liu, F. Zhang, P. Zhang, C. Huang, L. Jiang, S. Wang, *Angew. Chem., Int. Ed.* **2014**, *53*, 2915.
- [21] S. S. Banerjee, D. H. Chen, *Chem. Mater.* **2007**, *19*, 6345.
- [22] S. Noel, B. Liberelle, L. Robitaille, G. De Crescenzo, *Bioconjugate Chem.* **2011**, *22*, 1690.



## ORIGINAL ARTICLE

Year : 2017 | Volume : 10 | Issue : 1 | Page : 129-133

Epidemiological study of hardiness profile of blind people

[Sanjeev Vasantao Chincholikar](#)

Professor, Community Medicine, MIMER Medical College, Talegaon Dabhade, Pune, Maharashtra, India

Click [here](#) for **correspondence address** and email

Date of Web Publication                      5-May-2017



### Abstract

**Objective:** To study the risk factors in psychosocial profile of blind people undergoing vocational training. using a screening test ,Personality based hardiness index and suggest recommendations if any. **Study design:** Cross sectional study. **Participants:** Blind people. **Study Variables:** Sex, socioeconomic status, literacy, psychiatric morbidity. **Statistical analysis:** Fishers Exact test,  $\chi^2$  test. **Results:** Recently introduced technique of Personality based hardiness index was tested for its utility for screening of blind persons to detect possible psychological maladjustments and hardiness. Analysis of results of Personality based hardiness index revealed that 9% subjects were non hardy. Most of the non hardy subjects were

1. males 13% as compared to females 3%
2. belonging to lower socioeconomic class (100%)
3. illiterates 34.3% as compared to literates 2%
4. residing in rural area (12.7%) as compared to person in urban area (0%)

The overall results of the above detailed tests brought some salient risk factors that can be strongly associated with psychosocial maladjustments and hardiness in the handicapped persons. These risk factors are Lower socioeconomic class, Rural residence, Illiteracy, Sex These risk factors that emerged out of the statistical analysis of the data can be immensely useful in the planning stages of rehabilitation.

**Keywords:** Literacy, socioeconomic class, personality based hardiness index, rural area, males

**How to cite this article:**

Chincholikar SV. Epidemiological study of hardiness profile of blind people. Ann Trop Med Public Health 2017;10:129-33

**How to cite this URL:**

Chincholikar SV. Epidemiological study of hardiness profile of blind people. Ann Trop Med Public Health [serial online] 2017 [cited 2018 Oct 18];10:129-33. Available from: <http://www.atmph.org/text.asp?2017/10/1/129/196522>

Introduction 

The psychiatric research for decades was confined to mental hospitals and psychiatric clinics, and was characterized by lengthy interviews, case records, and case studies. The application of public health principles to mental disorders was tried only recently, with the aim of expanding the mental health research beyond the mental health hospital and the psychiatric clinics. It is at stage of implementation in field that the difficulties in practicing these scientific principles are experienced. Resource crunch, in respect of technical manpower, poses the main hurdle among other things, especially in a developing country like India. It is generally agreed that psychological aspects are the common victims of these circumstances. A very substantial lack of manpower trained in psychology, psychiatry, social sciences, and related fields has been the real hurdle in this respect.<sup>[1]</sup>

The Personality based hardiness index is the measurable personality characteristics and dynamics of those who appear immune to the development of stress related disorders, and comprises a variable personality based hardiness index .The notion of hardiness is derived from existential theories of psychology, which states that individuals require meaning and commitment in their life to become fulfilled and psychologically healthy. In the Intrinsic Indies existential theories, the three factors, which are considered to be important for the actualization for the fulfillment of an individual, are : commitment, control, and challenge.

**Commitment:** The ability to believe in the truth, importance, and interest value of when is and what one is doing, and thereby the tendency to fully involve oneself in many situations of life including work, family, interpersonal relationship, and social institutions. It is also described as the tendency to be curious about and involve oneself in whatever is happening rather than avoid doing vigorous interaction with the environment.

**Control:** The tendency to believe and act as if one can influence the course of events rather than feeling like the passive victim of circumstances. The persons high in control seek explanation for why something is happening not with respect to others' action or fate but rather with an emphasis on their own responsibility.

**Challenge:** The belief that the change rather than stability is the normative mode of life. From a challenge's perspective , much of the disruption associated with the occurrence of a stressful life events can be anticipated as an opportunity and incentive for personal growth rather than a simple threat to security. The challenge leads a person to be a catalyst in the environment, and

to practice responding to the unexpected events. Also, they are characterized by openness and tolerance for ambiguity. This characteristic allows an individual, high on the factors, to integrate and effectively appraise the threat even in the most unexpected stressful life events. In effect, these individuals expect the unexpected. They are not thrown off guard by an anticipated turn of events.

The person high on hardiness places stressful events in a broad perspective, where they are less threatening, and also actively engages in transforming the situation at hand. Though he may be under more strain for a short period of time, yet he will be relieved of the stresses in the end. In contrast, those low on hardiness are believed to be more likely to not see the forest for the trees, and hence, be more easily overwhelmed and reluctant to interact with the change in the world around them.

Those doing research on hardiness as a factor in development of physical and psychological symptoms are clear to point out that the personality factors are not the only variables in stress illness equation. Life events, social support, physiological predispositions, and health habits also play a major role in the likelihood of developing an illness.

For this study, the third generation hardiness test has been used. This latest version of the hardiness test consists of 50 rating scale items that can be completed in a few minutes. The test has been carefully constructed both conceptually and empirically.

Therefore, the present study was carried out in two institutions, which have been carrying out vocational rehabilitation of blind persons for a long time. The research was undertaken with a view to study the risk factors in the hardiness profile of blind people utilizing the above-mentioned personality based hardiness index technique and then suggest recommendations if any.

## Objectives

1. To study the risk factors in the hardiness profile of blind people using the above-mentioned psychological screening technique.
2. To suggest some recommendations to those undergoing vocational training if any.

## Material and Methods

The study was conducted in two institutions from January 1992 to January 1993.

- Technical Training Institute of Blind Men, Poona Blind Men's Association situated in Hadpasar.

- The Poona School and Home for the blind girls situated near Kothrud.

The respective authorities of above institutions admit blind subjects having inability to count fingers at a distance of 6 meters as certified by Civil Surgeon of the concerned district.

The permission was obtained from respective authorities of above two institutions for conducting this study.

All the blinds enrolled in above two institutions at the time of the study were included.

The information regarding the types of questions was given to all blinds included in the study, and the answers were obtained by interview technique.

For the present study, the personality hardiness index followed by Kobasa and Maddi<sup>[1],[2],[3]</sup> was used. The index consisted of 50 scale rating items.

For the present study, 47 of these 50 items were selected, as 3 of them were deemed by consulting psychiatrist to be ambiguous. The 47 selected item consisted of 14 positive and 33 negative statements. Each statement was read and explained to the subject to elicit answers. All subjects above the age of 14 years were considered for hardiness test as recommended by Kobasa and Maddi.

For the 14 positive statements scoring was done as follows:

For the choice, score 0 was given because of complete disagreement with a correct statement. For choice,<sup>[1]</sup> score 1 and for choice,<sup>[2]</sup> scores 2 were given, respectively. For choice,<sup>[3]</sup> the subject was given score 3 because of complete agreement with a correct statement.

The scoring system was exactly reverse for the 33 negative statements therefore, response 0 got score 3, and response 3 got score 0. At the end, the scores obtained by a given subject for all 47 statements were totaled. A subject scoring equal to or more than 50% of the maximum possible score, that is  $47 \times 3 = 141$ , was classified as hardy, which means well-equipped to cope up with psychological stresses. While the one whose score was less than 50% was labeled as non hardy.

The experience for scientific utilization of personality hardiness was obtained by working in the psychiatry department under the guidance of qualified psychiatrist. The Personality based hardiness index was used in the present study for screening of blind subjects to study the risk factors in the psychosocial profile of blind people.

## Results and Discussion

The Hardiness score was calculated among blind subjects, and subjects were classified as hardy



and non hardy. It can be observed from [Table 1] that 8.88% of study subjects were non hardy. This would mean, that 8.88% of study subjects were ill-equipped to cope up with the stressful conditions of life, and were more prone to develop psychological maladjustments. These subjects would need intervention in the form of psychological counseling for improving their hardiness for a successful psychological rehabilitation.

HARDINESS STATUS	NUMBER	PERCENTAGE
NON HARDY	15	8.88
HARDY	154	91.12
<b>TOTAL</b>	<b>169</b>	<b>100.00</b>

Table 1: Personality Based Hardiness Status Amongblind Subjects

[Click here to view](#)

When hardiness results were co-related with the sex of the subjects by using the test of significance, as observed from [Table 2], there was, statistically, a significant difference between the two at 95% confidence limit.

Hardiness status	MALE	FEMALE	TOTAL
Non hardy	13	2	15
hardy	85	69	154
<b>TOTAL</b>	<b>98</b>	<b>71</b>	<b>169</b>

Table 2: Hardiness Results According To Sex

[Click here to view](#)

$$\chi^2=4.35, D.F.=1, P<0.05$$

It would appear that males are relatively less hardy than females. The observed difference in the hardiness in both the sexes could perhaps be due to the difference in levels of exposure to socioeconomic stresses and frustrations outside the protection of the home.

Ray in 1962<sup>[4]</sup> and Sethe in 1977<sup>[5]</sup> observed higher percentage of male population registered at psychiatric facilities in India.

Rudolf Pinter *et al*<sup>[6]</sup> in their study of deaf observed that men were more neurotic and introvert than women.

Springer and Rosler<sup>[7]</sup> in their study of deaf observed that deaf boys were more neurotic than girls.

It can be observed from [Table 3] that there was, statistically, a significant difference between the two groups at 95% confidence limit.

Hardiness status	RESIDENCE		TOTAL
	URBAN	RURAL	
Non hardy	0	15	15
hardy	51	103	154
<b>TOTAL</b>	<b>51</b>	<b>118</b>	<b>169</b>

Table 3: Hardiness Results As Per Urban And Rural Residence

[Click here to view](#)

Applying Fishers exact test P=0.003424

This would mean that blind subjects in rural area were more prone to get psychological

maladjustments than their urban counterparts.

All 51 urban dwellers showed presence of hardiness.

This would mean that blind subjects in rural area need more careful attention especially in the area of psychological counseling for ensuring better results of rehabilitation process. The mental morbidity revealed in various rural surveys among general population varies from 18.24 per thousand to 102.8 per thousand. The mental morbidity revealed in various urban surveys among general population, varies from 0 per thousand to 38 per thousand.<sup>[8],[9]</sup>

[Table 4] shows the hardiness results as per socioeconomic status. None of the subjects from class II and class III showed non hardiness. Owing to unacceptably small values in some of the cells of the table, which would undermine the utility of  $\chi^2$  test, the data for class II, class III (upper and lower middle class), class IV, and class V were pooled for statistical analysis.

Hardiness status	SOCIOECONOMIC CLASS					TOTAL
	I	II	III	IV	V	
Non hardy	0	0	0	02	13	15
hardy	0	11	37	71	35	154
TOTAL	0	11	37	73	48	169

Table 4: Hardiness Results as Per Socioeconomic Status

[Click here to view](#)

When hardiness results were co-related with socioeconomic status of the subjects by using the test of significance, as observed from the table, there was, statistically, a significant difference between the two at 95% confidence limit.

$$\chi^2=4.964, D.F.=1, P<0.05$$

It appears that hardiness of an individual varies according to socio-economic status, as none of the blind subjects in class II and class III were non hardy, and 27.08% of those in class V showed non hardiness.

It would mean that as socio-economic status become better, hardiness increases, that is, the subjects belonging to lower socio-economic classes may have more risk of getting psychiatric maladjustments than those in the higher classes. This confirms that socio-economic status is one of the important factors in deciding the probable psychological maladjustment among blind subjects.

It is a known fact that even in case of persons without any disabilities, the adverse socio-cultural factors present in the lower socio-economic classes make the subjects more vulnerable to psychiatric morbidities. Blindness or other handicaps further complicate the picture.

Several studies made in different parts of world have shown that lower socio-economic classes have a higher rate of mental disorders.

B. Sen. *et al.*<sup>[10]</sup> in their study observed that more than half of the families of social class V had psychiatric morbidity.

Tanksale<sup>[11]</sup> in her study of blind observed a significant relationship between better self-

adjustment and higher socio-economic class.

When hardiness were correlated with literacy of blind subjects, it was observed from the table that there was, statistically, a significant difference between hardiness results in the 2 groups at 95% confidence limits (applying fisher's exact test,  $P=9.271 \times 10^{-8}$ ). It appears that non hardiness was more in Illiterate as compared to Literates as [Table 5] reveals that only 2.19% of Literates were non hardy.

Hardiness status	LITERATE	ILLITERATE	TOTAL
Non hardy	3	12	15
hardy	134	20	154
TOTAL	137	32	169

Table 5: Literacy And Hardiness Results

[Click here to view](#)

This would mean that literacy is one of the crucial risk factors that decide the occurrence of psychological maladjustment. Thus, while planning rehabilitation process, more efforts will be needed to provide Illiterate blind subjects more facilities for education that will help them avoid psychological disturbances.

Prajakta Tanksale<sup>[11]</sup> in her study observed high association between education of blind subjects and adjustment of blind persons.

The overall results of the above detailed tests brought some salient risk factors that can be strongly associated with psychosocial maladjustments and psychiatric morbidities in the handicapped persons.

These risk factors are:

1. Male sex
2. Lower socioeconomic class
3. Rural residence
4. Illiteracy

These risk factors that emerged out of the statistical analysis of the data can be immensely useful in the planning of stages of rehabilitation. Hence, they can be integrated in the planning stages of rehabilitation of blind persons.

### ***Financial support and sponsorship***

Nil.

### ***Conflicts of interest***

There are no conflicts of interest.

## References

1. Kobasa SC. Stressful life events, personality and health, an enquiry into hardiness. Journal of personality and social psychology 1979;37:1-11. †  
[\[PUBMED\]](#)
2. Kobasa SC, Maddi SR. Existential personality theory in R Corsini (ed), current personality theory itasca, 1977. †
3. Maddi SR, Kobasa SC, Kahn S. Hardiness and health: A prospective study. Journal of personality and social psychology 1982;42:168-77. †  
[\[PUBMED\]](#)
4. Dattas Ray. Social stratification of mental patients. Indian J Psychiatry 1962;4:3. †
5. Sethi BB, Manchanda R. Social factors and mental illness, an analysis of first admission to a psychiatric hospital. The International journal of social psychiatry 1980;26:200-7. †
6. Pinter R, Eisenson R, Stranton M. The psychology of the physically handicapped. Newyork Appleton Centry Crofts, INC. †
7. Springer NN, Rosler. A comparative study of deaf and hearing children. Jeducatioal psychology 1938;29:459-66. †
8. Surya Mental morbidity in Pondicherry. All India Institute of Mental Health 1964;9:56. †
9. Nandi DN, Ajmary S, Ganhuli H, Banerjee G, Boral GC, Ghosh A. Sarkars The incidence of mental disorders in one year in a rural community in west Bengal. Ind j psychiatry 1976;18:79. †
10. Sen B, Nandi DN, Mukherjee SP, Mishra DC, Banerjee G, Sarkar S. Psychiatric morbidity in an urban slum dwelling community. Indian journal of psychiatry 1984;28:p185-93. †
11. Prajakta Tanksale. The problem of social adjustment and rehabilitation of the blind A dissertation submitted to Nagpur University Nagpur for Degree of Doctor of philosophy, in the faculty of social sciences April 1988. 22-35. †



### Correspondence Address:

Dr. Sanjeev Vasantrya Chincholikar  
Professor, Community Medicine, MIMER Medical College, Talegaon Dabhade, Pune,  
Maharashtra  
India

 Login to access the email ID



**Source of Support:** None, **Conflict of Interest:** None



Check

**DOI:** 10.4103/1755-6783.196522



Tables

[\[Table 1\]](#), [\[Table 2\]](#), [\[Table 3\]](#), [\[Table 4\]](#), [\[Table 5\]](#)



## Pattern of Gastric Cancer at Tertiary Rural Hospital in Central India - 10 Year Retrospective Study

<b>* Dr. Tushar Khachane</b>	Asst. Professor Dept. of Surgery MIMER Medical College Talegaon Dabhade Pune, * Corresponding Author.
<b>Dr. Sangram Karandikar</b>	Asso. Professor, Dept. of Gen. Surgery, Terna Medical College, Nerul, Navi Mumbai
<b>Dr. Siddharth Rao</b>	Asso. Professor, Dept. of Gen. Surgery, MGIMS, Sewagram

**ABSTRACT**

Cancer of gastrointestinal tract is one of the most common causes of cancer related deaths in India. The present research carried out at a tertiary rural hospital in Central India was aimed to study the clinical profile of gastric cancers in this region. 147 cases of primary malignant tumors of stomach treated during a 10 year interval between July 1994 to June 2004 were studied retrospectively and data analyzed using standard methods.

The incidence of cancer was highest in 6th and 7th decade with male preponderance. All cases of stomach cancer were in advanced stage underlining the need for early diagnosis and a favorable outcome.

<b>KEYWORDS</b>	Cancer, Gastric
-----------------	-----------------

**Introduction:**

Cancer is emerging as a major problem globally both in more developed and in less developed countries (1). The incidence of most digestive cancers in India are moderate or low (2). But cancer of gastrointestinal tract is one of the most common causes of cancer related deaths in India (3). Differences in the regional distribution of cancer and its outcome as documented by a worldwide network of population based cancer registries help to identify causative and risk factors influencing survival.

Attempts were made to study the pattern of gastric cancers presented during ten years from July 1994 to June 2004 at Kasturba hospital attached to Mahatma Gandhi Institute of Medical Sciences, Sewagram, Wardha. The clinicopathological aspects were critically analyzed in the study.

**Aims and Objectives :**

- 1) To study the demographic variables in gastric cancers.
- 2) To study the pattern of clinical presentation of gastric cancers.
- 3) To study the extent of disease at presentation in gastric cancer.

**Materials and Methods :**

The present study was carried out at Kasturba Hospital attached to MGIMS, Sewagram. A total of 147 cases of primary malignant tumours of stomach seen and treated during 10 year interval between July 1994 to June 2004 were studied retrospectively from the case records. The parameters studied included : Age, Sex, duration of symptoms, nature of symptoms and signs and pathological features.

The tumours were staged according to the extent of the disease i.e. local, locoregional and distant. The information was recorded in a specially designed proforma and data later analyzed using standard statistical methods.

**Observations :**

**Table 1 : Age distribution by sex for patients with stomach cancer from year 1994 - 2004**

Age (Years)	No.	Percentage	Male	Female	Ratio (M : F)
10 – 19	0	0	0	0	
20 – 29	5	3.4	3	2	
30 – 39	18	12.2	11	7	
40 – 49	34	23.2	26	8	
50 – 59	35	23.8	22	13	2.5 : 1
60 – 69	38	25.2	29	9	
70 – 79	15	10.3	13	2	
80 – 89	2	1.3	1	1	
Total	147	100	105	42	

10 – 19	0	0	0	0	2.5 : 1
20 – 29	5	3.4	3	2	
30 – 39	18	12.2	11	7	
40 – 49	34	23.2	26	8	
50 – 59	35	23.8	22	13	
60 – 69	38	25.2	29	9	
70 – 79	15	10.3	13	2	
80 – 89	2	1.3	1	1	
Total	147	100	105	42	

The age range was seen to have spanned from 3<sup>rd</sup> to 9<sup>th</sup> decade. The peak incidence was seen in 6<sup>th</sup> and 7<sup>th</sup> decade. 105 males had cancer of stomach as compared to 42 females resulting in Male : Female ratio of 2.5 : 1.

The mean age of presentation in cancer of stomach was 52.5 years.

**Table 2 : Profile of symptomatology in Stomach Cancer**

Symptoms	No. of Patients	Percentage
Weight loss	120	81.6
Abdomen Pain	110	74.8
Nausea	91	61.9
Vomiting	88	51.8
Anorexia	135	91.8
Mass	44	29.9
Dysphagia	16	10.8
Malaena	32	21.7

The commonest symptom was anorexia (91.8 %), closely followed by weight loss (81.6 %) Abdominal pain, nausea and vomiting were also present in majority of patients 74.8 %, 61.9 % and 59.8 % respectively. 5 patients with stomach cancer had an acute presentation. Of these 2 patients presented with haematemesis, 2 patients with perforation peritonitis and 1 patient with acute obstructive symptoms.

**Table 3 : Profile of objective signs in stomach cancer.**

Signs	No. of Patients	Percentage
Pallor	116	78.9
Palpable mass	44	29.9
Visible peristalsis	12	28.1

Succusion splash	8	20
Troiser's sign	9	6.1
Jaundice	2	1.3
Blumershelf	2	1.3
Ascites	15	10.2

Pallor was found in 78.9 % and was the commonest sign. Ascites (10.2 %) was the commonest sign of distant metastasis.

The mean duration of time interval between onset of symptoms was 6.7 months (range 1-36 months)

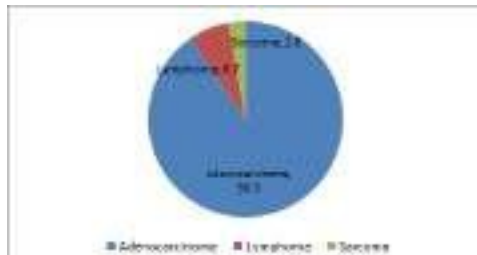
**Table 4 : Distribution of stomach cancer by anatomic site**

Site	No. of Patients	Percentage
Proximal 1/3 rd	13	8.8
Middle 1/3 rd	61	41.8
Distal 1/3 rd	73	49.8

Stomach cancer was commonest in distal third (49.8 %) and least common in proximal third (8.8 %)

**Table 5 : Histological types in stomach cancer**

Type	No. of Patients	Percentage
Adenocarcinoma	76	90.5
Mucin secreting	15	
Signet ring cell	5	
Lymphoma	7	6.7
Sarcoma	3	2.8



Adenocarcinoma was the commonest histological type. 27 % cases of adenocarcinoma had well differentiated histology. The remaining cases were either moderately differentiated (43.8 %) or poorly differentiated (29.2 %)

**Table 6 : Staging of cancer stomach according to extent of the disease.**

Stage	No. of Patients	Percentage
Local	0	0
Locoregional	45	30.7
Distant	102	69.3

Out of total 147 patients with cancer of stomach, 69.7 % patients had distant spread of the disease while 30.7 % had locoregional extent. No patient had a stomach cancer confined to organ only.

**Discussion :**

The incidence rates of gastric cancers in India are moderate or low but there is no room for complacency because most of them are currently diagnosed in a stage well beyond cure. The study of pattern of gastric cancers, a retrospective review of 10 years was carried out at Kasturba Hospital, Sewagram. The hospital caters predominantly to rural population.

The rural urban ratio of patients attending the hospital is 3 : 1.

The information was analysed with regard to age, sex, length of history, presenting symptom and sign and pathological type. The tumors were staged according to the extent of the disease i.e. local, locoregional and distant.

The study indicates a peak age incidence in 6<sup>th</sup> and 7<sup>th</sup> decade. MOA Malik et al (4) reported similar peak age incidence while K.

L Luna Devi (5) reported peak age incidence in 5<sup>th</sup> and 6<sup>th</sup> decade. The mean age of cancer of stomach was found to be 52.5 years. J. Beuten et. al (6) reported mean age at presentation as 65 years. While Laurence SB (7) reported it to the 62 years.

The male female ratio of malignant tumor of stomach in the present study was 2.5 : 1. Diehl et al (8) observed it as 2.1 : 1 and H. Goldsmith (9) in his review also reported the same. In the present study it was found that the distal 3<sup>rd</sup> was the commonest site involved (59.8 %) followed by 31.4 % in middle third. The proximal 3<sup>rd</sup> was involved in 8.8 % cases only. In an epidemiological survey conducted by Tata Memorial Hospital (10) it was reported that prox. third was involved in 23.5 %. while distal 3<sup>rd</sup> and middle 3<sup>rd</sup> were involved in 43.8 % and 18.7 % respectively.

Dinshaw A (11) and B. R. Prabhakar et al (12) reported 95 % incidence of adeno concinoma of stomach. In the present study 90.5 % patients with cancer of stomach had adenocarcinoma.

The clinical features of Ca stomach were analysed in the present study.

**Table 7 : Symptomatology profile of Ca stomach.**

Presenting symptom	H. Goldsmith (9) 1970	H. Wanebo (13) 1993	Diehl et al (8) 1983	Present Study (2004)
1) Weight loss	52.1	61.6	88	81.6
2) Abdominal Pain	48.1	51.6	90	74.8
3) Anouxia	21.1	32	-	91.8
4) Nausea	3.7	34.3	-	61.9
5) Malaena	-	20.2	3	21.7
6) Mass	33.3	-	10	29.9
7) Vomiting	20.7	-	7	59.8

**Conclusion :**

The peak age incidence of cancer of stomach was in 6<sup>th</sup> and 7<sup>th</sup> decade with males outnumbering females 2.5 : 1. Loss of appetite was the commonest symptom with pallor being the commonest sign. The distal 3<sup>rd</sup> of stomach was the commonest site and histologically adenocarcinoma was the most common. All case of stomach cancer were in advanced stage. Early diagnosis is essential for a favourable outcome of treatment. Health education of patients along with efforts by medical fraternity is the need of the hour.

**REFERENCES**

- 1) Stewart BW and Kleihues P (Eds) 2003 : World Cancer Report IARC Press, Lyon
- 2) KN Mohandas, P. Jagannath. Epidemiology of digestive cancer in India. Indian J. Gastroenterology, 2000 : 19 : 74 – 78.
- 3) Geeta Malkan, KM Mohandas, Epidemiology of digestive cancer in India. Indian J. Gastroenterology 1997 : 16 : 98.
- 4) MOA Malik, ZA Zakial, Div., SHEL Mashi Cancer of the alimentary tract in Sudan, Cancer 1976 37 : 2533:2542
- 5) K. R. Leena Devi, N. Suvarna, Pattern of Gastrointestinal Tumours in North Kerala, Indian Journal of Cancer 1980 : 17 : 159 – 160.
- 6) J. Benton Dupont, J. Filleus Lec George R. Burton, Isidore Cohn Adenocarcinoma of the Stomach. Review of 1497 cases. Cancer 1978; 41 : 941 – 947.
- 7) Lawrence S. Bizer, Adenocarcinoma of the Stomach : Cancer, 1983 : 51 : 743 – 745.
- 8) James T. Diehl, Robert E. Hermann, Auram M. Cooperman, Stanly O. Hoerr, Gastric Carcinoma, Annals of Surgery July 1982; 198 : 9-12
- 9) Harry S. Goldsmith, Bimal C. Ghosh, Carcinoma of the stomach, The American Journal of Surgery 1970 : 120 : 317 – 319.
- 10) K. M. Mohandas, Aabha Nagral, Epidemiology of digestive tract cancers in India Stomach and gastrointestinal lymphomas. Indian Journal of Gastroenterology 1998 : 17 : 24-27.
- 11) Dinshaw KA, Rao DN, Shroff PD, Hospital Cancer registry : Annual Report 1994. Mumbai : Tata Memorial Hospital 1997.
- 12) B. R. Prabhakar, B. S. Tang, Asha Sood, Gastrointestinal, Malignant tumours in Amritsar. Indian Journal of Surgery April 1981, 343 – 346.
- 13) Harold J. Wanebo, B. J. Kennedy, Joan Chmiel, Glen Steele, David Winchester and Robert Osteen Annals of Surgery Nov. 1993, 218 (5) : 583 – 592.
- 14) N. Ananth Krishnan, P. Jagannath, Satya Prakash, R.B. Mehta, Indian Journal of Surgery. 1981. Oct – Nov 779 – 784.



Contents lists available at ScienceDirect

Journal of Environmental Management

Journal homepage: [www.elsevier.com/locate/jenvman](http://www.elsevier.com/locate/jenvman)

23

Review

## Budding trends in integrated pest management using advanced micro- and nano-materials: Challenges and perspectives

Neha Khandelwal<sup>a</sup>, Ranjit S. Barbole<sup>b</sup>, Shashwat S. Banerjee<sup>c</sup>, Govind P. Chate<sup>b</sup>,  
Ankush V. Biradar<sup>d</sup>, Jayant J. Khandare<sup>b, e, \*\*</sup>, Asbok P. Giri<sup>a, \*</sup>

<sup>a</sup> Nano Molecular Biology, Biochemical Sciences Division, CSIR-National Chemical Laboratory, Pune-411008, Maharashtra, India

<sup>b</sup> Maharashtra Institute of Medical Education and Research (MIMER) Medical College, Solapur District, Dist. Pune-413007, India

<sup>c</sup> Organic Material and Catalysis Division, CSIR-Central Salt and Mercuric Chemical Research Institute, Bhawanagar-364002, Gujarat, India

<sup>d</sup> Maharashtra Institute of Pharmacy, MIT Campus, Pune-411008, Maharashtra, India

### ARTICLE INFO

#### Article history:

Received 5 July 2016

Received in revised form

15 September 2016

Accepted 21 September 2016

Available online xxx

#### Keywords:

Nanobiotechnology

Pest management

Insecticides

Biopesticides

Controlled delivery

Formulations

### ABSTRACT

One of the most vital supports to sustain human life on the planet earth is the agriculture system that has been constantly challenged in terms of yield. Crop losses due to insect pest attack even after extensive use of chemical pesticides, are major concerns for humanity and environment protection. By the virtue of unique properties possessed by micro and nano-structures, their implementation in Agri-biotechnology is largely anticipated. Hence, traditional pest management strategies are now forestalling the potential of micro and nanotechnology as an effective and viable approach to alleviate problems pertaining to pest control. These technological innovations hold promise to contribute enhanced productivity by providing novel agrochemical agents and delivery systems. Application of these systems envisage to achieve: i) control/release of agrochemicals, ii) site-targeted delivery of active ingredients to manage specific pests, iii) reduced pesticide use, iv) detection of chemical residues, v) pesticide degradation, vi) nucleic acid delivery and vii) to mitigate post-harvest damage. Applications of micro and nano-technology are still marginal owing to the perception of low economic returns, stringent regulatory issues involving safety assessment and public awareness over their uses. In this review, we highlight the potential application of micro and nano-materials with a major focus on effective pest management strategies including safe handling of pesticides.

© 2016 Elsevier Ltd. All rights reserved.

### Contents

1. Introduction	00
2. Interaction of NPs with insect physiological status: an essential and important aspect (reviewed viewpoint)	00
3. Rationales for micro and nano-technological approach: insect management	00
3.1. Microbe-derived bioactives	00
3.2. Plant derived products and their application	00
3.3. Nucleic acid delivery	00
4. Reinforcing nano or micro based pesticides: techniques and applications	00
4.1. Micro/nanocomplexed formulations	00
4.2. Nanoparticles as advanced delivery systems	00
4.3. Delivery via adsorption/encapsulation	00
4.4. Delivery via entrapment	00

\* Corresponding author. Nano Molecular Biology, Biochemical Sciences Division, CSIR-National Chemical Laboratory, Pune-411008, Maharashtra, India.

\*\* Corresponding author. Maharashtra Institute of Medical Education and Research (MIMER) Medical College, Solapur District, Dist. Pune-413007, India.

E-mail addresses: [apgiri@ncl.res.in](mailto:apgiri@ncl.res.in) (A.P. Giri), [jjkhandare@ncl.res.in](mailto:jjkhandare@ncl.res.in) (J.J. Khandare), [rajesh@ncl.res.in](mailto:rajesh@ncl.res.in) (R.S. Barbole).

<http://dx.doi.org/10.1016/j.jenvman.2016.09.027>

0304-3870/2016 Elsevier Ltd. All rights reserved.

Please cite this article in press as: Khandelwal, N., et al., Budding trends in integrated pest management using advanced micro- and nano-materials: Challenges and perspectives. Journal of Environmental Management (2016), <http://dx.doi.org/10.1016/j.jenvman.2016.09.027>



4.5. Interaction via surface functionalization .....	00
4.6. Inorganic micro and nano-pesticide delivery systems .....	00
4.7. Advance polymeric delivery systems in pest management .....	00
5. Other applications .....	00
5.1. Detection of pesticide residue .....	00
5.2. Pesticide degradation .....	00
6. Conclusions and future perspective .....	00
Acknowledgements .....	00
References .....	00

## 1. Introduction

A significant proportion of a nation's economy relies on its agriculture and also vitally contributes to the world's food basket. Constantly expanding population coupled with changing environmental conditions exerts pressure on agriculture to augment food production in order to satiate a greater demand of food supply (Gothray et al., 2010; McClung, 2014). The advent of synthetic pesticides and fertilizers, the major contributors to the green revolution, has indeed brought about transformational change in the structure sector. These strategies have paved their way in modern agriculture due to the lack of sufficient inherent quality of the crop plants in sustaining environmental stresses, e.g. pest invasion.

Since 1940 synthetic pesticides provided an effective solution to control pest populations on crop plants, losses due to the insect pests are estimated to be 27–42% on crops after application of synthetic pesticides, as opposed to >83% losses at the untreated crops (Oerke and Defore, 2004). However, in the due course of time, several insects have developed resistance to numerous pesticides (Dawlat et al., 2011). Further, excessive use of chemical pesticides (>2 million tons/year) has caused detrimental effects on the ecosystem raising concerns to safeguard crops in an eco-friendly manner (Kühler and Tribokorn, 2013; Van Den Bosch et al., 2011). Thus to address these challenges, 'integrated biotechnological approaches' and 'sustainable intensification techniques' are being explored (Tilman et al., 2011). An adaptation of biotechnological approaches to suppress pest populations involves modification of the living organisms and their bioactives. Towards this, transgenic plants expressing insecticidal compounds have captured significant attention around the globe. A classical example is the genetically engineered crop plants expressing cry toxin(s) of *Bacillus thuringiensis* (James et al., 2006). Development of transgenic plants either offers gene-pyramiding by expressing proteins with a different mode of actions or by domain swapping to maximize efficacy on the target insect pests (Dinjar et al., 2010; Carrone et al., 2015). Although, genetic manipulation imparts an excellent opportunity to develop improved biopesticides, its application has been limited due to the stringent regulatory guidelines and public acceptance over their use. In addition, various natural compounds have been identified as potent deterrents, growth inhibitors, and toxins against insect pests *in vitro*. But substantial studies related to their field applications are lacking due to various environmental and other constraints. This has generated an immediate requirement to harness an alternative technology that can offer eco-friendly, cost-effective, and sustainable solutions towards pest control.

Advancements in material science has offered flexible processes to design varying size of micro and nanostructures yielding desired features (Fig. 1). Industrial application of these materials reveals their innumerable advantages in various facets of science including agriculture. Micro and nanoparticles (NPs) if applied prudently can help to leverage biotechnological expedients via encapsulation,

adsorption or conjugation. This shall also provide benefits of safe handling of chemical pesticides by achieving precise and targeted delivery. Application of insect controlling active agents in the field suffers from fast evaporation, runoff, and UV degradation. Towards this, identification of NP based delivery systems are the key as they can offer: (i) enhanced activity against a wide spectrum of pests, (ii) greater stability and retention in external environmental condition and (iii) improved uptake (Ghani et al., 2012). Furthermore, these tools are anticipated to enhance the field conditions by reducing pest burden and mediating 'smart' delivery of active ingredients in terms of targeted and controlled release of agrochemicals and biological agents. Other advantages include their use as nanosensors-sensing chemical residues, as nanocides, in reducing pesticide use, facilitating pesticide degradation, and assist nucleic acid transfer targeted against insects (Fig. 2). Taken together, implementing sustainable biotechnological approaches with the application of novel materials anticipates a paradigm shift in global crop protection.

In the following sections, we focus on cataloguing developments in advanced micro and nano-based pest management strategies that may be suited for agronomical applications. In addition, our attempt was to cite challenges and recent advances in the burgeoning use of active ingredients by exploiting unique properties of novel materials towards pest control. For the interest of the readers, a brief section on the application of nanoparticles as residue detector and pesticide degradation have also been included from the perspective of environmental concerns.

## 2. Interaction of NPs with insect physiological status: an essential and important aspect remained unexplored

In line with the focus of the review, control of agricultural pests by nano-biotechnological means offer unprecedented advantages. Most of the devastating agricultural pests belong to two major classes named Lepidoptera and Coleoptera, responsible for major losses of field crops and stored grains. Herbivore insects depending on their feeding spectrum are divided into 'generalists' that feed on a variety of plants belonging to different families and 'specialists' that are confined to a single species of plant. In this way different insects have evolved distinct feeding habits which further determine their physiological status that varies with the diet composition. Studies have revealed that a particular insect possesses the capability to modify its biochemical composition when fed on different diets that enables them to detoxify plant defensive compounds while providing better opportunity for the utilization of nutrients (Dawlat et al., 2013; Satti et al., 2014). This presents a challenging prospect to devise a sustainable and targeted strategy for the control of particular pest population in the different environment and crops.

Applied technology of MNPs in the pest management has been gathering attention across the globe for their wide spectrum of tunable physico-chemical properties. Despite the advantages

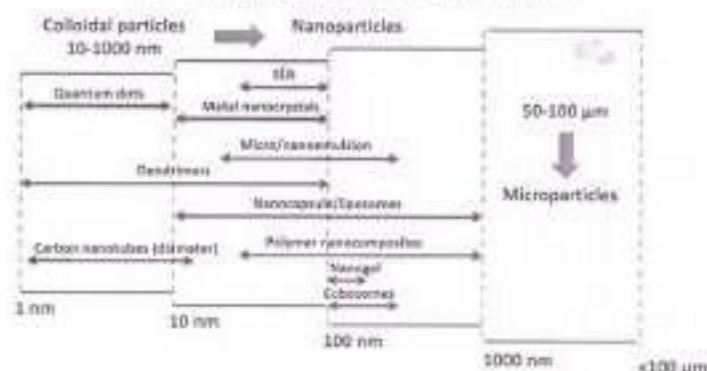


Fig. 1. Representation of size range of different types of nano- and micro-particles.



Fig. 2. Applications and advantages of micro-nano systems in integrated pest management.

possessed by nano-based pest control, their extensive application in the field has remained elusive. Before manoeuvring into application, it is imperative that multitude of physical parameters needs to be critically evaluated viz. light, temperature, humidity, and biological factors such as insect feeding habits, motility, detoxification strategies by insects and phytochemistry. The translocation of particulate materials and their interaction with insect body fluids have not been much investigated, exploring which may facilitate precise location of materials and their selective engineering. Hence, the studies determining the transport, release and fate of NPs with respect to insect physiology remain scarce. With relevance to the invertebrate system, gut pH of herbivores ranges from 5 to 13 which seek for the selection of particles exhibiting ‘smart’ pH-responsive properties to overcome such challenge. Furthermore, targeted release of the nano-encapsulated bioactive in the specific pH milieu has to cross the barrier of pH gradient which it receives while passing from the plant surface to the insect gut system. We recently demonstrated the unloading of defensive protein immobilised on silica nanoparticles to target insect digestive system exhibiting alkaline pH (Khandekar et al., 2013). Engineering of such materials to make it acceptable for a desired condition is plausible and readily achievable owing to the advancement in chemical and biological molecular knowledge. Furthermore, several insect display variations in redox potential which is an indicative of oxidising or

reducing condition of the gut environment. Ingestion of plant allelochemicals that generates reactive oxygen species can induce oxidative stress in the insects upon feeding. However, insects have developed mechanism to evade the plant defense system for instance, *Manduca sexta* can maintain reducing condition in midgut by the secretion of antioxidants (Chapman et al., 2013).

The exposure of nanoparticles (NPs) to oxidation-reduction state may challenge their stability and of immobilized protein, which in principle may impact the protein-protein interaction and hence efficacy in the feeding insects. Metallic NPs such as Silver (Ag) or Gold (Au) are considered as redox species requiring the evaluation of their redox properties and reactivity in physiological conditions. Exposure of insects to Ag NPs has shown to induce oxidative stress, which was thwarted by the enhanced production of antioxidant enzymes such as superoxide dismutase, peroxidase and catalase (Vasile and Iani, 2015). Thus, to determine the insect response upon exposing it to varied nanostructures require a careful examination to devise an effective strategy for the prolonged stability and effectivity of particulate materials.

NPs have the tendency to adsorb a dense layer of proteins which are highly dynamic in nature forming a ‘corona’ like structure. Proteins that are abundantly present are known to adsorb on NPs, which can be replaced by the proteins present in low amount but has high affinity to the NP surface (Hoi et al., 2009). Interestingly, several reports are available on the interaction of cooese proteins with nanosurface influencing translocation, uptake and fate of the NPs in the biological system. It can be assumed that entry of particles through feeding exposes it to distinct biochemical composition present in the mouth parts and in the gut environment of the insect. However, the interactions of the NPs with proteins, native to the insect system, are still obscure. Lepidopteran insects predominantly contain serine proteases which are active at alkaline pH, but several coleopteran insect digestive system is dominated with cysteine proteases that are active at a slightly acidic pH. Interaction of NPs with proteins in a distinct physicochemical environment affects release, retention and efficacy. Furthermore, the properties viz. size, shape, charges, hydrophobicity and surface chemistry of the particles determines the selectivity and specificity of their interaction. The role of these features in governing the efficacy and applicability of nanomaterials towards insect growth or survival is the subject of research. We propose that studying these factors will be useful for designing micro or nano-manipulation for effective control of pests in an eco-friendly way. This will also bring light in evaluating the retention of nanoparticles from the view of



environmental concerns. Till date, though reports have demonstrated the efficacy of NPs in regard to insect management, these parameters have been overlooked which needs a critical viewpoint in order to successfully commercialize the micro or nano-pest control strategies for their application in the agriculture fields.

### 3. Rationales for micro and nano-biotechnological approach in pest management

Past few decades have witnessed the increasing use of methods involving biological means for controlling pests. Towards this, modest research support was aimed at screening attributes of living organisms, plants and microbes and their products to form biopesticides. The commercial success of any biopesticides is largely determined by its efficacy, safe handling, cost effective, longer shelf life and non-target safety along with displaying no phytotoxic effects. These features can be addressed by designing robust materials exhibiting stability under environmental conditions and contribute to maintaining the effectiveness of bioactive agents. By combining these organisms with biological ingredients to form a formulation is expected to endow with consistent responses at field level. Biopesticide formulations often exert a synergistic effect with multiple modes of actions, reducing the danger of developing resistance to pests as opposed to synthetic pesticides typically having a single mode of action (Hutcheon et al., 2014).

#### 3.1. Microbe-derived bioactives

Microbial agents like bacteria, protozoa, fungus, viruses and nematodes have been investigated and successfully used either alone or in combinations as biocontrol agents. Several industries are exploiting the features of bacteria and fungi in reducing or managing pest populations due to their narrow host range. Examples include the use of several species of *Trichoderma*, *Neurospora*, *Beauveria*, *Metarhizium* in agriculture. Several species of *Neocyphopogon* endophytes have potent insecticidal properties and are commercially available (Clare et al., 2012). In addition, various registered products include microbe-derived bioactives that exert deleterious effects on the insect pests and are optimized for large scale production. Selection of microbes requires high throughput screening among thousands of isolates. Genetic engineering of microbes has made it feasible to modulate sub-optimal features of pesticidal microbes such as efficacy, stability and virulence by overproduction of bioactives with enhanced activity or introducing insecticidal genes that are obtained from other living organisms (Kluger and Wang, 2010; Leizer et al., 2006). *Bacillus thuringiensis* based biopesticides have dominated the marketplace since half century and have been genetically mutated to produce strains with novel insecticidal proteins (Clare et al., 2012). Maintaining the efficacy of microbial agents in the field is the utmost prerequisite, which can be achieved by selecting diverse complement of adjuvants and blend it with target agents/molecules to augment efficacy and environmental compatibility. Though data on recipe preparation for the commercial microbial formulation is limited, its components should provide advantageous properties viz. improved uptake, enhanced spread, reduced evaporation and desiccation along with providing protection from harsh environmental conditions such as UV radiation and rainfastness (Hynes and Boyerchik, 2006). For example, the addition of Timpal LPW to the virus suspensions contributed to reducing LD<sub>50</sub> in target pest *Spodopoptera exigua* (Lepidopteran) (Munillo et al., 2003).

Despite the global realization of effective pest control, the commercial success of biopesticides is still facing challenges due to biological, ecological, and regulatory constraints. Nevertheless, improvements in the pesticide research and their acceptance by

industries and the public sector are continuing to grow. Simultaneously, recent research interventions have advanced our knowledge in various solid and liquid based formulation technologies to expand biopesticide applicability. Magnetic immobilization of microbial cells onto a hybrid product generated from the amalgam of gelatin gum polymer and Fe<sub>3</sub>O<sub>4</sub> nanoparticle has endowed them with the higher degradation ability of organic contaminant, carbazole (Wang et al., 2007). For efficient and controlled delivery of bioactives various surface modifications and combination of materials have also been explored. Double-shelled microcapsules of avermectin, a microbial-based insecticide was prepared by coating chitosan over surface functionalized silica shell. Shell thickness of nanoparticles provided UV and thermal protection besides with controlled release of avermectin (He et al., 2012a, b). Noteworthy, use of Bt biopesticides to insect control is escalating with a mounting interest in exploring novelties to further its effective utilization. Potential of nanoparticles in pest eradication/suppression have received a recent recommendation to develop fitnanopesticides providing protection to high-value crops (Mahabaleswamy and Anjan, 2012).

#### 3.2. Plant-derived products and their application

Over the past decades, plant-derived compounds and extracts have been investigated for their capability to control insect pests. Inherent plant protection from pests is governed by the action of defensive traits through the production of secondary metabolites such as alkaloids, benzoxazinoids, cyanogenic glucosides, phenolics, and terpenoids (Mishra et al., 2015). This arsenal of structurally and functionally diverse natural molecules exhibit repellent, toxic or antifeedant effects on insects (Bauer et al., 2012). Our recent studies have shown enhanced insecticidal effects portrayed by *Dermanis* species by increased levels of metabolites such as camphor, limonene and  $\beta$ -caryophyllene against *M. ornigera* (Singh et al., 2014). *In vivo* studies have also demonstrated the potential of caffeic acid in deterring growth and development of lepidopteran pest (Joshi et al., 2014). Furthermore, wound inducible plant proteinase inhibitors, a well-studied class of defensive proteins, was found to interfere with insect protein digestion, resulting in the arrested growth, lowered fecundity and fertility of *M. ornigera* (Lorenz et al., 2005, 2007; Mishra et al., 2010). Despite the intensive research demonstrating the biological efficacy of plant metabolites, only a limited number of plant-based products are registered (Table 1). Products such as neem (*Azadirachta indica*) seed extract, azadirachtin, pyrethrin, and limonene are amongst the widely accepted botanical insecticides (Jensen et al., 1990). Azadirachtin, a triterpenoid isolated from neem, interferes with the embryonic development of *Spodopoptera exigua* (Carrara et al., 2011). *Helicoverpa armigera* have also shown to be highly susceptible to the neem seed extract (Bhattach et al., 2011; Nigam et al., 1994; Weisner, 2000).

Pesticides based on the plant essential oils (EOs) and plant-derived compounds hold special status of 'exempted active ingredients'. They have reduced risk to the environment and are exempted from registration along with extensive toxicological and environmental tests. A few examples are: cinnamon, citronella, lemon grass, garlic, thyme, pure compounds like eugenol and thymic acid (Carrara et al., 2012). Though many of them act as natural repellents against various arthropods, our focus here is on those compounds that are efficient in controlling the menace of crop pests. Various formulations of azadirachtin have been developed in the form of emulsion, microcapsules, and MNPs, achieving greater stability and efficacy against pests such as *Plutella maculipennis*, *Zobryta subfocata* (Fonseca et al., 2011; da Costa et al., 2014). In another example, a citrus extract consisting  $\beta$ -limonene was

**Table 3**  
 Selected examples of plant-derived compounds applied through conjugation on nanoparticles or prepared as formulations against insect pests.

Class	Plant-derived compound	Mode of action	Details of formulation	Effective against	Reference
Insecticides	$\alpha$ -pinene linalool	Repellent	Adorn on silica nanoparticle	Spodoptera litura Aedes aegypti (Lepidoptera)	Sato et al., 2014
	Quercetin	Insecticidal	Drydown 15 Insecticide, 872X, 875A-10, 0.1% Silver 1-77	Resistant Anopheles stephensi Diptera (Anopheles)	Phillis et al., 2002
Transmembrane	Alkaloids Menthol	Disrupts membrane	Nanoformulation in colloidal suspension (water at 2% (w/v), menthyl acetate 0.1% (w/v), Span 40 0.5% (w/v), polyvinylpyrrolidone 0.5% (w/v), and Tween 80 0.5% (w/v))	Phytophthora blight (Lepidoptera)	Debnath et al., 2013
Alkaloids	Nicotine	Neurotoxic (mode of action: Nicotinic AChR ion channel)	Nicotine dispersion (3 ml 8.5ml/ml nicotine, 30 ml 8.5ml/ml)	Aphis (Homoptera)	Chakraborty et al., 2005
Wood-boring Pest	Pyrethrin in herb	Digestive enzyme inhibition (insecticide)	Water suspension (500 mg/100 ml) loaded on silica nanoparticles	Anticarsia gemmatilis (Lepidoptera)	Tanaka et al., 2012; Chakraborty et al., 2015
Essential oils	Eucalyptol	Antifeedant	Microencapsulation in PEI coated nanoparticles	Trialeurodes vaporariorum	Yang et al., 2009

formulated as an emulsion that demonstrated up to 100% mortality to mealybug and scale insects (Hollingsworth, 2005). Formulation of botanicals in an appropriate media is imperative in the view of overcoming limitations pertaining in field application as well as for enhanced bioactivity.

Repellent and antifeedant activities of plant secondary compounds,  $\alpha$ -pinene and linalool were elevated to 25% against *Spodoptera litura* and *Aedes aegypti* when formulated with silica NPs. Nanoformulation granted improved shelf life to these terpenes for the purpose of their long-term use in the field (Bhui et al., 2014). Among conventional pesticides, synthetic pyrethroid derived from a plant (*Chrysanthemum* species) holds an essential component, which can control a wide range of insects. Historically, pyrethrum is recognized as a potent killer of insects. However, it is highly unstable when exposed to light and UV radiation. Thus, the synthetic derivatives are formed by chemical modifications to render stability to pyrethrin in order to maintain its efficacy (Clark, 1997). Similarly, the neonicotinoid class of insecticides containing plant-derived nicotine has captured a significant portion of the insecticide market. However, considering the environmental toxicity posed by these synthetic pesticides, it is essential that use of formulations implicate non-toxic effect on non-target insects and safety towards humans by guarded pesticide handling. In a study, nicotine-based formulation was prepared using sodium caseinate as a stabilizing agent. Dispersion of increasing concentration of nicotine oleate sought three formulation systems in the form of emulsion, suspension and suspension. This study revealed greater bioactivity and stability of formulation majority in the form of emulsion and suspension (Casanova et al., 2002).

Thus, to achieve substantial stability and biological activity, appropriate liquid and solid formulations can be designed that propose promising opportunities for pest control in an environmentally benign way. Botanical insecticides pose a narrow range of stability under environmental conditions, including thermal degradation, product inactivation and rapid evaporation (de Oliveira et al., 2014). Furthermore, commercial level of success also depends on properties such as controlled release of the active compound, improved physicochemical stability, greater retention and better uptake. This has enabled researchers to explore delivery mechanisms by exploiting MNPs or emulsions and polymeric nanoparticles that are depicted to hold beneficial characteristics than their bulk counterparts.

### 3.3. Nucleic acid delivery

RNA interference technology is a new tactic for insect control. This method relies on post-transcriptional silencing by double-stranded RNA (dsRNA) mediated downregulation of specific genes by degrading respective messenger RNA (mRNA)s. dsRNA upon encounter with endonuclease called 'dicer', produce small interfering RNA (siRNA), one strand of which is responsible for target degradation (Carroll and Oleschinski, 2007). So far, the potential of dsRNA to control insects has been evaluated by microinjection into the insect gut, oral feeding assays and transgenic expression (Price and Gauthreaux, 2009). Studies have suggested that the efficient delivery of dsRNA is an insect is an important factor to achieve efficacy. For instance, microinjection of dsRNA in the insect hemocoel efficiently downregulated the midgut aminopeptidase-N gene of *Spodoptera litura*, but feeding the dsRNA construct to the insect did not result in downregulation of this gene (Rajagopal et al., 2002). This differential response is assumed due to the complexity of insect physiology that exists in different species and respond differently to oral uptake and injected RNA (Price and Gauthreaux, 2009).

The efficiency of introducing RNAs in insects suffers challenge of lower stability, poor delivery, and uptake as well as degradation by nucleases. Hence, it is projected to use an advanced nano or micro delivery system, such as an encapsulated or conjugated dsRNA to achieve exceptional results. Advanced materials including cationic polymers, dendrimers, and functionalized nanoparticles are considered as an effective gene delivery materials (He et al., 2012a, b). In a study, fluorescent nanoparticles were developed containing a dye in the center, poly (phenylene) dendrimers form the inner layer, whereas the outer layer is composed of a cationic polymer. The inner layer of dendrimers assists in preventing the aggregation of dye in water milieu whereas amino group functionalized outermost polymeric shells aid in enhanced aqueous solubility. This structure comprised of positively charged polymer shell to facilitate binding of negatively charged DNA or dsRNA. In vivo analysis revealed efficient uptake of genetic materials while exhibiting low cytotoxicity (Liu et al., 2015).

Application of NPs conjugated RNA for the disruption of target gene activity in the insect may exert negative consequences on its biological function. However, the knockdown efficiency varies with the type of NP used along with the ratio of NP-dsRNA conjugated



complex and require optimization. In an interesting study, three different types of NPs (i.e. carbon quantum dots, chitosan and amine-functionalized silica NPs) were used to conjugate the same amount of dsRNA. Though the loading efficiency in all the cases was reported to be 100%, their efficiency in gene suppression varied with carbon quantum dots showing the efficient suppression of *Aedes aegypti* gene (Das et al., 2015). This demonstrates that the oral route of delivering genetic materials conjugated with MNPs in insects for the gene suppression offers a non-toxic and economically viable approach. It also offers an easy method for controlling insects by avoiding a tedious process of generating plant transgenics. However, before administration, a detailed assessment of the use of RNAi delivery systems is required for its successful administration and protection in the field conditions.

#### 4. Reinforcing nano or micro based pesticides: techniques and applications

Small materials comprising various sizes of MNPs has a profound impact on their functionality in medical and agricultural applications. Nanotechnology refers to a technique involving synthesis, engineering, modification and implementation of materials > solutions having particles or droplet size ideally below 100 nm (Fig. 1) (Bhandari et al., 2012). Several sized NPs such as carbon nanotubes, dendrimers or quantum dots have been explored well for drug delivery purposes but is still in its infancy in the delivery of agrochemicals. The size of the NPs largely influences the binding of active ingredients such as protein/peptide or DNA/RNA and loading efficiency. Especially, for agricultural application, efficient loading of bioactives are desirable. In addition to size, surface chemistry and particle composition has a crucial importance in pesticide delivery and particle uptake.

Use of nano or micro based pesticides applied through nano-micro-emulsions, nanocapsules or MNPs offers unparalleled advantages over the conventional delivery systems. They propose to provide a wide range of solubility, thermal stability, biodegradability, large surface area and permeability (Bergeson, 2010; Bouamrane et al., 2009). For the successful application of bioactives, it is desirable that the pesticide formulations must include the following traits, viz. (i) improved activity, (ii) increased spreading and retention ability on plant surfaces, (iii) stability in the external environmental milieu and (iv) ease of handling (Müller and Griebelmann, 2001). Formulations are prepared in different ways by assessing various physicochemical properties of bioactive agents. In several instances, there is a practical difficulty in applying or spreading the active ingredients directly for effective insect control. Furthermore, the active ingredients may be chemically unstable, difficult to handle and may have a short shelf life. Thus, 'active ingredients' are generally formulated using excipients which provide a protective shield and may act as adjuvants. Generally, these formulations are differentiated by physical classes, e.g. emulsions, ready to use aerosols, smoke or fog generators, micro-encapsulated materials, pastes, gels and other injectable baits. Pesticide formulation may consist of: (i) pesticidal active ingredients that control the target pest, (ii) the vehicle, e.g. organic solvent or mineral clay, (iii) surface-active ingredients including stickers and spreaders (e.g. emulsifiable concentrates) and (iv) other ingredients, such as stabilizers, dyes, and chemicals to enhance the pest control activity.

Water insoluble pesticides can be formulated using micro-encapsulation and nanoemulsion formulation methods to enhance their bioavailability in aqueous environment (Usaj, 2001; Wang et al., 2007). A pesticide delivery system was developed containing pesticide, surfactant, and water by two-step milling process (Choi et al., 2011). In this formulation, a general milling process was

used to form a micro-suspension and then a nano-milling process using Zirconium oxide beads provided the second milling step. Formation of nanosuspension concentrates containing pesticide imparted enhanced dissolution of poorly soluble insecticides, (e.g. carbosulfan) along with increased stability. Evaluation of its biological activity against diamond black moth was shown to be highly efficient at low effective concentration (Choi et al., 2011). This study represented the high efficacy of nanosuspension as compared to micro-suspension. Development of such novel processes can be extended to address other problems faced by poor bioavailability or stability of biological or chemical pesticides for their safe and targeted use in contrasting environments. Further potential advantages of the use of MNPs and mode of delivery of active ingredients in IPM have been provided in the subsequent subsections.

#### 4.1. Micro/nanoemulsion formulations

Due to the differential solubility of active ingredients, emulsions are prepared by dispersing liquid droplets (as a dispersed phase) into another fluid as a continuous phase (e.g. oil/water or water/oil emulsion). This system could be further stabilized by adding surface-active ingredients (Sathishkumar et al., 2008). Such formulations are routinely used with certain modifications depending on the environment, crop, target insect pests and their feeding habits. Currently, development of formulation is focused with an objective of high loading of active ingredients and for wide spectrum applications, resulting in greater efficacy and applicability against target insect pests. Towards this, micro/nanoemulsions may achieve this aim in delivering a high payload of bioactives.

Micro/nanoemulsion-based pesticide formulations have advantage over the conventional pesticidal emulsions due to their long-term thermodynamic stability and small droplet size (Wang et al., 2007). Altogether, these systems boasts wide range of solubilizing ability allowing loading of different polar and non-polar compounds in an acceptable range (Sathishkumar et al., 2008). Thus, it is possible to develop microemulsions complementary to the chemical bio-actives with desirable features. A microemulsion-based formulation carrying plant protease inhibitor (PI) protein were developed and was evaluated for safety and efficacy when applied to the plant surfaces (Tambure et al., 2012). PI formulation composed of water: isopropanol: butanol (WB) microemulsion was found to be effective against *H. urticae* and caused no adverse effect on the plants as compared to the other microemulsions in the study. Interestingly, WB microemulsion was found to increase the retention of PI protein on leaf by possibly endowing the property of penetration (Tambure et al., 2012). Despite providing advantageous properties microemulsion systems in agronomical application are very limited. A few examples include, developing novel formulations by incorporating cyhalothrin, an organic pesticide in the microemulsion system (Zhou et al., 2009). Similarly, water insoluble agrochemical, *β*-cypermethrin formulations were developed by incorporating it into the microemulsion concentrate. Dilution of this concentrate with a large amount of water forms a stable nanoemulsion system displaying enhanced wetting, spreading and penetrating properties (Wang et al., 2007). This suggests that such systems can be efficiently utilized and modified to contain biologically or chemically active ingredients and might prove to be a promising system for hydrophilic or hydrophobic compounds. Such microemulsions can have immense potential in the agriculture industry owing to its increased dispersion over larger contact area, improved wettability and enhanced penetration properties (Paul and Maudh, 2001). While bio-formulation intend to cause no harmful effect on the environments, the possibility of the phytotoxic effect on the target crops after multiple applications must be recognized and needs to be tested over extended period to develop

a suitable and ecologically acceptable system.

#### 4.2. Nanoparticles as advanced delivery systems

Nanoscience and its transformation into nanotechnology platforms are anticipated to offer better solutions for targeted delivery. Towards this, both organic and inorganic components have been widely explored in fabricating nano-sized systems, deliberating the prudent applications in engineering and biomedical sciences.

In general, nanosystems offer several tasks in parallel including loading of cargo molecules, either small or large, through the conjugation process (Khandetwal et al., 2012). Therefore, the nanosystems are typically prepared using biologically relevant biopolymers (e.g. sodium alginate, chitosan etc.) and hard matters (e.g. Zeolites, iron oxide, nanoporous silica, etc.) that suggest numerous applications. Furthermore, additional complexities are chemically tuned by adding multifunctional components, thus, leading to robust chemical diversities. Methods such as encapsulation, covalent bonding, adherence, and adsorption, render significant impact on the 'smart' delivery approach to achieve controlled payload release (Ghannadi et al., 2011) (Fig. 1). Most of the approaches that have been developed to fabricate the multicomponent nanosystems rely upon the adsorption of molecules on their surfaces (Arlawan et al., 2010; Khandetwal et al., 2015). Conversely, the chemical conjugation methods can considerably affect the efficiency of the delivery systems. Multiple agents may compete for the same surface binding sites and thus may alter the efficacy of both agents. Depending upon the biological significance and chemical properties of the bioactives, selection of suitable materials is critical. This further relies on the interaction of bioactives with nano structures that can affect their delivery and hence efficacy.

#### 4.3. Delivery via adsorption/immobilization

The property of NPs to adsorb proteins and revealing their interaction has been the subject of intensive research in nanotoxicology or nanomedicine applications. Due to small size and large surface area they serve as an excellent template for the adsorption of the large number of proteins and other biomolecules involving hydrogen bonds or through hydrophobic interactions (Dastghoibi et al., 2015). Interestingly, the process and properties can be exploited to adsorb bioactive compounds on the nanosurface for the targeted delivery of the active ingredients in agricultural applications. Application of silica NPs, described in the later section, has unique advantages pertaining to surface functionalization, surface area and particle size. Mesoporous silica nanostructures with varied pore diameters, and structures were synthesized to evaluate the factors important in the adsorption and release of synthetic insecticide imidacloprid, an insect neurotoxin. The adsorption isotherm study revealed that particle with larger surface area shows higher adsorption by accumulating large number of imidacloprid particles. After adsorption, strong reduction in the particle surface area or pore diameter was observed as compared to other structures with lesser surface area (Poppe et al., 2011). Loading of natural or chemical agrochemicals occurs through physical interaction at the nano-bio interface that may cause significant conformational changes leading to a possibility of disruption or enhanced activity of bioactives. Studies suggest that parameters like hydrophobicity and particle size are the vital determinants for maintaining the native structure of proteins (Maitani et al., 2011). Owing to the plasticity of the particle size and surface area fine tuned with desired surface chemistry modifications, it is plausible to control the surface hydrophobicity and surface curvature leading to high adsorption and enhanced stability of proteins

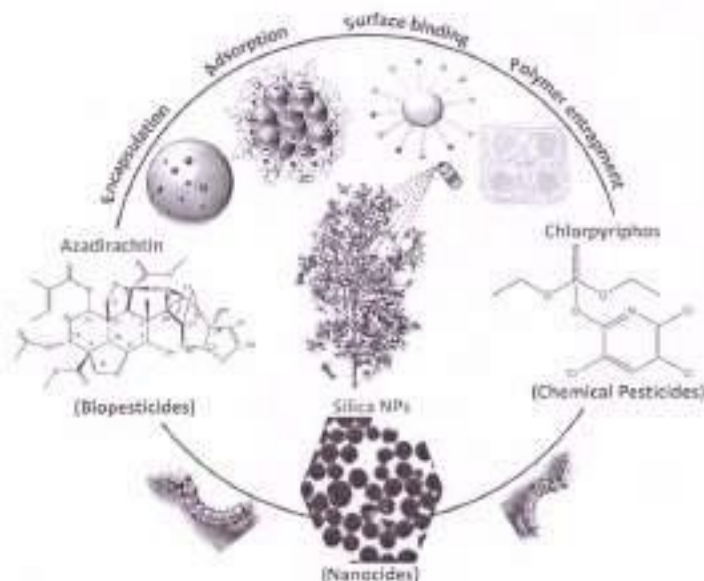


Fig. 1. Schematic representation of nanomaterials and their interaction with active ingredients. Bioactive delivery by encapsulation, adsorption, binding on the surface through ligands and entrapment in the polymer are shown. Different biological or chemical pesticides along with nanocides can be formulated appropriately for their controlled delivery on plants in managing pest infestation. The figure shows examples of each class of pesticides such as Azadirachtin, chlorpyrifos and silica NP.

Please cite this article in press as: Khandetwal, N., et al., Binding trends in integrated pest management using advanced micro- and nano-materials: Challenges and perspectives, Journal of Environmental Management (2016), <http://dx.doi.org/10.1016/j.jenvman.2016.03.071>



along with achieving efficient release. In our recent study, we have utilized the adsorption property of NP to form a single protein corona by using silica nanoparticles and mixing it with protein (protease inhibitor). With increasing concentration of protein, its adsorption on the NP surface was observed to be greater as calculated by quantifying the remaining amount of proteins. Interestingly, the electrostatic interaction at the nano-bio interface facilitated the adsorption of positively charged proteins on negatively charged silica surface as measured (Khoshdel et al., 2015).

#### 4.4. Delivery via encapsulation

In context with field application of bioactives, their protection from environmental factors such as UV degradation, rain leachiness, evaporation losses, temperature stability is essential. An ideal encapsulating material for bioactives protects the sensitive compounds from getting ineffective and facilitates their controlled and sustained release. The sensitivity of azadirachtin, a potent insecticidal compound, to environmental conditions led the researchers to screen different materials for the preparation of nanoparticles that can enhance its stability while obtaining efficient encapsulation and optimized release. Sodium alginate nanocarriers loaded with different coating agents such as natural rubber, starch and PEG showing over 80% encapsulation efficiency (Rajasekhar and Sakthapathi, 2009; Jesu et al., 2012). Encapsulating vehicles, in general, may contain a selective material that act as a nanocarrier or coating agent and a reticulating agent. Together these materials control the encapsulation efficiency and release rate for the bioactives in desired environment. Several examples pertaining to agricultural application of natural compounds have been provided in the above sections that make use of encapsulation methods for their targeted delivery. Such nanoformulations display less toxicity to non-target insects as compared to their respective commercial bulk counterparts.

Plant derived products or extracts have gained a prominent position in agriculture, especially, in the production of organic foods. de Oliveira et al. (2014) reviewed application of plant based insecticidal compounds such as azadirachtin, neem, calyculin, thymol, eugenol, including essential oils of garlic, rosemary and citrus plants. Plant-based EO are the complex mixture of metabolites that appear to be non-toxic in isolation, but exert a synergistically antagonistic effect on the pest (Ismail et al., 2011). Though their significance in the protection of stored grains was known traditionally, re-evaluation of their efficacy in the agricultural system by combining approaches from nanotechnology envisages great potential in agronomy. Synthesis of nanocarriers takes into account the effect of encapsulation efficiency, release profiles and stability of botanicals for their successful development and application. Coating of nanoparticles restricts the exposure of active ingredient to light and temperature thereby preventing the degradation by microbes. In addition, it facilitates slow release of bio-actives as compared to the uncoated nanoparticles. Polymers such as PEG, sodium alginate, chitosan or solid-lipid nanoparticles offer such advantages. For instance, loading of garlic EO on poly (ethylene glycol) (PEG) coated nanoparticles displayed over 80% efficacy against *T. monorepus* up to 5 months against free oil showing only 31% controlling efficiency (Yang et al., 2009). Nano-carriers with PEG coating does not interfere with the activity of natural compounds such as enzymes or proteins, exhibits a wide range of solubility and are biocompatible thereby ensuring lack of toxicity. In a study, nanoformulation of PEG was employed for the gradual release of plant secondary metabolites, geraniol and bergamot terpenes; it ensured enhanced contact toxicity through disrupting digestive physiology of storage pests *Tribolium castaneum* and *Blattella germanica* (Camilleri et al., 2014). PEG polymeric matrix

has not only led to the enhanced stability of the compounds by allowing controlled release, but reduced volatility have augmented its bioavailability with minimum active concentration. As a consequence longevity of active ingredients as compared to free essential oils can be accomplished due to slow and consistent release. In another example, EO extracted from cumin (*Cuminum cyminum*) were entrapped in nanogels formed by the combination of myristic acid and chitosan to exhibit their fumigant toxicity against grain weevil *Sitophilus granarius* and flour beetle *Tribolium castaneum*. Results indicated enhanced toxicity of nanogel loaded essential oil as compared to free oil which showed an insecticidal activity loss in 32 days (Elsay et al., 2014). Thus, overall observations manifest that loading or encapsulation of oils or nanoparticles is preferable to achieve controlled delivery and to maintain stability of sensitive compounds. Encapsulation of EO extracted from *Artemisia arborescens*, an important medicinal plant was reported. Biological significance of *Artemisia* EO against various arthropod pests has been well documented. The drawback due to its physico-chemical degradation has led to the use of solid-lipid nanoparticles rendering physical stability, enhanced shelf life and reduced evaporation of the oil (Liu et al., 2006). Its encapsulation in alginate beads also exhibited its slow release. These results reinforce the possibility of the extensive use of these nano or micro systems in agronomy for control pesticide delivery. The application of various inorganic and organic material with relevance to insect management are provided in the below sections.

#### 4.5. Interaction via surface functionalization

Covaleent attachment of structural moieties onto the surface for the adsorption or coupling of the active ingredients is the utmost requirement to attain desired results. Surface chemistry of nano-materials grants opportunities to carry out certain modifications that become the primary determinant of their interaction with biomolecules and biological system. For the application of nano-materials in insect pest management, suitable surface chemistry plays a key role not only in determining its efficacy, but maintaining stability and can avoid ecotoxicity by specific conjugation of chemical moieties. Modulation of surface properties enhances the uptake or bioavailability in specific conditions. For instance, problem pertaining to the distribution of hydrophobic pesticides in insect physiological system can be resolved by entrapping the active ingredient onto carrier with hydrophilic surface moieties mediating their effective distribution. Nanocarriers based on dendrimers were successfully used for emapping pesticide molecules after surface functionalization with amine groups to enhance their hydration (Liu et al., 2015). Silica NPs due to the presence of large number of silanol groups on the surface allows it to be readily functionalized with various organic groups to carry out desired functions. For instance, surface functionalization of silica particles with 3-mercaptopropyltrimethoxysilane and hexamethyldisiloxane have shown enhanced efficacy against lepidopteran pest (Sobhanli et al., 2012). Modification of surface chemistry also affects release profile of bioactives and can circumvent the problems of bioactive outburst thereby rendering sustained release. Use of the selective coating matrix such as PEG function to contain the bioactive encapsulated and facilitate slow release.

#### 4.6. Inorganic micro and nano-pesticide delivery systems

In the view of increasing concern over an indiscriminate use of pesticides, MNT was suggested to be the potential carrier of pesticides, allowing an optimized level of exposure in the environment with reduced and effective dose. Inorganic micro and nanoparticle-based formulations for pesticide delivery have attracted great

along with achieving efficient release. In our recent study, we have utilized the adsorption property of NP to form a single protein corona by using silica nanoparticles and mixing it with protein (proteinase inhibitor). With increasing concentration of protein, its adsorption on the NP surface was observed to be greater as calculated by quantifying the remaining amount of protein. Interestingly, the electrostatic interaction at the nano-bio interface facilitated the adsorption of positively charged proteins on negatively charged silica surface as measured (Khandalwal et al., 2015).

#### 4.4. Delivery via encapsulation

In context with field application of bioactives, their protection from environmental factors such as UV degradation, rain fastness, evaporation losses, temperature stability is essential. An ideal encapsulating material for bioactives protects the sensitive compounds from getting ineffective and facilitates their controlled and sustained release. The sensitivity of azadirachtin, a potent insecticidal compound, to environmental conditions led the researchers to screen different materials for the preparation of nanoparticles that can enhance its stability while obtaining efficient encapsulation and optimized release. Sodium alginate nanocarriers (and with different coating agents such as natural rubber, starch and PEG

showing over 80% encapsulation efficiency (Rajvan and Sakthipanthi, 2009; Joshi et al., 2012). Encapsulating vehicles, in general, may contain a selective material that act as a nanocarrier or coating agent and a reticulating agent. Together these materials control the encapsulation efficiency and release rate for the bioactives in desired environment. Several examples pertaining to agricultural application of natural compounds have been provided in the above sections that make use of encapsulation methods for their targeted delivery. Such nanoformulations display less toxicity to non-target insects as compared to their respective commercial or bulk counterparts.

Plant derived products or extracts have gained a prominent position in agriculture, especially, in the production of organic foods. de Oliveira et al. (2014) reviewed application of plant based insecticidal compounds such as azadirachtin, rotenone, calyculin, thymol, eugenol, including essential oils of garlic, rosemary and citrus plants. Plant-based EO are the complex mixture of metabolites that appear to be non-toxic in isolation, but exert a synergistically antagonistic effect on the pest (Juman et al., 2011). Though their significance in the protection of stored grains was known traditionally, re-evaluation of their efficacy in the agricultural system by combining approaches from nanotechnology envisages great potential in agronomy. Synthesis of nanocarriers takes into account the effect of encapsulation efficiency, release profiles and stability of botanicals for their successful development and application. Coating of nanoparticles restricts the exposure of active ingredient to light and temperature thereby preventing the degradation by microbes. In addition, it facilitates slow release of bio-actives as compared to the uncoated nanoparticles. Polymers such as PEG, sodium alginate, chitosan or solid-lipid nanoparticles offer such advantages. For instance, loading of garlic EO on poly (ethylene glycol) (PEG) coated nanoparticles displayed over 80% efficacy against *T. castaneum* up to 5 months against free oil showing only 31% controlling efficiency (Yang et al., 2009). Nano-carriers with PEG coating does not interfere with the activity of natural compounds such as enzymes or proteins, exhibits a wide range of solubility and are biocompatible thereby ensuring lack of toxicity. In a study, nanoformulation of PEG was employed for the gradual release of plant secondary metabolites, geraniol and bergamot terpenes. It entrapped enhanced contact toxicity through disrupting digestive physiology of storage pests *Tribolium castaneum* and *Blattopertha germanica* (Corralan et al., 2014). PEG polymeric matrix

has not only led to the enhanced stability of the compounds by allowing controlled release, but reduced volatility has augmented its bioavailability with maximum active concentration. As a consequence longevity of active ingredients as compared to free essential oils can be accomplished due to slow and consistent release. In another example, EO extracted from ramin (*Cumoum gymmiun*) were entrapped in nanogels formed by the combination of myristic acid and chitosan to exhibit their fumigant toxicity against granary weevil *Sitophilus granarius* and flour beetle *Tribolium castaneum*. Results indicated enhanced toxicity of nanogel loaded essential oil as compared to free oil which showed an insecticidal activity loss in 12 days (Diaz et al., 2014). Thus, overall observations manifest that loading or encapsulation of oils in nanoparticle is preferable to achieve controlled delivery and to maintain stability of sensitive compounds. Encapsulation of EO extracted from *Artemisia arbuscula*, an important medicinal plant was reported. Biological significance of *Artemisia* EO against various arthropod pests has been well documented. The drawback due to its physico-chemical degradation has led to the use of solid-lipid nanoparticles rendering physical stability, enhanced shelf life and reduced evaporation of the oil (Liu et al., 2008). Its encapsulation in alginate beads also exhibited its slow release. These results reinforce the possibility of the extensive use of these nano or micro systems in agronomy for control pesticide delivery. The application of various inorganic and organic material with relevance to insect management are provided in the below sections.

#### 4.5. Insecticide via surface functionalization

Covalent attachment of structural moieties onto the surface for the adsorption or coupling of the active ingredients is the utmost requirement to attain desired results. Surface chemistry of nano-materials grants opportunities to carry out certain modifications that become the primary determinant of their interaction with biomolecules and biological system. For the application of nano-materials in insect pest management, suitable surface chemistry plays a key role not only in determining its efficacy, but maintaining stability and can avoid ecotoxicity by specific conjugation of chemical moieties. Modulation of surface properties enhances the uptake or bioavailability in specific conditions. For instance, problem pertaining to the distribution of hydrophobic pesticides in insect physiological system can be resolved by entrapping the active ingredient onto carrier with hydrophilic surface moieties mediating their effective distribution. Nanocarriers based on dendrimers were successfully used for entrapping pesticide molecules after surface functionalization with amine groups to enhance their hydration (Liu et al., 2015). Silica NPs due to the presence of large number of silanol groups on the surface allows it to be readily functionalized with various organic groups to carry out desired functions. For instance, surface functionalization of silica particles with 3-mercaptopropyltriethoxysilane and hexamethyldisilazane have shown enhanced efficacy against lepidopteran pest (Dehman et al., 2012). Modification of surface chemistry also affects release profile of bioactives and can circumvent the problems of bioactive elution thereby rendering sustained release. Use of the selective coating matrix such as PEG function to contain the bioactive, encapsulated and facilitate slow release.

#### 4.6. Inorganic micro and nano-pesticide delivery systems

In the view of increasing concern over an indiscriminate use of pesticides, MNPs was suggested to be the potential carrier of pesticides, allowing an optimized level of exposure in the environment with reduced and effective dose. Inorganic micro and nanoparticle-based formulations for pesticide delivery have attracted great



attention over the last few years as they offer high stability, chemical versatility and biocompatibility (Fig. 4A). Inorganic nanomaterials, e.g. iron oxide, silica, and calcium phosphate nanoparticles envisaged unprecedented opportunities in delivering bio-actives (Debnath et al., 2012; Banerjee et al., 2015). For example, silica nanoparticles have burgeoned to be the most widely explored material for pesticide delivery as they offer inimitable advantages (Fig. 4B). They possess markedly different features viz. physical and chemical stability, tunable pore sizes, high surface area and distinct surface properties, making them superlative for molecules of varied sizes, shapes and functionalities (Khundhvir et al., 2015; Torrey et al., 2007). In addition, silica nanoparticles provide stability to bio-active molecules from chemical to physical parameters such as temperature, moisture, plant's chemical secretions, soil pH and composition. These characteristics must be considered in the efficient delivery of many peptide and protein molecules.

Various reports on the utilization of functionalized silica as nanocarriers or carriers with varying size have been demonstrated for their plausible application in pest management. Recently, we investigated the potential of silica based nanospheres and rods immobilized with proteinase inhibitor peptide (Khundhvir et al.,

2015). The nanosystem based formulation possessed a critical property of pH-triggered release, thus, offering an advantage of controlled release of immobilized proteinase inhibitor peptide. Silica nanoparticles exhibited a high peptide loading capacity accounting for 82%. The interaction of proteinase inhibitor peptide with silica nanosphere was driven by the charge and ionic strength as evident from the variation in peptide loading at different pH. Additionally, other forces such as particle size, curvature and aggregation were suggested to play their role at the interface. Interestingly, an *in vitro* release study showed pH-dependent peptide release of 50% at pH 10 and *in vivo* study demonstrated higher efficacy for proteinase inhibitor peptide with silica nanoparticle as compared to the control.

It was reported that treating insects with silica NPs (15–30 nm) resulted in higher mortality than when the insect was treated with bulk silica (Debnath et al., 2011; Wen et al., 2009). The possible mode of action of silica particles on insect physiological system is suggested by blocking the cuticular lipid layers for the passage of water resulting into dehydration of the insect (Barik et al., 2008). Amorphous nanosilica was also shown to be effective against smudge gram pest and field pest. Surface functionalized silica NPs

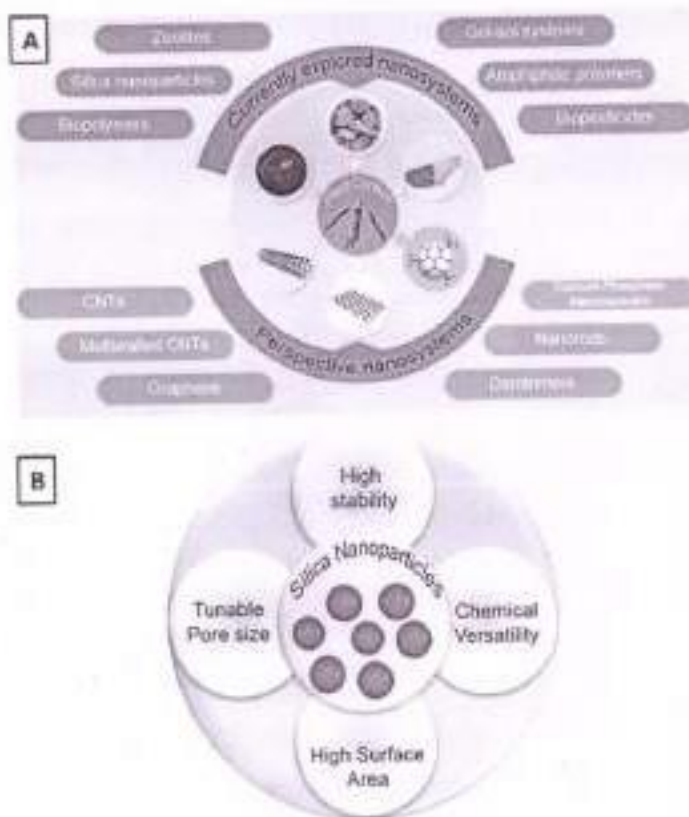


Fig. 4. Present and futuristic micro- and nano-formulations and delivery systems exhibiting potential to be used in the insect pest control in agriculture. (A) Currently explored nanosystems in pest management, i.e. Nanosystems of zinc, porous zeolites, alginate/chitosan polymers, WGA, and/or prospective nano-delivery systems such as silica, lipopeptides (e.g. CNT, graphene etc.), dendrimers and calcium phosphates. (B) Properties of silica nanoparticles beneficial for pesticide delivery applications.

Please cite this article as: Khundhvir, N., et al., Boding trends in integrated pest management using advanced micro- and nano-materials: Challenges and perspectives, Journal of Environmental Management (2016), <http://dx.doi.org/10.1016/j.jenvman.2016.09.071>

possess the advantages of imparting desired features to carry specific functions. A study revealed that surface functionalized silica nanoparticles, i.e., hydrophobic, hydrophilic or lipophilic coatings have a differential effect on *Sitophilus oryzae* mortality (Goswami et al., 2010). Similarly, silica nanoparticles capped with 3-mercaptopropyltriethoxysilane and hexamethyldisilazane was assessed against *S. oryzae* (Debnath et al., 2012) and found significantly effective. Silica nanoparticles have also been used for delivery of pesticides with the short half-life. For example, avermectin an insect chloride channel inhibitor that blocks neurotransmission shows a major problem in the field due to UV inactivation, Li et al. investigated porous hollow silica nanoparticles to deliver avermectin. These nanoparticles not only protected avermectin from UV degradation by encapsulation but also controlled its slow release. Furthermore, the nano-pesticide formulation exhibited a sustained-release pattern for nearly 30 days (Li et al., 2007). Under similar lines, insecticidal effect of nanostructured alumina was tested against two storage pests, *Sitophilus oryzae* and *Rhyzopertha dominica* (Stadler et al., 2010). Results demonstrate that exploitation of nanostructures with various functionalizations can impart significant effect on controlling pest population and present a scope for further testing their role as nanocides in pest management.

Other inorganic materials such as clay have also been studied for potential use in pesticide delivery. Clay nanoparticles form stacked platelet-like structure with a nanometer scale dimension of each platelet. Nano-clays provide more interactive surfaces when exfoliated and dispersed well due to the high aspect ratio (Chomade et al., 2011). Singh et al. developed pesticide delivery systems containing neem leaf powder, kaolin, and bentonite. The formulation demonstrated controlled and sustained release due to the presence of kaolin and bentonite particles while the release of thiram from kaolin-based formulation was found to be greater compared to bentonite (Singh et al., 2008). The clay based polymeric beads facilitate safe handling and finally supports efficient delivery (Roy et al., 2014).

Insecticidal effect of silver nanoparticles (AgNP) was investigated in two lepidopteran insects, castor semilooper (*Ahura jatara* L.) and asian armyworm (*Spodoptera litura* F.). Insects displayed delayed growth due to the accumulation of silver nanoparticles in their gut and a larger proportion of AgNP was detected in their fecal matter (Yan et al., 2014). More studies are needed to make a reliable assessment of the benefits and risks of using silver nanoparticles. Further insights in this research are anticipated over the coming years to address the present knowledge gap, by exploring other stractive inorganic nanosystems such as zinc oxide nanoparticles, calcium phosphate, etc (Ranjan et al., 2015).

#### 4.7. Advance polymeric delivery systems in pest management

Many new polymer based systems are being introduced as nanocarriers, however, progress is limited due to stringent clinical regulations, toxicity profiles, and overall therapeutic efficacy. New polymeric nanocarriers are being designed and explored in vivo, and their biocompatibility and delivery capacity is being correlated with bioavailability, tissue distribution and its elimination (Yasir and Rana, 2015).

Preparation of pesticidal nanoformulation requires their entrapment usually in biodegradable polymers for slow and sustained release. In general, few natural polymers like chitosan and alginates can serve as important functional nanocarriers for application purposes by encapsulating bio-actives/chemical pesticides. In particular, sodium alginate, an acid resistant poly (saccharide) anionic polymer, has been widely explored as a drug carrier because of its biocompatibility and non-toxicity. The prime mechanism governing the active ingredient release in the

physiological fluids is through the sodium-calcium exchange. The delivery of pesticidal compound through alginates has also been demonstrated. For example, the delivery of imidacloprid in the form of nanoformulation was achieved by utilizing sodium alginate biodegradable polymer (Bhugat et al., 2013). The pesticide entrapment efficiency was observed to be more than 98%; however, the formulation showed less cytotoxicity in *in vitro* studies over unformulated pesticide. Also, *in vivo* studies showed a significant reduction in leafhopper population on okra leaves after the treatment. Calcium alginate is rich in divalent salts and once it is introduced in the environment, the insoluble calcium alginate converts into a soluble alginate. This subsequently results in the solubilization of nanoformulation at alkaline pH and release of the pesticide is achieved (Kumar et al., 2014). Entrapment of Chlorpyrifos in a polymer based matrix formed by the combination of starch and alginate via crosslinking with CaCl<sub>2</sub> has produced pesticidal nanospheres (Bardisa, 2013; Roy et al., 2009). Interestingly, nano-pesticidal structures are bestowed with greater environmental and economical advantages such as low toxicity to non-targets due to release in a controlled manner as compared to bulk or commercial formulations. In a recent study, silver NPs were employed for nano-encapsulation of diazinon and chlorpyrifos, stabilized by the starch obtained from cassava. While the entrapment efficiency for the both the pesticides was over 95%, their release profiles exhibited slow and long lasting discharge in a buffered medium (Jhepoanagi et al., 2016). This study represents a facile, rapid and a cost effective method of synthesizing pesticidal nanostructures in the range of 23–30 nm which can further be extended for a large scale production. Application of highly hydrophobic pesticides is usually problematic for their low solubility in aqueous environments and risk to transdermal exposure if solubilized in an organic solvent. Efficacy of hydrophobic pesticides is largely dependent on their degree of dispersion. Effective dispersion can be achieved by designing an appropriate nano delivery system to generate stable dispersions. Bifenoxin, largely used to protect cotton plants from insects, were suspended in a nanoparticle formulation for improved uptake by insects and enhanced release. For this, flash nanoprecipitation technique was applied, which involves rapid mixing in a controlled chamber to achieve high supersaturation of active ingredient leading to rapid nucleation and growth. The growth is restricted by the adsorption of amphiphilic polymer on the surface. This technique creates nano-sized particles of <200 nm with stable dispersions (Liu et al., 2008). By choosing an appropriate polymer, the efficacy of different hydrophobic compounds can be improved with enhanced bioavailability. Various novel approaches using polymeric gels have been designed with major emphasis on environment-friendly management of fruit flies. Low molecular mass gelator consisting nanogels was prepared from a pheromone, methyl eugenol (Bhugat et al., 2013). The pheromone nanogels showed greater stability under all environmental conditions. At the same time, it has controlled and reduced the rate of evaporation of pheromone significantly. The nano-gel pheromone demonstrated an effective management of *Bactrocera dorsalis*, a prevalent pest for a number of fruits e.g. guava. This study demonstrated a practical low-cost green polymeric delivery strategy for crop protection.

Dendrimers are hyperbranched polymers and are used in drug delivery due to monodispersity, nano size and multiple modifications for surface functionalization (Khandalwal and Mishra, 2006). Use of fluorescent dendrimers for synthetic pesticide thiamethoxam showed promising results (Liu et al., 2015). Nanoparticle-mediated gene delivery including dendrimers and cationic polymers have received greater attention for delivery of nucleic acids (Jin et al., 2009). Interaction of nucleic acids with cationic polymers is electrostatically driven which provides the protection from



degradation and subsequently facilitate cellular uptake. Fluorescent nanoparticulate dendrimers were employed to assist their transfer across the cell membrane. The dsRNA for a chitinase-like gene was synthesized, mixed with fluorescent nanoparticles, and fed to the Asian corn borer (*Ostrinia furnacalis*). The results showed adverse effects on the insects such as small body size and failure to come individuals to molt (He et al., 2015a, b). These studies highlight new avenues in the utilization of pesticides based nano-systems. Overall, these strategies provide advantages of easy synthesis in bulk, flexibility to modifications, environmental stability, targeted delivery, and thus reducing the harsh effects of chemical pesticides.

### 5. Other applications

#### 5.1. Detection of pesticide residue

One of the important aspects of sustainable agricultural practices is to apply an effective concentration of pesticides in the crops. A significant amount of spray pesticide leaches off into the soil and groundwater consequently polluting the environment and demanding multiple applications. Furthermore, the persistence of pesticide residue in the harvested or processed food is of high importance to assess. Detection of pesticide residue in the environment needs to be monitored for the risk assessment purposes and to determine exposure limit (Barry et al., 2009). Several immunological assays were developed, though with a detection limit of one residue per assay thereby requiring several tests for the complex mixture. Also, the lack of quantitative measures for the accurate pesticide detection with minimal cost/resources was another constraint. An upsurge in micro and nano-based technological innovations suggest advantages of developing advanced microanalytical biosensors (Barry et al., 2009). Application of MNPs coupled with the range of biomolecules forms a novel detection system. Such systems offer the benefits of quick and simultaneous detection of residues in a complex system with greater sensitivity at nano-micro scale. Attachment of proteinaceous molecule or oligonucleotides on the nanostructures imparts them with the property of bio-recognition. By the virtue of target analytes to take part in specific chemical reactions upon interacting with biosensors, their detection becomes feasible by performing tests like colorimetric, fluorescent, conductometric or change in electric potential.

Biosensors developed for the detection of organophosphates (OPs) and carbamate pesticides are mainly based on their ability to inhibit cholinesterase enzyme. Cholinesterase (ChE) hydrolyses its normal substrate, acetylcholine into choline and acetic acid. Variation in pH due to the acid formation can be determined by measuring the pH indicating presence of pesticidal components. In a more sensitive and reliable detection system, ChE and choline oxidase (ChOD) were immobilized on Au-Pt metallic nanoparticles based electrode. Choline being a non-electroactive species was processed into  $H_2O_2$  by the action of ChOD for its further oxidation. The combined effect of bimetallic NPs assisted in electron transfer process by the increased surface area for the potentiometric detection of pesticidal residue (Suresh et al., 2012). In another highly sensitive method, polyvinyl pyrrolidone capped cadmium sulfide (CdS) quantum dots nanostructures were used for the detection of trichlorfon, based on the principle of inhibition of ChE. Enzymatically produced thiocholine from an artificial substrate acetylthiocholine was electrochemically distinguished (Li et al., 2010). Similarly, carbon nanotubes were developed for the identification of carbaryl with a detection limit of  $4.9 \times 10^{-10}$  M. Gold NPs (Au-NPs) hold intriguing properties for the preparation of biosensors and also providing a favorable microenvironment for the immobilization of the biomolecules. Furthermore, Au-NPs act as

signal transducers facilitating facile and direct transfer of electrons from immobilized electroactive species and the electrode. Their application is noticeable in the detection of the potential insecticides namely, methyl parathion, carbaryl, malathion, diazinon. Another electrochemical sensor employing specific detection methods such as molecular imprinting for organophosphate OPs such as parathion, methyl parathion, and fenitrothion were developed to circumvent the use of biomolecules with the benefits of high selectivity and improved precision. Zirconia NPs, exhibiting high affinity to the phosphoric group, was deposited on gold electrode facilitating OPs adsorption for its electrochemical detection. The study suggests the scope of field monitoring of OPs by designing portable electrochemical sensors and feasible NP printed gold electrode (Liu and Liu, 2005). Recent studies have reported novel enzyme-based nano-biosensors for the detection of an OE, paraoxon with the advantage of requiring very low concentration of starting sample (10–1000 nM) with detection limit close to  $5 \times 10^{-9}$   $\mu$ M. The nanomagnet silica core-shell was conjugated to OP hydrolase (OPH). Coumarin 1, a competitive inhibitor of OPH was used as a fluorogenic probe. Upon excitation, nanomagnet silica core-shell caused a quenching effect to intensely radiations emitting from coumarin. Paraoxon, competing for the enzyme active site, resulted in the reduction of emission, which is a direct measure of paraoxon concentration (Khatkar et al., 2015).

#### 5.2. Pesticide degradation

To reduce the potential exposure of pesticides in the environment, their removal via nano-based degradation methods were explored. As many conventional approaches are time-consuming and incur a high cost, contaminant removal by nanomaterials promotes rapid action with low cost (Adegun et al., 2016; Ghani et al., 2016). Photocatalytic degradation of hexachlorobenzene, cypermethrin and bifenthrin pesticides using titanium oxide NPs was demonstrated. At the interface of pesticide and  $TiO_2$  NP, a series of electron transfer reactions takes place along with the production of peroxide. Presence of hydroxyl radicals further accelerates photo-degradation (Yu et al., 2007). Dispersion of  $TiO_2$  over a porous zeolite silica was found to be effective in degradation of commercial pesticidal preparation of imidacloprid and phosphamidon (Tharwa et al., 2011). Degradation of various chemical classes was also evaluated though are not discussed in this review considering its limited scope.

### 6. Conclusions and future perspective

The thrust of MNT in agriculture is expanding at an accelerated rate and reaching almost every sector. In this review, application of MNT to curb the use of chemical pesticides and develop an environmental benign strategy for control of pest populations was given a major focus. Along with this, safe handling of pesticides and controlled delivery of agrochemicals using micro and nano-structures are also depicted. With the burgeoning potential of biopesticides, a comprehensive understanding of natural compounds and their properties is imperative. Understanding the potential of natural compounds and their utilization has been demonstrated in various studies for their effective role in controlling insect pest attack on plants. However, more studies of these compounds in the field are needed. Advances in MNTs have contributed to the successful development of nano or micro based formulations by achieving effective delivery, imparting enhanced activity, greater stability of the compounds and biodegradability. Importantly, choosing an ideal nanomaterial or formulation for field application is critical. Materials that are biocompatible, nontoxic and biodegradable are preferable and should be

investigated. It is critical to study both the short-term and long-term effects of the formulations on plant physiology to avoid adverse effects. Moreover, by integrating current agricultural technology with advancements in nanotechnology, improved crop productivity can be achieved while minimizing hazardous environmental and human health effects.

#### Acknowledgements

NK thank the Council of Scientific and Industrial Research (CSIR), Government of India, New Delhi for Senior Research Fellowship. Project funding under CSIR network programs in XII plan (BSC0107 and BSC0120) to National Chemical Laboratory is greatly acknowledged. JC would like to acknowledge financial support Department of Biotechnology, Government of India, New Delhi. AVB acknowledges the Director CSIR-NCL and CSMCRI for allowing to publish this work and Science and Engineering Research Board, Department of Science and Technology, Government of India for funding. We thank Dr. Bhushan Dholalia, for editorial assistance.

#### References

- Arora, A., Ghosh, M., Gaudenzi, A. 2010. Optimization of ultrasonic-assisted dispersive solid-phase microextraction based on nanoparticles followed by spectrophotometry for the simultaneous determination of five colorimetric dyes. *Ultrasonics Sonochem.* 17, 407–413.
- Arora, A., Ghosh, M., Gaudenzi, A., Mishra, N. 2010. Response surface methodology approach for optimization of simultaneous and sensitive ultrasonic-assisted adsorption onto Mn doped ZnO-ZnO<sub>2</sub> loaded on AC: kinetic and isotherm studies. *Indian J. Chem.* 48, 1433–1439.
- Banerjee, M., Tudu, R., Ghosh, G., Chak, G.P., Banerji, A.V., Choudhury, M.B., Ghosh, R., Ghosh, J. 2015. Calcium phosphate nanoparticles: green mediated carbon nanotubes for pH triggered controlled release drug release. *J. Mater. Chem. B* 3, 3811–3824.
- Bardhan, S. 2013. Optimization of encapsulation conditions of chitosan-coated nanoparticles. *J. Pharm. Pharm. Sci.* 5, 1246–1249.
- Burk, T., Saha, B., Saha, V. 2008. Nanotechnology: new avenue to pest control. *Biotechnol. Bioeng.* 100, 252–258.
- Chen, R.C., Liu, Y., Wang, J., Liu, G., Tian, C.A. 2008. Nanotechnology-based environmental sensors for monitoring chemical exposures. *J. Expo. Sci. Environ. Epidemiol.* 18, 1–18.
- Cheng, L.L. 2010. Nanosilver pesticide products: what does the future hold? *Inviron. Qual. Manag.* 19, 77–82.
- Cheng, D., Soriano, S.R., Bhattacharya, S. 2011. Efficient management of food pests by plant-derived nanoproducts. *Sci. Rep.* 1, 1–1344.
- Choudhary, S., Singh, R.P., Shrivastava, R. 2011. Bioefficacy of neem and Bt against pest insects *Melanoplus asiatica* in chickpea. *J. Agric. Sci.* 9, 87–89.
- Choudhary, H., Datta, S., Nandan, M.T., Hagar, M.I., Bhatt, A.S., De Haze, C., De Vries, E.L., Wijkman, S.W., Maras, H.J., Sips, A.J. 2008. Review of health safety aspects of nanotechnologies in food production. *Regul. Toxicol. Pharm.* 33, 53–62.
- Choudhary, C.L., Dey, R.E., Datta, S.G. 2012. Natural products as sources for new pesticides. *J. Nat. Prod.* 75, 1211–1242.
- Corina, C., Găvruta, R., Tabăra, R.E. 2010. Optimizing pyreneol transport: Methods for sustainable pest management. *Nat. Biotechnol.* 28, 161–168.
- Czizmadia, H., Bero, E., Balazs, C., Valkó, A., Mészáros, M.E., Kovács, M. 2002. Nanoparticle formulations based on nicotine disease resistance by natural extracts. *J. Agric. Food Chem.* 50, 8359–8364.
- Cyprus, R.P., Simpson, S.J., Douglas, A.E. 2013. The farmer, biocontrol and Food. Cambridge University Press.
- Das, C.P., Ma, H.S., Wang, K.S. 2011. New approach in pesticide delivery using nanotechnology: research and applications. *Ind. Eng. Chem. Res.* 50, 1612–1643.
- Das, J.M. 1997. Insecticides as tools in probing vital receptors and enzymes in suitable membranes. *Procs. Biochem. Phys.* 57, 221–224.
- Das, A.N., Wadley-Srinivas, V., Srinivas, A.K., Divyana, J.R., Goudarzi, G.G., Goudarzi, M.E., Rayan, T.A., Mee, L.C. 2011. Microscopic analysis of *Spodoptera litura* (Lepidoptera: Noctuidae) midgut: development before and after treatment with azadirachtin, neemazal, and deltamethrin. *J. Econ. Entomol.* 100, 747–755.
- de Lima, J.T., Faria, M.A., Costa, E.S., De Souza, J.R., Mavedola, J.V., Jorini, A.L.B. 2014. Effect of different formulations of neem oil-based products on control *Diatraea saccharalis* (Lepidoptera: Tortricidae) on maize. *J. Stored Prod. Res.* 58, 49–53.
- De, J., Ghosh, N., Das, C., Das, J., Das, S.R. 2010. Chlorophyll a quantum dot- and silica nanoparticle mediated DNA delivery for gene silencing in *Arabidopsis thaliana* model system. *ACS Appl. Mater. Interfaces* 2, 1953–1957.
- Demireven, M., Ghosh, M., Adhikari, A., Gaudenzi, A., Langreck, M., Tseng, J., Agarwal, S., Gupta, M.P. 2015. Ultrasonic-assisted adsorption of reactive green dye onto ZnO–Co-NiO<sub>2</sub> equilibrium isotherms and kinetic studies—response surface optimization. *Appl. Surf. Sci.* 304, 780–788.
- Dhawan, V.P., Choudhary, V.P., Ghosh, P.R., Ghosh, R.R., Gupta, V.S., Gu, A.P. 2013. Molecular insight into resistance mechanism of *Leishmania* insect pest against insecticides. *J. Proteome Res.* 12, 4727–4737.
- de Oliveira, J.L., Targui, E.Y.S., Sakell, M., Alkhatib, H., Frazão, L.E. 2014. Application of nanotechnology for the encapsulation of botanical insecticides for sustainable application: prospects and previous. *Nanoscale Adv.* 12, 1530–1541.
- Debnath, N., Das, J., Seth, B., Choudhary, R., Bhattacharya, S.C., Gaudenzi, A. 2011. Encapsulation effect of silica nanoparticles against *Helicoverpa zea* (L.). *Procs. Biochem. Phys.* 59, 99–105.
- Debnath, N., Mitra, S., Das, J., Gaudenzi, A. 2012. Synthesis of surface functionalized silica nanoparticles and their use as entomotoxic nanocides. *Procedia Technol.* 22, 252–258.
- Datta, R.M., Stevens, J.A., Lee, T.E., Gupta, V.S., Ghosh, R.R., Anandhan, M.S. 2010. Comparison of polyoxin type I and II proteinase inhibitors gene action proteinase against insect damage in the field. *Proc. Natl. Acad. Sci. U. S. A.* 107, 1201–1205.
- Das, M.E., Costa, E.S., de Souza, M.Z.D.F., Fernandes, J.B., Wadley, J.M., Srinivas, A.L. 2015. Development of a new method to prepare nano-nanoparticles loaded with extracts of *Andropogon* species, their characterization and use in controlling *Phaenicia sericata*. *J. Agric. Food Chem.* 63, 9324–9328.
- Das, M., Ghosh, H.Z., Adhikari, A., Gaudenzi, A. 2010. Response surface methodology approach for optimization of adsorption of basic Green 8 from aqueous solution onto ZnO@SiO<sub>2</sub> 2-MP-NC. *Kinetic and isotherm study. Spectrochim. Acta Mol. Biomol. Spectrosc.* 75, 232–240.
- Dattavadi, Y., Bhattacharya, M.V., Palitkar, R.M. 2011. Perspectives for nano-technology enabled protection and nutrition of plants. *Biotechnol. Adv.* 29, 790–803.
- Das, T., Gaudenzi, J., Ghosh, W., Johnson, T., Frykhol, N., Kulk, J., Maitra, P., Mohan, L., Srinivas, A. 2012. Novel nanosilica-coated core of Ag<sup>+</sup> loaded nanoparticles. *Sci. Rep.* 2, 290–295.
- DeGroot, P.L., Reddyrajah, J.R., Chou, J.R., Haddad, S., Lawrence, G., Wan, J.F., Potts, J., Robinson, A., Thomas, S.M., Srinivas, C. 2010. Food security: the challenge of feeding 9 billion people. *Science* 327, 822–828.
- Dasgupta, J.W., Gaudenzi, M.M., Prasad, S.A., Kulk, H. 2014. Efficient cell transfection by chitosan-coated poly (D,L-lactide-co-glycolide) and biological polyethylene glycol. *Colloids Polym. Sci.* 292, 110–116.
- Dasgupta, S.H., Wadhawan, P.S. 2007. Water in nano-sized phases. *Nat. Nanotechnol.* 2, 1271–1272.
- Dasgupta, S., Roy, J., Sengupta, S., Choudhary, N. 2010. Novel applications of modified lipid nanoparticles of nanotechnology against insect pests and pathogens. *Thin Solid Films* 518, 1222–1227.
- De, R., Das, J., Pal, M., Mukherjee, K., Gu, C., Saha, J. 2012a. Fluorescent nanoparticle-mediated siRNA toward genetic control of maize pests. *Adv. Mater.* 24, 4580–4594.
- De, S., Zhang, W., Li, D., Li, P., Zhu, Y., Ai, M., Li, J., Cai, Y. 2010. Preparation and characterization of double-shelled mesoporous nanoparticles based on copolymer matrix of silica–polyacrylate–chitosan. *J. Microchem. Biotechnol.* 11, 1270–1278.
- Dhalwani, N.C. 2010. Ultrasonic: a novel method for control of metabolic and cellular events. *J. Evol. Biochem.* 98, 772–778.
- Dhalwani, N., Ghosh, H.Z., Ghosh, M., Palitkar, R.M. 2014. The biochemistry behind insecticide efficacy. *Indian Chem. Process* 2, 12.
- Dhawan, V.P., Sengupta, S.M. 2008. Bioactive molecules for the art and science of nanotechnology-based pest control. *Ind. Eng. Chem.* 40, 845–848.
- Dhawan, V., Ghosh, C., Ghosh, I. 2013. Food associated toxins in ecological networks. *Trans. R. Soc. Open Sci.* 10, 128–142.
- Dhawan, V.P., Sengupta, S.M., Sengupta, T.A., Srivastava, L.A., Srinivas, P., Saha, B., Maitra, M. 2010. Facile formulation of silica–silver–nanoparticle encapsulated chitosan and chitosan for enhanced insecticide delivery. *New J. Chem.* 40, 1777–1784.
- Dhawan, V.P., Das, J., Sengupta, S., Kulkarni, J. 2010. Insecticidal and antifungal applications of neem oils and their relationship to azadirachtin content. *J. Agric. Food Chem.* 48, 1480–1487.
- Dhawan, V.P., Srinivas, S., Haddad, C. 2010. Commercial opportunities for production based on plant essential oils in agriculture: industry and consumer products. *Phys. Chem. Res.* 48, 197–204.
- Dhawan, V., Srinivas, S., Sengupta, S.M., Srinivas, A., Choudhary, N. 2012. Biodegradable polymer based encapsulation of neem oil nanosuspension for controlled release of Ag<sup>+</sup>. *Colloids Polym. Sci.* 290, 1720–1726.
- De, S., Lewis, J.C., Yi, K. 2005. Nanoparticle-mediated gene delivery. *Methods Mol Biol.* 144, 347–377.
- De, S., Wadhawan, P., Sharma, N., Mukherjee, S., Srinivas, G., Choudhary, H., Seth, B., Gupta, V., Gu, A. 2014. Way toward “green pesticides”: molecular characterization of insecticidal activity of coffee acid against *Helicoverpa zea* (L.). *J. Agric. Food Chem.* 62, 10447–10454.
- Dhalwani, N., Ghosh, H.Z., Adhikari, A., Bhattacharya, T., Karan, S., Choudhary, M. 2015. An organophosphorus hydrolysis-based biosensor for direct detection of parathion using silica-coated magnetic nanoparticles. *Appl. Biochem. Biotechnol.* 178, 259–271.
- Dhalwani, J., Ghosh, M., Datta, R.M., Wang, R. 2012. Mathematical modeling systems in nanotechnology: opportunities and challenges. *Chem. Soc. Rev.* 41, 3024–3040.





# Novel Concept of Attaching Endoscope Holder to Microscope for Two Handed Endoscopic Tympanoplasty

Mubarak M. Khan<sup>1</sup> · Sapna R. Parab<sup>1</sup>

Received: 6 July 2015 / Accepted: 17 September 2015 / Published online: 6 November 2015  
© Association of Otolaryngologists of India 2015

**Abstract** The well established techniques in tympanoplasty are routinely performed with operating microscopes for many decades now. Endoscopic ear surgeries provide minimally invasive approach to the middle ear and evolving new science in the field of otology. The disadvantage of endoscopic ear surgeries is that it is one-handed surgical technique as the non-dominant left hand of the surgeon is utilized for holding and manipulating the endoscope. This necessitated the need for development of the endoscope holder which would allow both hands of surgeon to be free for surgical manipulation and also allow alternate use of microscope during tympanoplasty. To report the preliminary utility of our designed and developed endoscope holder attachment gripping to microscope for two handed technique of endoscopic tympanoplasty. Prospective Non Randomized Clinical Study. Our endoscope holder attachment for microscope was designed and developed to aid in endoscopic ear surgery and to overcome the disadvantage of single handed endoscopic surgery. It was tested for endoscopic Tympanoplasty. The design of the endoscope holder attachment is described in detail along with its manipulation and manoeuvring. A total of 78 endoholder assisted type 1 endoscopic cartilage tympanoplasties were operated to evaluate its feasibility for the two handed technique and to evaluate the results of endoscopic type 1 cartilage tympanoplasty. In early follow

up period ranging from 6 to 20 months, the graft uptake was seen in 76 ears with one residual perforation and 1 recurrent perforations giving a success rate of 97.435 %. Our endoscope holder attachment for gripping microscope is a good option for two handed technique in endoscopic type 1 cartilage tympanoplasty. The study reports the successful application and use of our endoscope holder attachment for gripping microscope in two handed technique of endoscopic type 1 cartilage tympanoplasty and comparable results with microscopic techniques.

Level of evidence: IV.

**Keywords** Justtack · Endoscope holder · Endoscopic cartilage tympanoplasty

## Introduction

Endoscopic surgeries have gained popularity not only in Otolaryngology but also in other surgical fields. Endoscopes and the Hopkins rod lens system have revolutionized the medical field in last half century. Endoscopic approach for paranasal sinuses is well known. The well established techniques in tympanoplasty are routinely performed with operating microscopes for many decades now. Endoscopic ear surgeries provide minimally invasive approach to the middle ear and evolving new science in the field of otology which is in its nascent stage. Migrating from classical Wullstein's microscopic tympanoplasty techniques to endoscopic tympanoplasty techniques is slow and tough but still a new horizon rising in the field of otology. Rigid endoscopes have been used by otorhinolaryngologists for sinus surgery and recently even for otologic surgeries. The advantages of endoscopic sinus surgeries are well known. In otologic surgery too,

---

Electronic supplementary material The online version of this article (doi:10.1007/s12070-015-0916-6) contains supplementary material, which is available to authorized users.

---

✉ Mubarak M. Khan  
drmubarakkhan@yahoo.co.in; ent.khan@gmail.com

<sup>1</sup> Department of Otorhinolaryngology, M.I.M.E.R. Medical College, Pune 410507, India



Fig. 1 Endoscopic view of middle ear showing inaccessible areas by microscope

endoscopes have several advantages to offer. (1) It allows visualization of the whole tympanic membrane and the ear canal without having to manipulate the patient's head or the microscope, (2) it extends the operative field in transcanal procedures into structures usually hidden from the microscope (anterior tympanic perforation, posterior retraction pocket, facial recess, and hypotympanum) (Fig. 1), (3) it visualizes structures from multiple angles as opposed to the microscope's single axis along the ear canal [1]. Disadvantage of the endoscopic surgeries is that it is one-handed surgical technique as the non-dominant hand of the surgeon is utilized for holding the endoscope. During the haemorrhage and drilling, it becomes difficult to use suction and instruments both along with endoscope in single handed technique. Even during fogging, one needs to remove endoscope again and again for lense cleaning. As endoscopic ear surgery (EES) is in developing stage, many of the times during drilling one needs to use microscope. And whenever one wants that multiple magnifications to visualize middle ear structures sometimes during ontological surgeries, microscope may be needed. This necessitated the need for development of the endoscope holder attachment which would allow both hands of the surgeon to be free for surgical manipulation during EES and allow alternate use of microscope whenever needed during tympanoplasty. The purpose of this study was to report the early and preliminary experience with the endoscope holder attachment for gripping microscope for endoscopic cartilage tympanoplasty. Incorporating the endoscope holder attachment into the armamentarium of Otorhinolaryngologic surgeries will not only contribute to the concept of documentation but will also augment the expanding uses of endoscope both for diagnostic and therapeutic use. The use of endoscope holder attachment in otolaryngologic surgeries may be considered as a new horizon. The idea is not just to hold the endoscope during surgeries, but to move and manipulate it as the left hand does it more or less. Operating Microscopes have range of

motion in space during ontological surgeries for focusing the desired object for magnification. This whole range of motions can be applied for driving the endoscope smoothly in any biological cavities once an endoscope holding attachment is fixed to optical system of any operating microscope (*Patent Application No. 3300-Mum-2013*): [2]. Robotic arms can do this, but they are too expensive. Hence this is an economical way to simulate it. Every otologist is well versed with the use of the microscope for ear surgeries. Operating microscope can be either mounted on floor stand, or ceiling or can be fitted on to the operating table in portable version. These operating microscopes have 360 degree rotation and motion in space for focusing and magnification of object. The same motions can be helpful for driving the endoscope in biological cavities. This is achieved by holding endoscope with metallic plate and gripping the optical system of any microscope just above objective lense (*Patent Application No. 3300-Mum-2013*): [2].

## Materials and Methods

Prior to developing the endoscope holder attachment, we performed the single handed technique of EES for 5 years. However due to the technical difficulties of single handed surgery, the Endoholder attachment was devised.

A total of 78 consecutive primary endoscopic type 1-cartilage tympanoplasties for pars tensa perforations were operated with our endoscope holder attachment gripping to microscope (Fig. 2). from September 2013 to November 2014 in M.I.M.E.R Medical College and Sushrut ENT Hospital with a follow up period ranging from 6 to 20 months. There was no ossicular chain impairment. There were 43 males and 33 females in the study group. The mean age of the study group was  $28.75 \pm 4.46$  years. The youngest patient was 11 years of age and the oldest was 47 years of age. The average preoperative Air Bone Gap in the study group was  $33.25 \pm 2.74$  dB and post operative AB gap closed up to  $8.57 \pm 2.24$ .



Fig. 2 Endoscope holder with Microscope gripping attachment (Justtach)

**Design of Our Endoscope Holder Attachment to Microscope (Patent Application No. 3300-Mum-2013): [2]**

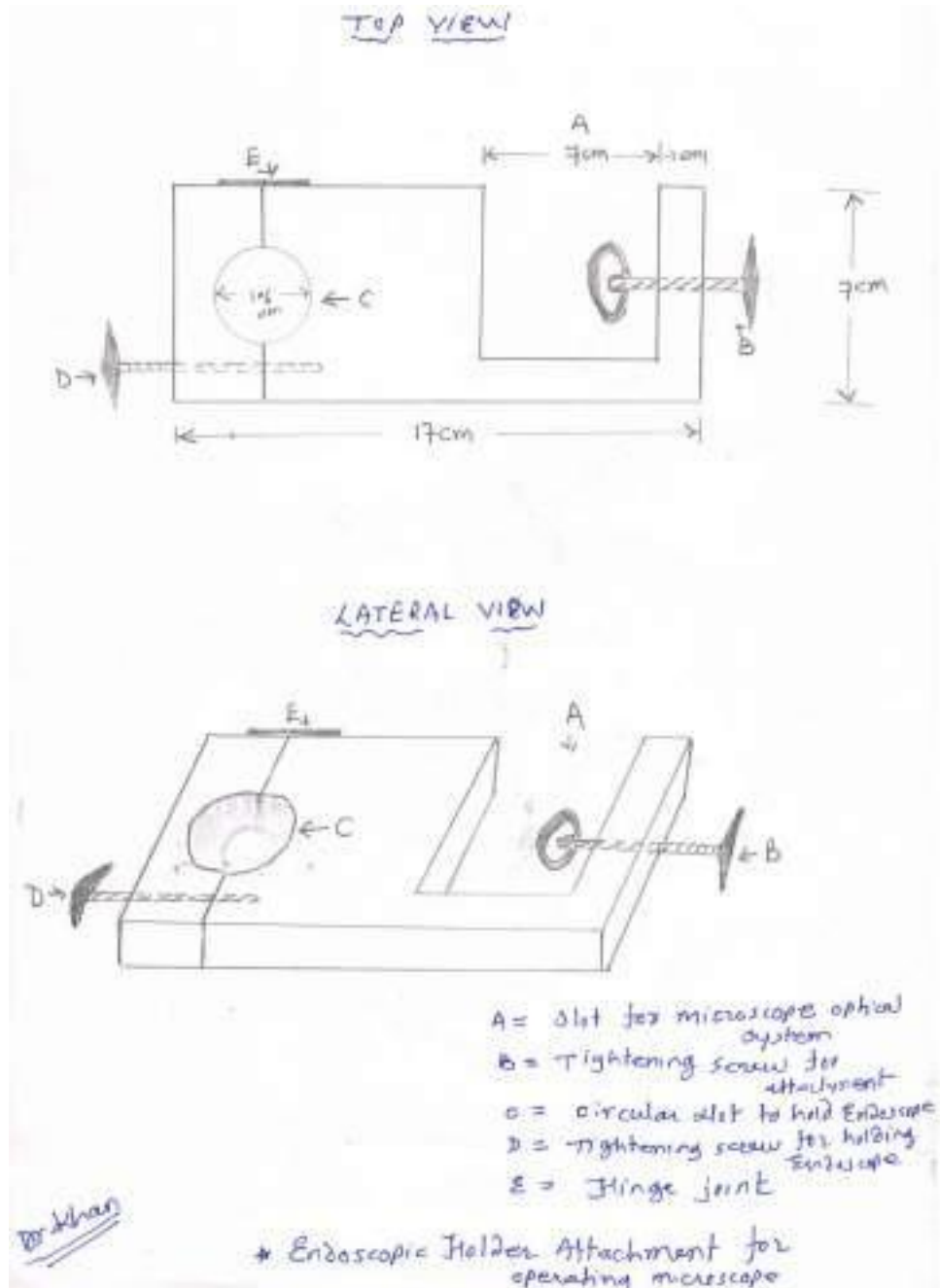
The object of the present innovation is to create a device of simple construction, and therefore low cost, which makes it possible

- (a) To easily hold any rigid endoscope to any medical operating microscope's optical body

- (b) To use endoscope and operating microscope alternately during surgery

The innovation achieves this objective by using a piece of a metallic plate of 170 9 70 12 mm in dimensions with a circular slot measuring 16 9 16 mm in diameter (Fig. 3C) and square slot (Fig. 3A) is rigid endoscopic holder can be affixed to optical system of any operating ENT microscope with 1 tightening screw (Fig. 3B) with the optical observation instrument of the microscope intact.

Fig. 3 Diagrams of endoscope holder with Microscope gripping attachment (Justtach) submitted to patent office





The circular slot (Fig. 3C) of 16 mm diameter in metallic plate half of which is on main attachment linking to optical system and half of which opens outside to accommodate any rigid endoscope for fixation (action is represented by figures). This opening part of metallic plate is attached to main part with hinge joint (Fig. 3E) with 90 degree of motion. This opening part then can be fixed to main part of metallic plate with adjustable screw (Fig. 3D). In other variant instead of fixing screw (Fig. 3B) on right lateral side, it is on front side. The inner part of circular slot (Fig. 3C) is reinforced with soft silicone or malleable plastic thin material to hold neck of endoscope which holds it firmly and does not cause undue pressure on gentle optical fibers of any rigid endoscope. This slot (Fig. 3C) is at 60 mm distance from its attached end and can be made of any suitable diameter to accommodate different rigid endoscopes of different diameters.

Thus all actions of operating microscopes are utilized for rigid endoscope which are very valuable when this endoscope holder is directly attached and secured to optical system of any operating microscope.

The described apparatus is combined, in particularly advantageous embodiments, with known operating microscopes and in particular with portable stands, with stands for wall or ceiling attachment, and with stands which have a table base or a floor-clamping device. Combination with a vertically adjustable horizontal arm or with a swivel arm is particularly suitable. The basic idea is to apply all microscope motions in space to drive the endoscope. Our endoscope holder attachment is universal and is compatible with all Endoscopes and cameras of all the brands.

#### *Operating Theatre Requirements*

Zero degree 4 mm endoscope with triple charge coupled device Camera (Karl Storz, Germany) is held in slot for endoscope on Endoholder attachment and this assembly is firmly fixed to optical system of microscope just above objective lens (Fig. 4). The horizontal arm of microscope stand balanced to avoid undue and uncontrolled vertical motion of microscope. Incorporating the endoscope into the microscope stand with endoscope holder augments the advantages and applicability and allows alternate use of both (Fig. 5).

#### *Preparation of the Patient*

The patient is prepared and draped in the usual fashion with the ipsilateral shoulder pulled down. The ear canal is infiltrated with 2 % lidocaine with 1 in 2,00,000 adrenaline. All patients were operated under general anaesthesia except 5 who were operated under local anaesthesia. Pre-operatively, the patient is explained about the endoscopic

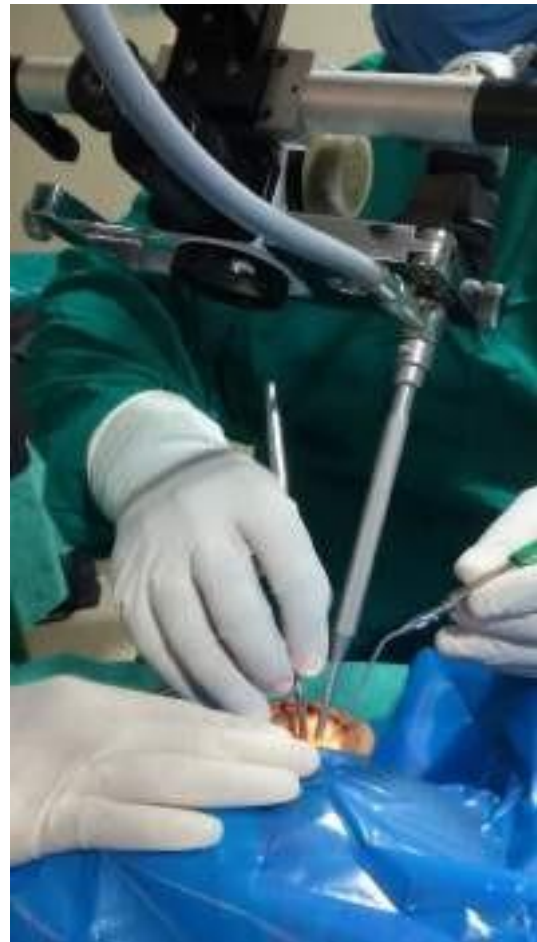


Fig. 4 Endoscope holder with Microscope gripping attachment (Justtack) in use for Endoscopic Tympanoplasty

procedure and is instructed not to move the head in case of local anaesthesia. The assistant steadies the head of the patient by placing the hand over the head of the patient to avoid any accidental head movement and injury in case of local anaesthesia (Fig. 6).

#### *Adapting to the Technique of Two Handed Technique of Endoscopic Tympanoplasty*

After developing the Endoholder attachment to microscope, initially the application and use was demonstrated on Cadaveric temporal bone for endoscopic middle ear dissections (Fig. 7). During the early days of practice of cadaveric temporal bone endoscopic two handed dissection, the manipulations of the endoscope mounted on endoscope holder into and out of the ear canal was practiced. The next step was targeted towards hand eye coordination and the two handed technique of instrumentation (dominant hand for micro ear instruments and non-dominant hand for suctioning). We have dissected five wet



Fig. 5 Endoscope holder with Microscope gripping attachment (Justtach) in use for Endoscopic Tympanoplasty in Operation theatre



Fig. 7 Endoscope holder with Microscope gripping attachment (Justtach) in use for cadaveric dissection demonstration in courses



Fig. 6 Endoscope holder with Microscope gripping attachment (Justtach) in use for Endoscopic Tympanoplasty under local anaesthesia



Fig. 8 Cadaveric dissection demonstration. Middle ear Endoscopic anatomy

temporal bones each before performing the EES with the Endoholder attachment (Fig. 8). As the endoscope holder attachment is firmly gripping the Operating Otomicroscope, hence the familiar movement of fine focusing was used for the further smooth advancement of the endoscope into the ear canal. After being thoroughly trained in two handed technique of EES, both the authors started with operating in patients with small perforations and later on to include tympanoplasties for large perforations.

*Procedure of Endoscopic Cartilage Tympanoplasty with Endoscope Holder (Figs. 9, 10, 11, 12, 13, 14, 15, 16)*

Instruments routinely used in microscopic ear surgery were used (rosen sickle knife, belluci's knife, picks, elevators,



Fig. 9 Tragal cartilage harvestation



Fig. 12 Endoscopic middle ear view



Fig. 10 Left anterior perforation with transcanal incision



Fig. 13 Tragal cartilage slicing with slicer



Fig. 11 Elevation of TM flap



Fig. 14 Sliced tragal cartilage of 0.5 mm thick shield graft kept as underlay

and currettes. Using all aseptic precautions, permeal incision is taken. Tragal cartilage graft is harvested via the horizontal incision on the tragus (Fig. 9). After freshening the edges of the pars tensa perforation, tympanomeatal flap is elevated (Figs. 10, 11). Ossicular mobility is confirmed and thorough middle ear inspection done (Fig. 12). The tragal cartilage perichondrium graft is sliced [3–6] with Precise cartilage splitter (Kurz, Germany) to 0.5 mm thickness with perichondrium retained on one side (Fig. 13). The tragal cartilage is not reinforced by temporalis fascia. Sliced cartilage of 0.5 mm thickness kept as

underlay shield graft (Fig. 14). Tympanomeatal flap reposed back (Fig. 15). Through out during procedure suction is held in left hand to avoid the fogging and to achieve cooling of endoscope generated heat as reported in previous study [16]. Intermittent irrigation is done for cooling of endoscope as well as to achieve cleaning of endoscope lense [16]. This is possible only with two handed endoscopic technique using Endoholder (Fig. 16). The stability rendered to the endoscope with the endoscope holder aids and augments the technical usage of endoscope





Fig. 15 View after TM flap reposition



Fig. 17 1 Year post op view of successful type 1 endoscopic cartilage tympanoplasty



Fig. 16 Simultaneous irrigation and suction during EES for cleaning and cooling the endoscope

in ear surgery during all steps of the routine tympanoplasty (including freshening the edges of perforation, tympanomeatal flap elevation, and underlay technique placement of sliced cartilage graft). No canalplasty is done in this series. Wherever we faced problems of narrow canal, we used specially designed Karl Storz zero degree endoscope

of 14 cm long and 3 mm diameter to improve instrument access to middle ear. All procedures performed were recorded for documentation. All procedures were done using our Endoholder attachment exclusively. Advantages and disadvantages of the endoscope holder attachment, if any, during all surgeries were noted and documented precisely.

## Results

The endoscope holder assisted 78 endoscopic type 1 cartilage tympanoplasties have been operated from September 2013 to November 2014 for pars tensa perforations with follow up period ranging from 6 to 20 months, which is definitely a very short follow up to evaluate Tympanoplasty outcomes. This technique, being a developing art and novel concept of two handed technique of endoscopic cartilage tympanoplasty, is thus an early attempt to demonstrate and report the use of our endoscope holder for micro ear surgeries. During the early use of endoscope holder for tympanoplasty we started with small pars tensa perforations and then extended the use of the endoscope holder for large perforations (Table 1).

Endoscope is kept most of the times at the isthmus and if the patient moves a bit, the horizontal arm of the microscope can be easily moved in the upward direction due to its spring action. No middle ear injury is reported in our series.

In our early follow up period ranging from 6 to 20 months in 76 ears operated for endoscopic cartilage tympanoplasty, the graft uptake was seen in ears with one residual perforation and four recurrent perforations giving a success rate of



Table 1 Gender distribution of perforations

Perforations involving quadrants	Number of ears		
	Male	Female	Total
One	11	7	18
Two	14	11	25
Three	9	8	17
All	13	5	18
Total	47	31	78

97.206 %. Our previous study [3] with sliced tragal cartilage perichondrium graft using microscope gave a success rate of 98.2 %. The present study was carried out using the same technique of slicing the cartilage [3] to 0.5 mm thickness and using it for type 1 tympanoplasty by two handed technique with endoscope of 4 mm diameter held in our designed endoscope holder. Comparing the results present endoscopic primary cartilage tympanoplasty technique with our published microscopic primary cartilage tympanoplasty outcome [3] the results are equivalent in terms of outcome for short term follow up.

## Discussion

Even though it has been two decades since endoscopy was first used to explore mastoid cavities, the endoscope is used infrequently for surgical management of ear disease [7–13].

Endoscopic ear surgery allows a minimally invasive approach to the middle ear [14]. The endoscope also allows an elaborate view of the three main elements in tympanoplasty surgery: ear canal, tympanic membrane, and the tympanic ring [15]. In order to augment the applicability and to overcome the disadvantage of single handed technique of endoscopic surgery, the Endoholder has been designed. Initially after designing the holder, its use and applications were tested on dry temporal bone and also for office based oto-endoscopies. Later on its use and applicability was tested for cadaveric temporal bone dissection.

A total of 76 endoscopic cartilage tympanoplasties were operated with endoscope holder by both the authors. During endoscopic cartilage tympanoplasty with the endoscope holder we observed several advantages.

1. Our innovation patent app no 3300/mum/2013 describes.

a. Simple gripping of any operating microscope optical body with mechanically tightening screw to hold Rigid endoscope by means of endoscope holding metallic plate (rigid endoscope too is held

in circular opening with mechanical fixing) irrespective of whether microscope functioning or not.

- b. By gripping microscope optical system by this way, I use existing all microscope movement in space and apply simply to endoscope movement (which is very important for two hand techniques) [Note: I mean movement of microscope and not function. Hence both systems (endoscope and microscope) are functioning independently].
- c. Two handed technique means using both hands of surgeon for operation (at present in endoscopic ENT or other surgeries, surgeon hold endoscope in left hand and uses right hand for doing surgical steps).
- d. At present ear surgery is done by using microscope (90 %) and few surgeons use endoscope (10 %). presently disadvantage of EES is that one hand is compromised to hold endoscope. But many advantages of endoscopes are surpassing the microscope in ear surgery. Single hand technique will become two hand technique by using our simple innovation (Note: both endoscope and microscope are functioning independently).
- e. Why to hold endoscope in metallic plate grip it to microscope?
  1. To use both hands for surgery.
  2. To apply all movements (not functions) of microscope optical body for endoscope movement.
  3. By doing so endoscope can be moved more or less like using left hand which is important for any surgery.
  4. We are not using both system(endoscope and microscope) simultaneously.
  5. But both system can be used alternatively which give added advantages.
  6. Every ENT surgeon owns microscope for ear surgery. Now by using our innovation he will be able to do EES with two hands (at present no body in the world is doing this) with simply fixing one endoscope holding metallic plate.
  7. Anything which will be holding endoscope, if fixed to microscope optical body will automatically apply all movements of operating microscope for driving endoscope during surgery (this is the basis of our innovation).
  8. Presently EES is in nascent stage and mainly done as single handed technique. By our innovation it will be two handed technique and will open new horizons in many surgical fields including ENT.

9. Possibly after my demonstration in many congresses, microscope manufacturers may provide inbuilt metallic plate which will be holding endoscope (very simple but nobody thought till this date. Our innovation describe this firstly).
  10. Considering the many advantages of two handed technique in endoscopic surgery, our innovation is discovery of new thing which was unknown till this date and very much applicable in many areas.
- f. Our simple innovation is “holding rigid endoscope in metallic plate or by any other means and fixing it to operating microscope” the benefits are described in patent.
  - g. At present endoscopic Ear Nose Throat surgery or any other endoscopic surgery is carried out by holding rigid endoscope in left hand and operating with right hand. Our innovation will allow both hands to be used for surgery as endoscope is held metallic plate and secured to microscope. This allows application of all movements of microscope to endoscope.
  - h. Alternately means when I want to operate with endoscope I may use endoscope and when microscope, I will use microscope. Note here I am not using both the instruments simultaneously as described in many patents.
  - i. In simple ways: hold the rigid endoscope and secure it by fixing to microscope optical head for applying all its only mechanical movements to endoscope as your left hand does during holding endoscope for surgery.
  - j. All present patents describes simultaneous observation through endoscope and microscope. My purpose is different. Just applying microscope movements to rigid endoscope moving.
  - k. To summarize:
    1. Simple innovation of holding endoscope in metallic plate and fixing it to microscope optical body.
    2. By doing this idea is to use all microscope mechanical movements not functions for movement of endoscope in space.
    3. Instead of developing separate stand to hold endoscope, it can be held as described in our innovation. Thus a very cheap but beneficial alternative.
    4. Contemporary single handed technique in EES will be two handed technique.
    5. Both systems (endoscope and Microscope) works independently with their own

advantages and disadvantage and not remotely related functionally. Only implementation of microscope stand actions for driving endoscope in space mechanically during surgery.

#### Advantages of Our Endoscope Holder

1. Both the hands of the surgeon are free for operative intervention which is of paramount importance both for diagnostic and operative procedure.
2. When angled endoscope (30°, 45°, 70°) is mounted on the endoscope holder allows better visualisation of sinus tympani, facial recess, anterior tympanic cavity and hypotympanum with just rotation of the endoscope within the Holder.
3. The elevation of the tympanomeatal flap and tympanic membrane assessment is much better as the left hand holds the suction cannula continuously (similar to Microscope ear surgery).
4. It can be used effectively without compromising the surgical field.
5. As an effective alternative for documentation and a useful teaching aid.
6. As endoscope is fixed onto the holder, the stability of the endoscope, camera and image on the monitor is ensured throughout.
7. Minimizes the need for assistance.
8. No surgeon fatigue in holding the endoscope as the endoscope is fixed on the endoscope holder (as compared with single handed EES).
9. As the endoholder attachment is mounted on optical system of Microscope Stand, the fine focus of the microscopic stand can be utilized for additional manipulation/advancing into the external auditory canal.
10. Mastoid bandage is not required.
11. Success rate is equivalent in early follow up compared to microscopic technique [3] as the placement of graft is more precise due to the total view of the tympanic membrane (Fig. 17).
12. Fogging of the endoscope is avoided by use of suction cannula.
13. Canalplasty can be done with the drill in the right hand and suction in the left hand.
14. As endoscope and microscope are on same platform, the alternate use of both is possible. This is very much necessary for initial training in EES.

#### Disadvantages

1. At times, narrow canal can pose difficulty during endoscopic tympanoplasty, but can be circumvented

by canalplasty. In this series not a single canalplasty was carried. We use specially designed Karl Storz 14 cm long, 3 mm diameter 0° endoscope in narrow canal.

2. During hemorrhage, the manipulation of the endoscope in and out of the operative field may be time consuming.
3. Possible potential disadvantage is the thermal damage to the middle ear due to endoscope light carrying fibres has been reported previously and measures to avoid excessive temperature elevation in EES has been suggested [16]. This is circumvented by following simple techniques during the use of our endoholder assisted transcanal two handed endoscopic tympanoplasty.
  - a. The endoscope is kept at a distance mostly at the isthmus of external auditory canal.
  - b. Continuous suction is held in left hand during the procedure as suggested in previous study [16].
  - c. Intermittent irrigation gives the cooling effect to endoscope [16] and added cleaning of the tip of the endoscope which avoids frequent its removal for defogging and cooling as done in single handed EES.
4. Overall cost of the endoscope holder in addition to the routine ear instruments.
5. Care is to be taken to avoid accidental injury due to head movement to the tip of the endoscope.

The learning curve for endoscope holder aided endoscopic tympanoplasty may not as steep as that for routine endoscopic or microscopic surgery. Many experienced with endoscopic surgeries will find the technique easy to master, but surgeons who have limited themselves to an entirely microscopic otology practice are likely to find endoscope holder aided endoscopic surgery more difficult to perform. Despite this, with sufficient training and practice the technique may be adopted by all. It is important to remember that the initial steps of the surgery are the most difficult. Once comfortable with partial use of the endoscope holder movements and manipulation, most surgeons may prefer to use the endoscope holder aided endoscopic surgeries.

#### *Extending the Use of Endoscope Holder for Ear Surgeries*

At present we have demonstrated the early use of our endoscope holder for tympanoplasty. The further use and applicability of endoscope holder needs to be extended to ossiculoplasty and mastoid surgeries. It will be useful to collaborate and associate with other, more experienced

surgeons who are more familiar with endoscopic ear, sinus and laryngeal surgeries to predict its consistent progress.

## Conclusion

This Endoholder developed as a modification of microscopic stand, incorporates the endoscope onto the microscope stand and augments the applicability of the endoscope into ENT practice. With little practice, endoscope holder can be used routinely in all ENT surgeries. endoscope holder is a valuable adjunct to conventional endoscopic surgeries. The technique though useful has a different learning curve and training is useful to allow more familiarity when getting started.

## Compliance with Ethical Standards

Conflict of interest Application for Patent in respect of “Rigid Endoscope Holder and Endoscope Fixing Method with Microscope Gripping Attachment” bearing Application No. 3300/MUM/2013 in the name of Dr. Mubarak Khan to Patent controller of India. And “JUSTTACH” is tradename secured for this. Dr Sapna Parab has helped in preparing the manuscript and evaluated endoscopic holder actively during various otolaryngological surgeries independently and along with first author.

Ethical Approval All procedures performed in studies involving human participants were in accordance with the ethical standards of the institutional committee and with the 1964 Helsinki declaration and its later amendments or comparable ethical standards.

Informed Consent Informed consent was obtained from all individual participants included in the study.

## References

1. Tarabichi M (1999) Endoscopic middle ear surgery. *Ann Otol Rhinol Laryngol* 108(1):39–46
2. Khan MM, Parab SR (2014) Concept, design and development of innovative endoscope holder system for endoscopic otolaryngological surgeries. *Indian J Otolaryngol Head Neck Surg*. doi: [10.1007/s12070-014-0738-y](https://doi.org/10.1007/s12070-014-0738-y)
3. Khan MM, Parab SR (2011) Primary cartilage tympanoplasty: our technique and results. *Am J Otolaryngol* 32(5):381–387
4. Khan MM, Parab SR (2013) Reinforcement of sliced tragal cartilage perichondrium composite graft with temporalis fascia in type I tympanoplasty: our techniques and results. *J Rhinolaryng Otol* 1:57–62
5. Khan MM, Parab SR (2014) Sliced Island tragal cartilage perichondrial composite graft: early results and experience. *J Rhinolaryng Otol* 2:4–9
6. Khan MM, Parab SR (2015) Comparative study of sliced tragal cartilage and temporalis fascia in type I tympanoplasty. *J Laryngol Otol* 129(1):16–22
7. Tarabichi M. Endoscopic cholesteatoma, tympanoplasty and middle ear. Open access atlas of otolaryngology, head and neck operative surgery. <https://vula.uct.ac.za/access/content/group/ba5fb1bd-be95-48e5-81be-586fbaeba29d/Endoscopic%20chole>

- [steatoma,%20tympanoplasty%20and%20middle%20ear%20surgery.pdf](#)
8. Thomassin JM, Korchia D, Doris JM (1993) Endoscopic-guided otosurgery in the prevention of residual cholesteatomas. *Laryngoscope* 103:939–943
  9. Hawke M (1982) Telescopic otoscopy and photography of the tympanic membrane. *J Otolaryngol* 11:35–39
  10. Nomura Y (1982) Effective photography in otolaryngology-head and neck surgery: endoscopic photography of the middle ear. *Otolaryngol Head Neck Surg* 90:395–398
  11. Takahashi H, Honjo I, Fujita A, Kurata K (1990) Transtympanic endoscopic findings in patients with otitis media with effusion. *Arch Otolaryngol Head Neck Surg* 116:1186–1189
  12. Poe DS, Bottrill ID (1994) Comparison of endoscopic and surgical explorations for perilymphatic fistulas. *Am J Otol* 15:735–738
  13. McKennan KX (1993) Endoscopic ‘second look’ mastoidoscopy to rule out residual epitympanic/mastoid cholesteatoma. *Laryngoscope* 103:810–814
  14. Pothier D (2013) Introducing endoscopic ear surgery into practice. *Otolaryngol Clin N Am* 46(2):245–255
  15. Tarabichi M (2010) Endoscopic transcanal middle ear surgery. *Indian J Otolaryngol Head Neck Surg* 62(1):6–24
  16. Kozin ED, Lehman A, Carter M et al (2014) Thermal effects of endoscopy in a human temporal bone model: implications for endoscopic ear surgery. *Laryngoscope* 124(8):E332–E339



# Endoscopic Cartilage Tympanoplasty: A Two-Handed Technique Using an Endoscope Holder

Mubarak M Khan<sup>1</sup>, Sapna R Parab<sup>1</sup>

Affiliations expand

- PMID: 2653547
- DOI: [10.1002/lary.25760](https://doi.org/10.1002/lary.25760)

## Abstract

**Objectives/hypothesis:** Endoscopic ear surgery provides a minimally invasive approach to the middle ear. The disadvantage of endoscopic ear surgery is that it is a single-handed surgical technique. The nondominant hand of the surgeon is utilized for holding and manipulating the endoscope. This necessitated the need for the development of an endoscope holder that would allow both hands to be free for surgical manipulation. The aim of this article is to report our preliminary experience using our newly designed and developed endoscope holder, which allowed us to perform cartilage tympanoplasty utilizing both hands for surgery.

**Study design:** Retrospective nonrandomized clinical study.

**Methods:** The endoscope holder was designed and developed to aid in endoscopic ear surgery and to overcome the disadvantage of single-handed endoscopic surgery. The design of the endoscope holder is described in detail, along with instructions on how it can be used. A total of 179 endoscope holder-assisted cartilage tympanoplasties were performed to evaluate the feasibility of a two-handed technique and to evaluate the results of surgery.

**Results:** In an early follow-up period ranging from 6 to 20 months, the graft take was seen in 174 ears, with one residual perforation and four recurrent perforations, giving a success rate of 97%. The endoscope holder eliminates the disadvantages of single-handed surgery and is a good option for those who wish to perform endoscopic ear surgery using both hands.

**Conclusion:** The study reports the successful application and use of the endoscope holder in a two-handed technique of endoscopic tympanoplasty.

**Level of evidence:** 4. Laryngoscope, 126:1893-1898, 2016.

**Keywords:** Endoscope holder; endoscopic cartilage tympanoplasty.

© 2015 The American Laryngological, Rhinological and Otological Society, Inc.



**HEPATOPROTECTIVE EFFECT OF ECLIPTA ALBA AND PHYLLANTHUS FRATURNUS EXTRACT IN ANIMAL MODEL (RATS)**

**Dr. Tushar Khachane**

Asst. Professor, Dept. of Gen. Surgery, MIMER Medical College, Talegaon Dabhade, Corresponding Author

**Dr. John Premendran**

Ex. Prof. & HOD Dept. of Pharmacology, MGIMS, Sewagram

**ABSTRACT**

This exercise was undertaken to study the hepatoprotective effect of Eclipta Alba and Phyllanthus fraternus extract in CCl4 treated rats. CCl4 induced fatty liver and liver cell necrosis in the rats. 60 male albino rats each weighing not less than 150 gm were divided into 6 groups with 10 animals in each group. The groups included-a control, group treated with CCl4, group-treated with Liv-52 and 3 groups receiving the plant extracts isolated and in combination. The rats were sacrificed under light ether anaesthesia and diagnostic estimations were done to assess the liver functions. Biochemical study indicated high levels of SGPT & SCOT in CCl4 treated rats: 450.33±161.25 and 605.66 ± 16.67 respectively. Eclipta alba managed to bring down the levels to 223.47 ± 105.79 and 444.67 ± 76.62 respectively whereas phyllanthus fraternus treated rats indicated readings of 341.66 ± 22.47 and 428.33 ± 9.5 respectively. Histopathological studies revealed less congestion and very less fatty changes in the extract treated rats. Eclipta alba group had minimum abnormal changes. The profile appears to suggest marked beneficial effect of plant extracts in liver damage produced by CCl4.

**KEYWORDS**

Eclipta Alba	Phyllanthus fraternus	SGPT
Carbon tetrachloride (CCl4)	Fatty Liver	SGOT

**INTRODUCTION :**

There is no specific treatment for infective hepatitis in modern medicine. However there are several remedies suggested in Ayurvedic medicine. The extracts of Eclipta alba, Eclipta prostrata and Phyllanthus fraternus are being commonly and regularly used as a Folk-lore medicine in the South of our country for the treatment of infective hepatitis (1,2).

In order to study the efficacy and safety of this plant extract, the plant was identified, brought all the way from Tamilnadu and was cultivated in Sevagram, This study was carried out to test this extract in rats after inducing damage to the liver with carbon tetrachloride which induces fatty liver and liver cell necrosis (3) as ICMR Research Project in Department of Pharmacology MGIMS, Sewagram, Wardha (M.S.) from Jan'2010 to Apr'2010

**MATERIALS AND METHODS :**

Eclipta alba and Phyllanthus fraternus extract: It was prepared by drying the leaves of the plants and then evaporating the alcohol added, in shadow.

Drugs and chemicals : CC14 (Qualigens fine chemicals, Bombay), Liv-52 (Himalaya Drug Co., Bombay), GOT, GPT estimation kits (Kasturba Hospital, Sevagram).

Experimental animals : 60 male albino rats each weighing not less than 150 gm were divided into 6 groups with 10 animals in each group. The rats had free access to commercial pellet diet (Goldmohr rat feed, Lipton India Ltd.) and water.

- Group I : was treated with CC14
- Group II : plant extract – No. 1. (Eclipta alba)
- Group III : plant extract – No. 2. (phyllanthus fraternus)

- Group IV : plant extract – No. 1 + 2
- Group V : Liv 52 - an Ayurvedic preparation.
- Group VI : Control.

The details of the procedure are as follows.

**TREATMENTS :**

- Group I : CC14 + groundnut oil mixture injected I.P. 0.1 ml / kg body weight. 3 doses on alternate days (1st, 3rd, 5th day), sacrificed on 6th day.
- Group II : Eclipta alba fed orally for 10 days 100 mg/kg body weight. CC14 + groundnut oil injected I.P. on 6th, 8th, 10th day (0.1 ml / kg), sacrificed on 11th day.
- Group III : Phyllanthus fraternus fed orally for 10 days, 100 mg/kg body weight. CC14 + groundnut oil injected I.P. on 6th, 9th, 10th day (0.1 ml/kg); sacrificed on 11th day.
- Group IV : Eclipta alba + phyllanthus fraternus fed orally for 10 days 100 mg/kg body weight each. CC14 + groundnut oil injected I.P. on 6th, 8th, 10th day (0.1 ml/kg), sacrificed on 11th day.
- Group V : Liv 52 fed orally for 10 days (1 ml/kg body weight) CC14 + groundnut oil injected I.P. on 6th, 8th, 10th day (0.1 ml/kg). Sacrificed on 11th day (4).
- Group VI : Distilled water fed orally (1 ml/kg body weight). Groundnut oil injected on 6th, 8th, 10th day (0.1 ml/kg). Sacrificed on 11th day.

All rats were sacrificed under light ether anaesthesia and the following diagnostic estimations were done to assess the liver functions. Biochemical study :

The blood extracted from the rats was centrifuged and the serum was estimated for the levels of following enzymes:

- 1) SGPT (Serum Glutamate Pyruvate Transaminase)
- 2) SGOT (Serum Glutamate Oxaloacetate Transaminase) (5)

**Histopathological study :**

Small pieces of liver tissues were collected in 10% formalin for proper fixation. These tissues were processed and embedded in paraffin wax. Sections of 5-6 microns in thickness were cut and stained with haematoxylin and eosin (6).

**RESULTS :**

The results obtained from biochemical estimation are tabulated and statistically analysed in Table 1.

**Table 1 : EFFECT OF ECLIPTA ALBA & PHYLLANTHUS FRATRURNUS EXTRACTS ON BIOCHEMICAL PARAMETERS IN RATS SUBJECTED TO CCL INDUCED TOXICITY.**

	Group	Biochemical parameter	
		SGPT ± S.D.	SGOT ± S.D.
I.	CCl <sub>4</sub>	450.33 + 161.25	605.66 + 16.67
II.	Eclipta alba	223.47 + 105.79	444.67 + 76.62
III.	Phyllanthus fratrurnus	341.66 + 22.47	428.33 + 9.5
IV.	Eclipta alba + Phyllanthus fratrurnus	354.66 + 34.99	455.21 + 28.58
V.	Liv 52	380.33 + 116.97	476.66 + 19.42
VI.	Control	035.37 + 7.23	339.31 + 9.33

Group	Dose
I	0.1 ml/kg body wt.
II	100 mg/kg body wt.
III	100 mg/kg body wt.
IV	100 mg/kg body wt. (each drug)
V	1 ml /kg body wt.
VI	1 ml /kg body wt.

Significant difference : I & II, III, IV  
I & II, III, IV, V

between groups VI & I, II, III, IV, V  
VI & I, II, III, IV, V

**HISTOPATHOLOGICAL STUDY :**

Liver from control group showed normal appearance, smooth and regular under surface without any evidence of haemorrhage and necrosis. CCl<sub>4</sub> treated livers showed multiple area of necrosis. Most of livers were covered with white slough and there were multiple white patches. The undersurface of most of the livers were irregular. Livers from Eclipta alba, phyllanthus fratrurnus and Liv 52 groups showed mild haemorrhage and minimum fatty changes, Eclipta alba group being almost near normal.

Histology of liver from control group showed aortal triad, rows of hepatocytes or normal arrangement of hepatocytes with nuclei, while CCl<sub>4</sub> treated liver sections showed intense centrilobular necrosis, sinusoidal congestion and extensive fatty changes. Hepatocytes in centrilobular zone were enlarged and contained lipids. Hepatocytes in periportal zone were also enlarged and normal architectural pattern was destroyed with severe vacuolization of surviving periportal hepatocytes.

In Phyllanthus fratrurnus and Eclipta alba treated rats there was less congestion and very less fatty changes. Liv 52 group also showed similar characters. Eclipta alba group had the minimum abnormal changes.

**DISCUSSION :**

Carbon tetrachloride is known to cause fatty infiltration and

liver cell necrosis, CCl<sub>4</sub> gets converted to trichloromethyl radical which is toxic reactive metabolite (7). This activated radical binds covalently to the macromolecules and induces peroxidative degradation of membrane lipids of endoplasmic reticulum rich in polyunsaturated fatty acids. This lipid peroxidative degradation of biomembranes is one of the principle causes of hepatotoxicity.

Our findings confirmed the hepatotoxicity of CCl<sub>4</sub> and free radical mechanisms suggested for the toxic effect of this chemical. CCl<sub>4</sub> induced lipid peroxidation was inhibited significantly in Eclipta alba, Phyllanthus fratrurnus and Liv 52 treated groups. A possible mechanism of Eclipta alba and Phyllanthus fratrurnus as hepatoprotective agent could be an antioxidant effect and is comparable to that of Liv 52.

**CONCLUSION :**

Biochemical data of the present study showed significant lowering of SGPT and SGOT from their elevated levels following Eclipta alba and Phyllanthus fratrurnus extract administration.

It is difficult to infer the exact molecular and biochemical mechanism responsible for prevention of CCl<sub>4</sub> induced liver damage but the observations suggest marked beneficial effect of the plant extracts in liver damage produced by CCl<sub>4</sub>.

**REFERENCES :**

1. K.R. Kirtikar & B.D. Basu, (1984) Indian medicinal plants, 36 (1-67)
2. Unandr DW, Webster GL, Blumbeig BS, 1991. Uses and Bio-assays in Phyllanthus (Eupharbiaceae): A compilation II, the subgenus phyllanthus J Ethnopharmacol 34, (97-133).
3. Recknagel RO (1967) Carbontetrachloride hepatotoxicity Pharmac Rev. 19: (145-208).
4. Kale AK, Kulkarni KD, Goglekar G Y, Balwani J H (1966) Effect of Liv. 52 on growth and alcohol induced hepatic dysfunction in rats. Curr. Med Pract 10: (240-1).
5. Retiman, S. Frankel AS (1957) A colorimetric method for the determination of serum glutamic oxaloacetic and glutamic pyruvic transaminases. Am J Clin Pathol 28: (53-6).
6. Luna LG. (1966) Manual of histological staining. Methods of Armed Forces institute of Pathology, London (1-31).
7. Indian Journal of Pharmacology, (1994) September, Volume II, (117-121)





## Evaluation of Possum Score As Predictor of Morbidity And Mortality in Gastrointestinal Surgeries.

\* Dr. Sachin Naik

Professor and Head, Dept. of Gen. Surgery, MIMER Medical College, Talegaon Dabhade, Pune. \* Corresponding Author

Dr. Pankaj Nemade

Senior Resident, Dept. of Gen. Surgery, MIMER Medical College, Talegaon Dabhade, Pune.

Dr. Sandesh Gawade

Assistant Professor, Dept. of Gen. Surgery, MIMER Medical College, Talegaon Dabhade, Pune.

### ABSTRACT

There is high risk of postoperative complications in patients undergoing abdominal surgery. It may lead to prolonged hospital stay, disproportionate use of resources and increased mortality and morbidity. We assessed impact of complications in terms of hospital stay and ICU stay by study of predictive factors, the nature and frequency of postoperative complications in this retrospective observational study of 100 patients undergoing abdominal surgeries for various diseases in our centre. The incidence of cardiorespiratory, infective and surgical complications was assessed.

POSSUM (Physiological and Operative Severity Score for the enumeration of Mortality and morbidity) score was used for evaluation.

High-risk patients could be identified by simple clinical criteria. Development of clinical pathways would prove valuable. POSSUM may be considered an essential component of surgical audit as it does appear to provide an efficient indicator of the risk of morbidity and mortality in the general surgical patient.

### KEYWORDS

POSSUM score, Gastrointestinal surgery, ASA.

### Introduction

Recovery from surgery is fast and uncomplicated in most patients and the overall mortality rate after non-cardiac surgery is approximately 1-2 percent.<sup>1</sup> Established risk factors include increasing age, impaired cardiovascular function and type of surgery.<sup>2</sup> In gastroenterological surgery postoperative complications occur more frequently and the postoperative mortality rate is higher (4 percent) than in many other specialties.<sup>3</sup> Patients who develop complications and whose hospital stay is prolonged may consume a disproportionately large share of the available resources.<sup>4</sup>

Definitions of complications and risk factors related to gastroenterological surgery vary extensively.<sup>3</sup> The reported incidence of complications is also greatly dependent on patient selection. Recent studies have shown that preoperative screening may facilitate the selection of patients for appropriate perioperative management<sup>5</sup> Perioperative intervention on high risk patients undergoing major surgery may be beneficial to reduce the postoperative complications, risk of death or the length of hospital stay.

### Aims and objectives

The objective of this study was to see the feasibility and predictivity of possum score for morbidity and mortality in patients undergoing gastrointestinal surgeries. And further to determine the nature and the frequency of cardiorespiratory, surgical and infective complications after gastroenterological operations; their correlation with the predictive factors and assessment of their impact in terms of hospital stay and need for intensive care.

### Materials and methods

This study was an observational study incorporating 100 patients admitted at MIMER hospital, Pune who underwent gastroenterological surgeries for various diseases from Feb 2010 to July 2012. We compared our data with that published by other national and international centers.

POSSUM score was used for evaluation of the study patients. POSSUM score consisted of 4 different parameters viz. Physiology Severity Score, Operative Severity Score, Possum Predicted Morbidity and Possum Predicted Mortality scores. Patients with POSSUM Scores <25 were grouped as "low-risk", those with scores 25-50 were termed "medium risk", whereas those with scores >50 were considered high risk.

The following predictors were recorded viz. Age(years), Coronary heart disease, Heart failure, Hypertension, Diabetes, Duration of operation (min), Duration of intraoperative hypotension (min), Blood loss during surgery(ml), COPD/Asthma; and the correlation with the postoperative complications was studied.

### Results

It was observed that more than 50% of the patients with Age > 60years, history of CAD, Hypertension and COPD/Asthma had postoperative complications, which indicates that these are important predictive factors with positive correlation for complication; although our observation was not statistically significant.

It was observed that the patients with increased duration of surgery, excess blood loss during surgery (> 500ml) and intraoperative hypotension (min) requiring inotropic supports had postoperative complications, with statistically significant P value.

Patients with ASA III or more had postoperative complications, prolonged hospital and ICU stay. This means higher ASA grade is a significant predictor for complications and resource utilization.

Maximum complications occurred in patients undergoing exploratory laparotomy whereas 60% of the patients undergoing more than one operative procedure had postoperative complications. This indicates that type and number of operative procedures also have positive correlation with postopera-

tive complications.

It was noted that patients undergoing emergency surgeries had prolonged (>10days) of hospital stay as well as ICU stay, which indicates that patients undergoing emergency surgeries have increased morbidity and thereby increase the resource utilization in the hospital.

More than 30% of the patients having postoperative cardiorespiratory or more than one complications had postoperative prolonged hospital stay (>10 days) whereas patients with ≥05 days of postoperative ICU stay had more infective or more than one complications. This implies that ICU patients have increased morbidity with infective or >1 complications whereas IPD patients have increased morbidity with cardiorespiratory complications, thereby increasing the resource utilization in the hospital.

In our study, patients with high risk Possum Predicted Mortality Score had Mortality, which was statistically significant. Similarly, patients with high risk Possum Predicted Morbidity Score had postoperative prolonged hospital stay and ICU stay, which was statistically significant. This indicates that POSSUM score predicts the excess utilization of hospital resources by comparing the observed and expected scores.

**Fig. 1 Comparison Of Complications With Possum Predicted Morbidity Score.**

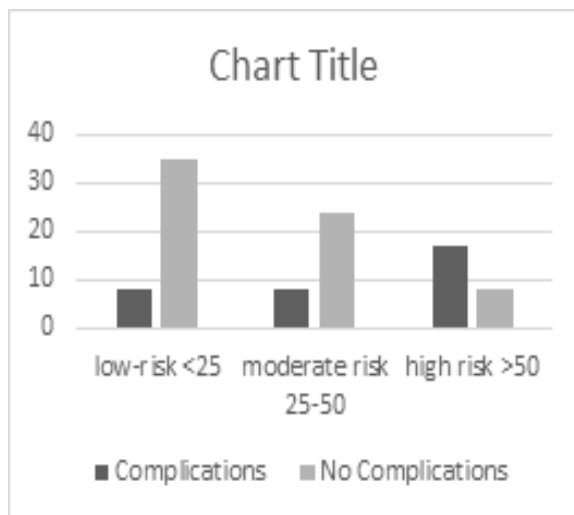


**Fig. 2 Comparison Of ASA with Complications**

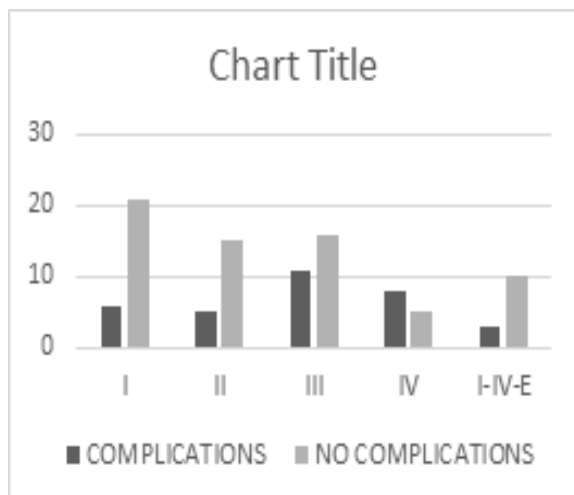


**Fig. 3 Comparison of duration of Hospital stay with POSSUM predicted Morbidity risk**

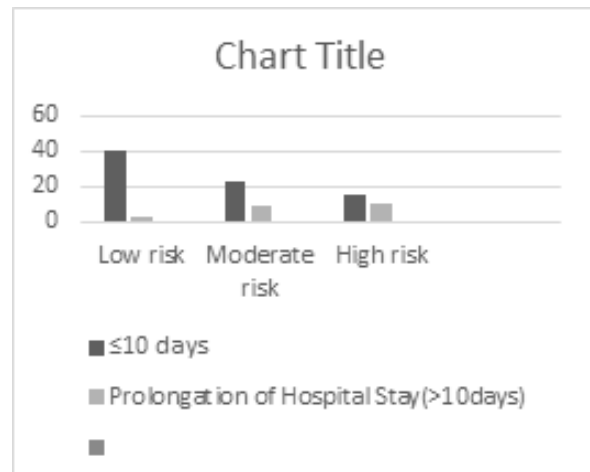


**Fig. 4 Comparison of ICU stay with POSSUM predicted Morbidity risk**

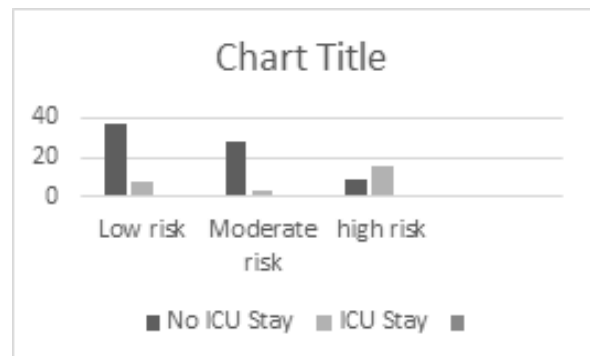
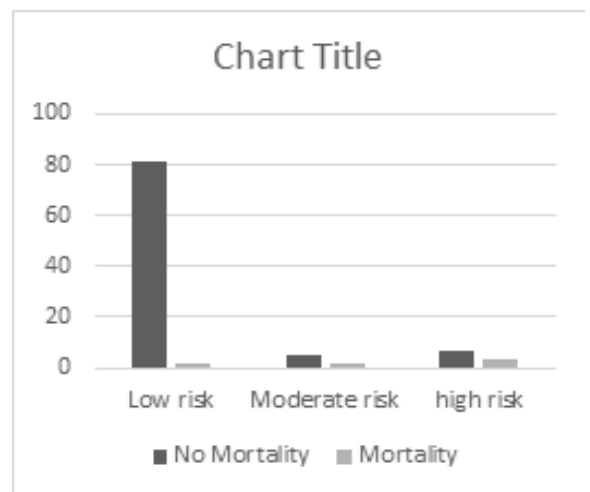


**Fig. 5 Comparison of Mortality with POSSUM predicted Mortality risk**



**Discussion**

According to the study by M. Lang, M. Niskanen, et al<sup>6</sup>, the main findings were that approximately one-half of patients undergoing gastroenterological surgery had postoperative complications, which resulted in a twofold increase in the length of hospital stay and costs of care. Complications have been reported to occur in up to two thirds of patients undergoing gastroenterological surgery, presumably because of wide definitions<sup>7</sup>.

According to our study, Cardiorespiratory complications occurred in 52.72% (29/55), whereas Surgical complications occurred in 14.5%(8/55) and infective complications occurred in 32.72% (18/55) of the complicated patients.

Complications were associated with easily recognizable clinical factors, such as increasing age, cardiovascular diseases and a prolonged operation, and occurred most often with rectal surgery as noted previously.<sup>1</sup>

According to the study by G. P. Copeland et al<sup>8</sup> to be of use in surgical audit, the scoring system must produce a valid assessment of the risk of mortality and morbidity.

Forrest and colleagues<sup>9</sup> showed that ASA classes III and IV were major predictors for severe cardiorespiratory outcome in a study which included only patients for elective surgery. According to another study by G. Prause et al<sup>10</sup>, the best predictor of survival was ASA grade II (0.4% mortality). For patients who were ASA grade III, the mortality ranged from 1.4% to 3.2%.

In our study, 61.5% (8/13) patients with Grade IV ASA had complications, whereas 40% (11/27) of grade III, 25% (5/20) of grade II, and 22.2% (6/27) of Grade I had complications; but it was not statistically significant with P>0.05.

Type and duration of surgery have long been known to influence the risk of postoperative complications.<sup>11,12</sup> According to the study by Dr. Michael Patrick<sup>13</sup>, duration of surgery was associated with postoperative length of stay (P <0.001) using univariate linear regression analysis. Therefore, it is important to control for these factors in estimating incidence of pulmonary and cardiac complications.

In our Study, 42.18% (27/64) with extended duration of surgery (>120min) had postoperative complications; whereas 16.6% (06/36) with <120min duration of surgery

It is widely agreed that the morbidity associated with anaesthesia and surgery is much higher in geriatric patients, especially in patients undergoing major surgery. Fowkes et al.<sup>14</sup> have found that the relative risk, in relation to anaesthesia and surgery of a concurrent disease such as ischemic heart disease was decreased with advancing age. This may imply that in the older age groups co-existing disease may be less important than other risk factors in determining morbidity.

As per our study, 52%(13/25) with Age >60years had post-operative complications; whereas 48%(12/25) with Age >60years had no postoperative complications; while the rate of post-operative complications was between 10-32% in <60 years age group in ascending chronological order but it was not statistically significant with P >0.05

As per our study, 100% (03/03) with >500ml blood loss during Surgery had postoperative complications; whereas 30.9% (30/97) with <500ml Blood loss during Surgery had postoperative complications. This result was statistically significant. (P <0.01)

In our Study, out of the total 100 patients undergoing all types of operative procedure; 33 patients had postoperative complications; out of which 39.39% (11/33) of the patients had cardiorespiratory complications; whereas 12.1% (04/33) of the patients had surgical, 27.7% (8/33) of the patients had infective and 21% (7/33) had more than 1 postoperative complications. This indicates that rate of cardiorespiratory complications were maximum after Exploratory Laparotomy and Cholecystectomy/Biliary Tract Surgeries with 16% and 19% incidence respectively.

In our Study, 16.6% (08/43) of the patients undergoing elective surgeries had postoperative prolonged hospital stay (>10 days); whereas 28.28% (16/57) of the patients undergoing emergency surgeries had postoperative prolonged hospital

stay (>10 days). This difference was not statistically significant. P >0.05

As per our Study, 06% (03/43) of the patients with low risk, 28.28%(09/32) with moderate risk and 40% (10/25) of the patients with high risk Possum Predicted Morbidity Score had postoperative prolonged hospital stay. This result was statistically significant. (P <0.005)

According to our data analysis, 02.4% (02/83) of the patients with low risk, 28.57%(02/07) with moderate risk and 30% (03/10) of the patients with high risk Possum Predicted Mortality Score had Mortality. This result was also statistically significant. (P <0.0001).

In our Study, 15.9%(07/44) of the patients with low risk, 09.6%(03/31) with moderate risk and 64% (16/25) of the patients with high risk Possum Predicted Morbidity Score had postoperative ICU stay. This result was statistically significant. (P <0.0001)

Patients with ASA grades I or II had a shorter post-operative length of stay (mean 12.6 days, median 10 days) than those in grades III or IV (mean 16.4 days, median 12 days). As per our data analysis, 37% (10/27) of the patients with ASA III, and 30% (04/13) of the patients with ASA IV had prolonged postoperative hospital stay This result was not statistically significant. (P >0.05)

## Conclusions

1. More than 1/3 patients undergoing Gastroenterological surgeries have complications including cardiorespiratory, surgical or infective, out of which more than ½ are cardiorespiratory complications.
2. The predictors like presence of CAD, Hypertension, DM, increased duration of surgery, increased amount of blood loss, increased duration of intra operative hypotension, higher ASA grade are associated with increased post-operative complications.
3. Scoring systems like POSSUM utilize these factors and can predict the morbidity and mortality risk. Higher POSSUM scores are associated with increased morbidity and mortality causing impact on resource utilization. POSSUM may be considered an essential component of surgical audit as it does appear to provide an efficient indicator of the risk of morbidity and mortality.

## REFERENCES -

1. Pedersen T, Eliassen K, Henriksen E. 1990. A prospective study of mortality associated with anaesthesia and surgery: risk indicators of mortality in hospital. *Acta Anaesthesiol Scand*. Apr;34(3):176-82.
2. Pedersen T, Eliassen K, Henriksen E. 1990. A prospective study of risk factors and cardiopulmonary complications associated with anaesthesia and surgery: risk indicators of cardiopulmonary morbidity. *Acta Anaesthesiol Scand*. Feb;34(2):144-55.
3. Lawrence VA, Dhanda R, Hilsenbeck SG, Page CP. 1996. Risk of pulmonary complications after elective abdominal surgery. *Chest*. Sep;110(3):744-50.
4. Guest JF, Boyd O, Hart WM, Grounds RM, Bennett ED. 1997. A cost analysis of a treatment policy of a deliberate perioperative increase in oxygen delivery in high risk surgical patients. *Intensive Care Med*. Jan;23(1):85-90.
5. Older P, Hall A, Hader R. 1999. Cardiopulmonary exercise testing as a screening test for perioperative management of major surgery in the elderly. *Chest*. Aug;116(2):355-62.
6. Lang M, Niskanen M, Miettinen P, Alhava E, Takala J. 2001. Outcome and resource utilization in gastroenterological surgery. *Br J Surg*. Jul;88(7):1006-14.
7. Hall JC, Brooks B. 1994. Australian national diagnosis related groups and abdominal surgery. *Aust N Z Surg*. 64:604-6.
8. Copeland GP, Jones D, Walters M, Brooks B. 1991. POSSUM: a scoring system for surgical audit. *Br J Surg*. Mar;78(3):355-60.
9. Forrest JB, Rehder K, Cahalan MK, Goldsmith CH. 1992. Multicenter study of general anesthesia. III. Predictors of severe perioperative adverse outcomes. *Anesthesiology*. Jan;76(1):3-15.
10. Prause G, Ratzenhofer-Comenda B, Pierer G, Smolle-Jüttner F, Glan-

- zer H, Smolle J. 1997. Can ASA grade or Goldman's cardiac risk index predict peri-operative mortality? A study of 16,227 patients. *Anaesthesia*. Mar;52(3):203-6.
11. Lubin MF, Walker HK, Smith RB [eds]. 1988. *Medical Management of the surgical patient* (2<sup>nd</sup> ed), Boston: Butterworths.
  12. Kroenke K, Lawrence VA, Theroux JF, Tuley MR. 1992. Operative risk in patients with severe pulmonary disease. *Arch Intern Med*; 152:967-71.
  13. Patrick Michael William. 2010. GROCOTT. Measuring morbidity following major surgery.
  14. Fowkes FG, Lunn JN, Farrow SC, Robertson IB, Samuel P. 1982. Epidemiology in anaesthesia. III: Mortality risk in patients with coexisting physical disease. *Br J Anaesth*. Aug;54(8):819-25.



See discussions, stats, and author profiles for this publication at: <https://www.researchgate.net/publication/303799453>

# Endoscopic management of cholesteatoma with Khan's Endoholder

Article in *The Journal of Laryngology & Otology* · May 2016

DOI: 10.1017/S002221511600270X

---

CITATIONS

0

READS

32

1 author:



**Mubarak M Khan**

Sushrut ENT Hospital & Dr Khan's Research Centre Talegaon Danhade

58 PUBLICATIONS 440 CITATIONS

[SEE PROFILE](#)

Some of the authors of this publication are also working on these related projects:



Human temporal bone [View project](#)



ENT Innovations [View project](#)

difference seen amongst the varying seniority of clinicians. These findings were corroborated by the sEMG readings.

*Conclusions:* ENT surgeons who perform prolonged microscopic work are at risk of musculoskeletal pain, which correlates with surgical experience suggesting an element of postural adaptation. Our prototype ergonomic support system can help delay the sensations of postural strain.

doi:10.1017/S002221511600270X

## Free Papers (F712)

ID: 712.2

### Endoscopic management of cholesteatoma with Khan's Endoholder

Presenting Author: Mubarak Khan

Mubarak Khan

*Mimer medical college*

*Learning Objectives:* Endoscopic ear surgery provides a minimally invasive approach to the middle ear. The disadvantage of endoscopic ear surgery is that it is a single-handed surgical technique. The nondominant hand of the surgeon is utilized for holding and manipulating the endoscope. This necessitated the need for the development of an endoscope holder that would allow both hands to be free for surgical manipulation. The aim of this article is to report our preliminary experience using our newly designed and developed endoscope holder, which allowed us to perform cholesteatoma surgery utilizing both hands for surgery.

*Study Design:* Retrospective nonrandomized clinical study.

*Methods:* The endoscope holder was designed and developed to aid in endoscopic cholesteatoma surgery and to overcome the disadvantage of single-handed endoscopic surgery. The design of the endoscope holder is described in detail, along with instructions on how it can be used. A total of 87 endoscope holder-assisted cholesteatoma surgeries were performed to evaluate the feasibility of a two-handed technique and to evaluate the results of surgery.

*Results:* Out of 87 Endoholder assisted cholesteatoma surgeries, 82 surgeries were performed exclusively with Endoholder and 5 needed combined approach (endoscope + microscope) suggesting 94% success in using exclusive Endoholder for endoscopic management of cholesteatoma.

The endoscope holder eliminates the disadvantages of single-handed surgery and is a good option for those who wish to perform endoscopic cholesteatoma surgery using both hands.

*Conclusion:* The study reports the successful application and use of the endoscope holder in a two-handed technique of endoscopic cholesteatoma management.

doi:10.1017/S0022215116002711

## Free Papers (F712)

ID: 712.3

### Long term hearing outcomes with the shape memory Nitinol stapes prosthesis: 10 year results

Presenting Author: Rebecca Heywood

Rebecca Heywood<sup>1</sup>, Mark Quick<sup>2</sup>, Marcus Atlas<sup>3</sup>

<sup>1</sup>Ng Teng Fong General Hospital, <sup>2</sup>Sir Charles Gairdner Hospital, <sup>3</sup>Ear Science Institute Australia

*Learning objectives:*

1. Understand the variability that ensues during crimping of stapes prostheses
2. Understand the benefits conferred by self-crimping shape memory prostheses
3. Learn about long term stability of hearing outcomes using self-crimping shape memory prostheses

*Introduction:* Self-crimping stapes pistons were introduced to remove the manual component of the crimping process during stapedectomy with a view to producing stable long term hearing improvement in a reproducible manner and reducing trauma to the middle and inner ear. The objective of this study was to assess the long term clinical hearing outcomes and their stability following stapedectomy using a self-crimping shape memory Nitinol prosthesis over a 10 year period.

*Methods:* Retrospective case review was performed in a tertiary referral centre. Thirteen adult patients underwent fourteen stapedectomy procedures using a self-crimping shape memory Nitinol prosthesis between November 2003 and February 2005. Pure tone audiometry was performed preoperatively, at three monthly intervals up to two years and at five and ten years postoperatively.

*Results:* Mean postoperative air conduction (0.5, 1, 2 and 3kHz) was 24.4 dB (standard deviation 8.3) at 1 year and 29.6 dB (11.2) at 10 years. Mean postoperative bone conduction (0.5, 1, 2 and 3kHz) was 18.6 (8.0) at 1 year and 25.0 (12.0) at 10 years. Mean postoperative air bone gap (0.5, 1, 2 and 3kHz) was 5.5 dB (3.0) at 1 year and 4.8 dB (3.9) at 10 years. Mean air bone gap closure was 23.3 (12.6) at 1 year and 24.2 (9.9) at 10 years. Mean change in high tone bone conduction level (1, 2 and 4kHz) was 5.4 dB (6.0) at 1 year and -0.2 dB (7.0) at 10 years, a mean deterioration of 5.6 dB (0.6 dB per year).

*Conclusions:* Excellent closure of the air bone gap is demonstrated and it remains stable over at least ten years. There is no evidence that circumferential firm fixation of the prosthesis hook around the long process of incus has a detrimental effect in the long term.

## Awareness of Infectious Occupational Health Risks and the Compliance of Recommended Vaccines Amongst the Medical Interns At Rural Hospital – A Pilot Study



### Medical Science

**KEYWORDS :** Occupational Health Hazards, Vaccination Awareness, Post Exposure Prophylaxis

**Dr. Sachin Naik**

Professor and Head, Dept. of Gen. Surgery, MIMER Medical College, Talegaon Dabhade, Pune.

**Dr. Rohan Patil**

Resident, Dept. of Gen. Surgery, MIMER Medical College, Talegaon Dabhade, Pune.

**Dr. Shrikant Ambalkar**

Consultant in Clinical Microbiology and Infection, King's Mill Hospital, Nottinghamshire, UK

### ABSTRACT

*Health professionals are at increased risk of exposure to infectious diseases, as they are exposed to potentially contaminated substances with a variety of pathogens. This was a cross-sectional questionnaire pilot study was conducted among 50 medical interns at M.I.M.E.R. Medical College & Dr.BSTR Hospital, Talegaon Dabhade, Pune 410507 in order to assess their current level of awareness. This study concludes that all medical interns should undergo a comprehensive training program regarding awareness of occupational health risks and vaccination coverage, reflecting the need for motivational policies, through activities for clarification and expansion of vaccination coverage.*

### INTRODUCTION

Health professionals are under an increased risk of exposure to infectious diseases, as during their work activities they are usually exposed to risks by biological agents due to contact with body fluids potentially contaminated with a variety of pathogens (1). Important measures to prevent some infections in the workplace consist of the immunization and monitoring of vaccination status of professionals, considered essential in infection control programs for these individuals (2).

Appropriate immunization of Health professionals, in addition to decreasing the overall rate of disease among vaccines, reduces the number of secondary cases, time associated to exposure management, and also provides protection to patients (3).

In India, Universal Immunization Program (UIP) conducted by Ministry of Health and Family Welfare (MoHFW), Government of India (GOI) does not present a specific protocol of vaccination coverage for this group of workers. In general the vaccines recommended by this program include: BCG, MMR, Polio, DPT and Hepatitis B (4).

Considering immunopreventable diseases in relation to medical students, it is recommended that corrective measures are taught while they are undergraduate medical course, before contact with patients, to avoid exposure to unnecessary risks. Also, the awareness of occupational diseases, the risk of transmission and the need for immunization should be present from the period of academic training. From this perspective, Higher Education Institutions are at a great responsibility to prepare students for safe clinical practice. (5)

Thus, in order to create this awareness among the medical students, it is essential to assess their current level of awareness. With this aim study was conducted among Medical Interns at M.I.M.E.R. Medical College & Dr.BSTR Hospital, Talegaon Dabhade, Pune 410507.

### OBJECTIVES

To assess knowledge, awareness and compliance among medical interns dental professionals regarding of Infectious Occupational Health Risks.

### MATERIALS AND METHODS

A cross-sectional questionnaire pilot study was conducted among 50 medical interns, who voluntarily participated in the

study. Data collection was done using structured questionnaire which was designed to assess the professional's knowledge and compliance regarding recommended vaccination and post exposure to needle prick injuries.

### RESULTS

A total of 50 respondents completed the questionnaire. Out of 50 respondents 96% were up to date with four routine vaccines recommended by MoHFW, GOI under UIP viz. BCG, MMR, Polio and DPT. 94% respondents have also received Hepatitis B. Considering Hepatitis B Vaccination 8% have received first dose, 12% have received second dose, 44% have received third dose and 30% have received booster dose as well however 6% have not taken HBV vaccine. After receiving complete course of Hepatitis B vaccine only 14% respondents checked Anti HBS Antibody level. Respondents who did not check for Anti HBs antibody level, 46% of them thought it is not important for them; for 28% Test was not available and cost was too high for 8% respondents. Annual influenza vaccine was not received by 92%. Respondents who did not receive Influenza vaccine out of them 62% thought it is not important; Vaccine was not available for 22% respondents and cost of vaccine was too high for 8% respondents. Regarding chickenpox vaccine, 68% Respondents have received it in childhood whereas 31% did not receive the same as depicted in Table I.

**Table I. Information about recommended vaccination:**

Questions	Responses	Frequency	Percentage
Are you up to date with your routine (BCG, MMR, Polio, DPT) vaccination?	Yes	48	96
	No	0	0
	Partial	1	2
	Don't Know	1	2
Hepatitis –B vaccination: Did you receive a complete course of Hepatitis –B vaccine?	No	3	6
	Dose 1	4	8
	Dose 2	6	12
	Dose 3	22	44
	Booster	15	30
Did you check your Hepatitis –B antibody (Anti HBs Antibody) level after the complete course of Hepatitis –B vaccination?	Yes	7	14
	Don't think it's important	23	46
	Test not available	14	28
	Cost too high	6	12

Questions	Responses	Frequency	Percentage
Influenza (Flu) – Do you get your annual Flu vaccine?	Yes	4	8
	Don't think it's important	31	62
	Vaccine not available	11	22
	Cost too high	4	8
Have you had chicken-pox in childhood?	Yes	34	68
	No	16	32

Table II depicts awareness about Post Exposure Prophylaxis. Considering the risk of transmission of blood borne viruses (HIV, Hepatitis B, Hepatitis C) after needle stick (injection needle) injury; 84% responded it to be High Risk, 14% responded Low Risk. 60% Respondents are aware of protocol for post exposure prophylaxis and follow up. After needle stick injury incident 18 % followed up on day zero, 6% followed on six weeks, 12% followed up on 3 months, 4% followed up on 6 months whereas 60% did not follow up after the same incident.

**Table II. Information about post exposure prophylaxis**

Questions	Responses	Frequency	Percentage
How do you perceive the risk of transmission of blood borne viruses (HIV, Hepatitis-B, and Hepatitis -C) after needle stick (injection needle) injury?	High Risk	42	84
	Low Risk	7	14
	No Risk	0	0
	Doesn't Matter	1	2
Have you got written protocol/ policy or are you aware of protocol for post exposure prophylaxis and follow up?	Yes	30	60
	No	20	40
Is there any proper follow up of needle stick injury incident?	No	30	60
	At Day 0	9	18
	6 weeks	3	6
	3 months	6	12
	6 months	2	4

Table III depicts awareness of respondents regarding health of staff they are working with in different departments of postings. Considering the overall percentage of staff members who have received complete course of Hepatitis B vaccination according to respondents; 2% responded staff to be completely vaccinated, 46% responded 50-75% of the staff is vaccinated, 14 responded less than 50% staff is vaccinated, 32 % respondents are not sure about the vaccination of staff whereas 6% responded staff is not vaccinated for hepatitis B. Main reasons for not having policy/protocols for prevention of occupational health risk of transmission of infectious diseases respondents and their staff; 12% respondents perceived it as low risk, for 8 % cost was factor and 80% responded lack of awareness.

Questions	Responses	Frequency	Percentage
What percentage of your staff members has received a complete course of Hepatitis-B vaccination?	None	3	6
	< 50%	7	14
	50- 75%	23	46
	100%	1	2
	Don't know or not sure	16	32
What are the main reasons for not having policy /protocol for prevention of occupational health risk of transmission of infectious diseases to you and your staff?	Perceived low risk	6	12
	Cost	4	8
	Lack of awareness	40	80

Table III. Information about Staff Health

**DISCUSSION**

Burden of occupational disease is increasing at an unprecedented rate. In 1985, to increase awareness among health care workers regarding the dangers of sharp injuries and other types of disease transmission, the Centers for Disease Control (CDC) and the Occupational Safety and Health Administration (OSHA) in the United States introduced the “Universal Precaution Guidelines, “which have become the worldwide standards in both hospital and community care settings.(6)

While assessing the immunization status of the Interns at a tertiary general hospital, our study identified 96% were up-to-date with their routine vaccination of BCG, MMR, Polio, DPT vaccines.

Baseline information regarding the immunization status of interns against hepatitis B was collected. It was observed that only 44 % interns had completed the three-dose HBV vaccination schedule. 8% have received first dose, 12 % have received second dose, 44% have received third dose and 30% have received booster dose as well but 6% have not taken HBV vaccine. Comparing to a study done by Acharya et al, 66.3% were completed three doses, 21.8% were partially immunized with either one or two doses, and remaining 11.9% were not immunized against hepatitis B. (7) Awareness regarding the checking the Anti HBs antibodies after complete vaccination of HBV was very poor as 86% interns did not check for it. Surprisingly 46% think that it is not important whereas Unavailability of the test (28%) and cost (12%) too remains other important factors for the same. More emphasize on awareness of the same should be implemented.

Annual Flu vaccine has been received by only 8% interns. However, from recent data in the USA, only 22% of Health Care Workers reported having received the vaccine. And 34.8% health care workers received in Hong Kong.

However, Health professionals are known to resist being vaccinated against influenza. That was confirmed by our study, where just 8% of interns had received the influenza vaccine last season. HOFMAN et al. found that the most common reasons for refusal were: fear of adverse effects, misconception that vaccination can cause influenza and unsuitable time/locations of vaccination - the third reason was the most common amongst medical house staff and students as compared to our study interns again thought it is not important followed by vaccine was not available and cost was too high. (3) Majority 84% of interns had perceived high risk regarding mode of transmission of blood borne viruses in the present study. Similar findings by Magdy et al.(9) and Singh et al.(10) among medical students, revealed that 77.7% and 86.7% of students had correct knowledge regarding mode of transmission of same respectively. Another study done by Kasetty et al.(11) among dental professionals, showed that 82.1% had correct knowledge regarding the mode of transmission. Whereas a study done by Khan et al.(8) among medical students of Karachi, found that only 57.1% had correct knowledge regarding the same.

Since 60% of the intern are aware of protocols for post exposure prophylaxis and follow up but there are no proper follow up of 60% interns after needle prick injuries. As medical interns are at increased risk of acquiring needle stick injury and increased prevalence rate of hepatitis B in India, interns should be routinely vaccinated upon entry into the medical institutes.(12)

Staff at Tertiary Hospital is at a greater risk at contracting blood borne diseases due to their constant contact with blood, body fluids, or sharps contaminated with blood. In the present study we found that 50-75% of staff has received complete vaccina-



tion of Hepatitis B. In a similar study conducted by Singhal et al., in 2011 they found that a significant number (41.7%) of Health Care Workers were unvaccinated even at an apex healthcare center.(13)

Main reason for not having policy/protocol for prevention of occupational health risk of transmission of infectious diseases to intern and staff is Lack of awareness.(80%) Hepatitis B vaccination protocol and needle stick injury prophylaxis are collated in Tables IV and V, respectively (14,15).

**Table IV.**

The vaccination schedule most often used has been three intramuscular injections. The following timing of injections are

1 <sup>st</sup> dose	At elected date
2 <sup>nd</sup> dose	4-10 weeks after the 1 <sup>st</sup> dose
3 <sup>rd</sup> dose	1-5 months after the 2 <sup>nd</sup> dose

**Dosage and administration**  
 Paediatric dose vaccine: 10 µg dose (in 0.5 ml suspension) is recommended for neonates, infants, and children up to 10 years of age  
 Adult dose vaccine: 20 µg dose (1.0 ml suspension) is recommended for adults and children above 10 years of age  
**Booster dose**  
 It would seem advisable to recommend a booster dose when the anti-HBs antibody titer falls below 10 IU/L, particularly for all people at risk  
 After the 0, 1, and 6 month primary immunization schedule a booster dose may be required 5 years after the primary course

**Table V.**

Vaccination and antibody response status of exposed HCWs	Treatment (source)		
	HbsAg <sup>+</sup> positive	HbsAg <sup>-</sup> negative	Unknown or not available for testing
Unvaccinated	HBIG <sup>+</sup> (1) and initiate HB vaccine <sup>+</sup> series	Initiate HB vaccine <sup>+</sup> series	Initiate HB vaccine <sup>+</sup> series
Previously vaccinated			
Known responder <sup>+</sup>	No treatment	No treatment	No treatment
Known non-responder <sup>-</sup>	HBIG <sup>+</sup> (1) and initiate or vaccination or HBIG <sup>+</sup> (2)	No treatment	If known high risk source, treat as if source were HbsAg positive
Antibody response unknown	Test exposed person for anti-HBs <sup>+</sup> If adequate, no treatment is necessary If inadequate <sup>+</sup> administer HBIG <sup>+</sup> (1) and vaccine booster	No treatment	Test exposed person for anti-HBs <sup>+</sup> If adequate <sup>+</sup> , no treatment is necessary If inadequate <sup>+</sup> administer vaccine booster and recheck titer in 1-2 months

From this table personnel have exposed with HBV or someone in workplace and those require post exposure prophylaxis. \*HBIG is active antigen, vaccine is inactivated. Also treat with HBIG administration. <sup>+</sup>HBIG is vaccine, is responder is a person with adequate level of serum antibody to HbsAg (≥ 100 IU/L or 10 IU/ml); is non-responder is a person with inadequate response to vaccination (i.e. anti-Hbs < 10 IU/ml). <sup>-</sup> is the status of being not able to HbsAg and remaining the vaccine series is preferred for non-responder who have not completed a second dose vaccine series. For person who previously completed a second vaccine series but failed to respond, two doses of HBIG are preferred. <sup>+</sup>antibody in HbsAg. HBV is secondary healthcare center.

**CONCLUSION**

Considering the results which we have obtained from this study, we would like to suggest that, all medical interns should undergo a comprehensive training program regarding awareness of occupational health risks and vaccination coverage, reflecting the need for motivational policies, through activities for clarification and expansion of vaccination coverage. However it needs a larger study to enlighten this topic.

**REFERENCES**

- Dinelli MI, I, Moreira TN, Paulino ER, Da Rocha MC, Graciani FB, De Moraes-Pinto MI. Immune status and risk perception of acquisition of vaccine preventable diseases among health care workers. *Am J Infect Control* 2009;37:858-60.
- Chehuen Neto JA, Sirimarc MT, Leite ICG, Gonçalves MPC, Delgado AA, Camilo GB et al. Undergraduates' Immunization Status at the UFJF Medical School. *Rev Bras Educ Med* 2010;34: 270-77.
- Silveira, M.B.V. ; Perez, D.A. ; Yamaguti, A. ; Saraiva, E.Z. ; Borges, M.G. & Moraes-Pinto, M.I. - Immunization status of Residents in Pediatrics at the Federal University of São Paulo, Brazil. *Rev. Inst. Med. Trop. Sao Paulo*, 53(2): 73-6, 2011.
- Universal Immunization Program, MOHFW, GOI [http://mohfw.nic.in/WriteReadData/1892s/Immunization\\_UIP.pdf](http://mohfw.nic.in/WriteReadData/1892s/Immunization_UIP.pdf)
- Ana Flávia Granville-Garcia ,Eveline Sales Rocha,Raulison Vieira de Sousa,Veruska Medeiros Martins, Andreza C. de L. Targino Massoni, Saul Martins Paiva; Knowledge of occupational diseases and immunization among healthcare students; *Rev Odonto Cienc* 2011;26(3):215-221
- Shwethashri R. Permi , Rahul Bhandary & Biju Thomas; Knowledge, awareness and compliance among dental professionals regarding percutaneous exposure

- incidents as occupational hazard; *NUJHS Vol. 5, No.4, 2015, December* ISSN 2249-7110
- Anita Shankar Acharya, Priyanka, Jyoti Khandekar, and Damodar Bachani, Assessment of Knowledge and Practices regarding Injection Safety and Related Bio-medical Waste Management amongst Interns in a Tertiary Care Teaching Hospital, Delhi; *International Scholarly Research Notices* Volume 2014 (2014), Article ID 670861, 5 pages <http://dx.doi.org/10.1155/2014/670861>
- Khan N, Ahmed SM, Khalid MM, Siddiqui SH, Merchant AA. Effect of gender and age on the knowledge, attitude and practice regarding Hepatitis B and C and vaccination status of Hepa-titis B among medical students of Karachi, Paki-stan. *J Pak Med Assoc* 2010; 60(6):450-5.
- Magdy A. Darwish and Nuha M. Al Khaldi. Knowledge about Hepatitis B Virus Infection among Medical Students in University of Dammam, Eastern Region of Saudi Arabia. *Life Sci J* 2013; 10(2):860-7.
- Singh A, Jain S. Prevention of Hepatitis B; knowledge and practices among Medical students. *Healthline* 2011; 2(2):8-11.
- Kasety S, Mohania A, Dwivedi D, Tijare M, Kallianpur S and Gupta S. A Cross-Sectional Study on the Knowledge of Hepatitis B Infection among Dental Professionals. *J Virology Micro-biol* 2013, Article ID 288280, DOI: 10.5171/2013.288280
- Purushottam A. Giri, Deepak B. Phalke; Knowledge and vaccination status of hepatitis B amongst medical interns of Rural Medical College, Loni, Maharashtra, India; *South East Asia Journal of Public Health* 2013;3(2):19-22
- Singhal V, Bora D, Singh S. Prevalence of Hepatitis B virus infection in healthcare workers of a tertiary care centre in India and their vaccination status. *J Vaccines Vaccin.* 2011;2:118.
- Serum Institute of India Limited. [Last accessed on 2013 Sep 10]. Available from: [http://www.seruminstitute.com/content/products/product\\_hepatitis.htm](http://www.seruminstitute.com/content/products/product_hepatitis.htm)
- Updated U.S. Public Health Service Guidelines for the Management of Occupational Exposures to HBV, HCV, and HIV and Recommendations for Postexposure Prophylaxis. [Last accessed on 2013 Sep 10]. Available from: <http://www.cdc.gov/mmwr/preview/mmwrhtml/rr5011a1.htm>

## ORIGINAL ARTICLE

**Epidemiological determinants of obesity in adolescent population Maharashtra, India.**Sanjeev Chincholikar<sup>1</sup>, Amit Sohani<sup>2</sup><sup>1</sup>Professor, Department of Community Medicine, MIMER Medical College, Talegaon Dabhade, Pune – 410507;<sup>2</sup>Medical officer, Z.P. Kolhapur, India

<a href="#">Abstract</a>	<a href="#">Introduction</a>	<a href="#">Methodology</a>	<a href="#">Results</a>	<a href="#">Conclusion</a>	<a href="#">References</a>	<a href="#">Citation</a>	<a href="#">Tables / Figures</a>
--------------------------	------------------------------	-----------------------------	-------------------------	----------------------------	----------------------------	--------------------------	----------------------------------

**Corresponding Author**

Address for Correspondence: Dr Sanjeev Chincholikar, Professor, Department of Community Medicine, MIMER Medical College, Talegaon Dabhade, Pune – 410507, Maharashtra, India  
E Mail ID: [aruna@mitmimer.com](mailto:aruna@mitmimer.com)

**Citation**

Chincholikar S, Sohani A. Epidemiological determinants of obesity in adolescent population, Maharashtra, India. Indian J Comm Health. 2016; 28, 2: 157-162.

**Source of Funding:** Nil **Conflict of Interest:** None declared

**Article Cycle**

**Received:** 20/04/2016; **Revision:** 10/05/2016; **Accepted:** 26/05/2016; **Published:** 30/06/2016

This work is licensed under a [Creative Commons Attribution 4.0 International License](https://creativecommons.org/licenses/by/4.0/).

**Abstract**

**Background:** For establishing effective intervention, it is important to identify major determinants in an early stage of life. Effective prevention of adult obesity will require prevention and management of childhood obesity. **Aims & Objectives:** To study the epidemiological determinants of obesity in adolescent girls. **Material & Methods:** All adolescent school going boys and girls in the age group between 10 to 19 years were included as per definition of adolescent. 585 students were selected by systematic sample i.e. every 3<sup>rd</sup> student was included in the study sample. A pretested standardized questionnaire which consisted of questions related to sociodemographic data was used to screen the population for obesity. **Results:** When body mass index was correlated with various socioeconomic variables, it was found that prevalence of obesity was more in males (overweight- 20.84%; obese- 5.43%) as compared to females (overweight- 16.92%; obese-3.14%), more in the upper socioeconomic status (27.27%) as compared to lower socioeconomic status(15%), more in subjects with more frequency of junk food(30.97%) as compared to having occasional junk food (20.93), more in subjects with more frequency of eating sweets ( 25.73%) as compared to occasional sweet eaters(13.59%). **Conclusion:** The dietary habits like more frequency of junk food, more sweet consumption, and socioeconomic status had a major impact on body mass index of children.

**Keywords**

Sex; Socioeconomic Status; Body Mass Index; Junk Food

**Introduction**

Obesity is widely regarded as a pandemic with potentially disastrous consequences for human health.(1,2) It is perhaps the most prevalent form of malnutrition. 65% of the world's population live in countries where overweight and obesity kills more people than underweight.

Available studies from Chennai and Delhi have shown prevalence of childhood obesity 6.2% and 7.4% respectively. (3) According to NHFS 3, in India 12.1% male and 16% female were either overweight or obese.(4) Many studies have shown that the prevalence of overweight among adolescent varies

between 10% to 30%. (5,6) For establishing effective intervention, it is important to identify major determinants in an early stage of life. Effective prevention of adult obesity will require prevention and management of childhood obesity. World Health Organization has also emphasized on urgent need of understanding the prevalence trend, factors contributing and developing strategies for effective intervention.

**Aims & Objectives**

1. To study the prevalence of overweight and obesity in adolescent population.

2. To determine the association of obesity with some epidemiological determinants

## Material & Methods

It was a cross sectional observational study that was carried out in 4 institutions (3 schools and 1 college) of semi-urban area of Maharashtra from Jan 2013 to Jan 2014. A pilot study of 100 adolescents was carried out for determining sample size and validating the questionnaire.

**Sample Size:** It was found that the prevalence of obesity was 15%. Prevalence of obesity is between 10% to 30% in India as reported by various studies (10,11,12,13). Finding of pilot study confirm the prevalence as 15% in the reference population also. Therefore, considering prevalence of obesity in adolescent as 15%, with 95% confidence interval ( $\alpha = 0.05$ ) power of test = 80% ( $\beta = 0.2$ ), estimated sample size for adolescent population including 5% non-responsive error was 575. Actual study was carried out on 585 students.

Out of all the schools and colleges which provided education up to 10<sup>th</sup> standard or above 10<sup>th</sup> standard were considered as reference population. As there were no government schools or colleges providing teaching up to 10<sup>th</sup> standard or above, thus only private schools and colleges were represented in data. Thus, reference population consisted of 17 schools and 3 colleges, all private. 3 schools and 1 college were selected by simple random sampling. 585 students were selected by systematic sample i.e. every 3<sup>rd</sup> student was included in the study sample. A pretested standardized questionnaire was used.

**Inclusion Criteria:** All adolescent school going boys and girls in the age group between 10 to 19 years were included as per definition of adolescent.

**Definition:** Height and weight of each individual was measured with the help of fiber plastic measuring tape up to the nearest millimeters and weighing scale up to the 0.5 kg respectively. Height was measured by asking the subject to stand erect without footwear on flat surface with heels together and upper limbs hanging closely to the sides of the body with the investigator standing on the left side of the subject. By placing hard cardboard on the head of the subject marking was made on the wall and later with the help of measuring tape height was calculated to the nearest millimeters. Before making the markings the head of the subject was positioned in such a way that the imaginary line drawn from tragus of the ear to the infra-orbital margin was

parallel to the ground. For the weight measurement standardized calibrated spring balance was used and subject was made to stand on platform of the balance without footwear. The weight was recorded nearest to 0.5 kg. Body mass index was calculated by dividing the weight in kilogram by square of height in meter.

**Ethical Clearance:** The study was reviewed and approved by ethical committee of parent institute approved the study. It was also approved by the concerned committee of the Maharashtra University of Health Sciences Nashik. Permission for the study was obtained from respective in-charges of schools and colleges.

## Results

It can be observed from [table I](#) that Prevalence of obesity was 4.5% while there were 20% overweight subjects. Prevalence of overweight and obesity was studied according to sex also and has been depicted in [table II](#). It was observed from the table that prevalence of obesity in a male population was more as compared to females. Similarly, prevalence of overweight was also found more in male population. Majority of the male and female were in the age group 10 to 13 years of age i.e. early adolescent.

Modified B.G. Prasad classification (2013), most widely used socio economic status classification, revealed that majority of the study population was from the upper socio economic status class. Only 6.49% subjects were from class IV. None belonged to class V. The table itself reflect the obvious reduction in obesity as socioeconomic class decrease. Owing to the unacceptable small value in one of the cells of the table, which would undermine the utility of chi-square test the data for class IV and class V were pooled for statistical analysis. As revealed from the [table III](#), there was a statistically significant difference between socioeconomic status and prevalence of either overweight or obesity.

$\chi^2 = 10.1504$ ,  $df=3$ ,  $p < 0.05$ .

Type of diet and frequency of meal has been studied with respect to prevalence of overweight and obesity. When association between prevalence of obesity and overweight with type of diet of study subjects was studied, it was observed from [table IV](#) that there was no statistically significant difference between the two, meaning that type of diet may not be related to overweight and obesity.

$\chi^2 = 0.31$ ,  $df= 1$ ,  $>0.05$ .

It was observed that out of 165 students taking vegetarian diet, 21.82% students were either overweight or obesity. It was also found that 420 students were taking mixed diet but out of them only 24.29% were either overweight or obese. As mentioned in review of literature use of junk food is reported to be associated with obesity. Association of frequency of junk food with prevalence of overweight and obesity in study subjects is given in table.

It can be seen from [table V](#) that use of junk food frequently has a role in development of overweight and obesity. It was observed that overweight and obesity was relatively less in those who take junk food occasionally (once in a week or less). It can be seen that 30.97% overweight subjects had frequent junk food. There was a significant association between frequency of junk food and prevalence of overweight as well as obesity.

$\chi^2 = 4.865957$ ,  $df=1$ ,  $p < 0.05$ .

From [table VI](#), It can be seen that consumption of junk food and sweets, frequently has a role in development of overweight and obesity.

$\chi^2 = 5.296657$ ,  $df= 1$ ,  $p < 0.05$ .

## Discussion

The detailed study brought out some salient features about demographic information, social status and nutritional status of the study subjects which has been discussed as below.

As revealed in table II, Prevalence of obesity in a male population was more as compared to females. Similarly, prevalence of overweight was also found more in male population. Goyal *et al*(7) in their study in 2010 found that age-adjusted prevalence of overweight was 14.3% among boys and 9.2% among girls. They also observed that prevalence of obesity was 2.9% in boys and 1.5% in girls. Kotian MS *et al*.(8) in their study in 2010, reported that, the prevalence of overweight among adolescents in both sexes was 9.9% and obesity was 4.8%. The prevalence of overweight was 9.3% among boys and 10.5% among girls; 5.2 and 4.3% were obese, respectively, which is comparable to our study. Arpita Mandal *et al*.(9) in their study recently, in Kolkata, India, evaluated 571 girls in the age group of 12 to 18 years. They observed that prevalence of overweight and obesity was 28.5% and 4.2% respectively. This prevalence of obesity in the above study is comparable to the prevalence of obesity among girls in our study. In a recently conducted study by Tabassum Nawab *et al*

(10) in Uttar Pradesh, it was found that prevalence of overweight and obesity was 9.8% and 4.8%, respectively. Prevalence of both overweight and obesity was higher among males. Similar findings are observed in our study.

Considering the different opinions among various researchers regarding which sex is more commonly affected group, it appears that a large representative sample will be required for settling this question. It appears that occurrence of obesity varies according to socioeconomic status; very few subjects are from class IV showed presence of either overweight or obesity. It would mean that subjects belonging to upper socioeconomic class may have more risk of becoming obese than those in lower classes. This confirms that socioeconomic status is one of the important factors in deciding the obesity among the adolescent population. Several studies in different part of the world including India showed that higher socioeconomic class have higher rate of overweight and obesity. In developing countries it has been observed that children from the upper socio-economic strata are more likely to be obese than children from the lower socio-economic strata.(11) Marwaha *et al*.(12) in a study carried out in Delhi, observed that, among the upper socio-economic status children, prevalence of overweight and obesity was 17% and 5.6% in boys and 19% and 5.7% in girls, respectively, whereas in the lower socio-economic status it was 2.7% and 0.4% in boys and 2.1% and 0.5% in girls, respectively.

Unnithan and Syamakumari (13) also reported that the prevalence of overweight and obesity were higher among urban children. Goyal RK *et al*.(7) in their study in western India, observed that prevalence of overweight among children was higher in middle socioeconomic status as compared to high socioeconomic status group in both boys and girls whereas the prevalence of obesity was higher in high socio-economic status group as compared to middle socioeconomic status group. The prevalence of obesity as well as overweight in low socioeconomic status group was the lowest as compared to other group.

One possible explanation for the different socioeconomic status - overweight and obesity relationship in developing countries such as India is that the influence of socioeconomic status on people's lifestyles such as diet, food consumption patterns, and public services such as health care and transportation and physical activity may differ.



Richer people have better access to meat and other energy-dense foods (which are much more expensive than other foods such as vegetables) than the poor. Middle socioeconomic status groups usually consume more vegetables and fruits. As revealed from table VI, there was statistically significant difference between frequency of eating sweets and prevalence of overweight as well as obesity. Obesity was more in study subjects who ate sweets frequently. 25.73% Students with overweight and obese subjects were frequent sweet eaters.

Caprio S. *et al* (14) from America reported a strong association between sugar-sweetened beverages and prevalence of childhood obesity. Andrew A (15) in his study observed that overweight and obesity decreases as sugar-sweetened beverage consumption is reduced.

#### **Eating habits and prevalence of overweight and obesity:**

According to the WHO expert committee (16), high intakes of energy-dense micronutrient poor foods which is the case in most of fast food is convincingly related with unhealthy weight gain and there is a possible relation between the high proportion of intake of food prepared outside home and unhealthy weight gain. Increased intake of energy-dense foods that are high in sugars and fat but low in proteins, micronutrients, vitamins and minerals play important role in childhood obesity. (17) A diet containing more energy than needed may lead to prolonged postprandial hyperlipidemia and deposition of triglycerides in adipose tissue resulting in obesity. (18) From a practical point of view all hypothesis concerning the genesis of obesity could be put down to over-nutrition, to a hyper energy food intake. This is a sound basis for preventive and therapeutic recommendations. (19) There was a significant association between frequency of junk food, sweets with prevalence of overweight as well as obesity. These results correlate well with previous reports which suggest that junk food (bakery items, pizza, burger, cheese, butter, oily items) chocolate intake tends to be more common among overweight and obese adolescents than among normal-weight adolescents. (20,21) Hanley JG *et al* (22) concluded that low consumption of fruits, green vegetables, and milk; increasing consumption of snacks, sweets, and soft drinks; and skipping breakfast; these eating habits result in continuous increase in adiposity among children. Tarek Tawfi, K Amin *et al* (23) in their study revealed that lean students consumed

more servings of fruits; vegetables; and dairy products, including milk, while overweight and obese children consumed significantly higher servings of egg, potato (especially fried), carbonated soft drinks, sugary drinks, and sweets per day. They also observed frequency of eating out was high among overweight and obese children.

Berkey CS *et al* (24) in their longitudinal study of preadolescent and adolescent boys and girls observed association between frequency of restaurant visit and obesity. Kotian MS *et al* (8) found that prevalence of overweight was higher in those adolescents who ate chocolates daily. Sameer H and Ghamdi AI (25) found a higher BMI in adolescent population who, ate more than three snacks per day. Goyal *et al*, (7) found a correlation between frequency of eating and overweight as well as obesity in adolescent population. They also observed correlation between junk food consumption and overweight as well as obesity

#### **Conclusion**

One thing that can be mentioned from the present study is that, as age increased gradually, students may have become cautious about their figure and health, and may have tried to consume less amounts of junk food, which was reflected in the lower prevalence rate of overweight, as well as obesity, in the higher age groups

It can be concluded that the dietary habits like more frequency of junk food, more sweet consumption, and socioeconomic status are the factors which had a major impact on body mass index of children. These risk factors may be considered as potential determinants of obesity.

#### **Recommendation**

Obese students should be counselled for nutrition, psychological changes, behavioural changes, pharmacological management and surgical intervention if necessary.

#### **Limitation of the study**

Out of all the schools and colleges which provided education up to 10<sup>th</sup> standard or above 10<sup>th</sup> standard were considered as reference population. As there were no government schools or colleges providing teaching up to 10<sup>th</sup> standard or above, thus only private schools and colleges were represented in data. Moreover, this being institutionalized study, community based studies on a larger representative sample of adolescent children will be needed for

confirming and quantifying the epidemiological determinants of obesity. The responses given by the study subjects at that were relied upon. Lastly, being a multifactorial disease all the associated risk factors could not be studied.

### Authors Contribution

All the authors had made substantial contributions to conception, design, data collection, analysis and interpretation of data; drafting the article, revising it critically for important intellectual content; and final approval of the version to be published.

### References

1. Park's textbook of Preventive and Social Medicine: 22nd Edition. Jabalpur India: BanarsidasBhanot Publishers; 2013; P. 367- 69.
2. Davidsons, Principles and Practice of Medicine. 21st edition, Churchill Livingstone Elsevierpublissher; 2011; P. 110.
3. Sidhu S, Kaur N, Kaur R. Overweight and obesity in affluent school children of Punjab. *Ann Hum Biol.* 2006 Mar-Apr;33(2):255-9. PubMed PMID: 16684697. [PubMed].
4. Bose K, Bisai S, Mukhopadhyay A, Bhadra M. Overweight and obesity among affluent Bengalee schoolgirls of Lake Town, Kolkata, India. *Matern Child Nutr.* 2007 Apr;3(2):141-5. PubMed PMID: 17355446. [PubMed].
5. Aggarwal T, Bhatia RC, Singh D, Sobti PC. Prevalence of obesity and overweight in affluent adolescents from Ludhiana, Punjab. *Indian Pediatr.* 2008 Jun;45(6):500-2. PubMed PMID: 18599939. [PubMed].
6. Kaneriya Y, Singh P, Sharma D. Prevalence overweight and obesity in relation to socio economic conditions in two different groups of school age children of Udaypur city (Rajasthan). *J Indian Assoc. community med* 2006; 7:133-5.
7. Goyal RK, Shah VN, Saboo BD, Phatak SR, Shah NN, Gohel MC, Raval PB, Patel SS. Prevalence of overweight and obesity in Indian adolescent school going children: its relationship with socioeconomic status and associated lifestyle factors. *J Assoc Physicians India.* 2010 Mar;58:151-8. PubMed PMID: 20848812. [PubMed].
8. Kotian MS, S GK, Kotian SS. Prevalence and determinants of overweight and obesity among adolescent school children of South karnataka, India. *Indian J Community Med.* 2010 Jan;35(1):176-8. doi: 10.4103/0970-0218.62587. PubMed PMID: 20606948; PubMed Central PMCID: PMC2888353. [PubMed].
9. Arpita M, Gopal Chandra M. Prevalence of overweight and obesity among the urban adolescent English Medium School girls of Kolkata, India. *IJPH* 2012;9(3):1-6
10. Nawab T, Khan Z, Khan IM, Ansari MA. Influence of behavioral determinants on the prevalence of overweight and obesity among school going adolescents of Aligarh. *Indian J Public Health.* 2014 Apr-Jun;58(2):121-4. doi: 10.4103/0019-557X.132289. PubMed PMID: 24820987. [PubMed]
11. Raj M, Sundaram KR, Paul M, Deepa AS, Kumar RK. Obesity in Indian children: time trends and relationship with hypertension. *Natl Med J India.* 2007 Nov-Dec;20(6):288-93. PubMed PMID: 18335794. [PubMed].
12. Marwaha RK, Tandon N, Singh Y, Aggarwal R, Grewal K, Mani K. A study of growth parameters and prevalence of overweight and obesity in school children from delhi. *Indian Pediatr.* 2006 Nov;43(11):943-52. PubMed PMID: 17151397. [PubMed].
13. Unnithan AG, Syamakumari S. Prevalence of Overweight, Obesity and Underweight among School Going Children in Rural and Urban areas of Thiruvananthapuram Educational District, Kerala State (India). *Internet J Nutr Wellness* 2008.p. 6. Available from <http://ispub.com/IJNW/6/2/7073>.
14. Caprio S. Calories from soft drinks--do they matter? *N Engl J Med.* 2012 Oct 11;367(15):1462-3. doi: 10.1056/NEJMe1209884. Epub 2012 Sep 21. PubMed PMID: 22998341. [PubMed].
15. Bremer AA, Lustig RH. Effects of sugar-sweetened beverages on children. *Pediatr Ann.* 2012 Jan;41(1):26-30. doi: 10.3928/00904481-20111209-09. PubMed PMID: 22224718. [PubMed].
16. Diet, nutrition and the prevention of chronic diseases. *World Health Organ Tech Rep Ser* 2003;916:61-7.
17. Global Strategy on Diet, Physical Activity and Health. Available from: [http://www.who.int/dietphysicalactivity/childhood\\_why/en/index.html](http://www.who.int/dietphysicalactivity/childhood_why/en/index.html)
18. Oliver M.Br. *Med. Bull.* 1981;37(1):49-58.
19. Oliver MF. Diet and coronary heart disease. *Br Med Bull.* 1981 Jan;37(1):49-58. Review. PubMed PMID: 7020866. [PubMed]
20. Klesges RC, Klesges LM, Eck LH, Shelton ML. A longitudinal analysis of accelerated weight gain in preschool children. *Pediatrics.* 1995 Jan;95(1):126-30. PubMed PMID: 7770289. [PubMed].
21. Wolfe WS, Campbell CC, Frongillo EA Jr, Haas JD, Melnik TA. Overweight schoolchildren in New York State: prevalence and characteristics. *Am J Public Health.* 1994 May;84(5):807-13. Erratum in: *Am J Public Health.* 2005 Jul;95(7):1093. PubMed PMID: 8179053; PubMed Central PMCID: PMC1615049. [PubMed].
22. Hanley AJ, Harris SB, Gittelsohn J, Wolever TM, Saksvig B, Zinman B. Overweight among children and adolescents in a Native Canadian community: prevalence and associated factors. *Am J Clin Nutr.* 2000 Mar;71(3):693-700. PubMed PMID: 10702161. [PubMed].
23. Amin TT, Al-Sultan AI, Ali A. Overweight and Obesity and their Association with Dietary Habits, and Sociodemographic Characteristics Among Male Primary School Children in Al-Hassa, Kingdom of Saudi Arabia. *Indian J Community Med.* 2008 Jul;33(3):172-81. doi: 10.4103/0970-0218.42058. PubMed PMID: 19876479; PubMed Central PMCID: PMC2763675. [PubMed].
24. Berkey CS, Rockett HR, Field AE, Gillman MW, Frazier AL, Camargo CA Jr, Colditz GA. Activity, dietary intake, and weight changes in a longitudinal study of preadolescent and adolescent boys and girls. *Pediatrics.* 2000 Apr;105(4):E56. PubMed PMID: 10742377. [PubMed].
25. Al-Ghamdi SH. The association between watching television and obesity in children of school-age in Saudi Arabia. *J Family Community Med.* 2013 May;20(2):83-9. doi: 10.4103/2230-8229.114767. PubMed PMID: 23983559; PubMed Central PMCID: PMC3748652. [PubMed].

**Tables****TABLE I PREVALENCE OF OVERWEIGHT AND OBESITY IN STUDY SUBJECTS**

BMI	Number of students	Percentage
Obese	26	4.44
Overweight	112	19.14
Normal range & below	447	76.41
Total	585	100

**TABLE II PREVALENCE OF OVERWEIGHT AND OBESITY ACCORDING TO SEX**

BMI	Male No. (%)	Female No. (%)	Frequency No. (%)
Students with normal weight and below	244 (73.71)	203 (79.92)	447 (76.41)
Overweight	69 (20.84)	43(16.92)	112 (19.14)
Obese	18 (5.43)	8 (3.14)	26 (4.44)
Total	331 (100)	254 (100)	585 (100)

**TABLE III ASSOCIATION OF SOCIOECONOMIC STATUS PREVALENCE OF OVERWEIGHT & OBESITY**

Socioeconomic status	Number of students No. (%)	Students with normal weight and below No. (%)	Students with overweight and obesity No. (%)
Class I	171(29.23)	119 (69.59)	52 (30.41)
Class II	214(36.58)	161 (75.23)	53 (24.77)
Class III	162(27.69)	136 (83.95)	26 (16.05)
Class IV	38 (6.49)	34 (89.47)	4 (10.53)
Class V	0(0)	0 (0)	0 (0)
Total	585(100)	447 (76.41)	138 (23.59)

$\chi^2 = 10.1504, df=3, p < 0.05.$

**TABLE IV ASSOCIATION OF TYPE OF DIET WITH PREVALENCE OF OVERWEIGHT AND OBESITY**

Type of diet	Number of students No. (%)	Students with normal weight and below No. (%)	Students with overweight and obesity No. (%)
Vegetarian	165(100)	129(78.18)	36(21.82)
Mixed	420(100)	318(75.71)	102(24.29)
Total	585(100)	447(76.41)	138(23.59)

$\chi^2 = 0.31, df= 1, p>0.05$

**TABLE V ASSOCIATION OF FREQUENCY OF JUNK FOOD WITH PREVALENCE OF OVERWEIGHT AND OBESITY IN STUDY SUBJECTS**

Frequency	Number of students No. (%)	Students with normal weight and below No. (%)	Students with overweight and obesity No. (%)
Occasional	430 (100)	340 (79.07)	90 (20.93)
Frequent	155 (100)	107 (69.03)	48 (30.97)
Total	585 (100)	447 (76.41)	138 (23.59)

$\chi^2 = 4.865957, df=1, p < 0.05.$

**TABLE VI ASSOCIATION OF FREQUENCY OF EATING SWEETS PER WEEK WITH PREVALENCE OF OVERWEIGHT AND OBESITY**

Frequency (per week)	Number of students No. (%)	Students with normal weight and below No. (%)	Students with overweight and obesity No. (%)
Occasional	103 (100)	89 (86.41)	14 (13.59)
Frequent	482 (100)	358 (74.27)	124 (25.73)
Total	585 (100)	447 (76.41)	138 (23.59)

$\chi^2 = 5.296657, df= 1, p < 0.05$

## Pirfenidone induced phototoxic reaction in an elderly man

Sir,  
Pirfenidone is an antifibrotic and anti-inflammatory agent used in the treatment of idiopathic pulmonary

fibrosis. It reduces fibroblast proliferation, inhibits transforming growth factor- $\beta$  stimulated collagen production and reduces the production of fibrogenic mediators. Although photosensitivity and rash are reported side effects in clinical trials, we were able to find only a few previously published reports of this adverse effect.<sup>[1]</sup>



A 70-year-old man presented with burning sensation and a rash for 20 days. He had intense erythema with desquamation involving the face, scalp [Figure 1], V area of the chest, shoulder area and upper back [Figure 2] extending to the dorsum of the hands along with involvement of the dorsa of feet upto the ankles. Fissuring was noted over the preauricular area. Characteristic sparing of the periorbital area (patient was using spectacles) and vest covered area was noted. Hair, nail, and mucosae were normal. Skin biopsy was not undertaken.

He had interstitial lung disease and was on treatment with bronchodilators (formetrol, once a day), mucolytics (N-acetylcysteine, 2 teaspoons thrice a day), and pirfenidone for the last 6 months. He had been started on 600 mg/day of pirfenidone 5 months back and the dose was gradually increased to 1200 mg/day. Ten days after escalation of the dose, the patient developed the rash suggesting a dose dependency of the phototoxic reaction. He was managed with oral prednisolone 0.75 mg/kg body weight in a tapering dose along with antihistamines, topical corticosteroids, broad spectrum sunscreens and strict photoprotection.

A diagnosis of drug-induced phototoxic reaction with pirfenidone was made based on clinical examination and history. The differential diagnosis of allergic contact dermatitis, irritant contact dermatitis, and subacute cutaneous lupus erythematosus were excluded on clinical grounds.

Costabel *et al.* stated that the cutaneous adverse effects of pirfenidone include phototoxic burn-like skin

rash on the sun exposed body areas.<sup>[2]</sup> Skin related photosensitivity reactions were observed in 12.2% and rash was noted in 32.2% of pirfenidone treated patients as reported in the CAPACITY studies.<sup>[3]</sup> Our patient can be categorized as Grade 3 (erythema with desquamation) which was reported in 0.2% of the drug cohort in the CAPACITY studies. Photosensitivity and rash led to the discontinuation of therapy in approximately 1% of the patient.<sup>[3]</sup>

The mechanism of pirfenidone-induced photosensitivity is likely to be phototoxic and is related to the drug's ability to absorb ultraviolet A and ultraviolet B. Absorption of ultraviolet light in the skin tissue could result in skin lesions due to generation of reactive oxygen species and lipid peroxidation.<sup>[4]</sup> Animal studies have shown the use of sunscreens with higher sun protection factor significantly reduce the severity of skin reactions.<sup>[5]</sup>

The standard approach for preventing and managing skin-related adverse effects include avoiding direct sun exposure, use of broad spectrum sunscreens, physical protection, and avoiding other phototoxic drugs. Costabel *et al.* have expanded the above guidelines by suggesting behavioral avoidance of indirect sunlight as well as intense artificial light sources, wearing of thick woven cloth and broad brimmed hats and avoiding sun exposure for a few hours following the intake of pirfenidone.<sup>[2]</sup> The management of the rash includes reduction of the drug dose and discontinuation of the drug in case of persistence of rash for more than 15 days. Slow re-introduction of the drug can be attempted once the symptoms have resolved.



**Figure 1: Erythema and scaling involving face, neck, shoulder sparing vest covered area, and periorbital region**



**Figure 2: Intense erythema involving upper back, nape of neck, and shoulders sparing the vest covered region**

As pirfenidone is also associated with gastrointestinal and neurological side effects, these also need to be carefully monitored. Dose reduction can lessen the gastrointestinal and dermatological side effects.<sup>[6]</sup>

#### Declaration of patient consent

The authors certify that they have obtained all appropriate patient consent forms. In the form the patient(s) has/have given his/her/their consent for his/her/their images and other clinical information to be reported in the journal. The patients understand that their names and initials will not be published and due efforts will be made to conceal their identity, but anonymity cannot be guaranteed.

#### Financial support and sponsorship

Nil.

#### Conflicts of interest

The authors have obtained appropriate patient consent for the information published in this article.

#### Rohini Pradip Gaikwad, Samipa S. Mukherjee<sup>1</sup>

Department of Dermatology, Venereology and Leprosy, MIMER Medical College, Talegaon Dabhade, Maharashtra, <sup>1</sup>Department of Dermatology, Bangalore Medical College and Research Institute, Bengaluru, Karnataka, India

**Address for correspondence:** Dr. Rohini Pradip Gaikwad, Flat Number 5, Hindustan Arcade, Tingrenagar Road, Vishrantvadi, Pune - 411 015, Maharashtra, India.  
E-mail: rohinigkwd@yahoo.co.in

#### REFERENCES

1. Koulelidis A, Zacharis G, Dolios P, Zouvelekis AT. Pirfenidone photosensitivity rash in a patient with idiopathic pulmonary fibrosis. *Pneumon* 2013;26:92.
2. Costabel U, Bendstrup E, Cottin V, Dewint P, Egan JJ, Ferguson J, *et al.* Pirfenidone in idiopathic pulmonary fibrosis: Expert panel discussion on the management of drug-related adverse events. *Adv Ther* 2014;31:375-91.
3. Noble PW, Albera C, Bradford WZ, Costabel U, Glassberg MK, Kardatzke D, *et al.* Pirfenidone in patients with idiopathic pulmonary fibrosis (CAPACITY): Two randomised trials. *Lancet* 2011;377:1760-9.
4. Seto Y, Inoue R, Kato M, Yamada S, Onoue S. Photosafety assessments on pirfenidone: Photochemical, photobiological, and pharmacokinetic characterization. *J Photochem Photobiol B* 2013;120:44-51.
5. Pharmaceuticals and Medical Devices Agency Japan. Pirfenidone Report. Available from: [http://www.pmda.go.jp/english/service/pdf/drugs/pirespa\\_oct2008\\_e.pdf](http://www.pmda.go.jp/english/service/pdf/drugs/pirespa_oct2008_e.pdf). [Last accessed on 2014 Mar 18]
6. Jiang C, Huang H, Liu J, Wang Y, Lu Z, Xu Z. Adverse events of pirfenidone for the treatment of pulmonary fibrosis: A meta-analysis of randomized controlled trials. *PLoS One* 2012;7:e47024.

This is an open access article distributed under the terms of the Creative Commons Attribution-NonCommercial-ShareAlike 3.0 License, which allows others to remix, tweak, and build upon the work non-commercially, as long as the author is credited and the new creations are licensed under the identical terms.

Access this article online	
<b>Quick Response Code:</b>	<b>Website:</b> www.ijdv1.com
	<b>DOI:</b> 10.4103/0378-6323.172899

**How to cite this article:** Gaikwad RP, Mukherjee SS. Pirfenidone induced phototoxic reaction in an elderly man. *Indian J Dermatol Venereol Leprol* 2016;82:101-3.

**Received:** February, 2015. **Accepted:** September, 2015.

# Cellular cannibalism in giant cells of central giant cell granuloma of jaw bones and giant cell tumors of long bones

[Gargi S Sarode](#)<sup>1</sup>, [Sachin C Sarode](#)<sup>1</sup>, [Shailesh Gawande](#)<sup>1</sup>, [Snehal Patil](#)<sup>1</sup>, [Rahul Anand](#)<sup>1</sup>, [Shankar Gouda Patil](#)<sup>2</sup>, [Prakash Patil](#)<sup>3</sup>

Affiliations expand

- PMID: 26991690
- DOI: [10.1111/jicd.12214](https://doi.org/10.1111/jicd.12214)

## Abstract

**Aim:** The aim of the present study was to investigate the relationship of central giant cell granuloma (CGCG) and giant cell tumor of long bones (GCT) with respect to cannibalistic giant cells (GCs).

**Method:** Sixteen cases each of CGCG and GCT were histopathologically analyzed for cannibalistic GCs. One hundred GCs were examined in each section, and the number of cannibalistic GCs was expressed in percentage.

**Results:** Cannibalistic GCs were seen in all cases of CGCG and GCT (100%). GCT showed significantly higher mean cannibalistic GC frequency ( $44.81 \pm 1.013$ ) than CGCG ( $32.06 \pm 1.398$ ), aggressive CGCG ( $38.17 \pm 1.579$ ), non-aggressive CGCG ( $28.40 \pm 0.6360$ ), non-recurrent CGCG ( $30.42 \pm 1.417$ ), and recurrent CGCG ( $37.00 \pm 2.483$ ). In aggressive CGCG, the mean cannibalistic GC frequency was significantly higher ( $38.17 \pm 1.579$ ) than the non-aggressive variant ( $28.40 \pm 0.6360$ ). Recurrent CGCG cases showed significantly higher mean cannibalistic GC frequency ( $37.00 \pm 2.483$ ) than non-recurrent cases ( $30.42 \pm 1.417$ ). Similarly, recurrent GCT showed significantly higher mean cannibalistic GC frequency ( $47.4 \pm 4.97$ ) than non-recurrent GCT ( $43.63 \pm 3.1$ ).

**Conclusion:** The distinctness of CGCG and GCT was observed in terms of mean cannibalistic GC count. The assessment of cannibalistic GC in CGCG and GCT could help in predicting the biological behavior and grading of the tumor.

**Keywords:** cannibalistic giant cell; cellular cannibalism; central giant cell granuloma; giant cell; giant cell tumor.

© 2016 John Wiley & Sons Australia, Ltd.

**Comment in**